UNIVERSIDAD COMPLUTENSE DE MADRID
FACULTAD DE CIENCIAS QUÍMICAS
DEPARTAMENTO DE QUÍMICA FÍSICA I

TESIS DOCTORAL

Superficies funcionales micro-nanoestructuradas obtenidas por combinación de litografía y segregación superficial

MEMORIA PARA OPTAR AL GRADO DE DOCTORA

PRESENTADA POR

Marta Palacios Cuesta

Directores

Olga García Ballesteros
Juan Rodríguez Hernández

Madrid, 2015

UNIVERSIDAD COMPLUTENSE DE MADRID

Facultad de CC. Químicas

Departamento de Química Física I

SUPERFICIES FUNCIONALES MICRO/NANOESTRUCTURADAS OBTENIDAS POR COMBINACIÓN DE LITOGRAFÍA Y SEGREGACIÓN SUPERFICIAL

TESIS DOCTORAL

Memoria presentada por

Marta Palacios Cuesta

Para optar al grado de Doctor

Directores: Dra Olga García Ballesteros y Dr. Juan Rodríguez Hernández

Instituto de Ciencia y Tecnología de Polímeros

MADRID 2015

La presente tesis doctoral ha sido realizada en el Departamento de Química y Propiedades de Materiales Poliméricos del Instituto de Ciencia y tecnología de Polímeros del Consejo Superior de Investigaciones Científicas (CSIC) bajo la dirección de la Dra Olga García Ballesteros y el Dr. Juan Rodríguez Hernández. Este trabajo ha sido posible gracias a la financiación de los proyectos MAT2011-22861 y MAT2009-12251 del Ministerio de Economía y Competitividad (MINECO) así como a la beca predoctoral del Ministerio de Educación para la Formación del Profesorado Universitario (FPU) (referencia *AP2009 0095*).

"Un hombre con una idea nueva es un loco, hasta que la idea triunfa."

Mark Twain

AGRADECIMIENTOS

Empezar agradeciendo a mis directores de Tesis, a la **Dra. Olga García Ballesteros** y al **Dr. Juan Rodríguez Hernández** por haberme dado la oportunidad de desarrollar una Tesis en el CSIC, por haber adquirido la responsabilidad de "adoptarme" profesionalmente hablando, guiarme, enseñarme el mundo de la investigación y formarme poco a poco durante estos años. Además, les quiero agradecer que hayan confiado en mí y que hayan valorado siempre mis ideas y mis aportaciones y por supuesto quiero agradecerles que no sólo sean grandes en ciencia sino que también hayan sido incluso mejores personas y se hayan preocupado por mí durante estos años.

A **Marta Liras** que aunque no es mi directora, me ha ayudado como la que más los años que ha estado compartiendo laboratorio con nosotras.

A la **Dra. Aitziber López Cortajarena** del IMDEA, por haberme ayudado en la parte más "bio" de la Tesis: los estudios con proteínas y bacterias, que han dado aplicabilidad a mis materiales.

Al **Dr. Adolfo del Campo**, del ICV, por la ayuda prestada en las medidas de perfilometría.

A **Sonia** y a **Elena** que además de compañeras del laboratorio, han sido antes amigas mías desde la carrera, por todos los ratos juntas. Y por supuesto a Elma, que fue de quién originalmente seguí los pasos.

A mis compañeros del ICTP, no quiero poner nombres porque seguro que me dejo a alguien. En estos años ha pasado mucha gente por aquí, que luego han seguido su camino por otros lados, gracias por compartir conmigo el día a día, las comidas, los *tupers* y todo lo demás.

A **Alberto**, mi amigo y mi compañero de Tesis, que no de laboratorio, por escucharme todos esos días cuando la química no quería salir, por tu carácter y tu alegría gaditana.

A **mis compañeros del máster**, aunque ya hace años, ahí es donde empezó todo. Algunos habéis seguido acompañándome durante el resto de los años aquí, otros decidisteis cambiar de ámbito profesional, que sepáis que guardo un recuerdo especial del buen ambiente que se podía respirar ese año.

Al **Prof. Gadegaard** por haberme dado la oportunidad de realizar la estancia de la Tesis en Glasgow y por brindarme la oportunidad de trabajar en la sala blanca de la Universidad, a Álex por ayudarme con la química y con el inglés allí.

A **Ángela, Clara, Raku, Santi** y **Víctor**, mis queridos "centimorgans", gracias por las cenas, las tapas, las excursiones y sobre todo por la risas y las anécdotas. Sé que algunos también entendéis también todo el esfuerzo que conlleva la Tesis, porque lo estáis viviendo en las propias carnes…

A mis **"Bailanchines",** porque con muchos de vosotros no solo he compartido pasos y figuras, sino que habéis entrado a formar parte de mi vida como amigos que se permanecerán aunque el baile termine, (cosa improbable, de todas formas). Gracias por los bailes, los congresos, los viajes pero sobre todo por estar conmigo algunas tardes y desconectar de todo bailando. A **Elena**, la primera bailanchina… ¡Bendita tarde de enero!, gracias también por todos estos años, por los viajes, por acompañarme en el camino tanto de la Tesis como en el de la Vida. A **Jota** por haber mi sido mi compañero en todos los cursos "extraescolares" y por preocuparse por mí.

A mis amigas **Leti, Eli, Sandra** y **Sory** por esas charlas, por las meriendas y porque sé que puedo contar con vosotras.

A mi **Silvi**, toda una vida, literalmente, gracias por acompañarme en el camino.

A mi **familia** porque sé que puedo contar con vosotros y en particular a mis **primas**, lo más parecido a hermanas que he tenido.

A **Javi**, porque siempre eres tan positivo, por tus energías, por todo lo que me ayudas y te preocupas por mí todos los días y por todo el camino que nos queda por recorrer juntos.

A mi **madre** y a mi **padre**, gracias por TODO, por la ayuda incondicional en todos los aspectos, gracias por quererme como lo hacéis y por apoyarme a todos los niveles, tanto profesionales como de la vida: ¡ESTE TRABAJO VA POR VOSOTROS!

A **Noita**, último miembro en llegar a la familia, gracias porque me has ayudado también sin saberlo, porque apareciste cuando me hacías falta, gracias por estar siempre siempre feliz y regalarme tu alegría independientemente de cuando llegue a casa.

A todos vosotros, que formáis parte de mi vida y quiero que la sigáis formando,

Gracias.

Acrónimos

ACRÓNIMOS

5FS –2,3,4,5,6-Pentafluorostyrene

AA –Acrylic acid

AFM – Atom force microscopy

ATR –Attenuated total reflectance

ATRP – Atom transfer radical polymerization

CuBr – Cupper (I) bromide

DPN – Dip pen nanolithography

DSC – Differential scanning calorimetry

DVB - Divinylbenzene

EBrIB – Ethyl-2-bromoisobutyrate

ECH – 3,4 epoxycyclohexyl methyl-3',4'-epoxycyclohexane carboxylate

EDC – Ethyl(dimehylaminopropyl) carbodiimide

EGDMA – Ethylene glycol dimethacrylate

FTIR – Fourier transform infrared spectroscopy

GFP – Green fluorescent protein

HEMA – 2-(hydroxyethyl methacrylate)

IRG 651- Irgacure 651, 2,2-dimethoxy-1,2-diphenylthan-1-one

MMA – Methyl methacrylate

MRSA – Meticillin-resistant *Staphylococcus Aureus*

NHS – N-hydroxysuccinimide

NIL – Nano imprint lithography

NMR – Nuclear magnetic resonance

OD – Optical density

P5FS - Poly(2,3,4,5,6-Pentafluorostyrene)

PAA –Poly(acrylic acid)

PAG – Photoacid generator

PBS – Phosphate buffered saline

PCT – Patent cooperation treatment

PDMS – Poly(dimethyl siloxane)

PEDGMA – Poly(ethylene glycol dimethylacrilate)

PETA – Pentaeritritol tryacrylate

PETRA – Pentaeritritol tetraacrylate

PGA – Poly(glutamic acid)

PMDETA – N,N,N',N'',N''-pentamethyldiethylentriamine

PMMA – Poly(methyl methacrylate)

POSS – Poly octasilsesquioxane

PS – Polystyrene

PU - Polyurethane

S – Styrene

SEC –Size exclusion chromatography

SEM – Scanning electron microscopy

SPL - Scanning probe lithography

STEM –Scanning transmission electron microscopy

TBST - Mixture of Tris-Buffered Saline and Tween 20

TEM – Transmission electron microscopy

TFMA – 2,2,2-Trifluoromethyl methacrylate

THF - Tetrahydrofurane

TPR – Tetratricopeptide protein

TSH – Triarylsulfonium hexafluoruro-antimonate salts mixed

UV - Ultraviolet

UVO - Ultraviolet ozone

WCA – Water contact angle

XPS –X-ray photoelectron spectroscopy

Índice

Prefacio

Los materiales poliméricos se usan, de manera generalizada, en la vida cotidiana, gracias a, su facilidad de procesado industrial, su gran versatilidad, su flexibilidad, resistencia a agentes químicos o a su buena relación peso/propiedades, entre otros. Sin embargo en algunos casos, sus propiedades superficiales no son adecuadas para algunas aplicaciones debido a su baja energía superficial. De hecho, un gran número de las utilidades que presentan los polímeros dependen, casi en exclusiva, de su superficie. Para éstas, no importa tanto cómo sea el interior del material y su desarrollo se va a ver afectado principalmente por las capas más externas de éste, las últimas micras/nanómetros superficiales. Por todo ello, el diseño y el control de estas superficies es imprescindible para poder adaptar los materiales poliméricos a los requerimientos necesarios en determinadas aplicaciones.

Estas adaptaciones superficiales pueden conllevar desde la funcionalización de la superficie, la modificación de su cristalinidad, la creación de microdominios o incluso variaciones de la rugosidad y de la topografía [1-4]. El control de la estructuración de una superficie y de la funcionalización de ésta, que pueden realizarse a través de procesos secuenciales o simultáneos, permite desarrollar nuevos materiales con propiedades superhidrofóbicas, superhidrofílicas, biocompatibles, adhesivas, lubricantes o *antifouling*, entre otras [5, 6].

En esta Tesis Doctoral se han adaptado métodos existentes y se han desarrollado otros nuevos que nos han permitido modificar la topografía de superficies poliméricas a la vez que se han generado superficies con diferente funcionalidad, de manera que se han transformado polímeros habituales, de los englobados en los llamados "*commodities*" de alto consumo, en materiales con alto valor añadido. Las metodologías desarrolladas, tanto de funcionalización como de modificación de la topografía superficial, además, han sido adaptadas de forma que no sea necesario el uso de grandes y costosos equipos o instalaciones especiales, como el empleo de salas blancas. Se perseguido que las tecnologías aquí desarrolladas sean potencialmente implantables a nivel industrial, tanto a nivel técnico como económico.

Esta Memoria está distribuida en cinco secciones. La primera sección corresponde a una introducción general donde se incluye un resumen de las técnicas de modificación

superficial que se emplean actualmente, tanto a nivel composicional como a nivel estructural, de manera que se engloban las técnicas que se han utilizado a lo largo de este Trabajo dentro de su propio contexto. Además, esta primera sección incluye las motivaciones que nos han llevado a desarrollar este trabajo y explica los Objetivos que nos planteamos en un principio y que finalmente han dado lugar a la presente Tesis Doctoral.

Las tres secciones siguientes se corresponden con los bloques estructurales de los que está compuesta esta Tesis. En cada uno de estos bloques se ha utilizado una técnica de microestructuración superficial diferente (fotolitografía, *hot embossing* y formación de arrugas superficiales) combinada con la funcionalización de la superficie, en todos los casos. Cada una de estas secciones se presenta con una breve introducción, y va seguida del/los artículo/s científico/s (o patente) a la que ha dado lugar, incluyendo un breve resumen del contenido de cada artículo en castellano.

Finalmente en la sección V se han incluido las principales Conclusiones de esta Tesis Doctoral.

Bibliografía

[1] C. Zhao, Y. Ma, L. Liu, D. Chen, L. Wang, W. Yang, Advances in photo-induced surface modification of polymer materials, *Gaofenzi Cailiao Kexue Yu Gongcheng/Polymeric Materials Science and Engineering*, 30, **2014,** 164-169.
[2] D. Li, Q. Zheng, Y. Wang, H. Chen, Combining surface topography with polymer chemistry: Exploring new interfacial biological phenomena, *Polymer Chemistry*, 5, **2014,** 14-24.
[3] M.S. She, T.Y. Lo, H.Y. Hsueh, R.M. Ho, Nanostructured thin films of degradable block copolymers and their applications, *NPG Asia Materials*, 5, **2013**.
[4] P.U. Dhanvijay, V.V. Shertukde, Review: Crystallization of biodegradable polymers, *Polymer - Plastics Technology and Engineering*, 50, **2011,** 1289-1304.
[5] P. Samyn, Wetting and hydrophobic modification of cellulose surfaces for paper applications, *Journal of Materials Science*, 48, **2013,** 6455-6498.
[6] C. Desrousseaux, V. Sautou, S. Descamps, O. Traoré, Modification of the surfaces of medical devices to prevent microbial adhesion and biofilm formation, *Journal of Hospital Infection*, 85, **2013,** 87-93.

SECCIÓN I: Introducción

SECCIÓN I

I. INTRODUCCIÓN GENERAL

Numerosas propiedades de los materiales poliméricos como la adhesividad [1, 2], la mojabilidad [3-5], la biocompatibilidad [6], las propiedades lubricantes [7], la cinética de las reacciones químicas o biológicas [8] o la absorción, dependen, casi en exclusiva, de su superficie. Algunos ejemplos se pueden encontrar en la misma naturaleza, donde algunos organismos han desarrollado morfologías específicas que cumplen funciones muy diversas [9-11]: desde la reducción de la adhesión de partículas para favorecer, así, la formación de estructuras deslizantes en las plantas carnívoras que les permiten atrapar insectos; hasta la obtención de superficies adhesivas, como se observa en la pata de la salamanquesa (Figura 1a) o la consecución de propiedades "autolimpiantes" gracias a superficies hidrofóbicas y multiestructuradas como el conocido caso de la hoja de loto (Figura 1b) .

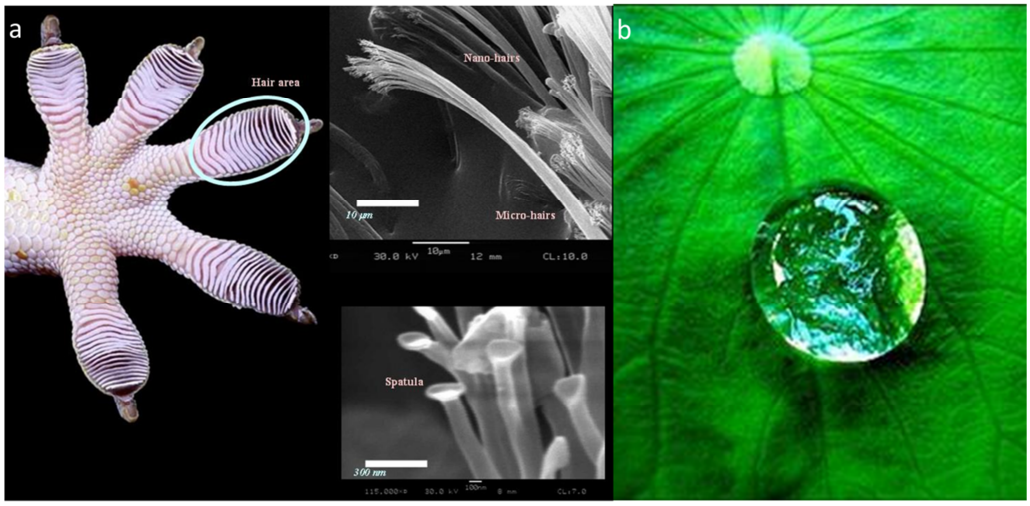

Figura 1*: a) Pata de una salamanquesa y micrografías por SEM de ampliaciones de la zona seleccionada. Gracias a esta microestructura el animal es capaz de adherirse a casi cualquier superficie. b) Superficie superhidrofóbica y autolimpiante de una hoja de loto [12]*

El desarrollo de superficies inspiradas en la naturaleza es muy complejo; se trata de superficies con patrones producidos a diferente escala (nano y micrométrica) con composiciones determinadas que favorecen una propiedad. Sin embargo, se han desarrollado superficies sintéticas bioinspiradas en las cuales existe la posibilidad de controlar algunos parámetros y conseguir, así, una determinada propiedad como se muestra, por ejemplo, en la Figura 2, donde se observa una superficie superhidrofóbica (la gota de agua no moja la superficie).

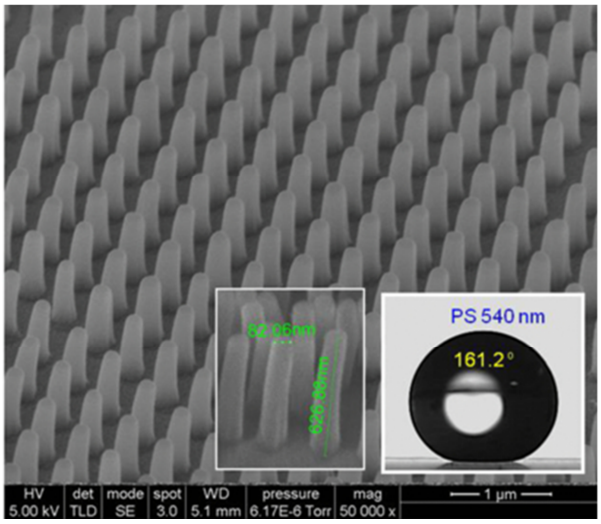

***Figura 2**: Superficie superhidrofóbica polimérica, creada por litografía[13] .*

En ocasiones, por tanto, la adaptación de un material a una determinada aplicación requiere del diseño de su superficie. Así, aparte de las propiedades mecánicas del material, para adaptarlo y adecuarlo a su uso final, se debe considerar a que medio va estar expuesto, es decir, tener en cuenta la interfase. Son varios los factores que juegan un papel fundamental en las propiedades finales de la superficie de un material. En esta Tesis Doctoral nos centraremos en dos de ellos principalmente: la funcionalidad y la estructura.

Muchos de los ejemplos que existen han considerado por separado algunas de las características superficiales tratando de ver cómo esa característica influye en una determinada propiedad. Por ejemplo, se han elaborado diferentes sistemas en las que la topografía afecta a la mojabilidad de una superficie.

Igualmente, la funcionalización química, es decir, la introducción de grupos funcionales en la superficie, ha sido clave para mejorar propiedades como la adhesión entre materiales poliméricos. Así, la primera se realiza mediante distintos métodos de fabricación que se pueden agrupar en dos grandes familias: las técnicas "*bottom-up*" (de abajo a arriba) y "*top-down*" (de arriba abajo). Mientras que en las primeras se desarrolla cada parte del sistema con amplitud de detalles y se va creciendo hasta llegar al sistema completo, en las segundas, se plantea el sistema en general, sin demasiado detalle, y desde ahí se va fragmentando y se van redefiniendo los detalles. La segunda requiere, normalmente, tratamientos químicos o físicos que modifican la parte más superficial del material.

La combinación de funcionalización y estructuración también ha sido explorada. Sin embargo, muchos de los ejemplos existentes (como se verá a lo largo de esta introducción) requieren de equipos sofisticados o de preparación en varias etapas.

En esta Tesis se propone el diseño de distintos sistemas que combinan la estructura con la funcionalidad y que, además, se pueden desarrollar de una manera directa y sencilla. Antes de abordar el trabajo realizado en esta Tesis se muestra un resumen de las estrategias empleadas para modificar la superficie y la funcionalidad por separado. También se ilustran con algunos ejemplos aquellos sistemas que combinan ambas. La última parte de este capítulo introductorio se centrará en las aplicaciones. Se han seleccionado las aplicaciones en las que nuestros materiales serán empleados.

I.1 Modificación de la topografía superficial

Existen numerosas técnicas para la estructuración de superficies [14] que se podrían agrupar, en una primera aproximación, atendiendo a si el objetivo es la generación de un patrón o, por el contrario, la replicación de éste. En este primer caso, se utilizan técnicas de escritura sobre superficies o las basadas en "inestabilidades superficiales". La replicación se lleva a cabo, por ejemplo, empleando una máscara (fotolitografía) o por litografía suave, más conocida por el término en inglés "*soft lithography*". A continuación se muestra una tabla que resume las principales técnicas de modificación superficial, atendiendo a la clasificación anteriormente descrita:

Tabla 1: *Principales técnicas de modificación superficial*

TIPO DE PROCEDIMIENTO		TÉCNICA	RESOLUCIÓN	CARACTERÍSTICAS
Replicación de un patrón: Se reproducen o duplican patrones idénticos o complementarios a una máscara o un original.	Máscara	**Fotolitografía** [15, 16]	10 nm → micras	Sustrato expuesto a la luz a través de una fotomáscara.
		Deposición [17, 18]	5 nm → micras	Se utilizan materiales vaporizables que se depositan en los huecos de la máscara.
		Grabado [19, 20]	10 nm → micras	La propia máscara actúa como una barrera física a la exposición del sustrato.
	Máster: *soft lithography*	***Hot embossing*** [21, 22]	< 100 nm → micras	El molde se imprime en un material deformable bajo fuerza mecánica.
		Moldeo por impresión [23, 24]	100 nm → micras	Utilizando un material flexible se hace una réplica de un molde el cual se rellena con un líquido prepolimérico que posteriormente se cura.
		Impresión por microcontacto [25-27]	>100 nm → micras	Con un sello con tinta se copia la impresión a un sustrato
		Estructuración con microfluidos [28, 29]	< 100 nm → micras	Los canales de una red de microfluidos se usan para distribuir el material desde un reservorio a la superficie de un sustrato.

TIPO DE PROCEDIMIENTO		**TÉCNICA**	**RESOLUCIÓN**	**CARACTERÍSTICAS**
Generación de un patrón: Formación o grabado de un patrón arbitrario.	Métodos de escritura:	Punta rígida [30, 31]	Submicrométrica	Modificación o desplazamiento de parte del material de la superficie con la punta.
		Partículas energéticas: fotones/ electrones [32] [33, 34]	10 nm	La escritura se realiza por la acción de un rayo de partículas energéticas. El más utilizado es el rayo de electrones. En este caso no hay contacto entre punta y superficie.
		Campo eléctrico [35]	Submicrométrica	Escritura se realiza por acción de un campo eléctrico.
		Campo magnético [36]	Submicrométrica	Escritura se realiza por acción de un campo magnético.
		Escritura por adición: *-Dip-pen nanolithography* (DPN) [37, 38] *- Inkjet printing* (IJP) [39, 40] *-Laser-induced vapor deposition* (LCVD) [41]	10 nm	Se deposita un material sobre la superficie de un soporte sólido

TIPO DE PROCEDIMIENTO		TÉCNICA	RESOLUCIÓN	CARACTERÍSTICAS
Generación de un patrón: Formación o grabado de un patrón arbitrario.	Inestabilidades superficiales	Auto-organización [42, 43]	nm - mm	Los diferentes componentes forman bloques de distinta composición que se pueden eliminar selectivamente.
		Técnica de secado [44, 45]	100 nm	Formación de pequeñas gotas de líquido, agujeros o estructuras poligonales.
		Estructuración superficial electrodinámica [46, 47]	Submicrométrica - micras	Se aplica una diferencia de campo eléctrico en las diferentes caras de una película polimérica que provocan el cambio y la estructuración superficial.
		Inducidas por gradiente térmico [48, 49]	Submicrométrica - micras	Aquí la diferencia es una diferencia de temperatura
		Figuras de respiración [50, 51]	Cientos de nm – ≈20 micras	Condensación de agua durante la evaporación del disolvente durante la formación de una película polimérica.
		Arrugas, crestas y plegamientos [52]	Micras-kilómetros	Causadas por una fuerza externa que sobrepasa un valor crítico, por lo que el material se dobla.
		Otras [53, 54], [55, 56] [57, 58], [59, 60]		

A lo largo de esta Tesis se han empleado técnicas de estructuración basadas en la utilización de máscaras definidas con distintos motivos y tamaños (fotolitografía), la preparación de moldes de PDMS que se han marcado sobre el material polimérico (*hot embossing*), así como otras que no requieren de los mismos. En particular, en este Trabajo se ha utilizado la formación de texturas superficiales también conocidas bajo el nombre de "arrugas" (del inglés "*wrinkles*"). Será por tanto de estas tres secciones de las que se hablará a continuación con más detalle.

I.1.1. Replicación de un patrón mediante la utilización de una máscara: Fotolitografía

En los procesos de replicación se reproducen o duplican patrones idénticos o complementarios a una máscara o un original (*master*). Si el sustrato es expuesto a irradiación por luz a través de una máscara, se habla de fotolitografía [15, 16].

El proceso de fotolitografía se basa en transferir el patrón de una fotomáscara a otra superficie. Todos los métodos fotolitográficos comparten el mismo principio (Figura 3) que consiste en la exposición de un material fotosensible a una radiación [14] a través de una fotomáscara obteniéndose el registro de una imagen. Así, solamente en las zonas expuestas a la radiación se producirán cambios en el material fotosensible. Tras un proceso de revelado y dependiendo de si se produce la degradación o el entrecruzamiento de este material (que suele ser un polímero), se obtendrá la imagen positiva (por ejemplo fotogeneradores de ácido o *photoacid generators (PAG) [60])* o la imagen negativa (por ejemplo el SU-8 [61]), respectivamente.

La litografía óptica se puede llevar a cabo siguiendo tres modos diferentes: proximidad, contacto y proyección [62]. La primera se suele usar únicamente en el ámbito de la investigación ya que el contacto físico puede contaminar y dañar la máscara, además, el tamaño del dibujo que se consigue en relación al de la máscara sólo puede ser 1:1. La fotolitografía de contacto soluciona algunos de estos inconvenientes, pero sigue manteniendo la misma relación de tamaños entre la máscara y el dibujo obtenido. Mientras que las técnicas de contacto o proximidad cubren toda la muestra, en los sistemas de fotolitografía por proyección, la máscara se proyecta sobre la oblea numerosas veces hasta completar el dibujo por completo.

En este caso, gracias a un sistema de lentes interpuestas, se desmagnifica el dibujo de la fotomáscara y se proyecta la imagen sobre toda la película fotosensible.

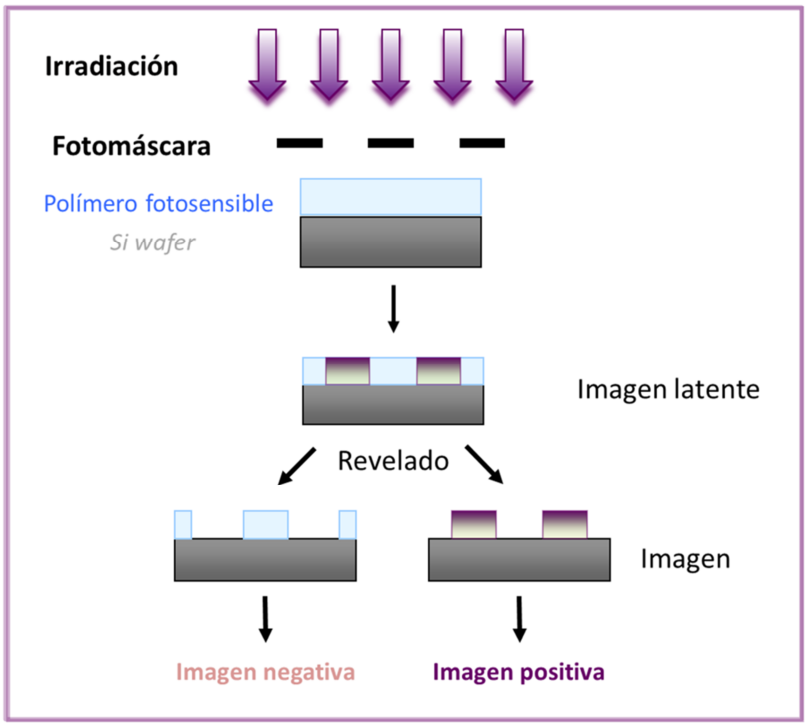

***Figura 3**: Esquema que muestra las diferentes etapas de un proceso fotolitográfico*

La posibilidad de proyectar una imagen con una resolución de tamaño más pequeño sobre esta película fotosensible depende de la longitud de onda de la luz incidente. El tamaño mínimo que un sistema de proyección puede desarrollar viene determinado por la siguiente ecuación:

$$CD = k_1 \cdot \frac{\lambda}{NA}$$

donde,

CD: Es el tamaño mínimo que se puede proyectar una imagen clara

λ: Es la longitud de onda de la luz utilizada

k_1: Es un coeficiente referido al proceso (y que suele ser 0.4) para procesos de producción industrial.

NA: es la apertura numérica de la lente desde la muestra

I.1.2. Replicación de un patrón a partir de un molde (master): Impresión en caliente (*Hot Embossing*).

Las técnicas de replicación de un patrón con un *máster* también se denominan técnicas de litografía suave (*soft lithography)*, se denominan así porque normalmente el *master* a replicar está compuesto de algún material flexible, tipo polidimetilsiloxano (PDMS) [63]. Aunque también se puede utilizar un *master* más rígido (como por ejemplo una resina fotosensible o una placa de silicio) [64]. Aquí, el *master* se imprime en un material deformable bajo fuerza mecánica. Esta técnica, que se representa en la Figura 4, también se conoce como impresión en caliente (*hot embossing)* [21, 22].

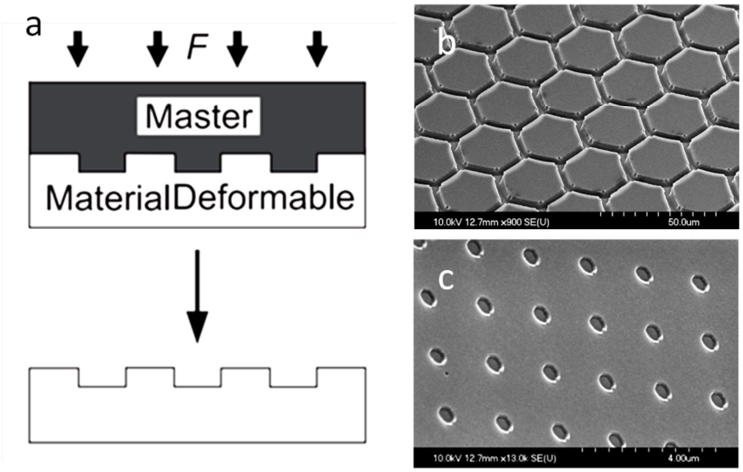

Figura 4*: a) Esquema de la técnica de litografía suave:* hot embossing [14]. *b) Micrografía por SEM de una superficie de PMMA , realizada por impresión en caliente con un molde hexagonal de PDMS [65]. c) Micrografía por SEM de una superficie de un copolímero de polimetacrilato de metilo copolimerizado con un polímero metacrílico con grupos fluorados de composición PMMA-co-TFMA 60:40, realizada por impresión en caliente con un molde de pilares de 500 nm en silicio.*

La impresión en caliente es una técnica con la que se pueden replicar micro/nanoestructuras de distintos dibujos o patrones en un polímero termoplástico usando un molde y aplicando unas determinadas condiciones de presión y temperatura [66]. Tanto en investigación como en la industria es uno de los procesos más instaurados y utilizados para la replicación de micro y nanoestructuras junto con el moldeo por inyección y la técnica de nanoimpresión asociada a UV.

Además, la impresión en caliente se usa, principalmente, a escala de laboratorio para producciones con bajo volumen de muestras. Sus ventajas, con respecto a otras técnicas, es que se pueden aplicar a un gran número de polímeros termoplásticos, el área de las muestras realizadas puede variar desde los pocas micras hasta áreas del orden de centímetros y, además, se pueden fabricar microestructuras con alta relación de aspecto sin que se generen tensiones en la parte interior de estas zonas [67].

A lo largo del tiempo se han desarrollado sucesivamente tres modos de *hot embossing*, incluyendo: plato-plato, rodillo-plato y rodillo-rodillo [21]. Este desarrollo ha permitido producir áreas nano/microestructuradas más allá de los límites comentados anteriormente. (Figura 5).

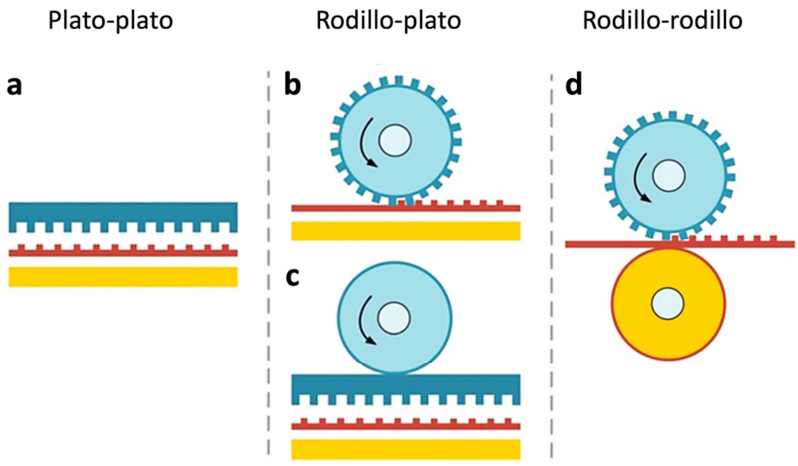

***Figura 5**: Esquema de los diferentes modos de fabricación por impresión en caliente [21]. a) Plato-plato, b) y c) Rodill- plato y d) Rodillo-rodillo.*

El modo plato-plato es el más convencional, ampliamente utilizado por la industria de fabricación de los CDs y DVDs, sin embargo es un método discontinuo y requiere un tiempo elevado para cada llevar a cabo todas las etapas del proceso, produce una alta deformación de las muestras y un área de replicación relativamente pequeña. Con el modo rodillo-plato se amplía el área de replicación de unos centímetros a varios metros cuadrados, mientras que con el método rodillo-rodillo se puede hacer llegar a obtener una producción en continuo.

- *Fases de la impresión en caliente*

Como se ha visto anteriormente, la impresión en caliente permite la replicación de todo tipo de polímeros termoplásticos conocidos, en áreas relativamente grandes. Se basa en el calentamiento del material termoplástico (a la vez que se aplica una determinada presión) hasta que éste se ablande y sea posible modelarlo. Este proceso se desarrolla a lo largo de cuatro etapas o fases: calentamiento del molde y muestra, estampación de la microestructura, enfriamiento y desmoldado [67].

El material original consta de una lámina polimérica con espesores que pueden variar desde las pocas micras hasta centímetros. Después de colocar la lámina entre los platos de la máquina de impresión en caliente, se conecta a una cámara de vacío que se cierra y se vacía para evitar inclusiones en las cavidades entre la estructura del molde rígido/semielástico y de la lámina polimérica.

En la Figura 6 se muestra un esquema de un proceso típico de impresión en caliente [68]. La primera etapa, que es además la que más tiempo consume, es la del calentamiento de los platos de los sustratos y de la lámina polimérica, cuya temperatura tiene que ascender por encima de la temperatura de transición vítrea (en el caso de polímeros amorfos) o por encima de la temperatura de fusión en caso de polímeros semicristalinos. En este punto el polímero se vuelve maleable para el siguiente paso de formación.

En este segundo paso se ha de controlar la velocidad y la presión que se aplica al polímero para que tome la forma del molde. Para asegurar una distribución homogénea de la temperatura y la presión, éstas se mantienen constantes durante un determinado tiempo que dependerá de las geometrías, el tamaño de las estructuras y el rango de flujos. La máquina para

la impresión en caliente, consiste en un conjunto de guías verticales y paralelas, con las que se pueden replicar partes poliméricas planas y paralelas también.

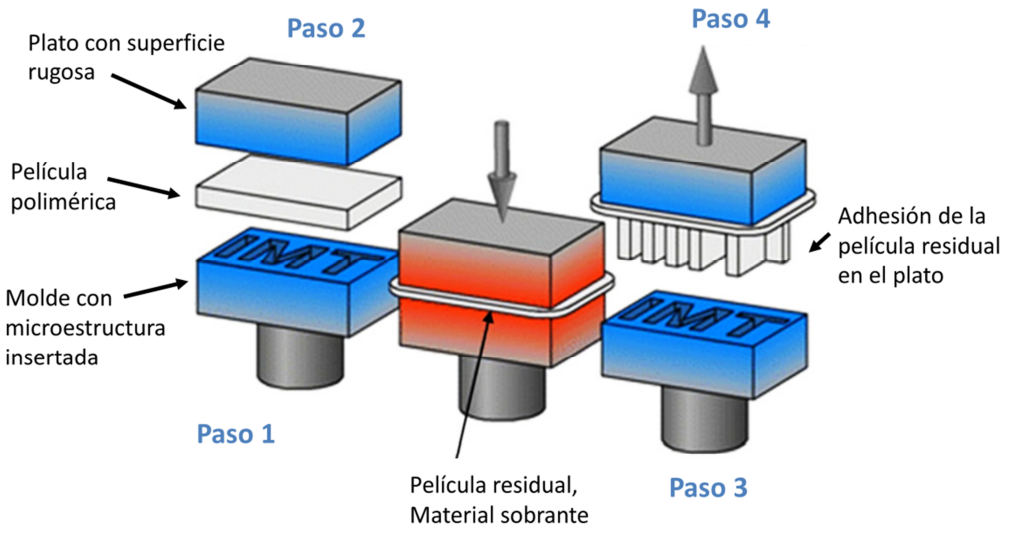

Figura 6: *Fases en el proceso general de impresión en caliente [21]. Paso 1) Calentamiento, Paso 2) Moldeado, Paso 3) Enfriamiento, Paso 4) Desmoldado.*

El tercer paso, tras el llenado de las cavidades y estructuras, es el enfriamiento de la muestra. Se debe mantener la presión aplicada en el paso anterior para prevenir la contracción de la muestra. En el cuarto y último paso se desmolda la pieza.

I.1.3. Inestabilidades superficiales: Generación de arrugas en superficies

La generación de inestabilidades superficiales es otra forma de estructuración de superficies que ha adquirido gran importancia recientemente. Las inestabilidades superficiales se producen espontáneamente, tanto a pequeña escala en sistemas confinados que o son inestables o que pueden ser inducidos en películas estables aplicando un estímulo externo. Una forma de crear inestabilidades superficiales en superficies poliméricas es la formación de arrugas, crestas e incluso de plegamientos [52] (Figura 7). En este caso, tras ejercer una fuerza (presión, estiramiento, hinchamiento), se provoca una inestabilidad en la superficie. La

relajación de estas inestabilidades hacia el equilibrio produce alteraciones en la topografía superficial para minimizar la energía superficial [52].

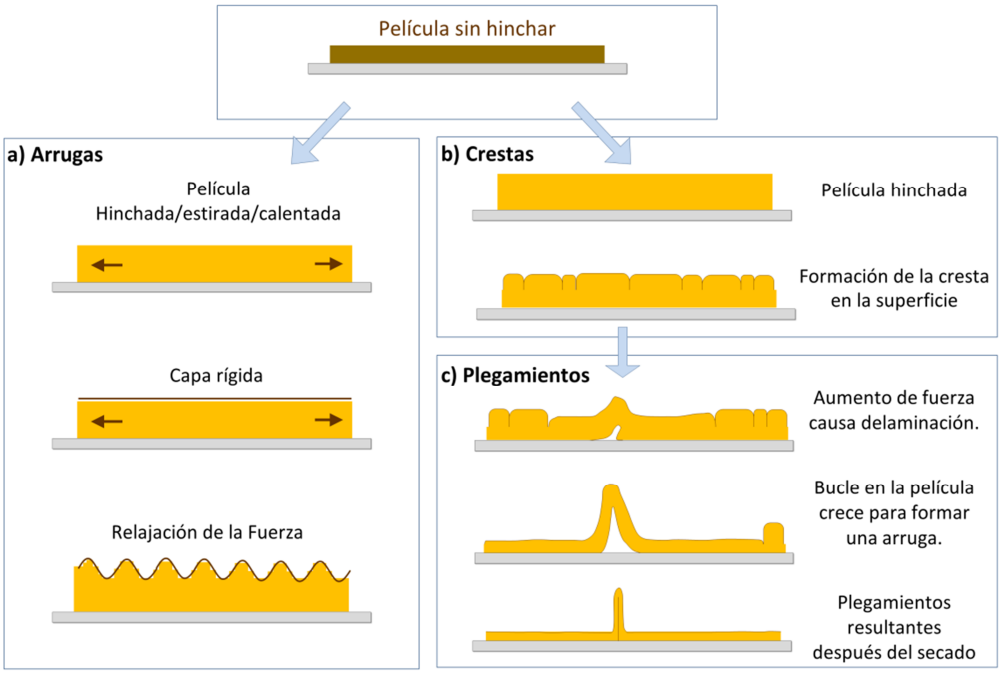

***Figura 7**: Formación de inestabilidades superficiales en superficies polimérica. [52] a) Arrugas, b) Crestas, c) Plegamientos.*

A día de hoy, se admite de manera general, que la formación de bucles o arrugas en las superficies poliméricas (que consiste en el curvamiento hacia fuera del plano) está causado por la aplicación de una fuerza externa (calor, estiramiento o compresión, hinchamiento) que es capaz de ejercer una fuerza que sobrepasa un valor crítico.

La formación de arrugas en superficies poliméricas puede llevarse a cabo siguiendo distintas estrategias que se pueden dividir en tres grandes categorías, según la estructura física/química de la película precursora [52]: Sistemas estructurados en capas, películas homogéneas y películas formadas por una variación gradual de una de las propiedades de la matriz (Figura 8). En el caso de esta Tesis Doctoral nos centraremos en un caso en particular de película homogénea que se forma en un espacio confinado (Figura 8 b1).

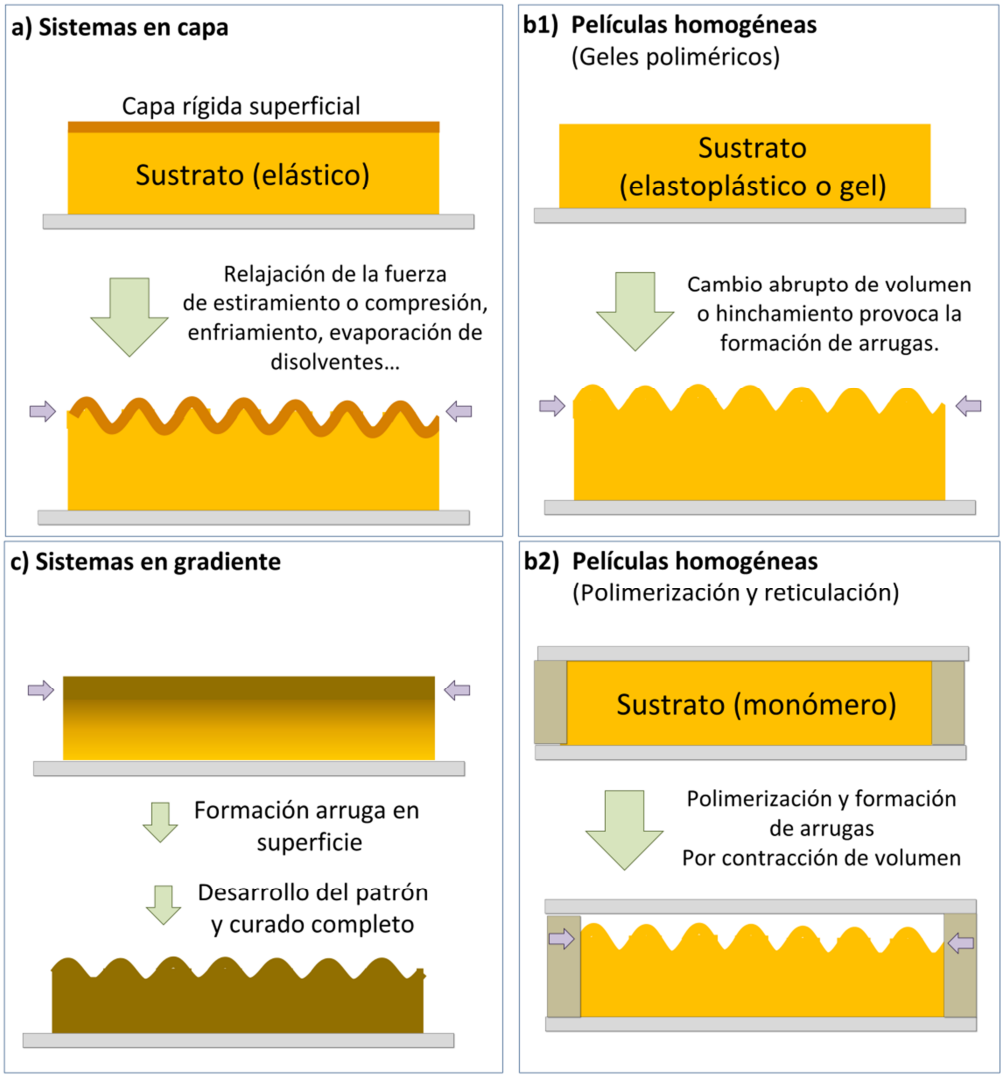

***Figura 8**: Estructuras de las películas que son capaces de formar arrugas superficiales [52]: a) Estructura multicapa constituida por un sustrato elastomérico recubierto por una capa rígida, b) Filmes homogéneos (típicamente hidrogeles entrecruzados), b1) y c) Película en gradiente, donde las propiedades mecánicas varían en función de la profundidad.*

I.1.3.1. Sistemas multicapa

- *Según el tratamiento llevado a cabo para formar la capa rígida*

El primer método descrito en la literatura sobre la formación de arrugas consistió en la evaporación de aluminio sobre el material flexible. La cobertura de metal se realiza sobre las películas poliméricas de PDMS una vez expandidas térmicamente que, al volverse a enfriar a temperatura ambiente, se contraen formando arrugas en la capa superior metálica. Después se comenzó a usar oro [69] o titanio [70].

Otro método empleado para la obtención de esta capa superior rígida es mediante la oxidación de la propia película de PDMS (con corriente de UV-ozono o con plasma) [69, 71-73]. Para llevar a cabo este procedimiento se realiza el estiramiento mecánico sobre las películas de PDMS en vez de hacerlo térmicamente. Aunque este método tiene la ventaja de utilizar un único material y no necesita la utilización de metales, la capa superior tiene la limitación de ser muy frágil, con una resistencia mecánica mucho menor que el resto del material, por lo que estas muestras sufren frecuentemente craqueos. En otros polímeros, como el poliestireno, se pueden utilizar gases fluorados para la creación de esta película rígida [74].

La utilización como capa rígida de coberturas de carácter polimérico es posterior. Se han descrito sistemas como poliestireno sobre PDMS expandido o multicapas de polielectrolitos con el módulo de *Young* muy superior al PDMS [75]. Dependiendo de cada método, se pueden crear microestructuras de arrugas superficiales que van desde los 150 nm [76] hasta los cientos de micras [77].

- *Según el estímulo empleado para inducir el plegamiento de la superficie*

Como se acaba de explicar anteriormente, las arrugas en sistemas multicapa se forman cuando se relaja la fuerza que se estaba ejerciendo sobre el sustrato. Aunque se ha mencionado brevemente en el apartado anterior, a continuación se enumeran las naturalezas de estas fuerzas para la formación de arrugas, que pueden ser: Arrugas formadas en respuesta a variaciones

térmicas [71, 74, 78, 79], a variaciones de esfuerzo mecánico [80-84] y arrugas autoinducidas [70, 85-87].

I.1.3.2. Sistemas con películas homogéneas

En este grupo se pueden incluir las películas elastoplásticas y los hidrogeles homogéneamente entrecruzados en los que la estructuración superficial se forma gracias a una transición de fase en volumen [88]. Además se pueden formar arrugas superficiales tras su hinchamiento (por un monómero o un disolvente) [85, 87, 89-91] o por el secado de un hidrogel desde su estado hinchado [92-94].

Un ejemplo de este tipo de sistemas ha sido desarrollado por *A. Crosby* y colaboradores [91]. Este grupo empleó una mezcla de monómeros y entrecruzantes que son irradiados mientras se aplica una corriente controlada de oxígeno. Los radicales de la capa superficial se quenchean por la presencia de oxígeno, de forma que la capa más superficial queda sin polimerizar y es capaz de hinchar la siguientes capas generando las arrugas.

Como se ha mencionado anteriormente, en los sistemas desarrollados en esta Tesis, ocurre una reducción abrupta de volumen durante la polimerización y esto es lo que provoca la formación de las arrugas (Figura 8 b1).

I.1.3.3. *Sistemas con variación de la composición en gradiente según la profundidad*

El mecanismo general aceptado de la formación de arrugas en este tipo de sistemas ha sido propuesto por *S. K. Basu* y colaboradores [95] y se muestra en la Figura 9. Aquí, una película gruesa se cura tanto por efecto de la temperatura como por la luz.

La primera capa líquida se polimeriza rápidamente y se crea un gradiente de entrecruzamiento a lo largo del espesor de la lámina y, por lo tanto, un gradiente de sus propiedades mecánicas. Este curado ocurre más rápidamente en la capa libre superficial. Esta capa se arrugará como consecuencia del estrés mecánico inducido por el entrecruzamiento y contracción de volumen posterior del resto del material [52]

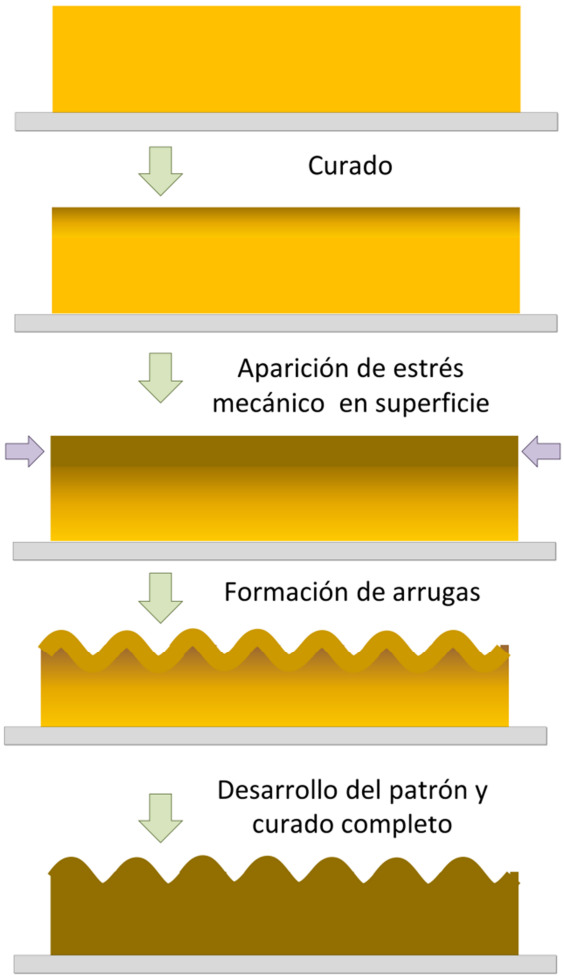

***Figura 9**: Mecanismo de formación de arrugas por polimerización en gradiente [52].*

.Como alternativa a estos sustratos también se han descrito, recientemente, sistemas fotoentrecruzables en dos pasos empleando distinta longitud de onda de fotopolimerización. En estos casos la fotopolimerización se realiza en dos etapas, primero se polimeriza y entrecruza la capa más superficial que queda flotando sobre el resto del material y después, cambiando la longitud de onda, se entrecruza el resto de la muestra y es la contracción de volumen lo que provoca la formación de arrugas en la capa más superficial [96].

I.2 Modificación de la funcionalidad superficial

Los métodos más habituales para la preparación de superficies funcionalizadas suponen la modificación física o química de las superficies. Así, se encuadrarán dentro de los tratamientos físicos aquellos que hacen uso de gases activos, vapores o radiaciones; mientras que, dentro de los tratamientos químicos se englobarían las reacciones químicas de las superficies, el *grafting* (injerto) o el recubrimiento por metales. En la Tabla 2 se hace un breve resumen de las principales técnicas físicas y químicas que se emplean actualmente para modificar la funcionalidad de las superficies.

***Tabla 2**: Principales técnicas de funcionalización de una superficie*

PROCEDIMIENTO	VARIANTE Y REFERENCIAS	TIPO DE GRUPO INTRODUCIDO	LIMITACIONES /VENTAJAS
Plasma	Polimerización por plasma [97, 98]	Polimerización y entrecruzamiento	En un sólo paso aunque no hay buen control de la composición química de la superficie después de la modificación. Costoso.
	Entrecruzamiento por plasma [99]	Entrecruzamiento	Bajo control de la composición
	Activación y funcionalización [100]	Grupos polares	
Recubrimientos metálicos	[101, 102]	Metales	Uso de metales pesados con las desventajas medioambientales que esto conlleva
Reacciones químicas	[103, 104]	-OH, -COOH, $-NH_2$ ...	Requiere el uso de disolventes orgánicos
Grafting (injerto)	*Grafting from* [105, 106]	Polímeros de todas las funcionalidades	Muy utilizadas en la química "click" Copolímeros de injerto con propiedades únicas con respecto a su estructura.
	Grafting to [107, 108]		
	Through [109, 110]		
Incorporación de monómeros/polímeros funcionales	[111, 112]	Diversidad de grupos	Se puede incorporar cualquier carga aunque no está anclada a la matriz
Segregación superficial	[113-115]	Funcionalidades hidrofóbicas e hidrofílicas	Control de la funcionalidad superficial Enriquecimiento del polímero funcional en la superficie

Dentro de esta Tesis Doctoral se han utilizado metodologías distintas para obtener superficies con composición química variable. Éstas son la incorporación de monómeros/polímeros funcionales en las mezclas, la segregación superficial y la modificación por reacción química.

I.2.1. Incorporación de monómeros/polímeros funcionales en las mezclas

La mezcla de dos o más polímeros/monómeros juntos persigue, en la mayoría de los casos, obtener una combinación única de propiedades de la que estos polímeros/monómeros tendrían por separado. Estas mezclas se usan como nuevos materiales en la actualidad ya que gracias a esto se puede acceder a un intervalo más amplio de propiedades si se comparan con los polímeros individuales [116]. Como resultado, la utilización de mezclas se hace conveniente, e incluso necesaria en algunos campos, tales como: la adhesión, la estabilidad de los coloides, materiales compuestos o materiales biocompatibles.

Aunque el desarrollo de estos materiales compuestos pueda parecer trivial, en la fabricación de éstos aparecen ciertas dificultades como la dependencia de la disponibilidad de polímeros funcionales y que las muestras deben de ser homogéneas, entre otras.

En esta Tesis se han utilizado monómeros que contienen grupos hidrófilos o hidrófobos que han permitido cambiar la composición química del material y, por tanto, la de su superficie.

I.2.2. Segregación superficial

Una alternativa a la preparación de mezclas poliméricas funcionales es la segregación superficial. Es un método que resulta interesante para la modificación de la composición química de la superficie de un material y que se basa en la capacidad de uno de los componentes de una mezcla (de naturaleza polimérica, en este caso) de migrar hacia la superficie de una matriz donde se encuentra disperso [113-115], de esta manera, la superficie queda enriquecida en esta sustancia, mientras que el resto del material queda inalterado en su composición. La segregación superficial se rige por dos fenómenos termodinámicos: la entropía y la entalpía [117, 118]. Esta última está relacionada con la energía superficial de los grupos funcionales de la molécula polimérica que va a migrar. En la interfase polímero-aire los

compuestos con flúor o las siliconas, por ejemplo, tienen una marcada tendencia a migrar hacia la superficie ya que estos grupos tienen una baja energía superficial, mientras que, otros grupos como el grupo alcohol, el grupo amina o el grupo ácido carboxílico tienen a esconderse en el interior de la matriz. Por su parte, las fuerzas entrópicas, se rigen por la topología de los polímeros y por su peso molecular (polímeros con pesos moleculares bajos tienden a migrar hacia la superficie más fácilmente). Hay que reseñar que, para que esta migración se produzca, es necesario que la muestra alcance la temperatura de transición vítrea de la matriz, que es la temperatura a la que comienza a existir movimiento macromolecular. Una vez producida la segregación y disminuir la temperatura a temperatura ambiente de nuevo, el movimiento vuelve a quedar congelado.

Por otra parte, es posible invertir este comportamiento anteriormente explicado variando las condiciones ambientales durante la segregación de las muestras, es decir, que si lo que se desea es la migración de un grupo hidrofílico hacia la superficie, se puede conseguir enfrentando el material a un ambiente húmedo (Figura 10).

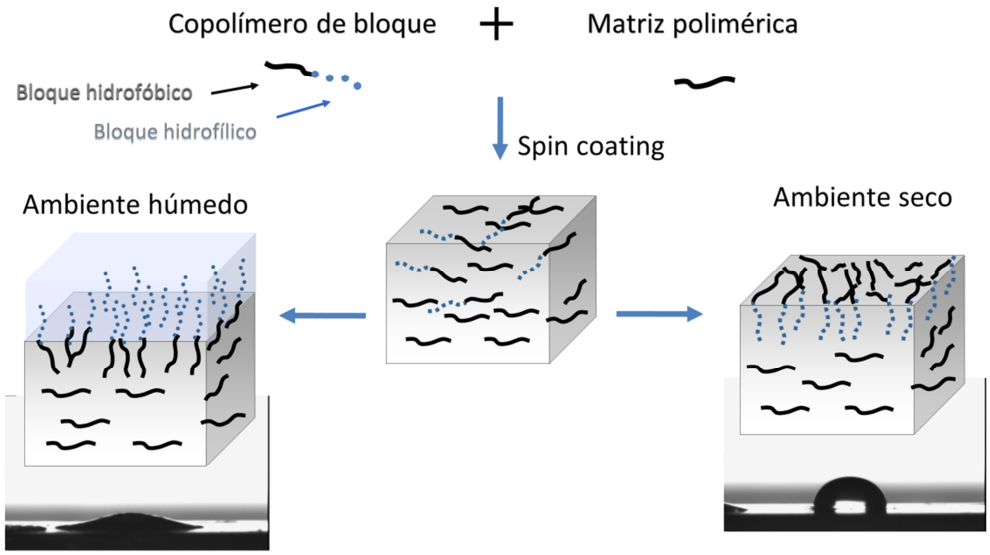

***Figura 10**: Esquema que muestra el proceso de segregación superficial de un copolímero de bloque que se encuentra disperso en un matriz polimérica al ser tratado en distintos ambientes: aire seco y aire húmedo [117].*

I.2.3. Modificación por reacción química

Las reacciones químicas son otro método de funcionalización de superficies, algunas de las más comunes son la aminolisis o la hidrólisis. Para esto, se ponen en contacto la superficie con grupos reactivos y el compuesto químico con el que van a reaccionar en una solución [103, 104]. Así se incorporan grupos hidroxílicos, carboxílicos o amino.

En el caso de esta Tesis Doctoral y tal y como se verá en el artículo 3, se han utilizado polímeros de Poliestireno con poliácido glutámico (PS-PGA). A los grupos ácidos se les introducen secuencias peptídicas con capacidad de reconocimiento de proteínas.

I.3 Control simultáneo tanto de la topografía superficial como de la funcionalidad. Estado del arte

Las técnicas de funcionalización y estructuración de superficies anteriormente descritas se han venido desarrollando en paralelo y de manera exponencial en las últimas tres décadas hasta desembocar en las avanzadas técnicas más actuales y, a pesar de los avances que se han llevado a cabo, tanto en el desarrollo de la funcionalidad controlada como de la topografía superficial, existen aún hoy pocos ejemplos en la literatura donde ambos procedimientos se tengan en cuenta simultáneamente. Según los datos recogidos en enero de 2015 del buscador científico *Scopus*, aparecen 15336 artículos para los criterios de búsqueda *patterned surface* y 141817 para *functional surface*, mientras que para la búsqueda de *patterned functional surface* la cifra desciende drásticamente hasta los 936 artículos.

Las **micro/nanoestructuras en superficies funcionales** se han obtenido, por ejemplo por: impresión por microcontacto [24] [119, 120], nanolitografía por *dip pen* [121, 122], dispositivos de microfluidos [123-125], litografía por haz de electrones [126], técnicas fotolitográficas o la combinación de alguna de estas técnicas entre sí.

A continuación se ilustrarán algunos ejemplos seleccionados en los que ambos parámetros (estructura y funcionalidad) han sido simultáneamente considerados.

Las técnicas de fotolitografía tienen una ventaja con respecto a las anteriores y es que se pueden utilizar en grandes superficies y para desarrollar estructuras 3D. Además presentan

una amplia versatilidad; por ejemplo, a partir de una monocapa funcional y por fotolitografía se pueden obtener distintas superficies con funcionalidad variable según se eliminen las diferentes partes de la estructura de este compuesto de la monocapa [127], tal y como se observa en la Figura 11.

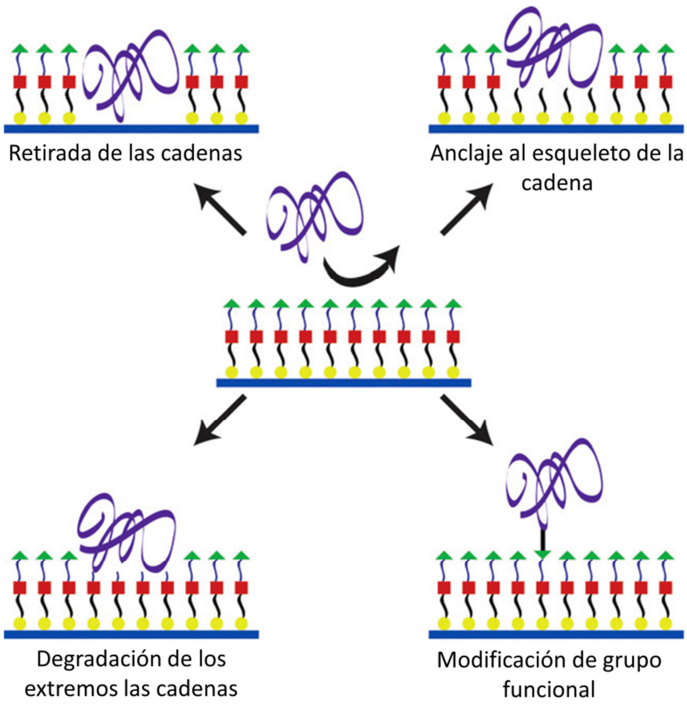

***Figura 11**: Modificación selectiva de una película multicapa [127]*

No sólo es posible la degradación o eliminación total o parcial de algunas moléculas integrantes de la monocapa, sino que se puede funcionalizar la superficie para luego anclar un grupo externo. Como ejemplo de estos procedimientos citaremos a *L. Li* y colaboradores que han desarrollado un método por el que funcionalizan polímeros fotodegradables para la preparación de superficies microestructuradas reactivas [128]. Para ello han sintetizado tres nuevos monómeros fotodegradables, con *o*-nitrobenzaldehído, con grupos alilo, propargilo y grupos epoxi y, gracias a este último se entrecruzan entre sí. Irradiando a través de una rejilla de TEM, se puede destruir selectivamente la película y las zonas remanentes pueden ser fácilmente modificadas por reacciones de química *click*, gracias a los grupos funcionales aún presentes en la superficie (Figura 12). Las películas resultantes presentan funcionalidad y se

tiene la libertad de estructurar la superficie. Aunque para un desarrollo industrial esta metodología no sería del todo viable ya que la totalidad de la película se basa en monómeros de síntesis, con el aumento de precio que eso conlleva.

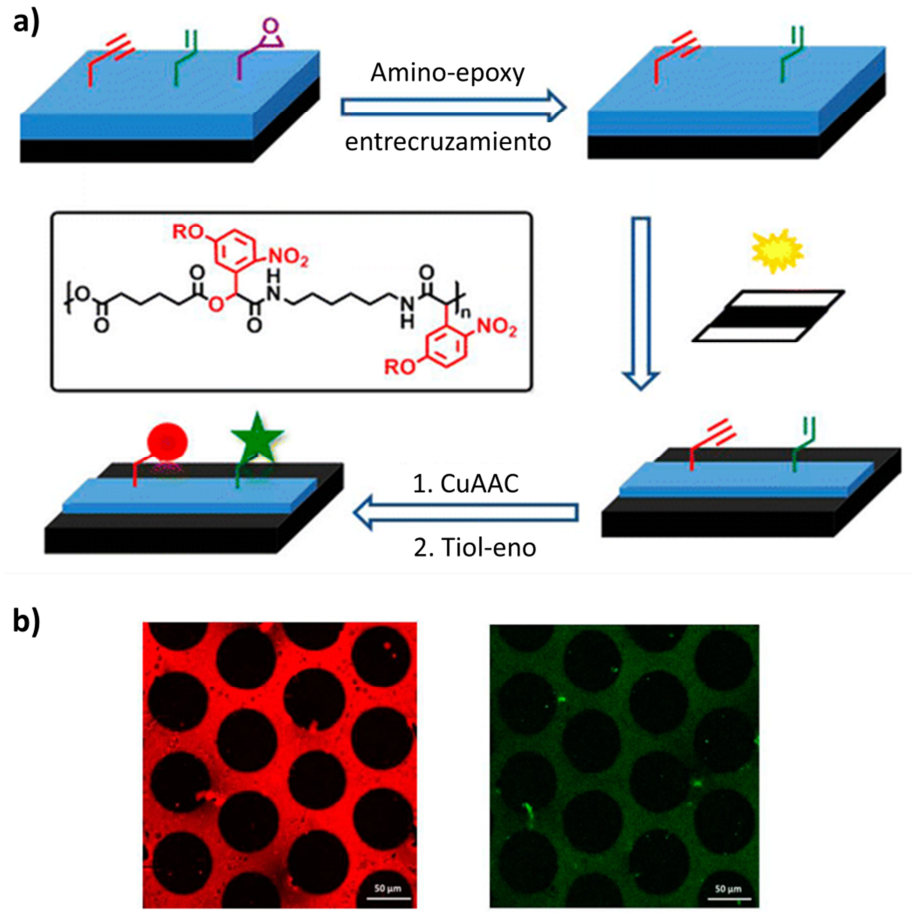

***Figura 12**: a) Representación esquemática del proceso de generación de patrones multifuncionales. b) Microfotografías obtenidas por microscopía confocal de fluorescencia de las películas estructuradas [128].*

De ahí la búsqueda de otros materiales más comerciales pero que mantengan las propiedades que ya se han conseguido alcanzar. Así, polímeros comerciales como el metacrilato de metilo (PMMA) o el poliestireno (PS), se presentan como excelentes candidatos para el desarrollo de este tipo de superficies. Por ejemplo, *S. Mattioli* y colaboradores han

irradiado con plasma de oxígeno películas de PS a través de una rejilla metálica de TEM obteniendo películas con canales micrométricos (zonas degradadas plasma) y topografía nanométrica (rugosidad) desarrollada dentro de estas zonas irradiadas por el plasma. Después, se recubre por deposición de vapor químico una capa de carbón amorfo hidrogenado [129]. Estas superficies han mejorado su mojabilidad y son biocompatibles con células óseas (Figura 13).

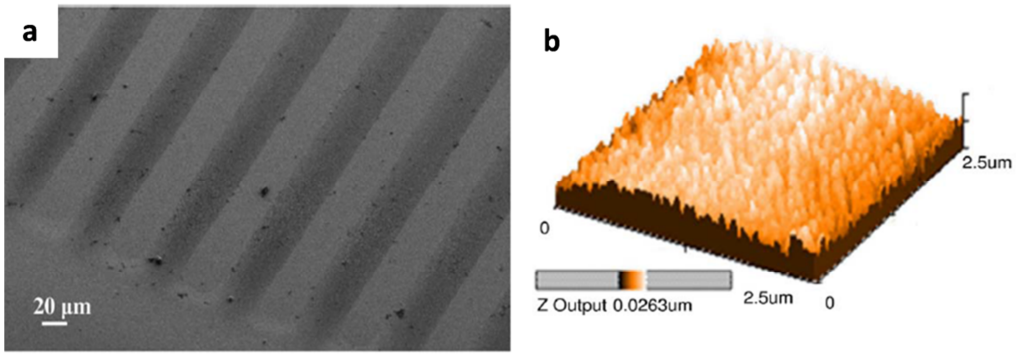

***Figura 13**: a) Superficie de PS nanoestructurado por irradiación con plasma a través de una máscara. b) Imagen de AFM donde se muestra la rugosidad de las zonas irradiadas por plasma [129].*

Las técnicas de impresión por microcontacto, son eficientes, no tienen un coste muy elevado y, una vez que el proceso está estandarizado, se pueden imprimir desde los pocos nanómetros hasta decenas de micras y se pueden utilizar para imprimir un elevado número de moléculas, biomoléculas, células e incluso microorganismos. La dificultad de su aplicación proviene de la complejidad de fabricación del molde para luego realizar la impresión. En el siguiente ejemplo se observa como estas técnicas están íntimamente relacionadas unas con otras y, en este caso, tal y como se observa en la Figura 14, es necesario del uso de la fotolitografía para la consecución del molde de PDMS.

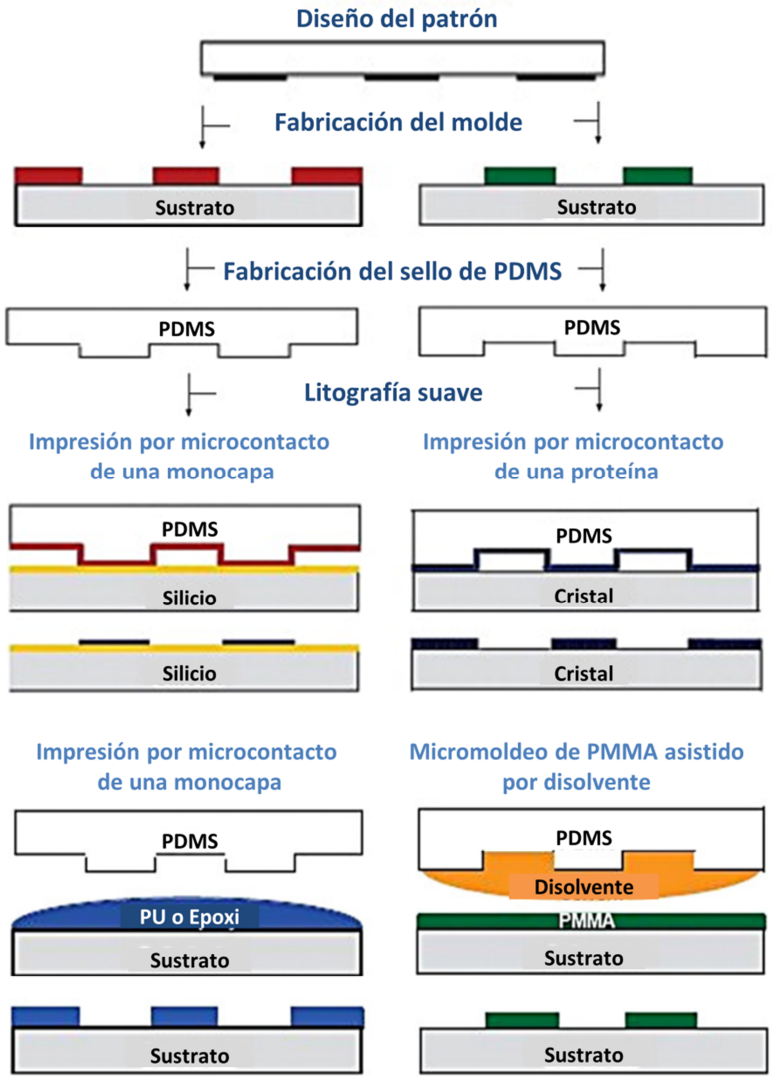

***Figura 14**: (a-c) Fabricación del máster en PDMS para la impresión por microcontacto, d) técnicas de soft lithography [24].*

I.4. Fotopolimerización y síntesis de polímeros por ATRP.

En esta Tesis, la fototopolimerización y la síntesis de aditivos funcionales mediante técnicas de polimerización controlada han sido fundamentales. A continuación se hará un breve resumen de ambas técnicas.

Tanto los distintos procesos de fotolitografía descritas, como la creación de arrugas superficiales son procedimientos basados en **reacciones de fotopolimerización** [130]. Este tipo de polimerización tiene muchas ventajas con respecto a la polimerización térmica entre las que se incluyen: que se pueden utilizar sistemas libres de disolvente, se puede llevar a cabo un estricto control del tiempo y también control espacial de la iniciación de las reacciones (indispensable en la fotolitografía, tal y como se ha explicado anteriormente) y, además, son reacciones rápidas.

La fotopolimerización por radicales libres emplea la energía de la luz para iniciar reacciones de formación de polímeros a partir de monómeros. La luz es absorbida por una especie química llamada fotoiniciador, cuya molécula se escinde y genera radicales libres que son, en último término, los responsables de iniciar las reacciones de polimerización que van permitir el curado o entrecruzamiento de la mezcla fotosensible.

El mecanismo general de fotopolimerización en estos sistemas incluye los tres pasos básicos de iniciación, propagación y terminación de las cadenas en crecimiento que se observa en el esquema 1.

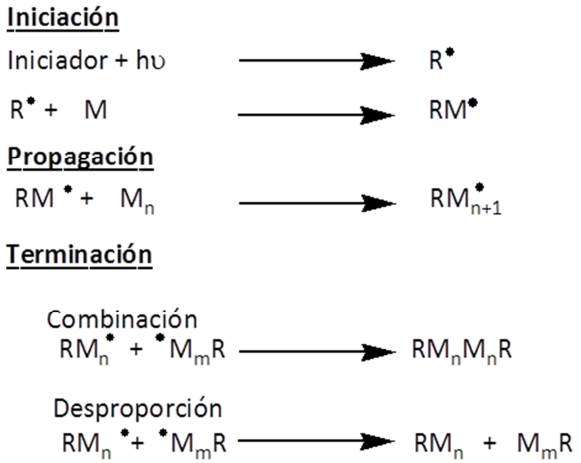

***Esquema 1**: Ilustración esquemática de un proceso de fotopolimerización radical.*

R• *Representa el radical iniciador formado a partir del fotoiniciador y desde el cual comienza a formarse la cadena polimérica.*

M, *Representa al monómero.*

En el caso de esta Tesis Doctoral se ha utilizado mayoritariamente el fotoiniciador Irgacure 651 (Irgacure 651, 2,2-dimetoxi-1,2-difeniltan-1-ona) que absorbe en la luz en la región ultravioleta.

Por otra parte, para la funcionalización de las superficies, tanto en la segregación superficial como en la adición de polímeros/monómeros funcionales a la mezcla, se han utilizado polímeros sintetizados por un método de polimerización controlada (**ATRP: Atom Transfer Radical Polymerization o Polimerización por Transferencia de Átomo).**

Este tipo de polimerización controlada surgió en 1995 y fue desarrollada por el Prof. *K. Matyjaszewski* [131] y, desde entonces y hasta la actualidad, ha tenido una gran repercusión en la síntesis de macromoléculas con composiciones, arquitecturas y funcionalidades bien definidas [132].

La generación de radicales por ATRP implica la formación de un haluro metálico que se somete a un proceso redox reversible, catalizado por un metal de transición (siendo el cobre, Cu, uno de los más utilizados y el que se ha empleado en esta Tesis), que está representado en el esquema 2.

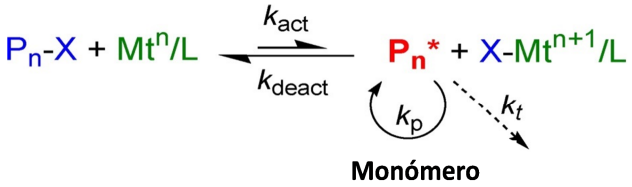

***Esquema 2**: Ilustración esquemática de un proceso de ATRP.*

La ATRP, como otras técnicas de polimerización controlada, está basada en la creación de radicales libres al principio de la reacción y de mantener su número constante mientras las cadenas van creciendo. Este efecto se consigue gracias al equilibrio dinámico entre las especies activadas y las especies dormidas. Por eso, la mayoría de las reacciones de terminación quedan suprimidas, consiguiendo así características tan remarcables como que se puede estimar el peso molecular de las cadenas, por ejemplo se pueden conseguir polímeros de pesos moleculares bajos, y que la polidispersidad de las cadenas en crecimiento sea también

baja (distribución estrecha de pesos moleculares) y, de esta manera, tanto las propiedades como las características e incluso las arquitecturas [133] de los polímeros sintetizados pueden ser controladas y hechas a medida.

El conocer de antemano las características de un polímero es esencial en el caso de la segregación superficial, ya que la migración de los polímeros que se introducen como aditivos en una mezcla con otros que actúan de matriz depende mucho del peso molecular o de la funcionalidad del polímero, entre otros aspectos. Por lo que si se desea es simplemente introducir un porcentaje de estos copolímeros en el material polimérico, es interesante también que su composición sea perfectamente definida.

En esta Tesis se han sintetizado diferentes polímeros con arquitecturas alternadas como de bloque, con distinta funcionalidad, tanto hidrofóbica como hidrofílica, que se han utilizado como matriz, individualmente o mezclados en diferentes proporciones con polímeros comerciales, consiguiendo, así, variar las propiedades en superficie.

I.5. Algunas aplicaciones de superficies estructuradas y funcionales.

El cambio estructural o químico de las superficies incide, directamente, en las propiedades que van a permitir el desarrollo de una aplicación. Adhesividad, mojabilidad, biocompatibilidad, la catálisis de las reacciones químicas o biológicas o la absorción dependen, casi en exclusiva, de su superficie. En el caso de esta Tesis Doctoral se ha perseguido la obtención de microestructuras poliméricas funcionales donde se puedan conseguir variaciones, entre otras, de las propiedades descritas anteriormente de manera controlada y nos permitan, así, potenciar el desarrollo de las siguientes aplicaciones.

I.5.1. Mojabilidad

La mojabilidad es la capacidad que tiene un líquido de extenderse y dejar una traza sobre un sólido. Depende, entre otros, de dos factores: la funcionalidad de la superficie y de la textura de ésta. Se determina, generalmente, a partir del ángulo que el líquido forma en la superficie de contacto con el sólido, denominado ángulo de contacto. A menor ángulo de contacto, mayor mojabilidad.

La mojabilidad depende de las fuerzas intermoleculares de los materiales en contacto. Las fuerzas adhesivas entre el líquido y el sólido provocan que el líquido se extienda por la superficie, mientras que las fuerzas cohesivas del líquido hacen que éste se abulte y tienda a evitarla.

El ángulo de contacto (θ) es el ángulo que forma el líquido respecto a la superficie de contacto con el sólido y está determinado por la resultante de las fuerzas adhesivas y cohesivas. Como la tendencia de una gota a expandirse en una superficie plana aumenta con la disminución del ángulo de contacto, este ángulo proporciona una medida de la inversa de la mojabilidad. Un ángulo de contacto pequeño (< 90°) indica que la mojabilidad es muy alta y el fluido se extenderá sobre la superficie; ángulos de contacto grandes (> 90°) significan que la mojabilidad es baja y el fluido disminuirá el contacto con la superficie, formando una gota compacta.

En el caso del agua, cuando una gota de agua se deposita sobre la superficie de un material, puede mantenerse de forma más o menos esférica o bien extenderse, comportamiento hidrofóbico e hidrofílico, respectivamente [134, 135]. Si las medidas se efectúan con gotas de aceite, estos comportamientos pasan a denominarse oleofóbico y oleofílico, respectivamente.

Para una gota medida sobre una superficie plana, la mojabilidad viene determinada por la energía libre superficial del sustrato sólido que, a su vez, viene determinada por la ecuación de *Young*:

$$cos\theta = (\gamma_{sv} - \gamma_{sl})\,\gamma_{lv}$$

Donde θ es el ángulo de contacto en el modelo de *Young* y γ_{sv} , γ_{sl} y γ_{lv} son las diferentes tensiones superficiales (líquido/vapor, sólido/vapor y sólido/líquido) del sistema. Así, en superficies planas, la contribución principal sobre la mojabilidad viene dada por la composición química de la superficie y los tipos de grupos funcionales que contiene.

Para superficies rugosas se usan los modelos de *Wenzel* y *Cassie Baxtel* [136]. El modelo de *Wenzel* predice que tanto la hidrofobicidad como la hidrofilicidad se refuerzan con la rugosidad de la superficie, asumiendo que el líquido penetra en la topografía superficial.

(Figura 15a). De esta manera el ángulo de contacto de la superficie rugosa se modifica por el factor de rugosidad, siguiendo la siguiente ecuación:

$$cos\theta_W = rcos\theta_Y$$

Donde θ_W es el ángulo de contacto aparente de la superficie rugosa, θ_Y es el ángulo de *Young* y *r* es el factor de rugosidad de dicha superficie que se define como el cociente entre la superficie actual sobre el área de la superficie proyectada.

Por otro lado, el modelo de *Cassie-Baxter* se puede utilizar sólo para superficies hidrofóbicas y predice que la hidrofobicidad se acentúa al quedarse atrapadas burbujas de aire en las estructuras de la topografía superficial (Figura 15b). Su expresión final es la siguiente:

$$cos\theta_{CB} = r_f f cos\theta_Y + f - 1$$

Donde *f* es el cociente entre el área de contacto y el área total superficial.

Para muestras hidrofílicas ha sido formulado otro tercer modelo, donde la gota se asienta en una superficie de un estado mixto (Figura 15c).

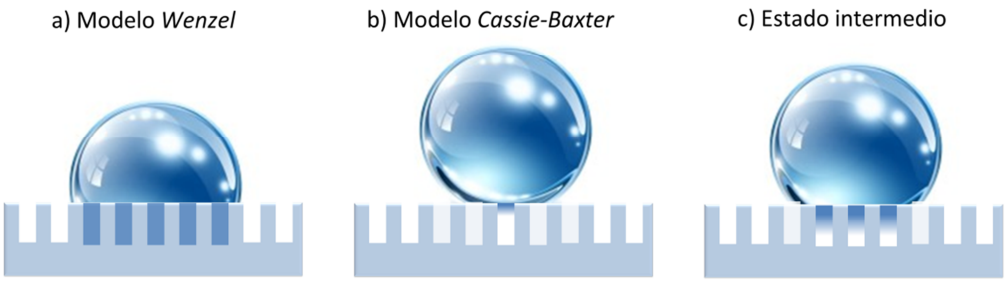

***Figura 15**: Efecto del comportamiento de mojado de una gota sobre un sustrato rugoso. a) Modelo de Wenzel donde la gota de agua moja toda la superficie rugosa. b) Modelo de Cassie-Baxter donde el aire queda atrapado en la rugosidad de la superficie c) Estado intermedio entre el modelo de Wenzel y Cassie-Baxter [102].*

Como resumen, decir que el control de la mojabilidad de superficies está directamente relacionado con el control de la composición química y la rugosidad. Ésta última está directamente relacionada con la estructura de la superficie. Además es importante señalar que la mojabilidad es crucial en el desarrollo de aplicaciones de carácter tecnológico como pueden ser: los recubrimientos para cristales, en el sector textil o pinturas autolimpiables. En la última década también se han desarrollado otras aplicaciones más específicas que se encuadran en campos tan diversos como la conservación y/o control de la energía o superficies con aplicaciones submarinas, la óptica, microelectrónica [137], sistemas de microfluidos y los recubrimientos [138, 139]

Por otra parte, tienen importancia las superficies con superoleofobicidad [140], donde un claro ejemplo de aplicación de éstas, podría ser el recubrimiento interno de los tanques de combustible para evitar así el desperdicio de combustible residual que queda adherido en las paredes del tanque.

I.5.2. Superficies con actividad biológica.

Dentro de las superficies funcionales microestructuradas tienen especial interés las que se fabrican para alguna actividad biológica. Como se ha descrito anteriormente, es interesante la adhesión selectiva de biomoléculas (por ejemplo proteínas) o de las propias células solamente en algunas zonas determinadas de la película. Ya que los fenómenos biológicos son complejos, en ocasiones es necesario estudiarlos en circunstancias confinadas.

La inmovilización precisa de microorganismos, y especialmente de bacterias, sobre superficies se ha conseguido utilizando diferentes técnicas de fabricación tales como la litografía suave *(soft lithography)* [141], impresión por microcontacto [142], *inkjet printing* [143], replicación con un molde [144-147] o diferentes técnicas litográficas como, litografía capilar [148], la litografía por rayo de electrones [149], nanolitografía *dip-pen* [145, 150] la fotolitografía [149, 151, 152] sobre multicapas funcionales [153].

La SPL (*Scanning probe lithography*) y, dentro de ésta, la DPN (*Dip pen lithography*), por ejemplo, tienen la capacidad de estructurar una amplia variedad de biomoléculas con una resolución mucho mayor que otras técnicas más convencionales como la

fotolitografía y la impresión por microcontacto. Tanto las proteínas, como enzimas, virus, y bacterias pueden ser estructurados en una superficie directamente o adsorbidos sobre los patrones creados por esta técnica. Por ejemplo, *D. Nyamjav* y colaboradores son capaces de inmovilizar células bacterianas vía nanolitografía *dip pen*. Se crean superficies de ácido mercaptohexadecanoico (MHA) con distintos patrones de líneas y bloques, que por unión electrostrática se unen a las paredes bacterianas [150].

La dificultad reside en la complejidad que tienen estas técnicas y la gran cantidad de equipos que necesitan para su desarrollo, además del tiempo, por lo que en esta Tesis se plantea la búsqueda de un método de fabricación de este tipo de sustratos para adhesión/inmovilización selectiva de proteínas/bacterias basado en la fotolitografía, más rápido y menos complejo y con una elevada versatilidad. Un ejemplo de este tipo de superficies lo encontramos en el trabajo de *P. Kim* y colaboradores fabrican estructuras con forma de pilar con alta relación altura/radio con precisión submicrométrica y después estudian el posicionamiento de las bacterias sobre estas estructuras, llegando a la conclusión de que las bacterias estudiadas (con forma de raíz) buscan maximizar su superficie de contacto con los pilares y, además, la distribución y estructuración de las bacterias varía dependiendo de la distancia entre pilares y del tamaño y anchura de éstos [151].

En general, los métodos mencionados tienen éxito para la inmovilización bacteriana en regiones de tamaño micrométrico, donde las bacterias pueden tanto aparecer aisladas como formando agregados. Tradicionalmente en el campo de la microbiología, la información de cómo las células responden a su ambiente, interactúan unas con otras o cómo funcionan procesos más complejos como la diferenciación celular o la expresión de los genes han sido obtenidos normalmente a partir de datos a nivel de una población de bacterias [154], aunque actualmente, en ocasiones, y tal y como se explicará en los siguientes apartados, es importante estudiar las bacterias de forma individual.

I.5.2.1. Reconocimiento de proteínas

Las proteínas constituyen un grupo de biomoléculas con una extraordinaria diversidad de funciones, muchas de ellas básicas para la vida. Curiosamente esta variabilidad funcional la

logran con una composición química que, en principio, es muy semejante entre todas ellas: una o varias cadenas de aminoácidos, más o menos largas que, en ocasiones, se unen a otro tipo de sustancias, de ahí la importancia de su reconocimiento específico. El reconocimiento de proteínas se refiere a la interacción entre dos moléculas a través de enlaces no covalentes. El conocimiento de los mecanismos físicos y químicos por los cuales una proteína reconoce un ligando específico es uno de los objetivos que se llevan estudiando desde hace más de tres décadas dentro de la investigación bioquímica [155].

Conocer el mecanismo de reconocimiento de una proteína a otra es importante para numerosos procesos bioquímicos, entre los que se incluyen la catálisis enzimática, la respuesta inmunológica o la señalización. Algunos de estos procesos ocurren en disolución, por lo que se pueden estudiar así *in vitro*, sin embargo, la esencia de estas reacciones es que se producen sobre superficies celulares o subcelulares. Por tanto, favorecer la manera de entender y explorar estos procesos superficiales es imprescindible para entender la verdadera naturaleza en la que se producen estos mecanismos de interacción. Por ejemplo, la inmovilización de proteínas sobre superficies sólidas es crucial para el desarrollo de tecnologías, tales como la miniaturización de dispositivos, para el diagnóstico o el reconocimiento de sustancias o ensayos bioquímicos [156-159].

I.5.2.2. Inmovilización y aislamiento de bacterias

En numerosos campos como la biomedicina, biosensores, ingeniería tisular, *biochips*, diagnosis e implantes, las interacciones célula-sustrato son la clave para el desarrollo de nuevas tecnologías [160, 161]. Entre los factores más determinantes de estas interacciones célula-sustrato están la química de la superficie frente a la topografía; o las micro- frente a las nanoestructuras [162].

En ocasiones es necesario el estudio de células microbianas de manera individual. Con estas técnicas se ha podido describir, de manera más completa, la distribución y las actividades de los microorganismos, así como, su comunicación química o su transferencia génica. Los métodos de aislamiento de bacterias han sido también esenciales para el conocimiento de las conexiones entre la bioquímica celular y el comportamiento de las células a un nivel de población [163]. Con estos métodos se han podido realizar, directamente,

medidas de las células individuales como la elasticidad o la presión osmótica [164]. También los estudios microfisiológicos de los metabolitos, las proteínas o de la actividad redox son otras de las áreas donde las técnicas para estudiar una sóla célula han sido desarrolladas [165-167].

Para el estudio de la adhesión bacteriana, es también necesario aislar una sola bacteria para ser capaces de elucidar este mecanismo de adhesión, ya que la adhesión entre células y las heterogeneidades de la superficie-célula también han de tenerse en cuenta. Existen pocos ejemplos en la bibliografía donde sea posible aislar células bacterianas y, normalmente, requieren el empleo de métodos costosos, lentos, laboriosos y que se desarrollan en varias etapas. Por ejemplo, *G. Zeng* y colaboradores describen un experimento de adhesión donde se emplea una sonda celular fabricada usando un *cantilever* de AFM sin punta y que está recubierto por una sustancia natural adhesiva basada en la dopamina [168]. De nuevo estos métodos se presentan como altamente complejos y se plantea como Objetivo adaptar el método fotolitográfico, explicado anteriormente para la fabricación de sustratos adhesivos solamente en determinadas zonas, al aislamiento de bacterias.

I.5.2.3. Estructuración de biomoléculas (proteínas) y células (bacterias)

Otra propiedad interesante para todos los campos relacionados con la biología es la recién nombrada adhesividad [169]. Es interesante el desarrollo de superficies estructuradas donde se puedan inmovilizar selectivamente biomoléculas como proteínas [170] o células como bacterias [171]. La habilidad para estructurar una superficie con moléculas biológicamente relevantes también es de gran interés ya desde hace años para diferentes campos de estudio, incluyendo biosensores, bioelectrónica, ensayos de crecimiento celular biología celular o la regeneración de tejidos [172]. Es importante el poder regular la posición de las células aprovechando la diferente adhesividad de las zonas donde se ha trasladado esta microestructura con una composición química determinada. Por ejemplo *A. Khademhosseini* y colaboradores estructuran ácido hialurónico sobre un cristal utilizando un sistema de microfluidos en PDMS, a la vez que intercalan bandas con fibronectina. Las células cardíacas solamente se adhieren a la fibronectina [173].

Por otra parte, la inmovilización de microorganismos de una manera controlada, también tiene un amplio rango de aplicaciones desde la biología celular, la construcción de

filmes biológicos o la elaboración de sistemas más sofisticados como biosensores o motores biomoleculares [174-178]. Por ejemplo *A. K. Adak* y colaboradores han desarrollado un método para detectar *S. Aureus* y otras bacterias, para ello fabrican formaciones proteína-ligando, de 10 micras, imprimiéndolas sobre una superficie. Estos ligandos son capaces de generar patrones de captura de bacterias y es posible obtener imágenes en condiciones de campo oscuro [178].

I.5.2.4. Superficies antibacterianas (antiadherentes)

Las superficies antiadherentes son aquellas que evitan la adherencia de elementos como el polvo, o que presentan propiedades biocidas que impiden la adherencia de organismos vivos a su superficie. Las superficies antiadhesivas son muy importantes y de gran aplicabilidad en campos como por ejemplo la Medicina. En la época actual, está ampliamente generalizado el uso de implantes de biomateriales en el cuerpo humano. Una vez implantados, es crucial que la integración de este material en los tejidos que le rodean sea más rápida que la adhesión de bacterias [179], previniendo, de esta manera, una colonización bacteriana en el implante. Las bacterias pueden alcanzar un biomaterial por diversos modos y a diferentes tiempos de post-implantación [180] pero, de forma generalizada, la colonización por bacterias de la superficie de un material sigue las mismas etapas [181]: 1) transporte de las células bacterianas a la superficie y adhesión reversible, 2) adhesión irreversible, 3) Formación de la microcolonia, 4) diferenciación y maduración del biofilme y 5) desprendimiento de las células y propagación de la infección.

Una vez implantado, la superficie del biomaterial se cubre primero con una capa compuesta, principalmente, por proteínas (fibronectina, vitronectina, fibrinógeno, albúmina e inmunoglobulinas) llamada película condicionante y que favorece las interacciones superficie-bacteria. En la primera etapa, las bacterias y las proteínas están unidas por fuerzas débiles tipo *Van der Waals* y cargas electrostáticas que se hacen posteriormente más fuertes, apareciendo interacciones específicas que incluyen proteínas de adhesión bacteriana [182] y sustancias poliméricas extracelulares.

De esta manera, se puede observar que un paso crucial en las patologías de adhesión de bacterias es su adhesión temprana, por lo que un primer enfoque para disminuir el número de estas infecciones sería el desarrollo de nuevos materiales que resistan o prevengan la

adhesión bacteriana y la formación subsecuente del biofilm [183, 184]. Por ejemplo, *A. K. Epstein* y colaboradores han estudiado un nuevo método para prevenir la adhesión bacteriana. Presentan una superficie estructurada con líquido inmovilizado que repele el 99.6% de la bacteria *Pseudomenas Aeruginosa*, en contraste con superficies de politetrafluoroetileno y otras superficies superhidrofóbicas que acumulan el biofilm en sólo unas horas [185].

Otra importante aplicación, son las superficies llamadas *antifouling* (antibacterianas). Muchas superficies submarinas presentan la acumulación indeseable de microorganismos, plantas e incluso de pequeños animales. Hasta hace no demasiado tiempo, la manera más efectiva de combatir este fenómeno pasaba por el empleo de las llamadas "pinturas antisuciedad", que aunque funcionaban correctamente y esto generaba amplios beneficios, presentan el inconveniente de que desprenden pequeñas cantidades de algunas sustancias tóxicas que afectan al medio ambiente (como por ejemplo metales pesados). Problema que podría quedar solucionado si la propiedad antisuciedad se obtiene gracias a la rugosidad superficial. Por ejemplo *C. M. Kirschner* y colaboradores describen en un artículo desde superficies naturales antisuciedad, como la piel de tiburones, hasta otro tipo de superficies antisuciedad sintéticas. En uno de los casos se consigue disminuir en un 86% la cantidad de una espora adherida en la superficie estudiada, simplemente variando la topografía superficial, teniendo en cuenta que el tamaño de estas microestructuras es determinante [186].

I.6 Motivación y justificación

Teniendo en cuenta todos los antecedentes expuestos nos planteamos como propósito la creación de plataformas poliméricas sub/microestructuradas fabricadas a partir de mezclas de monómeros y/o polímeros comerciales y, a la vez, ser capaces de funcionalizarlas mediante la incorporación de polímeros funcionales hechos a medida. Nuestra motivación es resolver algunos problemas o inconvenientes que surgen de la aplicación de las técnicas de estructuración superficial y funcional ya existentes, mediante el desarrollo de nuevas metodologías que nos permitan simultanear este tipo de procesos de forma más sencilla y generar sistemas más versátiles que faciliten, en último término, su implementación a nivel industrial.

Además de las técnicas fotolitográficas, nos propusimos la estructuración de superficies poliméricas de estos nuevos polímeros de síntesis aplicando otras técnicas como el *hot embossing* o la formación de arrugas debido a la aparición de inestabilidades superficiales. Hasta ahora, estas técnicas estaban más limitadas al uso de polímeros comerciales, por lo que el empleo de polímeros, en los que se pueda elegir la naturaleza y el número de unidades funcionales, amplía la versatilidad de este tipo de sistemas.

Hasta ahora, la única opción para funcionalizar estructuras creadas por *hot embossing* hacía necesario emplear más de una etapa en el proceso. *S. Neuhaus* y colaboradores, en 2012 crearon microestructuras con formas de cuadrados y líneas en un polímero comercial y luego las modificaron creando *polymer brushes* cambiando así su funcionalidad y la mojabilidad [187] . Otro problema que se plantea es el desmoldar las piezas fabricadas por esta técnica. Para solucionar esto, algunos autores describen el tratamiento del propio molde con algún compuesto de baja energía superficial [92]. La utilización de polímeros con la funcionalidad deseada, permite solucionar este inconveniente a la vez que se fabrican las piezas.

Por otra parte, la formación de arrugas también estaba limitada, desde el punto de vista de la funcionalidad, tanto las multicapas como en los filmes homogéneos o en gradiente en su composición. La complejidad de estas metodologías y la necesidad de utilizar soportes flexibles han limitado, en gran medida, su desarrollo industrial.

Hasta ahora, sólo hemos encontrado dos antecedentes bibliográficos recientes donde se describe la preparación de arrugas mediante la utilización de reacciones de fotopolimerización en dos sistemas diferentes. El primero de los métodos descritos, consiste en la irradiación UV en dos pasos de una mezcla de acrilatos [188], donde, en primer lugar, se irradia con una lámpara de excímero, luz monocromática de Xenón (< 230nm) con baja penetración en acrilatos (< 500 nm), que polimeriza sólo la capa superior de la disolución fotosensible. Esta capa polimeriza gradualmente a lo largo de su espesor y queda flotando sobre las capas inferiores, en disolución, aún no polimerizadas. De esta manera, consiguen formar las arrugas superficialmente. Para congelar este cambio estructural se realiza una segunda irradiación con una lámpara de mercurio, con mayor poder de penetración, que acaba polimerizando la totalidad de la película.

El segundo método descrito, desarrollado por *J. Crosby* y colaboradores, plantea la creación de arrugas a partir de la irradiación UV de disoluciones acrílicas formadas por mezclas de monómeros acrílicos mono- y polifuncionales, sometidas superficialmente a una corriente de oxígeno controlada [91]. En este caso, el proceso de fotopolimerización se ve impedido en las capas superiores puesto que los radicales iniciadores se inactivan por la presencia de oxígeno y la polimerización en esta capa más superficial no ocurre. Por otro lado, el resto de la mezcla se hincha por la capa no curada superficialmente generando tensiones que provocan la generación de las arrugas. Éste método tiene la desventaja principal de que, aunque se produce en un solo paso, son necesarios periodos de tiempo de hasta 20 minutos tras la irradiación para que se produzca el hinchamiento de las capas inferiores por parte de la disolución no polimerizada. Además, presenta el inconveniente de que el monómero sin polimerizar quedaría confinado dentro de la película final, con los consiguientes problemas de reactividad o de segregación al exterior, haciendo que este tipo de materiales, que no están totalmente polimerizados, presenten serios problemas para su aplicación en cierto tipo de usos, por ejemplo, en aplicaciones de tipo biológico o medioambiental (debido a posibles problemas de toxicidad).

En el desarrollo de esta Tesis Doctoral se han aplicado diferentes métodos para la estructuración superficial (fotolitografía, *hot embossing* y formación de arrugas superficiales) y la funcionalización (segregación superficial y utilización de polímeros/monómeros funcionales) para el desarrollo de nuevas plataformas poliméricas sub/microestructuradas y funcionales. Junto a estos métodos de modificación de superficies (detallados anteriormente en este mismo capítulo) es necesario nombrar la fotopolimerización y la polimerización controlada por ATRP, como técnicas que complementan a estos métodos recién citados y, sin los cuales no se habría podido llevar a cabo la fabricación de nuestras muestras.

Uno de los motivos por el que se ha elegido la fotolitografía como primer método de modificación de superficies es que esta técnica permite producir cambios selectivos en las zonas expuestas del material a la radiación. Es decir, que se pueden elegir previamente las zonas que se van a modificar, manteniéndose inalterada el resto de la superficie.

Por su parte, el *hot embossing* se usa principalmente en el laboratorio y para producciones con bajo volumen de muestras. Sus ventajas, con respecto a las técnicas

anteriores, es que se pueden utilizar un gran número de polímeros termoplásticos, el área de las muestras realizadas puede variar desde pocos nanómetros hasta áreas del orden de centímetros y, además, se pueden fabricar microestructuras con alta relación de aspecto sin que se creen tensiones en la parte interior de estas zonas [67], no se necesita una superficie fotoreactiva y, además, no hace falta que las muestras sean totalmente planas.

Por último, la tercera vía de variación de la topografía elegida ha sido la generación de inestabilidades superficiales mediante la creación de arrugas. Ésta, además de ser una tecnología sin costes elevados, es apropiada para la fabricación de grandes áreas superficiales.

I.7 Objetivos

El Objetivo principal de la presente Tesis Doctoral ha sido la creación de plataformas poliméricas sub/microestructuradas fabricadas a partir de monómeros y/o polímeros comerciales y funcionalizadas con polímeros funcionales sintetizados a medida por ATRP, mediante la adecuación y/o desarrollo de metodologías simultáneas de estructuración y funcionalización de superficies de fácil desarrollo y aplicación, tanto a nivel de laboratorio como a nivel industrial.

Para desarrollar este Objetivo Global ha sido necesario actuar en distintos frentes. Por un lado, sintetizando nuevos polímeros funcionales de distinta naturaleza (hidrofóbica/hidrofílica) por medio de procesos de polimerización controlada (ATRP), lo que ha permitido obtener polímeros con composiciones, arquitecturas y funcionalidades bien definidas. Por otro lado, desarrollando nuevas metodologías que nos permitan aplicar procesos simultáneos de estructuración superficial (fotolitografía, *hot embossing* y la creación de arrugas superficiales) y funcionalización mediante el empleo de mezclas de polímeros funcionales sintéticos (empleados como aditivos y/o en procesos de segregación superficial).

El desarrollo de estas nuevas superficies poliméricas estructuradas y funcionalizadas ha ido encaminado a la potenciación de nuevas propiedades: mojabilidad y/o adhesión y, en último término, a su aplicación como nuevas plataformas con actividad biológica, para el reconocimiento de proteínas o la adhesión y aislamiento de bacterias.

I.8 Bibliografía de sección I

[1] I.L. Onder, A. Okudan, Functionalization of Polystyrene with Cyclic Anhydrides and their Spectroscopic, Adhesive and Corrosive Characterizations, *International polymer processing*, 27, **2012,** 270-276.

[2] S. Yuan, G. Xiong, A. Roguin, C. Choong, Immobilization of Gelatin onto Poly(Glycidyl Methacrylate)-Grafted Polycaprolactone Substrates for Improved Cell–Material Interactions, *Biointerphases*, 7, **2012,** 1-12.

[3] C.P. Stallard, K.A. McDonnell, O.D. Onayemi, J.P. Ogara, D.P. Dowling, Evaluation of Protein Adsorption on Atmospheric Plasma Deposited Coatings Exhibiting Superhydrophilic to Superhydrophobic Properties, *Biointerphases*, 7, **2012,** 1-12.

[4] M. Kobayashi, Y. Terayama, H. Yamaguchi, M. Terada, D. Murakami, K. Ishihara, A. Takahara, Wettability and Antifouling Behavior on the Surfaces of Superhydrophilic Polymer Brushes, *Langmuir*, 28, **2012,** 7212-7222.

[5] B. Cortese, H. Morgan, Controlling the Wettability of Hierarchically Structured Thermoplastics, *Langmuir*, 28, **2012,** 896-904.

[6] W.-H. Kuo, M.-J. Wang, C.-W. Chang, T.-C. Wei, J.-Y. Lai, W.-B. Tsai, C. Lee, Improvement of hemocompatibility on materials by photoimmobilization of poly(ethylene glycol), *Journal of materials chemistry*, 22, **2012,** 9991.

[7] J.M. Lagleize, P. Richetti, C. Drummond, Effect of Surfactant Oligomerization Degree on Lubricant Properties of Mixed Surfactant-Diblock Copolymer Films, *Tribology letters*, 39, **2010,** 31-38.

[8] J.-F. Briand, I. Djeridi, D. Jamet, S. Coupé, C. Bressy, M. Molmeret, B. Le Berre, F. Rimet, A. Bouchez, Y. Blache, Pioneer marine biofilms on artificial surfaces including antifouling coatings immersed in two contrasting French Mediterranean coast sites, *Biofouling*, 28, **2012,** 453-463.

[9] E. Celia, T. Darmanin, E. Taffin de Givenchy, S. Amigoni, F. Guittard, Recent advances in designing superhydrophobic surfaces, *Journal of Colloid and Interface Science*, 402, **2013,** 1-18.

[10] M. Nosonovsky, P.K. Rohatgi, Biomimetics in materials science: Self-healing, self-lubricating, and self-cleaning materials, in: Springer Series in Materials Science, 2012, pp. 1-409.

[11] B. Bhushan, Y.C. Jung, Natural and biomimetic artificial surfaces for superhydrophobicity, self-cleaning, low adhesion, and drag reduction, *Progress in Materials Science*, 56, **2010,** 1-108.

[12] *http://www.vialattea.net/esperti/php/risposta.php?num=9599,http://www.quelleenergie.fr/magazine/batiments-durables/materiaux-autonettoyants-01939/.*

[13] Z.-H. Yang, F.-C. Chien, C.-W. Kuo, D.-Y. Chueh, Y.-C. Tung, P. Chen, Interfacial adhesion and superhydrophobicity modulated with polymeric nanopillars using integrated nanolithography, *Journal of Micromechanics and Microengineering*, 22, **2012,** 125026.

[14] M. Geissler, Y. Xia, Patterning: Principles and Some New Developments, *Advanced Materials*, 16, **2004,** 1249-1269.

[15] B. Sharma Rao, M.N. Asri, U. Hashim, T. Adam, Conventional photolithography and process optimization of pattern- size expansion technique for nanogap biosensor fabrication, in: Advanced Materials Research, 2014, pp. 89-94.

[16] N.E. Kurland, T. Dey, S.C. Kundu, V.K. Yadavalli, Precise patterning of silk microstructures using photolithography, *Advanced Materials*, 25, **2013,** 6207-6212.
[17] P. Prompinit, A.S. Achalkumar, A.S. Walton, R.J. Bushby, C. Wälti, S.D. Evans, Reversible metallisation of soft UV patterned substrates, *Journal of Materials Chemistry C*, 2, **2014,** 5916-5923.
[18] R.K. Kramer, C. Majidi, R.J. Wood, Masked deposition of gallium-indium alloys for liquid-embedded elastomer conductors, *Advanced Functional Materials*, 23, **2013,** 5292-5296.
[19] R. Di Mundo, F. Palumbo, G. Barucca, G. Sabato, R. d'Agostino, On the "Growth" of Nano-Structures on c-Silicon via Self-Masked Plasma Etching Processes, *Plasma Processes and Polymers*, 10, **2013,** 843-849.
[20] G. Grenci, G. Della Giustina, A. Pozzato, E. Zanchetta, M. Tormen, G. Brusatin, Negative hybrid sol-gel resist as hard etching mask for pattern transfer with dry etching, *Microelectronic Engineering*, 98, **2012,** 134-137.
[21] L. Peng, Y. Deng, P. Yi, X. Lai, Micro hot embossing of thermoplastic polymers: A review, *Journal of Micromechanics and Microengineering*, 24, **2014**.
[22] A. Kolew, M. Heilig, M. Schneider, D. Münch, R. Ezzat, N. Schneider, M. Worgull, Hot embossing of transparent high aspect ratio micro parts, *Microsystem Technologies*, 20, **2014,** 1967-1973.
[23] H. Lan, H. Liu, UV-nanoimprint lithography: Structure, materials and fabrication of flexible molds, *Journal of Nanoscience and Nanotechnology*, 13, **2013,** 3145-3172.
[24] A. Mujahid, N. Iqbal, A. Afzal, Bioimprinting strategies: From soft lithography to biomimetic sensors and beyond, *Biotechnology Advances*, 31, **2013,** 1435-1447.
[25] A.D. Dias, D.M. Kingsley, D.T. Corr, Recent advances in bioprinting and applications for biosensing, *Biosensors*, 4, **2014,** 111-136.
[26] J. Voskuhl, J. Brinkmann, P. Jonkheijm, Advances in contact printing technologies of carbohydrate, peptide and protein arrays, *Current Opinion in Chemical Biology*, 18, **2014,** 1-7.
[27] Q. Wei, B. Yu, X. Wang, F. Zhou, Stratified polymer brushes from microcontact printing of polydopamine initiator on polymer brush surfaces, *Macromolecular Rapid Communications*, 35, **2014,** 1046-1054.
[28] W.S. Guan, H.X. Huang, B. Wang, Topographic design and application of hierarchical polymer surfaces replicated by microinjection compression molding, *Journal of Micromechanics and Microengineering*, 23, **2013**.
[29] A. Ghosh, R. Ganguly, T.M. Schutzius, C.M. Megaridis, Wettability patterning for high-rate, pumpless fluid transport on open, non-planar microfluidic platforms, *Lab on a Chip*, 14, **2014,** 1538-1550.
[30] N.L. Abbott, A. Kumar, G.M. Whitesides, Using Micromachining, Molecular Self-Assembly, and Wet Etching to Fabricate 0.1-1-.mu.m-scale structures of Gold and Silicon, *Chemistry of Materials*, 6, **1994,** 596-602.
[31] S. Krämer, R.R. Fuierer, C.B. Gorman, Scanning Probe Lithography Using Self-Assembled Monolayers, *Chemical Reviews*, 103, **2003,** 4367-4418.
[32] A. Kitamura, T. Satoh, M. Koka, T. Kobayashi, T. Kamiya, Fabrication of micro-prominences on PTFE surface using proton beam writing, *Nuclear Instruments and Methods in Physics Research, Section B: Beam Interactions with Materials and Atoms*, 306, **2013,** 288-291.

[33] J. Jussot, E. Pargon, B. Icard, J. Bustos, L. Pain, Line width roughness reduction strategies for patterns exposed via electron beam lithography, in: Proceedings of SPIE - The International Society for Optical Engineering, 2014.
[34] D.X. Yang, A. Frommhold, X. Xue, R.E. Palmer, A.P.G. Robinson, Chemically amplified phenolic fullerene electron beam resist, *Journal of Materials Chemistry C*, 2, **2014,** 1505-1512.
[35] Z. Ahmad, M. Rasekh, M. Edirisinghe, Electrohydrodynamic direct writing of biomedical polymers and composites, *Macromolecular Materials and Engineering*, 295, **2010,** 315-319.
[36] U. Hartmann, MAGNETIC FORCE MICROSCOPY, *Annual Review of Materials Science*, 29, **1999,** 53-87.
[37] M. Hashimoto, R. Tong, D.S. Kohane, Microdevices for Nanomedicine, *Molecular Pharmaceutics*, 10, **2013,** 2127-2144.
[38] K.A. Brown, D.J. Eichelsdoerfer, X. Liao, S. He, C.A. Mirkin, Material transport in dip-pen nanolithography, *Frontiers of Physics*, 9, **2014,** 385-397.
[39] V. Romanov, S.N. Davidoff, A.R. Miles, D.W. Grainger, B.K. Gale, B.D. Brooks, A critical comparison of protein microarray fabrication technologies, *Analyst*, 139, **2014,** 1303-1326.
[40] Q. Xu, P. Ihalainen, J.H. Smått, A. Määttänen, P. Sund, C.E. Wilén, J. Peltonen, Template-induced fabrication of nanopatterned polymeric films by inkjet printing, *Applied Surface Science*, 313, **2014,** 237-242.
[41] S.C. Singh, Recent advances on laser based nanomaterials synthesis, in: Synthesis, Characterization and Applications of Multifunctional Materials, 2012, pp. 99-126.
[42] L. Xue, J. Zhang, Y. Han, Phase separation induced ordered patterns in thin polymer blend films, *Progress in Polymer Science*, 37, **2012,** 564-594.
[43] J.-U. Sommer, G. Reiter, The Formation of Ordered Polymer Structures at Interfaces: A Few Intriguing Aspects, in: G.J. Vancso (Ed.) Ordered Polymeric Nanostructures at Surfaces, Springer Berlin Heidelberg, 2006, pp. 1-36.
[44] R. Mukherjee, A. Sharma, U. Steiner, Surface Instability and Pattern Formation in thin Polymer Films, in: Generating Micro- and Nanopatterns on Polymeric Materials, Wiley-VCH Verlag GmbH & Co. KGaA, 2011, pp. 217-265.
[45] L.V. Govor, G. Reiter, G.H. Bauer, J. Parisi, Treelike branched structures formed in dewetting thin films of a binary solution, *Applied Physics Letters*, 89, **2006,** -.
[46] H. Schoberth, V. Olszowka, K. Schmidt, A. Böker, Effects of Electric Fields on Block Copolymer Nanostructures, in: A.H.E. Müller, H.-W. Schmidt (Eds.) Complex Macromolecular Systems I, Springer Berlin Heidelberg, 2010, pp. 1-31.
[47] G. Liu, W. Yu, H. Li, J. Gao, D. Flynn, R. Kay, S. Cargill, C. Tonry, M. Patel, C. Bailey, Microstructure formation in a thick polymer by electrostatic-induced lithography, *Journal of Micromechanics and Microengineering*, 23, **2013,** 035018.
[48] E. Bormashenko, S. Balter, R. Pogreb, Y. Bormashenko, O. Gendelman, D. Aurbach, On the mechanism of patterning in rapidly evaporated polymer solutions: Is temperature-gradient-driven Marangoni instability responsible for the large-scale patterning?, *Journal of Colloid and Interface Science*, 343, **2010,** 602-607.
[49] E. Schäffer, S. Harkema, R. Blossey, U. Steiner, Temperature-gradient–induced instability in polymer films, *Europhys. Lett.*, 60, **2002,** 255-261.
[50] M. Hernandez-Guerrero, M.H. Stenzel, Honeycomb structured polymer films via breath figures, *Polymer Chemistry*, 3, **2012,** 563-577.

[51] P. Escalé, L. Rubatat, L. Billon, M. Save, Recent advances in honeycomb-structured porous polymer films prepared via breath figures, *European Polymer Journal*, 48, **2012,** 1001-1025.
[52] J. Rodríguez-Hernández, Wrinkled interfaces: Taking advantage of surface instabilities to pattern polymer surfaces, *Progress in Polymer Science*.
[53] J.-W. Park, Y.-H. Cho, Surface-Induced Morphologies in Thin Films of a Rod−Coil Diblock Copolymer, *Langmuir*, 22, **2006,** 10898-10903.
[54] G. Nisato, B.D. Ermi, J.F. Douglas, A. Karim, Excitation of Surface Deformation Modes of a Phase-Separating Polymer Blend on a Patterned Substrate, *Macromolecules*, 32, **1999,** 2356-2364.
[55] H. Katsuragi, Diffusion-induced spontaneous pattern formation on gelation surfaces, *EPL (Europhysics Letters)*, 73, **2006,** 793.
[56] B. Bozzini, D. Lacitignola, I. Sgura, A Reaction-diffusion model of spatial pattern formation in electrodeposition, in: Journal of Physics: Conference Series, IOP Publishing, 2008, pp. 012051.
[57] S. Zhao, Z. Qiu, M. Yang, J. Meng, M. Fang, Crystallographic symmetry effect on the nucleation in non-equilibrium aggregation pattern, *Physica A: Statistical Mechanics and its Applications*, 387, **2008,** 5355-5361.
[58] R.-M. Ho, F.-H. Lin, C.-C. Tsai, C.-C. Lin, B.-T. Ko, B.S. Hsiao, I. Sics, Crystallization-Induced Undulated Morphology in Polystyrene-b-Poly(l-lactide) Block Copolymer, *Macromolecules*, 37, **2004,** 5985-5994.
[59] I. Siretanu, J.P. Chapel, C. Drummond, Water−Ions Induced Nanostructuration of Hydrophobic Polymer Surfaces, *ACS Nano*, 5, **2011,** 2939-2947.
[60] T.A.L. Burgo, T.R.D. Ducati, K.R. Francisco, K.J. Clinckspoor, F. Galembeck, S.E. Galembeck, Triboelectricity: Macroscopic Charge Patterns Formed by Self-Arraying Ions on Polymer Surfaces, *Langmuir*, 28, **2012,** 7407-7416.
[61] P. Abgrall, V. Conedera, H. Camon, A.M. Gue, N.T. Nguyen, SU-8 as a structural material for labs-on-chips and microelectromechanical systems (review), *Electrophoresis*, 28, **2007,** 4539-4551.
[62] K. Ronse, Optical lithography—a historical perspective, *Comptes Rendus Physique*, 7, **2006,** 844-857.
[63] M.H. Kim, O.O. Park, Hot embossing of polymeric nanostructures using poly(dimethylsiloxane) replica molds based on three-dimensional colloidal crystals, *Microelectronic Engineering*, 91, **2012,** 121-126.
[64] Y. Fan, T. Li, W.M. Lau, J. Yang, A rapid hot-embossing prototyping approach using SU-8 molds coated with metal and antistick coatings, *Journal of Microelectromechanical Systems*, 21, **2012,** 875-881.
[65] M. Palacios-Cuesta, I. Vasiev, N. Gadegaard, J. Rodríguez-Hernández, O. García, Direct micrometer patterning and functionalization of polymer blend surfaces by using hot embossing, *European Polymer Journal*, 59, **2014,** 333-340.
[66] L. Peng, Y. Deng, P. Yi, X. Lai, Micro hot embossing of thermoplastic polymers: a review, *Journal of Micromechanics and Microengineering*, 24, **2014,** 013001.
[67] A. Kolew, D. Münch, K. Sikora, M. Worgull, Hot embossing of micro and sub-micro structured inserts for polymer replication, *Microsystem Technologies*, 17, **2011,** 609-618.
[68] M. Worgull, Chapter 5 - Hot Embossing Process, in: M. Worgull (Ed.) Hot Embossing, William Andrew Publishing, Boston, 2009, pp. 137-177.

[69] C.-C. Fu, A. Grimes, M. Long, C.G.L. Ferri, B.D. Rich, S. Ghosh, S. Ghosh, L.P. Lee, A. Gopinathan, M. Khine, Tunable Nanowrinkles on Shape Memory Polymer Sheets, *Advanced Materials*, 21, **2009,** 4472-4476.

[70] H. Vandeparre, S. Gabriele, F. Brau, C. Gay, K.K. Parker, P. Damman, Hierarchical wrinkling patterns, *Soft Matter*, 6, **2010,** 5751-5756.

[71] N. Bowden, W.T.S. Huck, K.E. Paul, G.M. Whitesides, The controlled formation of ordered, sinusoidal structures by plasma oxidation of an elastomeric polymer, *Applied Physics Letters*, 75, **1999,** 2557-2559.

[72] D.B.H. Chua, H.T. Ng, S.F.Y. Li, Spontaneous formation of complex and ordered structures on oxygen-plasma-treated elastomeric polydimethylsiloxane, *Applied Physics Letters*, 76, **2000,** 721-723.

[73] Y. Zhao, W. Huang, Y. Fu, Formation of micro/nano-scale wrinkling patterns atop shape memory polymers, *Journal of Micromechanics and Microengineering*, 21, **2011,** 067007.

[74] M.D. Huntington, C.J. Engel, A.J. Hryn, T.W. Odom, Polymer Nanowrinkles with Continuously Tunable Wavelengths, *ACS Applied Materials & Interfaces*, 5, **2013,** 6438-6442.

[75] T. Boudou, T. Crouzier, K. Ren, G. Blin, C. Picart, Multiple functionalities of polyelectrolyte multilayer films: new biomedical applications, *Advanced Materials*, 22, **2010,** 441-467.

[76] A. Chen, D.K. Lieu, L. Freschauf, V. Lew, H. Sharma, J. Wang, D. Nguyen, I. Karakikes, R.J. Hajjar, A. Gopinathan, E. Botvinick, C.C. Fowlkes, R.A. Li, M. Khine, Shrink-Film Configurable Multiscale Wrinkles for Functional Alignment of Human Embryonic Stem Cells and their Cardiac Derivatives, *Advanced Materials*, 23, **2011,** 5785-5791.

[77] M. Palacios-Cuesta, M. Liras, A. del Campo, O. García, J. Rodríguez-Hernández, Versatile Approach for the Fabrication of Functional Wrinkled Polymer Surfaces, *Langmuir*, 30, **2014,** 13244-13254.

[78] E.P. Chan, K.A. Page, S.H. Im, D.L. Patton, R. Huang, C.M. Stafford, Viscoelastic properties of confined polymer films measured via thermal wrinkling, *Soft Matter*, 5, **2009,** 4638-4641.

[79] T. Okayasu, H.L. Zhang, D.G. Bucknall, G.A.D. Briggs, Spontaneous Formation of Ordered Lateral Patterns in Polymer Thin-Film Structures, *Advanced Functional Materials*, 14, **2004,** 1081-1088.

[80] C. Jiang, S. Singamaneni, E. Merrick, V.V. Tsukruk, Complex Buckling Instability Patterns of Nanomembranes with Encapsulated Gold Nanoparticle Arrays, *Nano Letters*, 6, **2006,** 2254-2259.

[81] T.R. Hendricks, I. Lee, Wrinkle-Free Nanomechanical Film: Control and Prevention of Polymer Film Buckling, *Nano Letters*, 7, **2006,** 372-379.

[82] D. Mertz, J. Hemmerlé, J. Mutterer, S. Ollivier, J.-C. Voegel, P. Schaaf, P. Lavalle, Mechanically Responding Nanovalves Based on Polyelectrolyte Multilayers, *Nano Letters*, 7, **2007,** 657-662.

[83] A.J. Nolte, M.F. Rubner, R.E. Cohen, Determining the Young's modulus of polyelectrolyte multilayer films via stress-induced mechanical buckling instabilities, *Macromolecules*, 38, **2005,** 5367-5370.

[84] J.Y. Chung, J.-H. Lee, K.L. Beers, C.M. Stafford, Stiffness, Strength, and Ductility of Nanoscale Thin Films and Membranes: A Combined Wrinkling–Cracking Methodology, *Nano Letters*, 11, **2011,** 3361-3365.

[85] E.P. Chan, E.J. Smith, R.C. Hayward, A.J. Crosby, Surface wrinkles for smart adhesion, *Advanced Materials*, 20, **2008,** 711-716.
[86] H.S. Kim, A.J. Crosby, Solvent-Responsive Surface via Wrinkling Instability, *Advanced Materials*, 23, **2011,** 4188-4192.
[87] E.P. Chan, A.J. Crosby, Fabricating microlens arrays by surface wrinkling, *Advanced Materials*, 18, **2006,** 3238-3242.
[88] B. Li, Y.P. Cao, X.Q. Feng, H. Gao, Mechanics of morphological instabilities and surface wrinkling in soft materials: A review, *Soft Matter*, 8, **2012,** 5728-5745.
[89] M. Guvendiren, S. Yang, J.A. Burdick, Swelling-Induced surface patterns in hydrogels with gradient crosslinking density, *Advanced Functional Materials*, 19, **2009,** 3038-3045.
[90] M. Guvendiren, J.A. Burdick, S. Yang, Kinetic study of swelling-induced surface pattern formation and ordering in hydrogel films with depth-wise crosslinking gradient, *Soft Matter*, 6, **2010,** 2044-2049.
[91] D. Chandra, A.J. Crosby, Self-wrinkling of UV-cured polymer films, *Advanced Materials*, 23, **2011,** 3441-3445.
[92] K. Huraux, T. Narita, B. Bresson, C. Frétigny, F. Lequeux, Wrinkling of a nanometric glassy skin/crust induced by drying in poly(vinyl alcohol) gels, *Soft Matter*, 8, **2012,** 8075-8081.
[93] L. Pauchard, C. Allain, Buckling instability induced by polymer solution drying, *Europhysics Letters*, 62, **2003,** 897-903.
[94] R. Rizzieri, L. Mahadevan, A. Vaziri, A. Donald, Superficial wrinkles in stretched, drying gelatin films, *Langmuir*, 22, **2006,** 3622-3626.
[95] S.K. Basu, L.E. Scriven, L.F. Francis, A.V. McCormick, Mechanism of wrinkle formation in curing coatings, *Progress in Organic Coatings*, 53, **2005,** 1-16.
[96] R. Schubert, T. Scherzer, M. Hinkefuss, B. Marquardt, J. Vogel, M.R. Buchmeiser, VUV-induced micro-folding of acrylate-based coatings. 1. Real-time methods for the determination of the micro-folding kinetics, *Surface and Coatings Technology*, 203, **2009,** 1844-1849.
[97] R. Morent, N. De Geyter, S. Van Vlierberghe, A. Beaurain, P. Dubruel, E. Payen, Influence of operating parameters on plasma polymerization of acrylic acid in a mesh-to-plate dielectric barrier discharge, *Progress in Organic Coatings*, 70, **2011,** 336-341.
[98] N. De Geyter, R. Morent, S. Van Vlierberghe, M. Frère-Trentesaux, P. Dubruel, E. Payen, Effect of electrode geometry on the uniformity of plasma-polymerized methyl methacrylate coatings, *Progress in Organic Coatings*, 70, **2011,** 293-299.
[99] T. Desmet, R. Morent, N.D. Geyter, C. Leys, E. Schacht, P. Dubruel, Nonthermal Plasma Technology as a Versatile Strategy for Polymeric Biomaterials Surface Modification: A Review, *Biomacromolecules*, 10, **2009,** 2351-2378.
[100] V.N. Vasilets, G. Hermel, U. König, C. Werner, M. Müller, F. Simon, K. Grundke, Y. Ikada, H.J. Jacobasch, Microwave CO2 plasma-initiated vapour phase graft polymerization of acrylic acid onto polytetrafluoroethylene for immobilization of human thrombomodulin, *Biomaterials*, 18, **1997,** 1139-1145.
[101] T. Tsujioka, Selective metal deposition on organic surfaces for device applications, *Journal of Materials Chemistry C*, 2, **2014,** 221-227.
[102] Advences in Polymer Science: Long-Term properties of Polyolefins, Springer, 2004.
[103] Y.-P. Jiao, F.-Z. Cui, Surface modification of polyester biomaterials for tissue engineering, *Biomedical Materials*, 2, **2007,** R24.

[104] Y. Cao, W. Liu, G. Zhou, L. Cui, Tissue engineering and tissue repair in immunocompetent animals: tissue construction and repair, *Handchirurgie· Mikrochirurgie· Plastische Chirurgie*, 39, **2007,** 156-160.
[105] S. Saha, G.L. Baker, Surface-tethered conjugated polymers created via the grafting-from approach, *Journal of Applied Polymer Science*, 132, **2015**.
[106] M. Dübner, N.D. Spencer, C. Padeste, Light-Responsive Polymer Surfaces via Postpolymerization Modification of Grafted Polymer-Brush Structures, *Langmuir*, 30, **2014,** 14971-14981.
[107] A. Ortega, D. Alarcón, F. Muñoz-Muñoz, A. Garzón-Fontecha, G. Burillo, Radiation grafting of pH-sensitive acrylic acid and 4-vinyl pyridine onto nylon-6 using one- and two-step methods, *Radiation Physics and Chemistry*, 109, **2015,** 6-12.
[108] J.K. Sprafke, J.M. Spruell, K.M. Mattson, D. Montarnal, A.J. McGrath, R. Pötzsch, D. Miyajima, J. Hu, A.A. Latimer, B.I. Voit, T. Aida, C.J. Hawker, Revisiting thiol-yne chemistry: Selective and efficient monoaddition for block and graft copolymer formation, *Journal of Polymer Science, Part A: Polymer Chemistry*, 53, **2014,** 319-326.
[109] J.A. Johnson, Y.Y. Lu, A.O. Burts, Y.-H. Lim, M.G. Finn, J.T. Koberstein, N.J. Turro, D.A. Tirrell, R.H. Grubbs, Core-Clickable PEG-Branch-Azide Bivalent-Bottle-Brush Polymers by ROMP: Grafting-Through and Clicking-To, *Journal of the American Chemical Society*, 133, **2011,** 559-566.
[110] C. Grande, M. Tria, M. Felipe, F. Zuluaga, R. Advincula, RAFT "grafting-through" approach to surface-anchored polymers: Electrodeposition of an electroactive methacrylate monomer, *The European Physical Journal E: Soft Matter and Biological Physics*, 34, **2011,** 1-10.
[111] M. Khanzadi, S.M. Jafari, H. Mirzaei, F.K. Chegini, Y. Maghsoudlou, D. Dehnad, Physical and mechanical properties in biodegradable films of whey protein concentrate-pullulan by application of beeswax, *Carbohydrate Polymers*, 118, **2014,** 24-29.
[112] F. Franzoso, S. Tabasso, D. Antonioli, E. Montoneri, P. Persico, M. Laus, R. Mendichi, M. Negre, Films made from poly(vinyl alcohol-co-ethylene) and soluble biopolymers isolated from municipal biowaste, *Journal of Applied Polymer Science*, 132, **2015**.
[113] A. Synytska, D. Appelhans, Z.G. Wang, F. Simon, F. Lehmann, M. Stamm, K. Grundke, Perfluoroalkyl End-Functionalized Oligoesters: Correlation between Wettability and End-Group Segregation, *Macromolecules*, 40, **2006,** 297-305.
[114] P.A.V. O'Rourke-Muisene, J.T. Koberstein, S. Kumar, Optimal Chain Architectures for the Molecular Design of Functional Polymer Surfaces, *Macromolecules*, 36, **2003,** 771-781.
[115] J.S. Lee, M.D. Foster, D.T. Wu, Effects of Branch Points and Chain Ends on the Thermodynamic Interaction Parameter in Binary Blends of Regularly Branched and Linear Polymers, *Macromolecules*, 39, **2006,** 5113-5121.
[116] V. Mittal, Functional Polymer Blends: Synthesis, Properties, and Performance, Taylor & Francis, 2012.
[117] A. Bousquet, G. Pannier, E. Ibarboure, E. Papon, J. Rodríguez-Hernández, Control of the Surface Properties in Polymer Blends, *The Journal of Adhesion*, 83, **2007,** 335-349.
[118] A. Muñoz-Bonilla, E. Ibarboure, E. Papon, J. Rodriguez-Hernandez, Engineering polymer surfaces with variable chemistry and topography, *Journal of Polymer Science Part A: Polymer Chemistry*, 47, **2009,** 2262-2271.
[119] O. Akbulut, A.A. Yu, F. Stellacci, Fabrication of biomolecular devices via supramolecular contact-based approaches, *Chemical Society Reviews*, 39, **2010,** 30-37.

[120] C. Wendeln, B.J. Ravoo, Surface Patterning by Microcontact Chemistry, *Langmuir*, 28, **2012,** 5527-5538.
[121] C.-C. Wu, D.N. Reinhoudt, C. Otto, V. Subramaniam, A.H. Velders, Strategies for Patterning Biomolecules with Dip-Pen Nanolithography, *Small*, 7, **2011,** 989-1002.
[122] A.B. Braunschweig, F. Huo, C.A. Mirkin, Molecular printing, *Nat Chem*, 1, **2009,** 353-358.
[123] A.C. Siegel, S.K.Y. Tang, C.A. Nijhuis, M. Hashimoto, S.T. Phillips, M.D. Dickey, G.M. Whitesides, Cofabrication: A Strategy for Building Multicomponent Microsystems, *Accounts of Chemical Research*, 43, **2010,** 518-528.
[124] S.J. Maerkl, Next generation microfluidic platforms for high-throughput protein biochemistry, *Current Opinion in Biotechnology*, 22, **2011,** 59-65.
[125] K. Liu, Z.H. Fan, Thermoplastic microfluidic devices and their applications in protein and DNA analysis, *Analyst*, 136, **2011,** 1288-1297.
[126] C.M. Kolodziej, H.D. Maynard, Electron-Beam Lithography for Patterning Biomolecules at the Micron and Nanometer Scale, *Chemistry of Materials*, 24, **2011,** 774-780.
[127] M.J. Hynes, J.A. Maurer, Lighting the path: photopatternable substrates for biological applications, *Molecular BioSystems*, 9, **2013,** 559-564.
[128] L. Li, X.-X. Deng, Z.-L. Li, F.-S. Du, Z.-C. Li, Multifunctional Photodegradable Polymers for Reactive Micropatterns, *Macromolecules*, 47, **2014,** 4660-4667.
[129] S. Mattioli, S. Martino, F. D'Angelo, C. Emiliani, J.M. Kenny, I. Armentano, Nanostructured polystyrene films engineered by plasma processes: Surface characterization and stem cell interaction, *Journal of Applied Polymer Science*, 131, **2014,** n/a-n/a.
[130] Y. Cai, J.L.P. Jessop, Photopolymerization, Free Radical, in: Encyclopedia of Polymer Science and Technology, John Wiley & Sons, Inc., 2002.
[131] J.-S. Wang, K. Matyjaszewski, Controlled/"living" radical polymerization. atom transfer radical polymerization in the presence of transition-metal complexes, *Journal of the American Chemical Society*, 117, **1995,** 5614-5615.
[132] K. Matyjaszewski, Atom Transfer Radical Polymerization (ATRP): Current Status and Future Perspectives, *Macromolecules*, 45, **2012,** 4015-4039.
[133] K. Matyjaszewski, N.V. Tsarevsky, Macromolecular Engineering by Atom Transfer Radical Polymerization, *Journal of the American Chemical Society*, 136, **2014,** 6513-6533.
[134] E. Celia, T. Darmanin, E. Taffin de Givenchy, S. Amigoni, F. Guittard, Recent advances in designing superhydrophobic surfaces, *Journal of Colloid and Interface Science*, 402, **2013,** 1-18.
[135] X.J. Feng, L. Jiang, Design and Creation of Superwetting/Antiwetting Surfaces, *Advanced Materials*, 18, **2006,** 3063-3078.
[136] E. Martines, K. Seunarine, H. Morgan, N. Gadegaard, C.D.W. Wilkinson, M.O. Riehle, Air-Trapping on Biocompatible Nanopatterns, *Langmuir*, 22, **2006,** 11230-11233.
[137] T. Shimoda, T. Masuda, Liquid silicon and its application in electronics, *Japanese Journal of Applied Physics*, 53, **2014**.
[138] F. Xu, P. Datta, H. Wang, S. Gurung, M. Hashimoto, S. Wei, J. Goettert, R.L. McCarley, S.A. Soper, Polymer Microfluidic Chips with Integrated Waveguides for Reading Microarrays, *Analytical Chemistry*, 79, **2007,** 9007-9013.

[139] H. Qi, Y. Du, L. Wang, H. Kaji, H. Bae, A. Khademhosseini, Patterned Differentiation of Individual Embryoid Bodies in Spatially Organized 3D Hybrid Microgels, *Advanced Materials*, 22, **2010,** 5276-5281.
[140] T. Darmanin, F. Guittard, Wettability of conducting polymers: From superhydrophilicity to superoleophobicity, *Progress in Polymer Science*, 39, **2014,** 656-682.
[141] A. Cerf, J.-C. Cau, C. Vieu, Controlled assembly of bacteria on chemical patterns using soft lithography, *Colloids and Surfaces B: Biointerfaces*, 65, **2008,** 285-291.
[142] L. Xu, L. Robert, Q. Ouyang, F. Taddei, Y. Chen, A.B. Lindner, D. Baigl, Microcontact Printing of Living Bacteria Arrays with Cellular Resolution, *Nano Letters*, 7, **2007,** 2068-2072.
[143] T. Xu, S. Petridou, E.H. Lee, E.A. Roth, N.R. Vyavahare, J.J. Hickman, T. Boland, Construction of high-density bacterial colony arrays and patterns by the ink-jet method, *Biotechnology and Bioengineering*, 85, **2004,** 29-33.
[144] B. Rowan, M.A. Wheeler, R.M. Crooks, Patterning bacteria within hyperbranched polymer film templates, *Langmuir*, 18, **2002,** 9914-9917.
[145] S. Rozhok, C.K.F. Shen, P.L.H. Littler, Z.F. Fan, C. Liu, C.A. Mirkin, R.C. Holz, Methods for fabricating microarrays of motile bacteria, *Small*, 1, **2005,** 445-451.
[146] S. Rozhok, Z. Fan, D. Nyamjav, C. Liu, C.A. Mirkin, R.C. Holz, Attachment of motile bacterial cells to prealigned holed microarrays, *Langmuir*, 22, **2006,** 11251-11254.
[147] C.M. Costello, J.-U. Kreft, C.M. Thomas, D.M. Hammes, P. Bao, S.D. Evans, P.M. Mendes, Exploiting additive and subtractive patterning for spatially controlled and robust bacterial co-cultures, *Soft Matter*, 8, **2012,** 9147-9155.
[148] K. Suh, A. Khademhosseini, P. Yoo, R. Langer, Patterning and Separating Infected Bacteria Using Host–Parasite and Virus–Antibody Interactions, *Biomedical Microdevices*, 6, **2004,** 223-229.
[149] P. Krsko, J.B. Kaplan, M. Libera, Spatially controlled bacterial adhesion using surface-patterned poly(ethylene glycol) hydrogels, *Acta Biomaterialia*, 5, **2009,** 589-596.
[150] D. Nyamjav, S. Rozhok, R.C. Holz, Immobilization of motile bacterial cells via dip-pen nanolithography, *Nanotechnology*, 21, **2010,** 6.
[151] P. Kim, A. Epstein, M. Khan, L. Zarzar, D. Lipomi, G. Whitesides, J. Aizenberg, Structural Transformation by Electrodeposition on Patterned Substrates (STEPS): A New Versatile Nanofabrication Method, *Nano letters*, 12, **2012,** 527-533.
[152] W.G. Koh, A. Revzin, A. Simonian, T. Reeves, M. Pishko, Control of mammalian cell and bacteria adhesion on substrates micropatterned with poly(ethylene glycol) hydrogels, *Biomedical Microdevices*, 5, **2003,** 11-19.
[153] N.J. Lawrence, J.M. Wells-Kingsbury, M.M. Ihrig, T.E. Fangman, F. Namavar, C.L. Cheung, Controlling E. coli Adhesion on High-k Dielectric Bioceramics Films using Poly(amino acid) Multilayers, *Langmuir*, 28, **2012,** 4301-4308.
[154] B.F. Brehm-Stecher, E.A. Johnson, Single-Cell Microbiology: Tools, Technologies, and Applications, *Microbiology and Molecular Biology Reviews*, 68, **2004,** 538-559.
[155] T. Hutchens, J. Porath, Protein recognition of immobilized ligands: promotion of selective adsorption, *Clinical chemistry*, 33, **1987,** 1502-1508.
[156] K.B. Lee, S.J. Park, C.A. Mirkin, J.C. Smith, M. Mrksich, Protein nanoarrays generated by dip-pen nanotithography, *Science*, 295, **2002,** 1702-1705.
[157] J.D. Hoff, L.J. Cheng, E. Meyhöfer, L.J. Guo, A.J. Hunt, Nanoscale protein patterning by imprint lithography, *Nano Letters*, 4, **2004,** 853-857.

[158] G.M. Whitesides, E. Ostuni, S. Takayama, X. Jiang, D.E. Ingber, Soft lithography in biology and biochemistry, in, 2001, pp. 335-373.
[159] T. Blättler, C. Huwiler, M. Ochsner, B. Städler, H. Solak, J. Vörös, H. Michelle Grandin, Nanopatterns with bioiogical functions, *Journal of Nanoscience and Nanotechnology*, 6, **2006,** 2237-2264.
[160] M. Ochsner, M. Textor, V. Vogel, M.L. Smith, Dimensionality Controls Cytoskeleton Assembly and Metabolism of Fibroblast Cells in Response to Rigidity and Shape, *PLoS ONE*, 5, **2010,** e9445.
[161] M. Schuler, T.P. Kunzler, M. de Wild, C.M. Sprecher, D. Trentin, D.M. Brunette, M. Textor, S.G.P. Tosatti, Fabrication of TiO2-coated epoxy replicas with identical dual-type surface topographies used in cell culture assays, *Journal of Biomedical Materials Research Part A*, 88A, **2009,** 12-22.
[162] A.V. Singh, R. Patil, D.K. Thombre, W.N. Gade, Micro-nanopatterning as tool to study the role of physicochemical properties on cell–surface interactions, *Journal of Biomedical Materials Research Part A*, 101, **2013,** 3019-3032.
[163] P. Cluzel, M. Surette, S. Leibler, An Ultrasensitive Bacterial Motor Revealed by Monitoring Signaling Proteins in Single Cells, *Science*, 287, **2000,** 1652-1655.
[164] A.E. Smith, Z. Zhang, C.R. Thomas, K.E. Moxham, A.P. Middelberg, The mechanical properties of Saccharomyces cerevisiae, *Proceedings of the National Academy of Sciences*, 97, **2000,** 9871-9874.
[165] C. Cai, B. Liu, M.V. Mirkin, H.A. Frank, J.F. Rusling, Scanning Electrochemical Microscopy of Living Cells. 3. Rhodobacter s phaeroides, *Analytical chemistry*, 74, **2002,** 114-119.
[166] J.D. Pasteris, J.J. Freeman, S.K. Goffredi, K.R. Buck, Raman spectroscopic and laser scanning confocal microscopic analysis of sulfur in living sulfur-precipitating marine bacteria, *Chemical Geology*, 180, **2001,** 3-18.
[167] E.O. Potma, W.P. de Boeij, P.J. van Haastert, D.A. Wiersma, Real-time visualization of intracellular hydrodynamics in single living cells, *Proceedings of the National Academy of Sciences*, 98, **2001,** 1577-1582.
[168] G. Zeng, T. Müller, R.L. Meyer, Single-Cell Force Spectroscopy of Bacteria Enabled by Naturally Derived Proteins, *Langmuir*, 30, **2014,** 4019-4025.
[169] W.K. Cho, S.M. Kang, J.K. Lee, Non-biofouling polymeric thin films on solid substrates, *Journal of Nanoscience and Nanotechnology*, 14, **2014,** 1231-1252.
[170] L. Yuan, Q. Yu, D. Li, H. Chen, Surface Modification to Control Protein/Surface Interactions, *Macromolecular Bioscience*, 11, **2011,** 1031-1040.
[171] I. Armentano, C.R. Arciola, E. Fortunati, D. Ferrari, S. Mattioli, C.F. Amoroso, J. Rizzo, J.M. Kenny, M. Imbriani, L. Visai, The interaction of bacteria with engineered nanostructured polymeric materials: A review, *Scientific World Journal*, 2014, **2014**.
[172] B.G. Gerberich, S.K. Bhatia, Tissue scaffold surface patterning for clinical applications, *Biotechnology Journal*, 8, **2013,** 73-84.
[173] A. Khademhosseini, G. Eng, J. Yeh, P.A. Kucharczyk, R. Langer, G. Vunjak-Novakovic, M. Radisic, Microfluidic patterning for fabrication of contractile cardiac organoids, *Biomedical Microdevices*, 9, **2007,** 149-157.
[174] K. Salaita, Y. Wang, C.A. Mirkin, Applications of dip-pen nanolithography, *Nat Nano*, 2, **2007,** 145-155.
[175] Y.-K. Kim, S.-R. Ryoo, S.-J. Kwack, D.-H. Min, Mass Spectrometry Assisted Lithography for the Patterning of Cell Adhesion Ligands on Self-Assembled Monolayers, *Angewandte Chemie International Edition*, 48, **2009,** 3507-3511.

[176] A.I. Hochbaum, J. Aizenberg, Bacteria Pattern Spontaneously on Periodic Nanostructure Arrays, *Nano Letters*, 10, **2010,** 3717-3721.
[177] D.D. Doorneweerd, W.A. Henne, R.G. Reifenberger, P.S. Low, Selective Capture and Identification of Pathogenic Bacteria Using an Immobilized Siderophore, *Langmuir*, 26, **2010,** 15424-15429.
[178] A.K. Adak, J.W. Boley, D.P. Lyvers, G.T. Chiu, P.S. Low, R. Reifenberger, A. Wei, Label-Free Detection of Staphylococcus aureus Captured on Immutable Ligand Arrays, *ACS Applied Materials & Interfaces*, 5, **2013,** 6404-6411.
[179] M. Kaupp, A.S. Quick, C. Rodriguez-Emmenegger, A. Welle, V. Trouillet, O. Pop-Georgievski, M. Wegener, C. Barner-Kowollik, Photo-Induced Functionalization of Spherical and Planar Surfaces via Caged Thioaldehyde End-Functional Polymers, *Advanced Functional Materials*, **2014,** n/a-n/a.
[180] G. Subbiahdoss, D.W. Grijpma, H.C. van der Mei, H.J. Busscher, R. Kuijer, Microbial biofilm growth versus tissue integration on biomaterials with different wettabilities and a polymer-brush coating, *Journal of Biomedical Materials Research Part A*, 94A, **2010,** 533-538.
[181] D. Alves, M. Olívia Pereira, Mini-review: Antimicrobial peptides and enzymes as promising candidates to functionalize biomaterial surfaces, *Biofouling*, 30, **2014,** 483-499.
[182] C.C. De Carvalho, Biofilms: recent developments on an old battle, *Recent patents on biotechnology*, 1, **2007,** 49-57.
[183] T.S. Sileika, H.-D. Kim, P. Maniak, P.B. Messersmith, Antibacterial Performance of Polydopamine-Modified Polymer Surfaces Containing Passive and Active Components, *ACS Applied Materials & Interfaces*, 3, **2011,** 4602-4610.
[184] H. Han, J. Wu, C.W. Avery, M. Mizutani, X. Jiang, M. Kamigaito, Z. Chen, C. Xi, K. Kuroda, Immobilization of Amphiphilic Polycations by Catechol Functionality for Antimicrobial Coatings, *Langmuir*, 27, **2011,** 4010-4019.
[185] A.K. Epstein, T.-S. Wong, R.A. Belisle, E.M. Boggs, J. Aizenberg, Liquid-infused structured surfaces with exceptional anti-biofouling performance, *Proceedings of the National Academy of Sciences*, 109, **2012,** 13182-13187.
[186] C.M. Kirschner, A.B. Brennan, Bio-Inspired Antifouling Strategies, *Annual Review of Materials Research*, 42, **2012,** 211-229.
[187] S. Neuhaus, N.D. Spencer, C. Padeste, Anisotropic wetting of microstructured surfaces as a function of surface chemistry, *ACS Applied Materials and Interfaces*, 4, **2012,** 123-130.
[188] R. Schubert, T. Scherzer, M. Hinkefuss, B. Marquardt, J. Vogel, M.R. Buchmeiser, VUV-induced micro-folding of acrylate-based coatings: 1. Real-time methods for the determination of the micro-folding kinetics, *Surface and Coatings Technology*, 203, **2009,** 1844-1849.

SECCIÓN II: Fotolitografía y superficies funcionales

SECCIÓN II:

FOTOLITOGRAFÍA Y SUPERFICIES FUNCIONALES

En esta sección II se describen los trabajos en los que se ha utilizado la fotolitografía como método para la estructuración de las superficies poliméricas. La sección se divide a su vez en dos capítulos: el capítulo II.1 donde se ha desarrollado un método de estructuración superficial que aúna la fotolitografía por reticulación a partir de mezclas de monómeros metacrílicos con la segregación superficial de un copolímero funcionalizado; y el capítulo II.2 donde las estructuras superficiales se han conseguido también aplicando la fotolitografía para inducir procesos de fotoentrecruzamiento/fotodegradación pero, esta vez, sobre superficies poliméricas. Se ha escogido con este fin un polímero comercial, el poliestireno (PS) y se han empleado asimismo, copolímeros funcionales de naturaleza estirénica para variar simultáneamente la química de las superficies generadas.

CAPÍTULO II.1: Fotolitografía a partir de monómeros y segregación superficial

En este capítulo se ha planteado la segregación superficial como un método alternativo a la funcionalización química de una superficie que combinado con la fotolitografía, que induce la fotopolimerización de mezclas de monómeros metacrílicos, permite la creación de nuevas superficies inteligentes.

El desarrollo de este trabajo ha dado lugar a un artículo científico que se presenta a continuación:

Artículo 1: *Functional micropatterned surfaces prepared by simultaneous UV-lithography and surface segregation of fluorinated copolymers*

Se ha desarrollado un nuevo procedimiento que se centra en el diseño y preparación de superficies poliméricas microestructuradas y funcionales por combinación de dos técnicas simultáneas: la fotolitografía a partir de la irradiación con luz UV de una mezcla fotosensible de monómeros de naturaleza metacrílica y la segregación superficial controlada de un copolímero fluorado sintetizado previamente por ATRP y de naturaleza estirénica que se encuentra disuelto en la mezcla inicial fotosensible.

ARTICLE WWW.POLYMERCHEMISTRY.ORG JOURNAL OF POLYMER SCIENCE Polymer Chemistry

Functional Micropatterned Surfaces Prepared by Simultaneous UV-Lithography and Surface Segregation of Fluorinated Copolymers

Marta Palacios-Cuesta,[1] Marta Liras,[1] Christine Labrugère,[2] Juan Rodríguez-Hernández,[1] Olga García[1]

[1]Department of Chemistry and Properties of Polymers, Instituto de Ciencia y Tecnología de Polímeros, (ICTP-CSIC), Juan de la Cierva 3, Madrid 28006, Spain
[2]Centre de Caractérisation des Matériaux Avancés (CeCaMA), Institut de Chimie de la Matière Condensée de Bordeaux, 87, Avenue du Docteur Schweitzer, Pessac Cedex 33608, France
Correspondence to: J. Rodríguez-Hernández (E-mail: rodriguez@ictp.csic.es) or O. García (E-mail: ogarcia@ictp.csic.es)

Received 25 May 2012; revised 27 July 2012; accepted 31 July 2012; published online 24 August 2012
DOI: 10.1002/pola.26318

ABSTRACT: A new procedure focused on the design and preparation of structured and functional polymer surfaces by combination of two approaches acting simultaneously is developed. The elaboration of micrometer size patterned surfaces by UV-light lithography is reported where, in addition, the surface chemical composition can be controlled by surface segregation of a fluorinated copolymer incorporated in the photopolymerizable mixture. As evidenced by contact angle and XPS measurements, the surface composition can be modified depending on such factors as with the environmental conditions or the concentration of copolymer in the blend. Moreover, the functionality of the copolymer is enhanced by the surface pattern created. As a consequence, the wettability of the films can be modified depending on the pattern and composition of the blend. By using this methodology, functional adaptive sensitive surfaces with a well-defined topography will be obtained in one single step and without the use of tedious and time-consuming multistep procedures. © 2012 Wiley Periodicals, Inc. J Polym Sci Part A: Polym Chem 50: 4902–4910, 2012

KEYWORDS: annealing; additives; blending; Crosslinking; fluorinated surface; lithography; micropatterned surface; photolitography; surfaces, photopolymerization; surface functionalization; surface segregation

INTRODUCTION A large variety of properties in polymers including adhesion,[1] wettability,[2] or biocompatibility[3,4] rely on surfaces. Thus, surface modification both in terms of to- areas. These changes can be either from photocrosslinking[14] to chemical modification[15,16] or decomposition reactions.[17] The development of these procedures has also allowed the

Functional micropatterned surfaces prepared by simultaneous UV-lithography and surface segregation of fluorinated copolymers

Marta Palacios-Cuesta[a], Marta Liras[a], Christine Labrugère[b], Juan Rodríguez-Hernández[a]* and Olga García.[a]*

[a]Department of Chemistry and Properties of Polymers, Instituto de Ciencia y Tecnología de Polímeros, (ICTP-CSIC), Juan de la Cierva 3, 28006 Madrid, Spain.

[b]Institut de Chimie de la Matière Condensée de Bordeaux 87, Avenue du Docteur Schweitzer , 33608 Pessac Cedex, France

Correspondence to:

Olga García (ogarcia@ictp.csic.es)

Juan Rodríguez-Hernández (rodriguez@ictp.csic.es)

Abstract

A new procedure focused on the design and preparation of structured and functional polymer surfaces by combination of two approaches acting simultaneously is developed. The elaboration of micrometer size patterned surfaces by UV-light lithography is reported where, in addition, the surface chemical composition can be controlled by surface segregation of a fluorinated copolymer incorporated in the photopolymerizable mixture. As evidenced by contact angle and XPS measurements, the surface composition can be modified depending on such factors as with the environmental conditions or the concentration of copolymer in the blend. Moreover, the functionality of the copolymer is enhanced by the surface pattern created. As a consequence, the wettability of the films can be modified depending on the pattern and composition of the blend. By using this methodology, functional adaptive sensitive surfaces with a well-defined topography will be obtained in one single step and without the use of tedious and time consuming multi-step procedures.

Introduction

A large variety of properties in polymers including adhesion [1], wettability [2] or biocompatibility [3, 4] rely on surfaces. Thus, surface modification both in terms of topography (creation of surface patterns) and chemical functionality (control over the chemical composition) is a requirement for the employment of a polymeric material. Up to now, the investigation and development of both aspects have advanced in parallel. Thus, a large number of techniques are now available to obtain either structured or functionalized surfaces [5]. Different methods allow us to obtain surface patterns with controlled sizes and varied shapes. Nowadays, the most important techniques of patterning [6] involve: generation of patterns, replication of patterns and three-dimensional patterning. Surface patterns can be obtained by direct writing techniques [7], instability induced polymers [8] or patterning with block copolymers [9] and photolithography, while the replication of pattern is fundamentally formed by "soft chemistry" (nanoimprint lithography [10], hot embossing [11], microfluidic patterning [12] or microcontact printing) [13]. In photolithography, the polymer is usually irradiated with a UV/Vis light through a photomask obtaining changes only in the exposed areas. These changes can be either from photocrosslinking [14] to chemical modification [15, 16] or decomposition reactions [17]. The development of these procedures has also allowed the

expansion of technologies in fields as varied as optics, microelectronics, microfluidic devices or microbiology [18, 19].

On the other hand, techniques such as plasma, flame or chemical reactions allow us to modify the surface chemical functionality. However, these methods are difficult to reproduce, they usually lead to multifunctional surfaces and due to the harsh conditions required in most of the cases the surfaces are usually damaged during the treatment. Surface segregation improves some of the drawbacks of the methods mentioned above since this methodology allows the control of the type and density of functional groups. Moreover, upon environmental changes the system can rearrange thus reversibly modifying the surface functionality [20, 21]. Surface segregation consists on the selective surface enrichment of one of the components in a polymer blend. In this particular case we design a functionalized copolymer within a polymer blend able to move towards or from the surface. By segregation to the polymer/air or polymer/water vapor interface the composition and properties in the surface can be altered [22]. The principles that direct the segregation of functionalized copolymers from the matrix towards the polymer surface based both on enthalpic and entropic factors have been described previously [23].

In spite of the significant advances carried out on the development of systems with either controlled functionality or topography only few examples have been described in which both can be simultaneously controlled. Attempts to obtain surfaces with both controlled structure, with moieties sizes of tens of nanometers (macromolecule size), and functionality have been recently reported in which ‘‘top-down’’ and ‘‘bottom-up’’ approaches have been combined in the so-called templated self-assembly (TSA) approach [24-26]. Hence, topographically patterned surfaces [27] and/or chemically patterned substrates [28] are typical templates used to order block copolymer films at larger length scales. Equally, hydrophobic surfaces in which the roughness has been artificially modified have been fabricated with hierarchical structures such as electrodeposition, nanowire arrays, colloidal systems, or photolithography [29, 30]. As an alternative to those complex procedures, Brittain and coworkers described the preparation of tethered PS-*b*-PMMA brushes in which the surface chemical composition could be reversibly modified upon treatment with selective solvents [31]. More interestingly, this group demonstrated the structural variations at the surface after exposure either to a common solvent forming a smooth polymer layer or to cyclohexane in which the PS blocks are swollen. To the best of our knowledge all the approaches previously

reported concerned the preparation of structured polymer films using inorganic supports except the work elaborated by our group concerning the elaboration of functional surface with controlled topography combining surface segregation with breath figures [32].

Herein we report the elaboration of micrometer size patterned surfaces where, in addition, the surface chemical composition can be varied depending on the environmental conditions. For that purpose, we combined photolithography and surface segregation of a copolymer containing fluorinated moieties. While by using photolithography we will create patterned surfaces to control the surface microstructure (Figure 1A, 1B), surface segregation of copolymers containing fluorinated moieties allowed us to modify the surface functionality. By using this methodology, we will obtain functional adaptive sensitive surfaces with a well-defined topography in one single step without the use of tedious and time consuming multi-step procedures.

Experimental

Materials: Methyl methacrylate (MMA) (Aldrich 99%) was washed three times first with a basic aqueous solution (10% NaOH) and then in water. Then, the resulting monomer was dried on anhydric magnesium sulfate, filtered and distilled. Ethylene glycol dimethacrylate (EGDMA) (Aldrich 99%), 2,2,2-trifluoroethyl methacrylate (TFMA) (Aldrich 99%), N,N,N',N'',N''-pentamethyldiethylenetriamine (PMDETA) (Aldrich, 99%), copper (I) bromide (CuBr) (Aldrich 98%), ethyl-2-bromoisobutyrate (EBrIB), Irgacure 651 (IRG651) (2,2-dimethoxy-1,2-diphenylethan-1-one) (Ciba), dichlorodimethylsilane (Aldrich 98.5%) and the rest of solvents were employed as received. As supports, we used silicon wafers (Siegert Consulting e.k.), glasses 0.15 mm thickness (Menzel-Glaser), microscope slides 1 mm thickness (Menzel-Glaser). The mask employed were metallic copper grids (100 µm x 100 µm) typically employed for transmission electron microscopy (1000 mesh, 25 µm pitch) (SPI supplies).

Polymer Synthesis

The random copolymer of poly(methyl methacrylate-co-2,2,2-trifluoroethyl methacrylate) p(MMA-co-TFMA) was synthesized by Atom Transfer Radical Polymerization (ATRP) in order to obtain both low polydispersity and controlled chain lengths (Figure 1C).

The polymerization was performed in Schlenk flasks previously flamed and dried under vacuum. ATRP was carried out using the following stoichiometry [M1]/[M2]/[I]/[CuBr]/[L] 48:12:1:1:1 where M1= MMA, M2= TFMA, I=Initiator (EbrIB), L=Ligand (PMDETA) in toluene. The reactants were added under N_2. The reaction mixture was degassed by three-pump-thaw cycles and placed in a thermostatic oil bath at 90ºC. After the polymerization, the mixture were cooled to room temperature, diluted with dichloromethane and passed through a neutral alumina column to remove the copper salt. After removing the solvent, the polymers were precipitated in hexane, washed and dried under vacuum.

Preparation of the films

Photosensitive blends were prepared from mixtures of MMA/EGDMA varying the volume composition (85:15, 90:10 and 95:5). A radical photoinitiator, IRG651 (2-10wt%) and different amounts (10-20wt%) of the fluorinated synthetic polymer, p(MMA-co-TFMA) were additionally added. The photopolymerization of the films has been done with UV light irradiation using a Hamamatsu source (model Lightningcure L8868 equipped with a Hg-Xe lamp of 200W power). To prepare the films, 2 x 2 cm silicon wafers with a spacer of 50 µm were employed. The photosensitive mixture was placed in the center of the wafer and covered by a glass (silanized or cleaned with 0.15 mm thickness), the metallic grid and with a second glass cover. Schematic representation of all this assembly is showed in the Figure 1A.

The irradiation intensity was constant throughout the experiments (75% of the total lamp intensity) and focused on the samples with an optic fiber. The incident light intensity was maintained constant for all experiments at 6150 mW/m2, measured by a Luzchem radiometer SPR-01. The distance sample to light was constant (7.5 cm) for all the experiments and a microscope slide was used as a heat filter. After the irradiation time (4, 6 or 10 min for samples with 15, 10 and 5 v/v% of EGDMA, respectively), the samples were washed with hexane in order to remove the non-irradiated regions.

For some particular cases, the glass covers were silanized following this procedure: the covers were introduced in dichlorodimethylsilane solution for 60 seconds. After the treatment, the glass covers were rinsed with a mixture ethanol/water and ethyl acetate.

The sample treatment after polymerization consisted in annealing at 130°C under vacuum for 10 days.

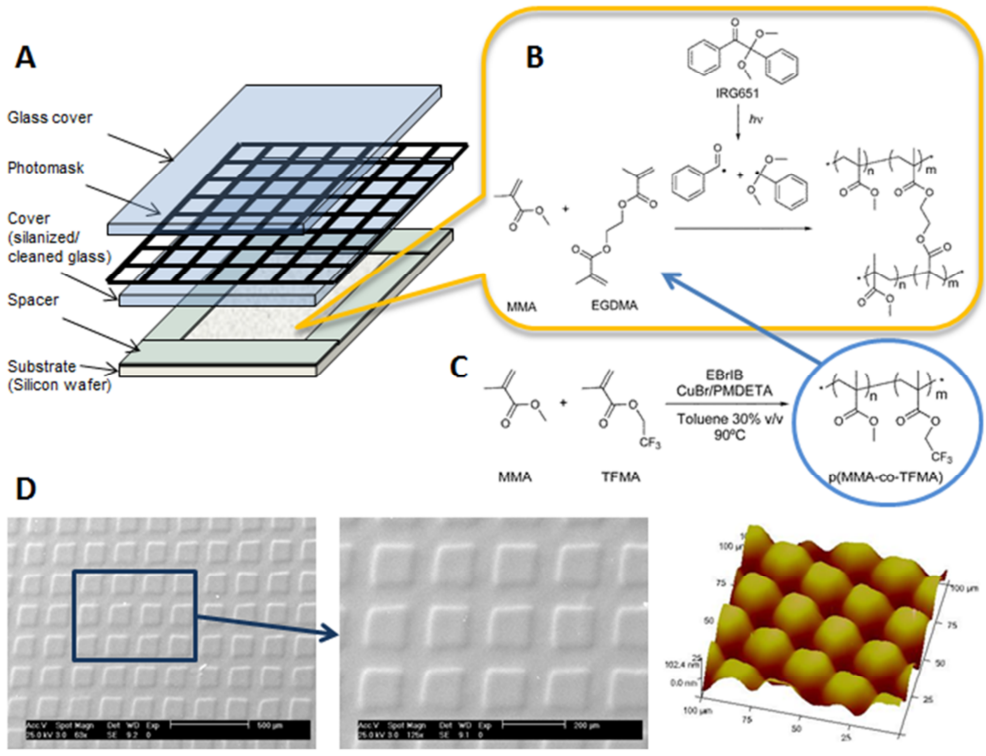

Figure 1: *a) Schematic procedure to fabricate structured surfaces via photolithography. b) Scheme of photopolymerization reaction using MMA, EGDMA and IRG651 as photoinitator. c) Scheme of ATRP reaction for the preparation of the copolymer p(MMA-co-TFMA). d) Scanning electron microscope images of the microstructures obtained by photopolymerization of MMA/EGDMA 85:15 and 10wt% of p(MMA-co-TFMA) using 5wt% IRG651 as photoinitiator (photomask with hole 100 µm) and an AFM image (photomask with hole 25 µm) at the same composition.*

Characterization

The ^{1}H and ^{13}C NMR spectra were registered at room temperature in $CDCl_3$ solution in Varian INOVA-300. Chemical shifts are reported in parts per million (ppm) using as internal

reference the peak of the trace of undeuterated solvent (δ 7.26). Size exclusion chromatography (SEC) analyses were carried out on chromatographic system (Waters Division Millipore) equipped with a Waters model 410 refractive-index detector. Dimethyl formamide (99.9%, Aldrich) containing 0.1% of LiBr, was used as the eluent at a flow rate of 1 mL min-1 at 50 ºC. Styragel packed columns (HR2, HR3 and HR4, Waters Division Millipore) were used. The molecular weights were estimated against poly(methyl methacrylate) standards. Poly(methyl methacrylate) standards (Polymer Laboratories, Laboratories, Ltd.) between 2.4×10^6 and 9.7×10^2 g mol^{-1} were used to calibrate the columns.

A detailed description of the photo-differential scanning calorimeter (Photo-DSC) employed can be found in previous publication[33]. All polymerizations were carried out in bulk at 30ºC under air atmosphere. Sample quantities of about 40µL were accurate weighted and spread as a layer over the base of the 6.5-mm diameter aluminum DSC pan. In order to identify the optimal conditions, IRG651 was selected as initiator and different proportions of MMA/EGDMA as monomer mixture. The incident light intensity was maintained constant at 10.95 mW/m^2. Power intensity of the light and emission spectra were also determined by a Luzchem SPR-01 spectroradiometer. Infrared spectra were obtained using a Spectrum One FT-IR spectrometer (Perkin-Elmer) fitted with an attenuated total reflectance (ATR) accessory under unforced conditions. The irradiated samples were placed in direct contact with the diamond crystal with no previous preparation. Measurements were collected at 8 cm^{-1} resolution and co-adding 6 scans per spectrum. Scanning electron microscopy (SEM) used for surface structural and cross-sectional analysis. Micrographs were taken using a Philips XL30 with an acceleration voltage of 25 kV. The samples were coated with gold-palladium (80/20) prior to scanning. The surface composition of selected blends was obtained by X-ray photoelectron spectroscopy (XPS). XPS spectra were recorded with a 220i-XL Escalab from VG (Netherlands). The films supported on silicon wafer were put under high vacuum (UHV) to reach the 10^{-8} Pa range. The non-monochromatized Mg-ray source was used at 100 W, and a flood gun was used to compensate for the nonconductive samples. The spectra were calibrated in relation to the C1s binding energy (284.6 eV), which was applied as an internal standard. Fitting of the high-resolution spectra was provided through the Advantage program from VG. Atomic force microscopy (AFM) measurements were conducted on a Multimode Nanoscope IVa, Digital Instrument/Veeco operated in tapping mode under ambient condition, allowing estimation of surface topography and roughness. Contact angles were measured with deionized

water on a goniometer KSV theta (KSV instruments, Ltd., Finland) at room temperature. Water droplets of 2µl were placed on the films and a charged coupled device camera was used to capture the images of the water droplets for the determination of the contact angle.

Results and Discussion

We employed photopolymerizable mixtures of two monomers in which the functional copolymer has been dissolved in order to construct a crosslinked film with the copolymer embedded within the network. Thus, methyl methacrylate (MMA) and a variable amount of crosslinker, ethylene glycol dimethacrylate (EGDMA), were mixed with Irgacure 651 (IRG651) as photoinitator (Figure 1B). The statistical copolymer employed as additive contains fluorinated monomer units, more precisely poly(methyl methacrylate-co-2,2,2-trifluoroethyl methacrylate) p(MMA-co-TFMA) (Mn=11318 g/mol, PD=1.10, 23%mol of TFMA) and was synthesized by Atom Transfer Radical Polymerization (ATRP) (Figure 1C). Films of these mixtures deposited onto glass substrates were irradiated with no filtered UV light. A spacer of 50 µm was employed to ensure a constant film thickness.

In order to get further insight about the photopolymerization reaction photo-DSC experiments were carried out [33]. This technique allowed us to establish the optimal composition of photoinitiator and crosslinkable monomer mixture in the initial blend. DSC analysis of these systems evidenced that polymerizations do not occur either in absence of light or without photoinitiator in the initial mixture at room temperature (results not shown here).

The DSC traces obtained for different samples irradiated with UV light with variable quantity of photoinitiator are depicted in Figure 2A. The isothermal profiles have a characteristic behaviour with an abrupt rise of the -ΔH (which is proportional to the rate of polymerization) at the beginning of the reaction, when the light is switched on, followed by a slow decline as the monomer reacts. This is caused by a combination of both the relative increase in the propagation with almost no termination at this initial stage and the increase in the concentration of growing radicals. After a rapid increase, the reaction rate decreases due, on the one hand, to the monomer consumption in the system; on the other hand, to the fact that propagation reactions become diffusion controlled because of the reduction in the monomer mobility when vitrification is approached. When a difunctional monomer undergoes crosslinking reactions and forms complex polymeric networks the viscosity of the system rises

very rapidly, and when gelation of the medium is reached the reaction diffusion mechanism starts to control the reaction. The propagating radicals are trapped into the matrix and they slowly add unreacted functional groups until they encounter a second radical for termination.

In some cases, a second increase of the polymerization rate was observed as depicted in Figure 2A. In spite of the decrease of the reaction rate due to the termination process, in these particular cases (5% of IRG for all the compositions) the reaction rate increases again to a certain extent as evidenced by the presence of a second peak. This effect, previously described for other systems, can be explained by the fact that an increase of the viscosity leads simultaneously to two effects. On the one hand, the gel effect or autoacceleration that arises from a reduction in the rate of diffusion-controlled termination resulting from a reduction of the mobility of the growing radical chains. On the other hand, the reduction of the oxygen diffusion into the samples allows the reaction to continue and thus decreasing the termination [34]. It has to be mentioned that the effect of oxygen inhibition on free radical polymerization is well known. Oxygen is an efficient scavenger of both initiating and propagating species in radical polymerization and this process is usually extremely fast. The rate constants for quenching carbon-centred radicals by oxygen molecules, for example, generally exceed 10^9 $M^{-1}s^{-1}$, which is at the diffusion limit [35].

Two independent parameters were analyzed to optimize the composition employed for the formation of the network, i.e. the amount of photoinitiator in the mixture and the relative amount of crosslinking agent (EGDMA) to monomer (MMA). The curves depicted in Figure 2A correspond to samples composed of 85v/v% of MMA and 15v/v% of EGDMA and a variable amount of IRG651 from 2 to 10wt%. The sample with 10wt% of IRG651 exhibits a single peak indicating the fast polymerization and collapse of the system with a drop in the ΔH at 9 minutes most probably due to the vitrification of the matrix. Using 5wt% and 2wt% of IRG651 the curves indicate the initiation and propagation of the polymerization and the presence of an autoacceleration process. The autoacceleration detected in both cases appears at different irradiation times, i.e. after three minutes using 5wt% and after ten minutes using 2wt% of IRG651. Thus, a decrease of the amount of the photoinitiator produces a decrease in the reaction rate and thus the system vitrifies later. On the other hand, further increase in IRG651 concentration up to 10wt% is not directly related with high monomer conversion. The effect caused by excessive levels of light absorbing photoinitiating radicals, well known termed as “inner filter effect” [36], caused by an attenuation of the radiation intensity through the

sample by preferential absorption of IRG651 in the upper layers, as well as a drastic enhancement of the termination step by recombination with the primary radicals, produced a loss of the polymerization rate and the possibility of the presence of unpolymerized monomer in the photocured sample.

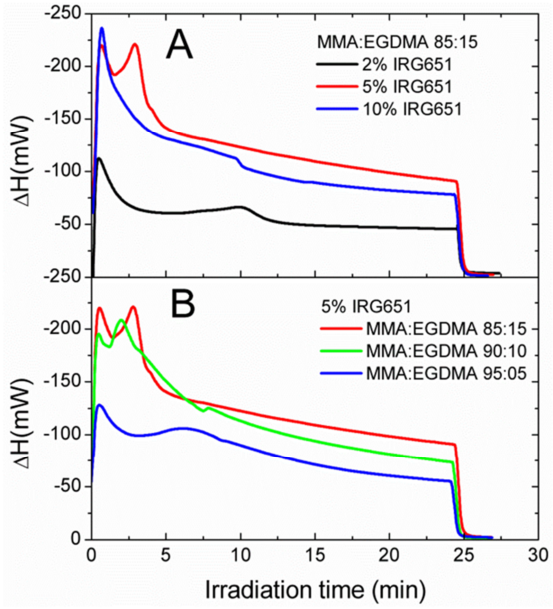

Figure 2. *a) DSC studies of different samples with composition MMA/EGDMA 85:15 and variable weight percentage of photoinitiator IGR651. b) DSC studies of different samples with compositions MMA/EGDMA in different proportion and 5wt % of IGR651.*

Similarly, in Figure 2B are depicted the photopolymerization DSC curves of MMA and EGDMA obtained varying the relative amount of both monomers while the amount of photoinitiator was optimized and keep constant at 5wt%. According to these results, and as expected, an increase of the amount of crosslinking agent produces a reduction of the photoinitiation time required to obtain the network.

Based on the above described results in this study we employed for the next experiments a mixture of MMA/EGDMA 85:15 and 5wt% of photoinitiator, besides this composition appears to be reactive enough to carry out the polymerization within few minutes (5 to 7 minutes) so that MMA evaporation can be neglected. Equally, the initiation and

propagation processes are produced first and the construction of the network occurs two or three minutes later. This behaviour help to achieve higher polymerization conversions compared to fast processes in which both processes occur simultaneously. Moreover, a relative fast network formation will favour the formation of well-defined surface patterns since diffusion will be decreased.

The irradiated films have been studied by FTIR-ATR (Figure 3A and B). In this graph are represented the spectra of mixtures MMA/EGDMA 95:5, 90:10 and 85:15 and for clarity purposes FTIR spectra of commercial PMMA and PEGDMA crosslinked by using UV light are also included. The bottom Figures 3A and 3B show an amplification of the region between 720 – 1030 cm^{-1} where the C=C bond can be easily detected at 812 cm^{-1}. The limited resolution of these signal in the spectra shown in Figure 3 difficult the quantification of the composition within the resulting photopolymerized films. However, a general trend in which the double bond signal increased with the amount of PEGDMA can be observed.

While in the composition with less percentage of EGDMA the number of free double bonds C=C is negligible, when the percentage of difunctional monomer in the mixture increases the number of these free bonds increases as well. Thus, a high percentage of EGDMA is associated to non-polymerized double bonds remaining in the network. From a chemical point of view, unreacted monomer with residual double bonds may lead to a variety of side-reactions. In order to improve the conversion of the polymerization reaction, and prevent from side reactions we additionally annealed the films under vacuum during 10 days at 130°C. The annealing process will thus produce two different effects: first, the conversion of the polymerization reaction will be enhanced and second, as we will see in the next paragraph, will have an effect on the variation of the surface composition. The first effect can be evidenced by FTIR as depicted in Figure 3B. In this graph are represented the spectra of a mixture MMA/EGDMA 90:10 before and after annealing and the FTIR spectra of commercial PMMA and PEGDMA crosslinked also by using UV light. The FTIR of the irradiated sample before annealed revealed the presence of residual double bonds in the polymer network. This signal at 812 cm^{-1} disappeared upon annealing and the spectra is similar to that of commercial PMMA. Thus, annealing favored the complete conversion of the residual double bonds.

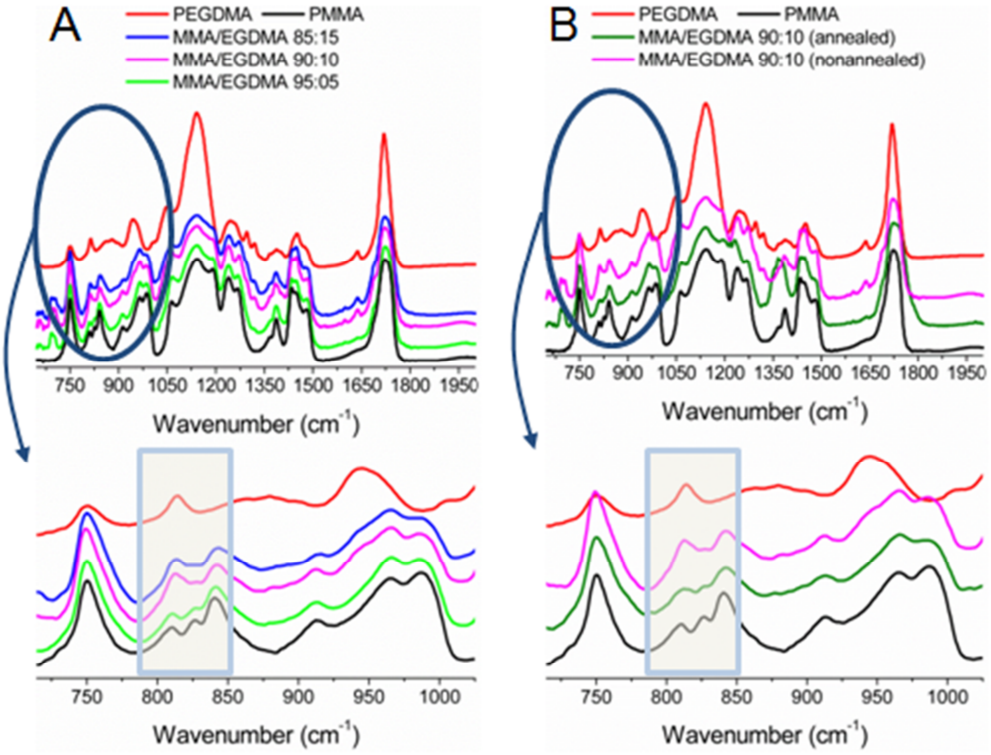

Figure 3. *a) FTIR spectra of the films obtained with initial mixtures MMA and EGDMA of 85:15, 90:10 and 95:05. The bottom graph is an amplification of the region 720-1030 cm^{-1}. b) Comparison of the FTIR spectra from a mixture of MMA/EGDMA 90:10 before and after annealing to air at 130ºC during 10 days. All the mixtures include 10 wt% of p(MMA-co-TFMA) and PEGDMA and PMMA spectra are included for comparative reasons.*

The mixtures above described were placed between two glass covers (either silanized or cleaned with piranha) using a spacer of 50 µm and irradiated by using UV light through a mask on the top as schematized in Figure 1A. As a consequence, the irradiated areas were photopolymerized and crosslinked whereas the non-exposed areas, under the grid, should remain unreacted. Upon rinsing the film with hexane, the non-crosslinked areas (soluble in hexane) could be removed. The irradiated areas remain unchanged since the formed polymer network formed by exposure to UV light is insoluble. As a consequence a surface pattern as shown in Figure 1D was created.

The lateral pattern resolution is limited by the high diffusion of the monomers in the initial polymerization stage. As a consequence, there exists also crosslinked material in the non-exposed areas. However, changes in the mixture composition and the incorporation of p(MMA-co-TFMA) clearly affect the quality of the surface pattern. The height difference between the non-irradiated and the irradiated areas versus the amount of crosslinking agent (EGDMA) are represented in Figure 4A. Equally, Figure 4A depicts the image profiles obtained by SEM of the samples with compositions MMA/EGDMA 85:15, 90:10 and 95:05 in which two different amounts of p(MMA-co-TFMA) were added (10wt% and 20wt%).

The films obtained from mixtures with increasing amount of EGDMA exhibit better resolved patterns since the depth increases with the amount of EGDMA. The height difference between the irradiated and non-irradiated areas increase with the percentage of EGDMA, as can be observed in the graph of the Figure 4A where in the 10wt% of copolymer series the average highs are 8.1 µm, 9.5 µm and 10.8 µm whilein the 20wt% series these highs are 8.7 µm, 10.4 µm and 13.0 µm, respectively. An increase of the EGDMA amount raises the viscosity of the photopolymerizable mixture thus limiting the diffusion of the monomers and improves the depth reached. The differences observed between the two series i.e. 10wt% of copolymer and 20wt% of copolymer have the same explanation. Since the copolymer introduced in the mixture is a solid, (which rises the viscosity of the sample), to the best of our knowledge, we can assume these differences in the pattern resolution to the lower mobility of the monomers in the mixture containing higher amount of copolymer.

The systems developed in this manuscript were additionally designed to exhibit variable surface chemical composition. The copolymer incorporated in the network can significantly modify the surface functionality upon migration to the polymer interface. This effect known as surface segregation has been already employed to control the surface composition of interfaces but their use has been limited to planar films. In our particular case, we formulated mixtures in which structuration and surface segregation (to modify the chemical functionality) can be simultaneously obtained.

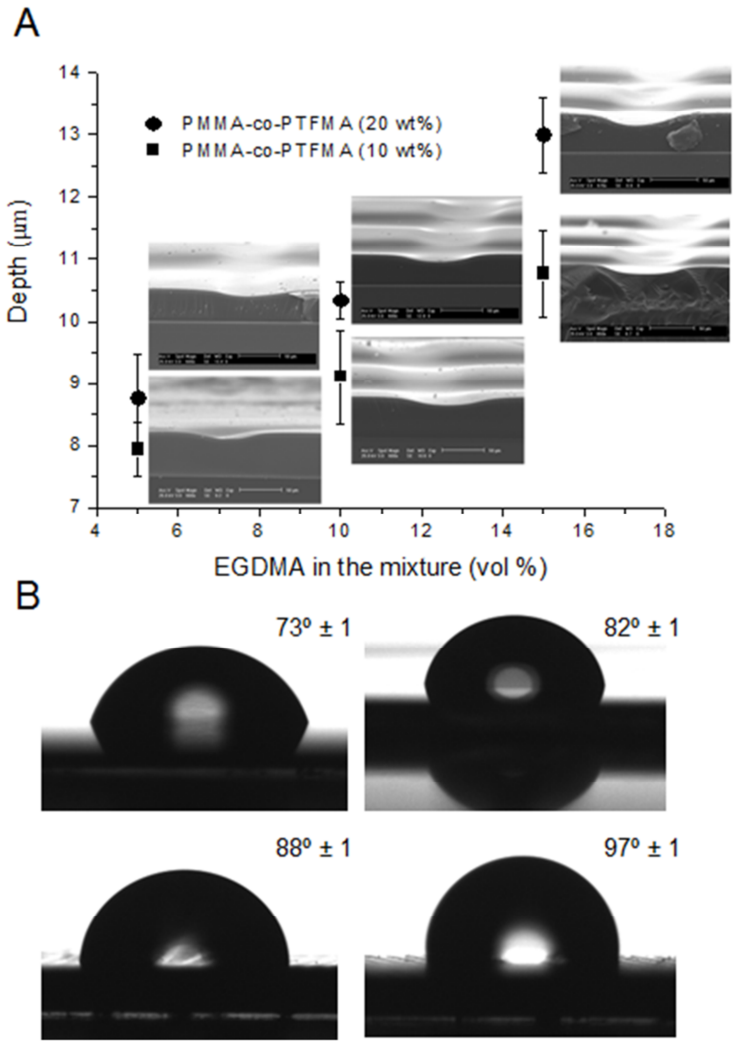

Figure 4. *A) Relation between the percentage of EGDMA and the height differences between the exposed and non-exposed areas. Squares correspond to a series of mixtures MMA/EGDMA with 10wt% of fluorinated copolymer and circles to the same mixtures but with 20wt% of fluorinated copolymer. Insets: SEM cross section images of each pattern. B) Contact angle measurements of films of PMMA (a), p(MMA-co-TFMA) (b), a network from a mixture p(MMA/EGDMA) 85:15 with 10wt% of p(MMA-co-PTFMA) and either a hydrophilic cover (c) or a hydrophobic cover (d). In both experiment photomask with 100 µm hole has been used.*

Information about the surface chemical composition was obtained by using XPS and contact angle measurements. The XPS results are summarized in Table 1. The values contained in Table 1 are representative from annealed and non-annealed samples, samples in which the amount of fluorinated copolymer has been varied and samples that have been prepared using either a silanized cover or a cleaned glass cover. The most significant changes on the chemical composition were obtained depending on the hydrophilicity of the cover employed before the irradiation. Whereas the employment of a hydrophilic glass leads to surfaces with low fluorinated content (less than 3%) the use of hydrophobic covers favours the migration of the fluorinated copolymer towards the polymer/cover interface during the photopolymerization. As a consequence, values of up to 6% - 8% of fluorinated at the surface were obtained for polymer networks containing 10wt% and 20wt% of copolymer by using hydrophobic covers. This effect can be explained by the low surface energy of the trifluorethyl moieties present in the copolymer structure that compensate the balance between the free energy gain associated with the surface tension and the free energy cost of demixing from the bulk [37].

Table 1. *XPS studies of samples MMA/EGDMA 85:15 with variable amount of p(MMA-co-TFMA), % atomic (Source RX Mg non-monochromatic, Ep=40 eV, correction Scofield, incertitude relative 5%).*

Sample number	Additive Composition [wt%]	Silanized cover	Annealed	Surface Chemical Composition		
				%C	%O	%F
1	10	Yes	No	71.7	22.0	6.2
2		No	No	79.9	18.2	1.9
3		Yes	Yes	70.6	22.3	7.1
4		No	Yes	77.4	19.7	2.8
5	20	Yes	No	67.5	24.7	7.8
6		Yes	Yes	71.5	21.6	6.9

When the photopolymerization was accomplished, the cover was removed and some of the films were then annealed to air at 130°C during 10 days. The effect of the annealing process can be analyzed by comparison of either samples 1 and 3 or samples 2 and 4. In both

cases the annealing leaded to an increase of the fluorinated content at the interface thus evidencing a surface migration of the copolymer towards the interface. As expected, an increase in the amount of copolymer employed in the initial mixture produces surfaces with higher content of copolymer. However an increase from 10 to 20wt% only produces an increase of ~1.6% in the fluorinated amount at the surface. This is most probably due to a saturation of the surface mostly composed of p(MMA-co-TFMA). Theoretically, a surface formed exclusively by the copolymer could lead to fluorinated contents at the surface of 8.5% taking into account that the copolymer has only a molar composition of 23% of TFMA monomer and 77% of MMA. This estimated value of the maximum fluorinated groups present at the surface is close to the experimental value obtained for the mixture containing 20wt% of copolymer, i.e. 7.8%.

The results obtained from the contact angle measurements are in good agreement with those described above resulting from the XPS measurements (Figure 4B). The contact angle values measured evidenced significant changes on the wettability not only due to the chemical composition of the surface but also due to the structuration at the micrometer length scale obtained by UV lithography. Whereas the contact angle values of planar films prepared by spin coating of both pure PMMA and p(MMA-co-TFMA) are 73° and 82° respectively, the structured films independently of the cover employed and using only 10wt% of p(MMA-co-TFMA), exhibit contact angles above 88°. It is generally admitted that below 90°, i.e. in the case of hydrophilic surfaces, the surface structuration should increase the contact angle [38]. However in our case, structuration leads to higher contact angles. The contact angles measured in planar films are close 90° so that structuration induces a change in the wettability to hydrophobic behaviour. However, this result evidences the role of the pattern on the wettability of the films.

More interestingly, the structured films prepared using a hydrophobic cover, possess contact angles ~10° higher than the structured films prepared using a hydrophilic cover. Thus, according with the XPS results the structured films prepared using hydrophobic covers possess a higher content of fluorinated groups at the surface and are more hydrophobic.

Conclusions

In summary, herein we have described a new procedure based on the design and preparation of structured and functional surfaces by combination of two approaches simultaneously developed. On the one hand, UV-light lithography was employed to create a surface pattern. On the other hand the design of the mixture containing a p(MMA-co-TFMA) copolymer allowed us to modify the surface chemical composition by surface segregation of the copolymer towards the polymer/cover or the polymer/air interface. Moreover, the functionality of the copolymer is enhanced by the surface pattern created. As a consequence both the structuration and surface functionalization influence the wettability of the films. The approach described herein can be employed with a large variety of systems based on photopolymerizable formulations and the final functionality will depend exclusively on the amount and type of functional groups contained in the additive employed for the mixture. Thus, taking into account both the recent developments on UV soft lithography, the large variety of different patterns (both in size, from micro- to nano-, and the type of drawing) that can be obtained at the surface and the possibility of modifying the surface composition (both in density and type of functional groups), the functional and microstructured polymeric systems presented in this manuscript open a wide range of possibilities and offers new challenges to the applicability for these new smart surfaces. These applications can verse either to bioengineering (from cell scaffolds or controlled growth of cells to cytophobic surfaces, only varying the employed copolymer additive) or to the preparation of hydrophobic/hydrophilic surfaces with special properties like adhesion or self-cleaning. In any case, this new developed method has the advantage of being fabricated in a single step which allows savings either in costs or time.

Acknowledgements

The authors gratefully acknowledge support from the Consejo Superior de Investigaciones Científicas (CSIC). Equally, this work was financially supported by the Ministerio de Ciencia e Innovacion (MICINN) through MAT2011-22861 and MAT2009-12251. M. Palacios thanks the Ministerio de Education for the FPU fellowship and M. Liras thanks to the CSIC for the JAE-Doc contract.

CAPÍTULO II.2: Estructuración superficial mediante fotolitografía a partir de películas de poliestireno (PS)

En el capítulo 2 de esta sección se consigue la creación de diversas estructuras de PS a partir la degradación y/o reticulación por irradiación con luz UV de películas poliméricas preparadas a partir de poliestireno (PS) comercial. Las diferentes estructuras se han generado empleando una única fotomáscara y variando, únicamente, las condiciones experimentales de la irradiación, así se han llegado a conseguir micro/nanoestructuras de dimensiones hasta 25 veces menores que el tamaño de la máscara empleada.

Una vez puestas a punto las condiciones experimentales que nos permiten generar cada tipo de estructura, éstas se han aplicado en filmes poliméricos funcionalizados. Los filmes se preparan a partir de nuevos copolímeros de naturaleza estirénica, sintetizados por ATRP, que incluyen bloques de diversa funcionalidad: fluorados (hidrofóbico), poliácido acrílico (hidrofílico) y poliácido glutámico (hidrofílico).

Sobre las micro/nanoestructuras generadas se consigue el anclaje específico de biomoléculas (en nuestro caso proteínas) o bacterias, sólo selectivamente en aquellas zonas de la superficie que están funcionalizadas. En primer lugar, utilizando las superficies de poliácido glutámico es posible el anclaje de una proteína fluorescente. Una vez demostrada la adhesión selectiva de proteínas se ensaya con éxito la inmovilización selectiva de bacterias fluorescentes sobre superficies de poliácido acrílico, consiguiendo incluso superficies tan definidas que permitan alinear o incluso llegar a aislar las bacterias.

Este capítulo ha dado lugar a tres artículos científicos que se expondrán a continuación:

Artículo 2: *Constructing robust and functional micropatterns on polystyrene surfaces by using deep UV irradiation*

En este artículo se describe un nuevo método de estructuración de superficies poliméricas basado en la aplicación de fotolitografía sobre las mismas, donde a partir de procesos de fotoentrecruzamiento y fotodegradación de películas de PS comercial se consigue la creación de diversas estructuras superficiales: estructura tipo caja cerrada, caja abierta, red o agujas. Estas diferentes estructuras se consiguen a partir del empleo de una única fotomáscara, variando únicamente las condiciones experimentales de irradiación de luz.

Una vez se han conseguido estas estructuras en PS, esta nueva metodología se ha aplicado, en un primero momento a un copolímero que contiene segmentos fluorados. Se ha estudiado la mojabilidad de las películas, que como era de esperar depende tanto de la naturaleza del copolímero sintetizado como de la morfología de la estructura superficial generada

Langmuir

Article

pubs.acs.org/Langmuir

Constructing Robust and Functional Micropatterns on Polystyrene Surfaces by Using Deep UV Irradiation

Marta Palacios, Olga García,* and Juan Rodríguez-Hernández*

Department of Chemistry and Properties of Polymers, Instituto de Ciencia y Tecnología de Polímeros (ICTP-CSIC), Juan de la Cierva 3, 28006 Madrid, Spain

ABSTRACT: We report the preparation of different surface patterns based on the photo-cross-linking/degradation kinetics of polystyrene (PS) by using UV light. Upon exposure to UV light, PS can be initially cross-linked, whereas an excess of the exposure time or intensity provokes the degradation of the material. Typically photolithography employs either positive or negative photoresist layers that upon removal of either the exposed or the nonexposed areas transfer the pattern of the mask. Herein, we present a system that can be both negative and positive depending on several aspects, including the irradiation time, intensity, or presence of absorbing active species (photoinitiators) using a general setup. As a result of the optimization of the time of exposure and the use of an appropriate cover or the incorporation of an appropriate amount of photoinitiator (in this particular case IRG 651), different tailor-made surface patterns can be obtained. Moreover, changes of the chemical composition of the polystyrene using, for instance, block copolymers can lead to surface patterns with variable functional groups. In this study we describe the formation of surface patterns using polystyrene-*block*-poly(2,3,4,5,6-pentafluorostyrene) block copolymers. The introduction of fluorinated moieties clearly modifies the wettability of the films when compared with that of the same structures obtained with PS. As a consequence we present herein a patterning methodology that can simultaneously vary not only the morphology but also the surface chemical composition.

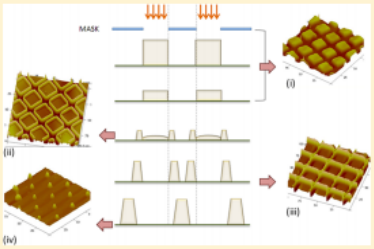

INTRODUCTION

The control of polymer interfaces is crucial to adapt the material for the requirements of a precise application. The

Equally, PS has been functionalized by using different approaches. For instance, Reinecke et al. reported the preparation of transparent polystyrene substrates by using a controllable surface chlorosulfonation reaction.[31] UV has also

Constructing robust and functional micropatterns on polystyrene surfaces by using deep UV irradiation

Marta Palacios, Olga García* and Juan Rodríguez-Hernández*

Department of Chemistry and Properties of Polymers

Instituto de Ciencia y Tecnología de Polímeros, (ICTP-CSIC),

Juan de la Cierva 3, 28006 Madrid, Spain.

Correspondence to:

Olga García (ogarcia@ictp.csic.es)

Juan Rodríguez-Hernández (rodriguez@ictp.csic.es)

Abstract

We report the preparation of different surface patterns based on the photocrosslinking/degradation kinetics of polystyrene (PS) by using UV-light. Upon exposure to UV-light PS can be initially crosslinked whereas an excess of the exposure time or intensity provokes the degradation of the material. Typically photolithography employs either positive or negative photoresist layers that upon removal of either the exposed or the non-exposed areas transferred the pattern of the mask. Herein, we presented a system that can be both negative and positive depending on several aspects including irradiation time, intensity or the presence of absorbing active species (photoinitiators) using a general setup. As a result of the optimization of time of exposure, the use of an appropriate cover or the incorporation of an appropriate amount of photoinitiator (in this particular case IRG 651) different tailor made surface patterns can be obtained.

Moreover, changes of the chemical composition of the polystyrene using for instance block copolymers can lead to surface patterns with variable functional groups. In this study we describe the formation of surface patterns using PS-*b*-P5FS block copolymers. The introduction of fluorinated moieties clearly modifies the wettability of the films when compared with the same structures obtained with PS. As a consequence we present herein a patterning methodology that can simultaneously vary not only the morphology but also the surface chemical composition.

Introduction

The control of the polymer interfaces is crucial in order to adapt the material for the requirements of a precise application. The design of the surface has to take into account the properties required for their final use such as biocompatibility, adhesion, wear resistance, wettability or optical behavior among others. In order to adapt the material for a targeted purpose several surface modifications can be carried out including the surface functionalization, modification of the crystallinity, creation of surface microdomains and morphology or variations on the roughness and topography [39-44]. In particular, from a chemical point of view several studies evidenced the significance of the control of both topography and functionality. An appropriate surface functionalization and patterning can lead

to materials with adhesive [45-47] or lubricant [48-50], biocompatible [51] or antifouling [52, 53] or even superhydrophilic [54-58] or superhydrophobic properties [59].

Among the polymers employed as models for surface functionalization and patterning polystyrene (PS) has been extensively employed. PS has been patterned by using different techniques including hot embossing [60], breath figures [61-63], polymer dewetting on chemically patterned substrates [64, 65], by using soft-lithography to pattern silicon substrates grafted with polystyrene chains [66], by UV-laser radiation to produce micro-drilling [67] or by scanning electrochemical microscopy [68]. Patterning has been also obtained by dewetting in thin polymer films by spatially directed photocrosslinking [65].

Equally, PS has been functionalized by using different approaches. For instance, Reinecke *et al.* reported the preparation of transparent polystyrene substrates by using a controllable surface chlorosulfonation reaction [69]. UV has been also employed to modify the surface chemical composition [70-72] or in combination with O_3 [73] just to mention few of them.

As a result of either surface functionalization or surface patterning steps the applications of the resulting materials is rather broad. For example, Knudsen et col.[74] proposed the use of polystyrene based resists as a cheaper alternative to other commercially available resists. Patterned polystyrene has been also extensively employed for biomedical purposes for instance in cell adhesion studies [68], the fabrication of medical devices able to measure the electrical activity of cells [67] or to improve the hemocompatibility [51].

Herein we propose the use of photolithography with UV light and the design of polystyrene based polymers to both modify structure and functionality simultaneously. Compared to previous approaches the possibility of modify both aspects in a single step supposes a clear advantage. Moreover both crosslinking [63] and degradation [75] produced when a photosensitive polymer is irradiated will play a key role on the resulting surface pattern. We describe how UV-photolithography can be used to obtain different structures with the same mask throughout the experiments as a result of the fine tuning of the photodegradation/crosslinking reactions. As a consequence we will describe how to vary the surface pattern from boxes to needles using two different polymers as a matrix, i.e. polystyrene

(PS) and a synthetic copolymer polystyrene-*block*-poly(2,3,4,5,6-Pentafluorostyrene) (PS-*b*-P5FS).

Experimental section

Polystyrene (PS), Irgacure 651 (IRG 651) (Ciba®), and the rest of solvents were employed as received. Glasses with 0.15 mm thickness (Menzel-Glaser) were employed as covers to limit the UV-light exposure. As a substrate we employed microscope slides with a 1 mm thickness (Menzel-Glaser). The masks used for this study were grids typically used for transmission electron microscopy (copper, 25μm pitch).

Polystyrene-*block*-poly(2,3,4,5,6-Pentafluorostyrene) (PS-*b*-P5FS) was prepared by ATRP in two consecutive polymerization steps following previously reported procedures [76].

The ^{1}H and ^{13}C NMR spectra were registered at room temperature in $CDCl_3$ solution in Varian INOVA-300. Chemical shifts are reported in parts per million (ppm) using as internal reference the peak of the trace of deuterated solvent (δ 7.26). Size exclusion chromatography (SEC) analyses were carried out on chromatographic system (Waters Division Millipore) equipped with a Waters model 410 refractive-index detector. Dimethylformamide (99.9%, Aldrich) containing 0.1% of LiBr, was used as the eluent at a flow rate of 1 mL min^{-1} at 50 ºC. Styragel packed columns (HR2, HR3 and HR4, Waters Division Millipore) were used. Poly(methyl methacrylate) standards (Polymer Laboratories, Laboratories, Ltd.) between $2.4x10^{6}$ and $9.7x10^{2}$ g mol^{-1} were used to calibrate the columns. The molecular weights were estimated against poly(methyl methacrylate) standards.

Atomic force microscopy (AFM) measurements were conducted on a Multimode Nanoscope IVa, Digital Instrument/Veeco operated in tapping mode at room temperature under ambient conditions. All the images are height images in which the clearer color corresponds to elevated areas whereas the darker color is related to deeper areas. The height measured is related to the crosslinking. Elevated areas result upon crosslinking since these areas are not removed upon rinsing. On the contrary, deeper areas correspond either to non-crosslinked areas or degraded.

For the preparation of the thin films a 30 mg/mL solution of PS homopolymer in THF was spin coated onto glass covers at 2000 rpm during 1 min. These films were then irradiated under UV spot light irradiation from source Hamamatsu model lightningcure L8868 provided by an Hg-Xe lamp with 200W power. The incident light intensity was focused on the samples with an optic fiber at a constant distance of 5.5 cm with either 50% or 100% of the total intensity of the lamp using a TEM copper grid as a mask. After irradiation the films were rinsed with THF in order to remove both degraded and non-crosslinked polymer.

Results and discussion

Polystyrene is one of the most employed commodity polymers nowadays and the photoinitiation degradation, crosslinking and oxidation reactions in air by UV light have been extensively explored and are now well known [74, 77-79]. It is generally admitted that, as described in Scheme 1, during the UV irradiation of PS, radicals are produced that can follow two types of mechanisms [80, 81]. When the reaction is carried out under vacuum, with no or low amount of oxygen, polystyrene can either produce the crosslinking between different chains or reactions of disproportion and unsaturation. The latter, with available double bonds, can eventually react with other radical species and form crosslinked structures. On the contrary, in the presence of oxygen, the proton abstraction from the polymer chain has associated an addition of an oxygen molecule. As a consequence, the oxygen produces the β-scission thus leading either to degradation of the polymer chain or acting as a bridge between two polystyrene chains. [82]

According to the above mentioned, by using UV-irradiation, PS can have a crosslinked structure thus providing additional chemical and thermal stability to the film. However, due to the variety of chemical processes (cross-linking, chain scission and photooxidation) [60-62, 64, 71, 75] occurring simultaneously in PS films upon exposure to UV light the experimental parameters that determine the primary reaction need to be controlled. Herein, we will first describe how the control over the degradation/crosslinking kinetics by modifying the environment (with and without oxygen), time of exposure and the use of a photoinitiator will allow us to prepare a large variety of surface patterns in one single step. Second, based on the variety of surface patterns obtained we will additionally modify the chemical composition. For that purpose we will use block copolymers, incorporating

hydrophobic moieties, in particular PS-*b*-P5FS, will permit the variation of the surface chemical composition and thus the surface properties such as the surface wettability.

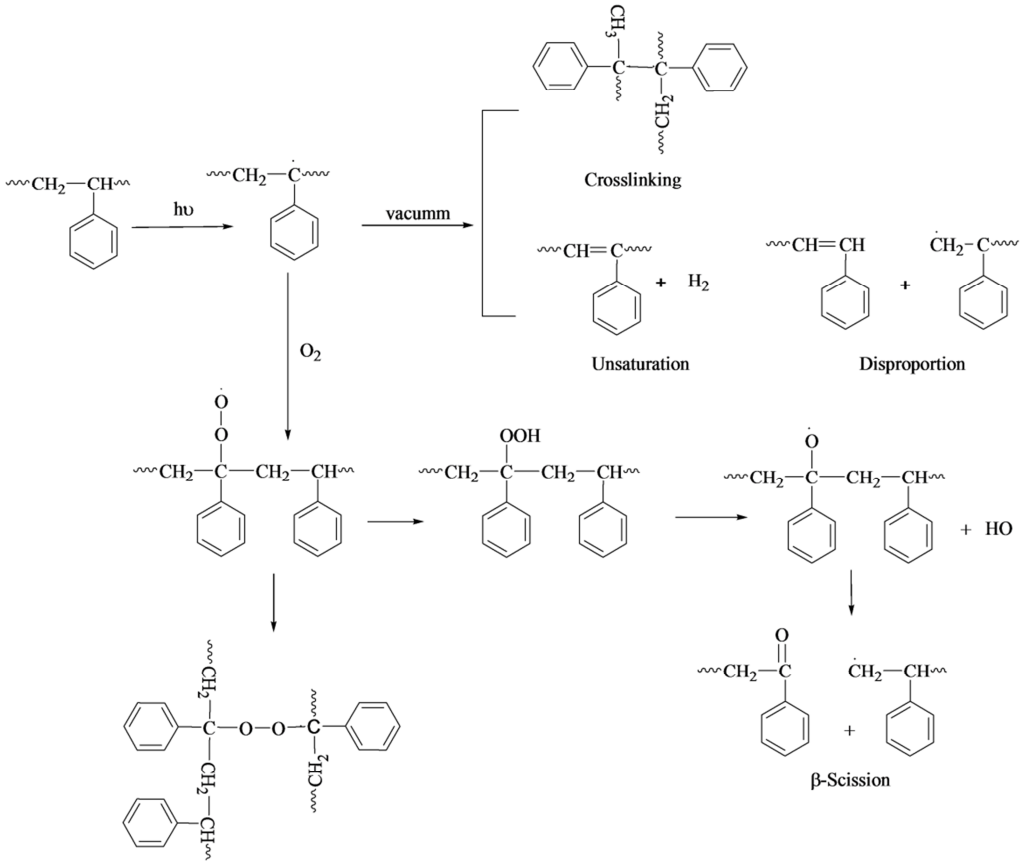

Scheme 1. *Reactions accomplished by PS upon irradiation with UV light. Depending on the presence or absence of oxygen the reaction mechanism can follow different reaction paths. Whereas in the absence of oxygen the reaction leads to crosslinking, in the presence of oxygen PS follow mainly β-scission reactions.*

The polystyrene thin films were prepared by spin coating from THF solutions (30 mg/ml). Spin coating allowed us to prepare films with controlled thicknesses by varying the solution concentration and rotation speed. Thicknesses of the films used throughout this study were varied between 280 nm and 420 nm as measured by AFM. The samples were irradiated at different times with a UV-light source at room temperature using a TEM copper grid as a mask. As a consequence, we obtained areas with different UV-light exposure during the

irradiation. After irradiation, the films were rinsed with THF, thus both degraded and non-crosslinked polymers were dissolved and removed while the crosslinked regions of the film remain insoluble.

In Figure 1, are depicted the AFM images of the PS films non-covered upon irradiation and subsequent rinsing varying the time of exposure to UV light from 15 minutes to 2 hours. As observed in the AFM images of the non-covered samples, upon 15 minutes of irradiation the films exhibit crosslinked polystyrene in the irradiated areas. After 30 minutes, the areas directly exposed to UV-light start to be degraded as indicated by the decrease in height observed in the images. Larger irradiation times produce a complete degradation of these areas. This result is in good agreement with the results reported by Kaczmarek et al. [75]. This group took advantage of the photodegradation of PS in a blend and selective removal of the photodegraded areas to induce changes in the final morphology of the film.

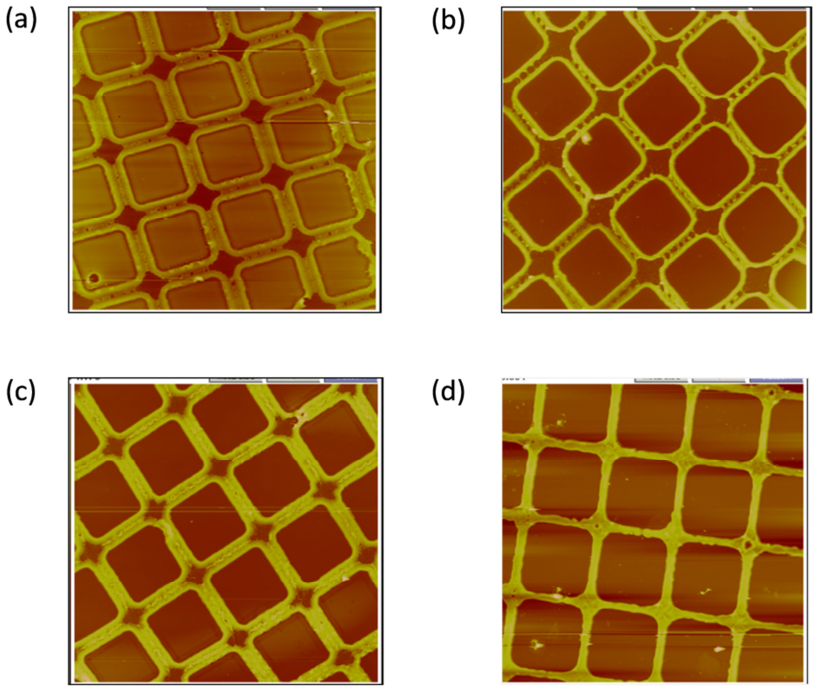

Figure 1. *AFM images of the microstructures formed by PS at different irradiation times (a to d for 15, 30, 60 and 120 minutes, respectively) using a 100% of light intensity. Films exposed to air.*

More interestingly, whereas degradation is the main mechanism when the irradiation times increase, the non-directly exposed areas exhibit a different behavior. An increase of the irradiation time produces the crosslinking reaction initially at the edge of the exposed-non exposed areas and later in the center of the non-exposed areas. To the best of our knowledge, the radicals may diffuse into the non-exposed and start to react from the edge to the center of the exposed-non exposed areas. The consequence of this process is the formation of complementary patterns as a result of the crosslinked polystyrene even if the film has not been exposed in these areas.

To further analyze the progression of the crosslinking reaction *vs.* degradation, in Figure 2 are depicted the cross sectional profiles of the AFM images obtained at different irradiation times for the samples above described, a sample covered with a quartz cover (in order to limit the presence of oxygen in contact with the film) and an additional non covered film irradiated using 50% of the maximum light intensity offered by the lamp employed (see experimental section). We can observe that the degradation of the areas directly irradiated is faster in those samples without cover for similar light intensities (100%) due to the presence of environmental oxygen that favors the photooxidation reaction to occur [83]. In addition, the crosslinking of the non-exposed areas also occurs quicker when no cover is used. On the contrary, the use of covers prevents, at least to some extent, the diffusion of oxygen into the film and the crosslinking reaction is favored at low irradiation times. Taking into account that the quartz covers employed do not absorb in the irradiation region we can assume that the kinetics of both degradation and polymerization decreased exclusively as a result of a reduction on the oxygen amount in contact with the film. As a consequence, the non-covered films crosslinking of the exposed areas was still observed after 30 minutes. The reduction of the UV-light intensity, series a, reduces the kinetics of the degradation process and the crosslinking of the exposed areas can be observed up to 1 h. Hence, the use of a cover or the reduction of the light intensity can be employed to finely tune the final pattern obtained.

The polymerization and degradation kinetics can be controlled not only limiting the oxygen in contact with the film but also by using a photoinitiator (herein we employ Irgacure 651) that can ‘a priori’ increase the crosslinking rate. In Figure 3 are depicted the AFM images for different polystyrene (covered with quartz) films varying the amount of IRG 651 within the film between 0 and 5wt%. IRG 651 has two effects on the photopolymerization kinetics. First, since the UV light employed has a maximum in the absorption wavelength of IRG 651, the

number of radicals created will increase and the initiation of the polymerization should occur faster. Second, an excess of the IRG 651 amount will favor the formation of a large amount of initiating radicals but will limit the crosslinking process increasing their recombination probability.

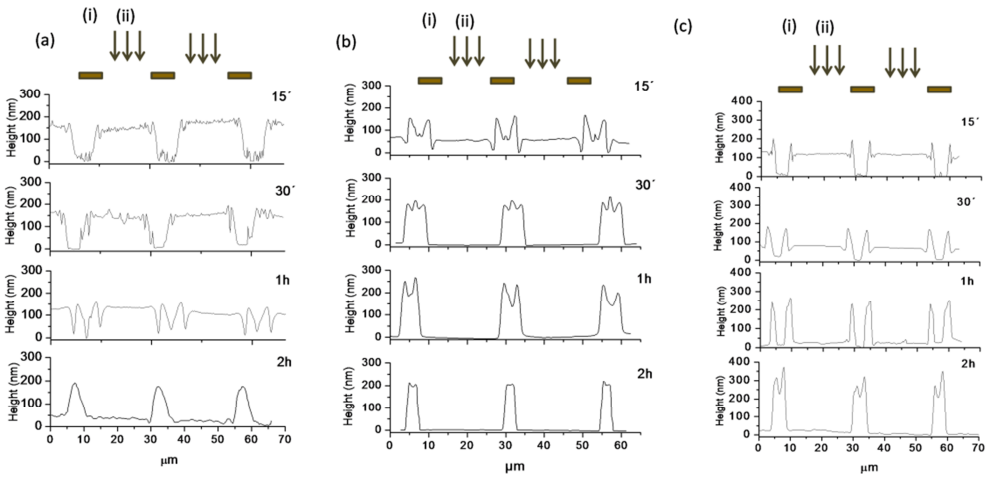

Figure 2. *Cross-sectional profiles of the crosslinked PS films non-covered a) 50% light intensity, b) 100% light intensity or c) 100% light intensity with a quartz cover at different irradiation times 15 min, 30 min, 1h and 2h.*

As shown in Figure 3, an increase of the amount of IRG 651 up to 3wt% favors the formation of radicals within the PS chains and enhanced the kinetics of chain scission. Above 3wt%, i.e. in the case of using 5wt%, degradation and/or recombination (i.e. preventing the formation of non-linear structures) in the directly irradiated areas is produced. Only in the sample irradiated 15 minutes the presence of crosslinked PS was observed. Similarly, the crosslinking in the non-irradiated areas is prevented as a result of the large number of radicals that recombine rather fast. This explains that after 2 h of irradiation the samples containing 1 and 3wt% of IRG 651 exhibit a larger crosslinking areas than the sample containing 5wt%.

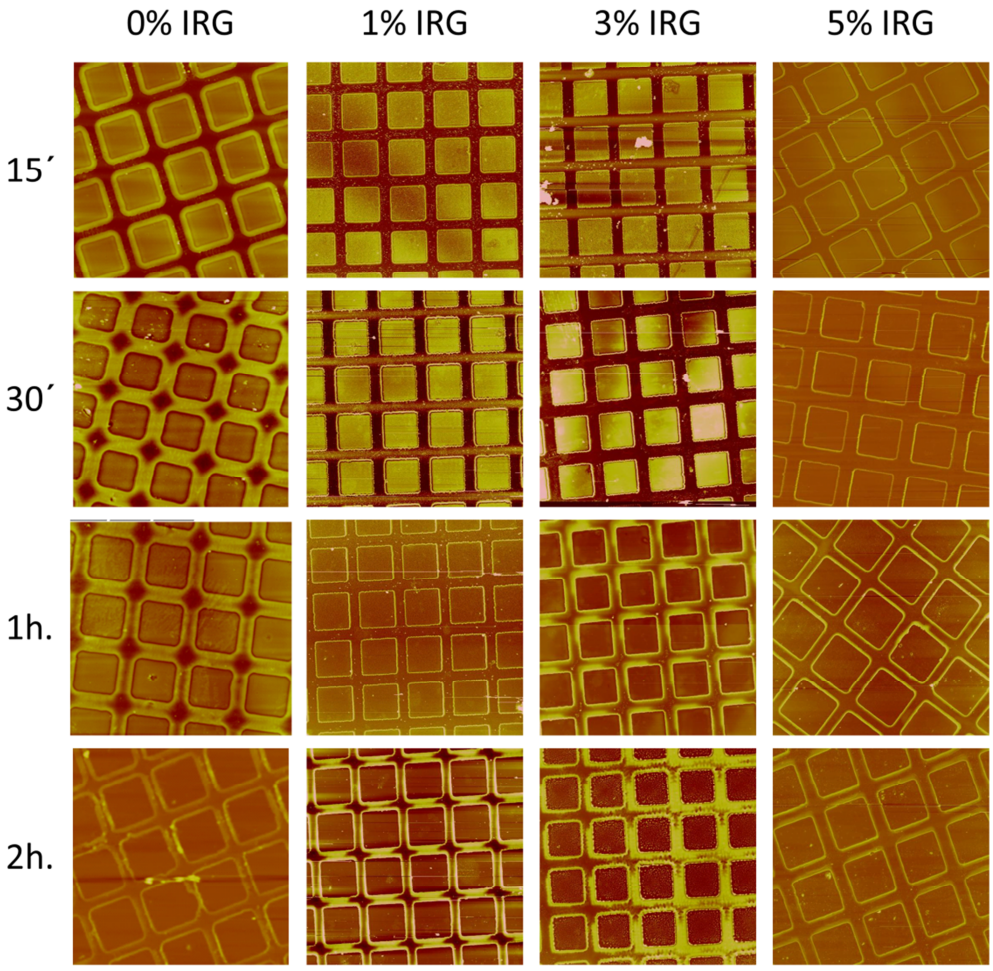

Figure 3. *AFM images of the films exposed to 100% UV-light for 15', 30', 1h and 2h. Moreover, the amount of IRG651 has been varied between 0 and 5wt%. Initially, an increase of IRG651 increases the number of radicals and favors both crosslinking and photodegradation to occur. However a large excess of IRG651 prevented the crosslinking as a consequence of the recombination of the initiating radicals created upon irradiation with UV-light.*

As depicted below, the kinetics of radical formation in the presence of a large amount of IRG 651 (5wt%) is rather fast and both degradation and recombination appears upon 15 minutes of irradiation. To control and tune the degradation kinetics a series of experiments

were carried out either using covers or leaving the film in contact with air while maintaining the same amount of photoinitiator. In figure 4 are depicted the cross sectional profiles and the AFM images obtained after irradiation of non-covered films (a), covered with a quartz (b) and using a glass cover (c).

Similar to what was observed in the previous cases, the introduction of a cover is expected to reduce the degradation of the directly irradiated areas avoiding a large amount of oxygen to be in contact with the film. However, as we will describe below the large amount of IRG 651 plays also an important role. In the series (a), i.e. films covered with quartz neither the exposed nor the non-exposed areas were crosslinked. We observe only a partial formation of polystyrene networks in the limit between the two. Due to the high amount of IRG 651 a large amount of radicals are created that can recombine, leading to linear structures and thus preventing from further crosslinking.

In the profiles of the series (b) we can distinguish the formation of crosslinked polystyrene in the directly irradiated areas even after 2h of exposure. This effect results from the fact that glass covers absorb in the region of the light employed and reduces the intensity of the light received by the film. As a consequence of the glass absorption the kinetics of radical formation decreased and the probability of recombination is reduced as well. The limitation on the number of radicals available for recombination favors the crosslinking reaction to occur.

In the series (c) concerning the films without cover, degradation occurs fast (less than 15 minutes) in the areas directly exposed to the UV-light. In this case, the large amount of radicals created during the irradiation react with the oxygen available favoring the degradation process instead of the recombination or even crosslinking. The areas of the films below the mask with lower amount of oxygen available are crosslinked. More interestingly, an increase of the exposure time continues the degradation even of the non-exposed areas. As a result, an additional surface pattern formed by pillars of crosslinked polystyrene can be obtained. Finally, too long irradiations will also produce the degradation of these pillars.

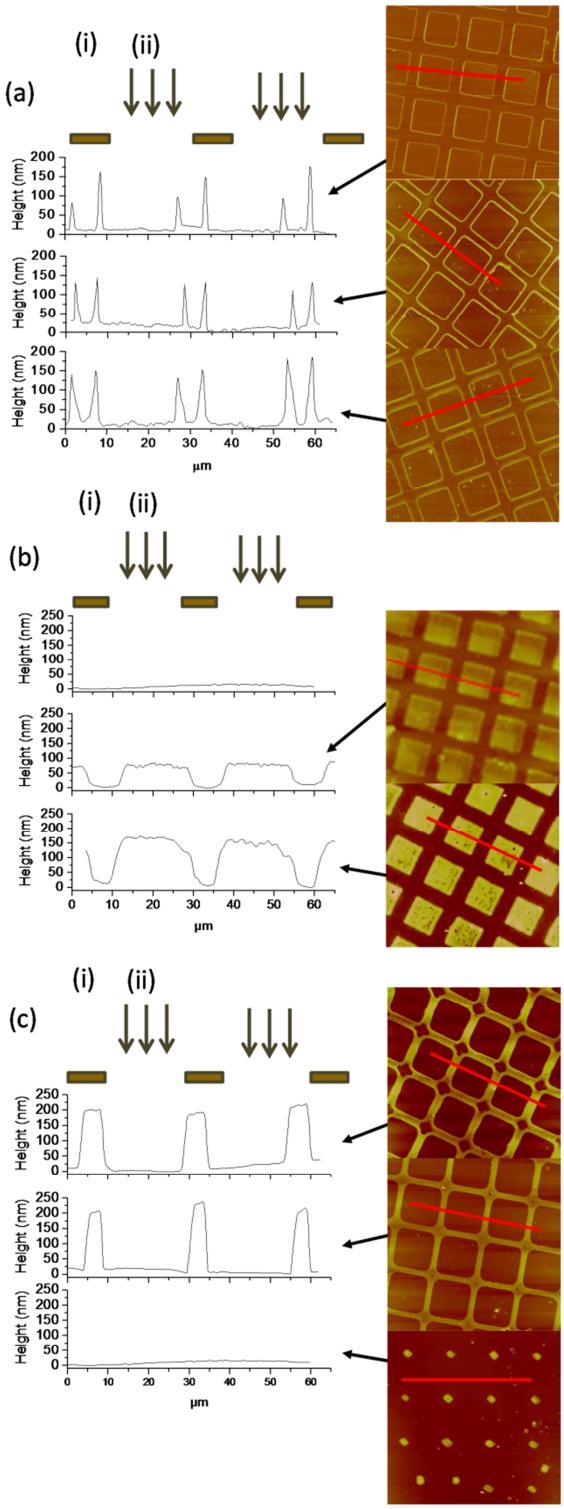

Figure 4. *AFM cross-sectional profiles polystyrene samples PS with 5wt% of IRG 651 irradiated at 100% total lamp intensity at three different exposure times 30 minutes, 1h and 2h: a) with quartz glass, b) with standard glass and c) non-covered.*

As a result of the combination of time of exposure, the use of an appropriate cover or the incorporation of an appropriate amount of photoinitiator (in this particular case IRG 651) different surface patterns can be tailor made. In Figure 5 are illustrated the different patterns observed by adjusting the previous experimental parameters and the modeled cross sectional profiles of each pattern. Short irradiation times, using mainly covers on the top of the samples protects from photooxidation, leads to crosslinked structures located in the directly exposed areas (i). In this case the non-exposed areas are protected by the mask. Since polystyrene do not receive UV-light remains linear and can be easily removed by rinsing with THF.

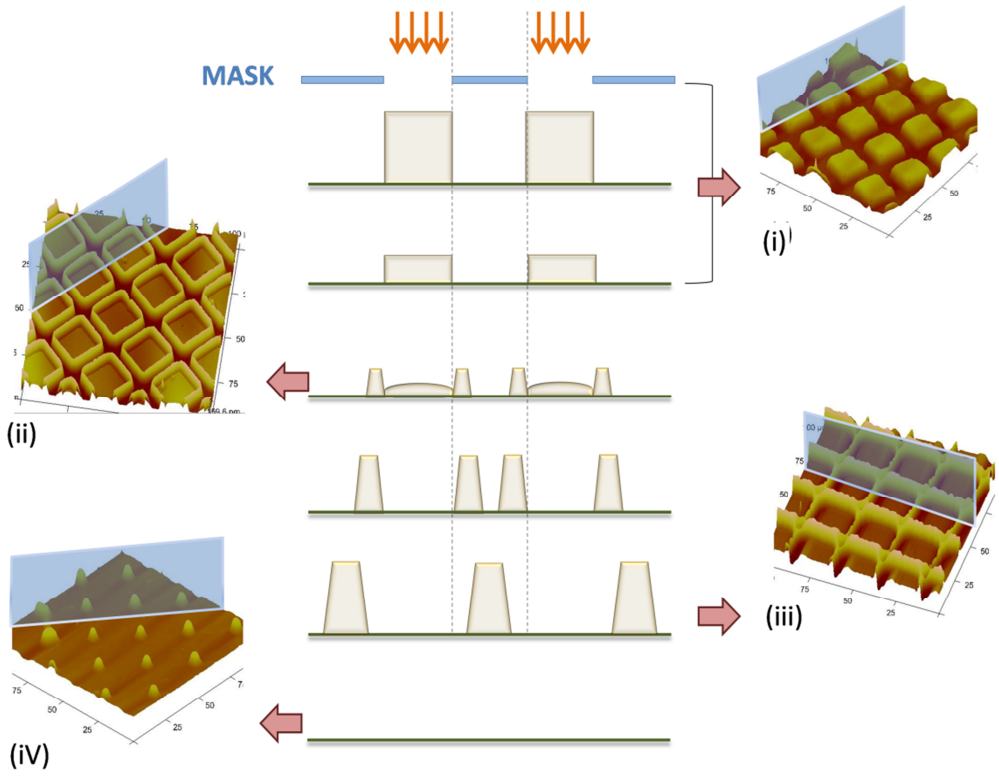

Figure 5. *Illustration of the different surface patterns that can be obtained by irradiation of polystyrene films with UV light as a function of the treatment followed.*

An increase of the exposure time or removing the cover produces similar effects, i.e. an increase of the degradation kinetics. The areas directly exposed to the UV light partially degrade as evidenced by a decrease of the height (ii) in the AFM images. Apart from the

degradation, at the edge of the exposed-non exposed areas we observed an increase of the crosslinking. Most probably the radicals created close to the light-shadow limits are able to diffuse and polymerize the non-exposed areas. The absence of direct light prevents from degradation thus leading to crosslinking. This observation is confirmed upon increase of either the irradiation time or the amount of photoinitiator that favors the total photooxidation of the directly irradiated regions (iii). Similarly to what has been already observed in step (ii), the non-exposed areas exhibit crosslinked polystyrene as a result of the radical diffusion and polymerization.

Finally, in step (iv) not only the exposed areas but also the non-exposed areas suffered degradation. As a result, only the areas where the mesh pattern crosses remain crosslinked forming pillars with average sizes of 5μm.

A major advantage of this approach consists on the possibility to combine within the polymer structure other functional groups. As a consequence not only the pattern can be varied but also the functionality can be simultaneously tuned depending on the functional polymer employed. In order to vary the chemical composition of the patterns created, a PS-*b*-P5FS block copolymer was prepared as a model system. The films of the block copolymer were prepared by spin coating using similar conditions as those employed for the PS films. The cross-sectional profiles resulting from the AFM images obtained for the different irradiation times eventually using cover and/or photoinitiator are represented in Figure 6. The tendency observed is rather similar to the described above for PS. Whereas the photodegradation occurs faster for both the non-covered samples or the samples covered with quartz, a dramatic decrease of this side reaction is observed using glass covers. Glass absorption and reduction of the oxygen available at the film surface prevents from photooxidation and favors the photocrosslinking. More interestingly, when using the PS-*b*-P5FS block copolymer at least 2h of irradiation is needed to observe the crosslinking in the directly irradiated areas. These results confirmed the tendency observed in Figure 4 for PS films containing the same amount of IRG 651 (i.e. 5wt%) within the films.

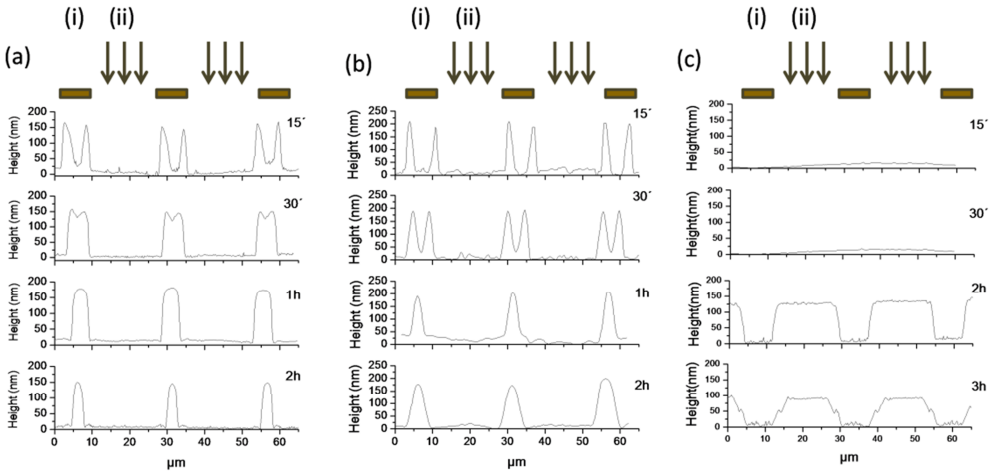

Figure 6. *AFM cross sectional profiles of PS-b-P5FS films upon exposure to 100% UV-light at different times. a) non-covered, b) non covered with 5wt% IRG 651 and c) with 5wt% IRG 651 covered with glass cover.*

The different chemical nature of the films can significantly vary the surface properties for instance on the surface wettability. In order to compare the changes of wettability as a function of the structure obtained upon UV-light irradiation, contact angle measurements of similar structures but based on either PS or the block copolymer were carried out. In Figure 7 are depicted the structures analyzed and the contact angle values measured depending on the polymer employed for their construction. In all the cases studied, the contact angle values obtained for the films prepared using the fluorinated block copolymer are higher than the equivalent structures obtained using PS. Moreover, whereas the wettability differences of the structures obtained upon short irradiation time, i.e. crosslinked PS in the directly irradiated areas are close to the 10º, the differences for the other two structures are significantly higher up to 40º. These results are in agreement with the work of Kong et al. [84]. These authors compared contact angle for similar surface structures (pillars) before and after plasma irradiation. After plasma irradiation the surface of the pillars was functionalized with hydrophilic functional groups and significantly reduced the contact angle. In our case the functionalization with hydrophobic groups significantly decreases the wettability of the surface.

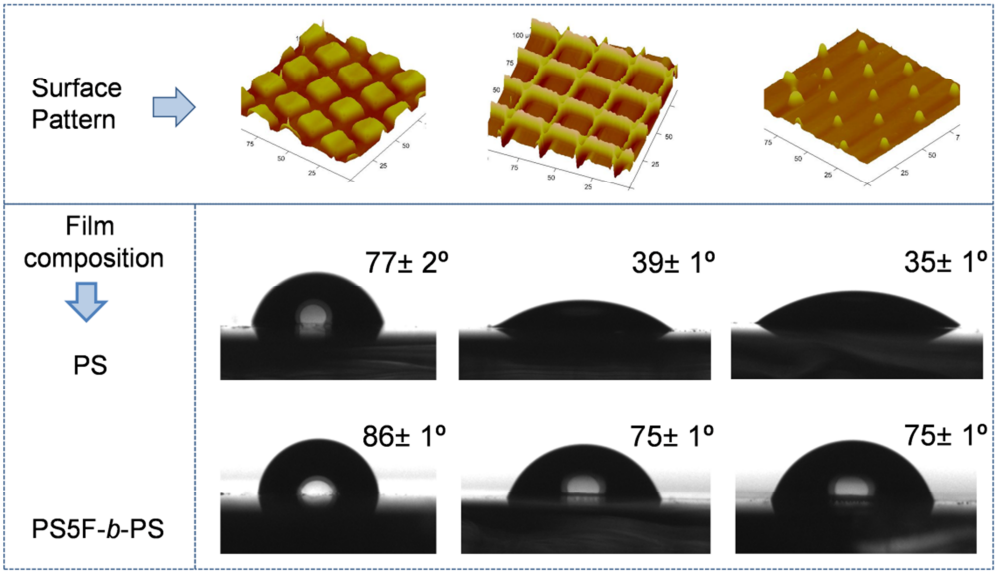

Figure 7. *Contact angle measurements as a function of the surface pattern created on either PS or PS-b-P5FS films upon different UV-light exposure times. Differences in contact angle for similar structures due to the chemical composition of the film can be observed.*

Conclusions

We developed an approach to create different patterns in PS samples by UV-light irradiation using a simple TEM-grid as a mask. We evidenced that short irradiation times or low irradiation intensities tends to crosslink polystyrene while longer irradiation times or an increase of the UV-light intensity provokes the photodegradation. Moreover, by adding an amount of photoinitiator to the polymer has two different impacts on the pattern formation. Low amounts of photoinitiator (up to 3%) favors both the photocrosslinking and photodegradation due to the major number of radicals present during the UV-irradiation. While an increase of the photoinitiator amount employed produces recombination and decreases the photocrosslinking kinetics.

In summary, upon optimization of the experimental conditions (irradiation time, intensity, cover employed and eventually the presence of a photoinitiator) different surface patterns can be tailor made in a straightforward manner using a single experimental setup.

As a proof of concept, we additionally extended the patterning approach to other polystyrene based block copolymer, PS5F-*b*-PS that will introduce functionality to the surface patterns. The wettability of the films is clearly affected by both the surface pattern and the chemical composition.

The simplicity of this approach and the possibilities to create a wide variety of surface patterns (depending on the mask employed) and functionalities (incorporated in the polystyrene chain) makes of this method an interesting alternative to other multistep approaches. A wide range of applications can benefit from this approach including the elaboration of novel polymer resists, the fabrication of platforms for selective adhesion or with antifouling properties or in the biomedical area as, for instance, substrates to construct protein arrays.

Artículo 3: *Versatile functional microstructured polystyrene-based platforms for protein patterning and recognition*

Una vez se ha optimizado la generación de micro/nanoestructuras en superficies de PS y PS fluorado (artículo 2), en este artículo se han puesto a punto las condiciones experimentales idóneas (fotoiniciador, cubierta de la disolución, tiempo de exposición, etc) para conseguir generar este tipo de estructuras que van desde las cajas hasta las agujas, pero esta vez sobre superficies poliméricas formadas a partir de un nuevo copolímero de PS funcionalizado con poliácido glutámico.

El empleo de este nuevo copolímero proporciona a las superficies generadas la presencia de grupos carboxílicos que resulta útil para el anclaje de secuencias polipeptídicas en posiciones precisas y permite el uso de estas superficies, mediante las post-modificación química de los grupos carboxilo para su utilización en reconocimiento de proteínas, lo que abre nuevas alternativas para la aplicación de estas superficies poliméricas estructuradas en aplicaciones biotecnológicas y biomédicas.

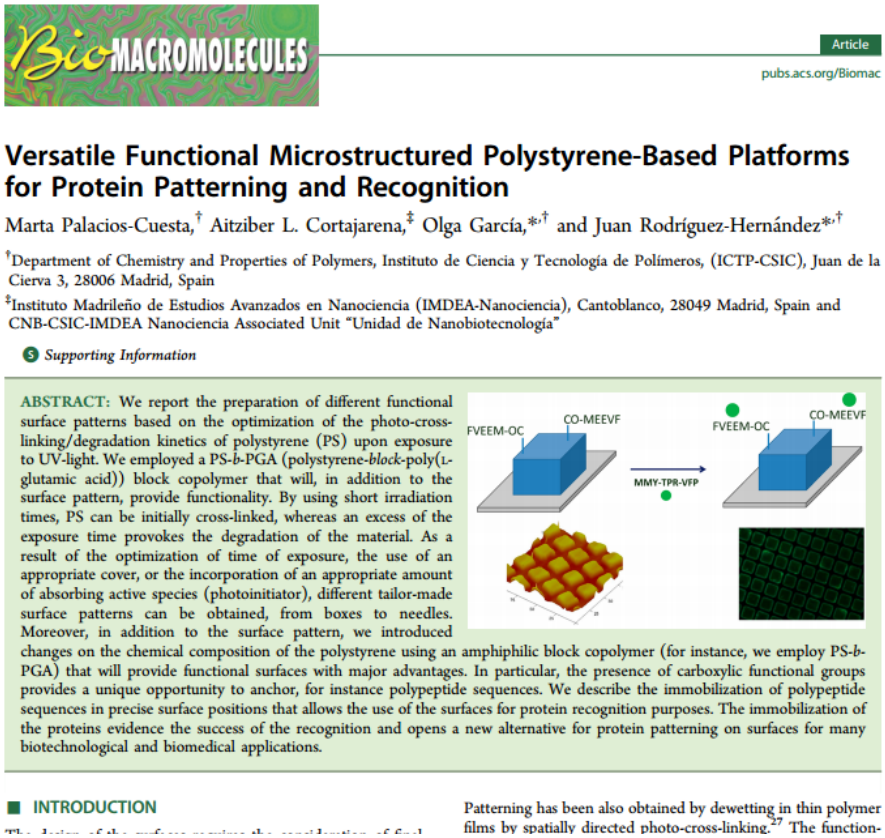

BioMACROMOLECULES

Article

pubs.acs.org/Biomac

Versatile Functional Microstructured Polystyrene-Based Platforms for Protein Patterning and Recognition

Marta Palacios-Cuesta,[†] Aitziber L. Cortajarena,[‡] Olga García,*[,†] and Juan Rodríguez-Hernández*[,†]

[†]Department of Chemistry and Properties of Polymers, Instituto de Ciencia y Tecnología de Polímeros, (ICTP-CSIC), Juan de la Cierva 3, 28006 Madrid, Spain

[‡]Instituto Madrileño de Estudios Avanzados en Nanociencia (IMDEA-Nanociencia), Cantoblanco, 28049 Madrid, Spain and CNB-CSIC-IMDEA Nanociencia Associated Unit "Unidad de Nanobiotecnología"

Supporting Information

ABSTRACT: We report the preparation of different functional surface patterns based on the optimization of the photo-cross-linking/degradation kinetics of polystyrene (PS) upon exposure to UV-light. We employed a PS-*b*-PGA (polystyrene-*block*-poly(L-glutamic acid)) block copolymer that will, in addition to the surface pattern, provide functionality. By using short irradiation times, PS can be initially cross-linked, whereas an excess of the exposure time provokes the degradation of the material. As a result of the optimization of time of exposure, the use of an appropriate cover, or the incorporation of an appropriate amount of absorbing active species (photoinitiator), different tailor-made surface patterns can be obtained, from boxes to needles. Moreover, in addition to the surface pattern, we introduced changes on the chemical composition of the polystyrene using an amphiphilic block copolymer (for instance, we employ PS-*b*-PGA) that will provide functional surfaces with major advantages. In particular, the presence of carboxylic functional groups provides a unique opportunity to anchor, for instance polypeptide sequences. We describe the immobilization of polypeptide sequences in precise surface positions that allows the use of the surfaces for protein recognition purposes. The immobilization of the proteins evidence the success of the recognition and opens a new alternative for protein patterning on surfaces for many biotechnological and biomedical applications.

INTRODUCTION

Patterning has been also obtained by dewetting in thin polymer films by spatially directed photo-cross-linking.[27] The function-

Versatile functional microstructured polystyrene-based platforms for protein patterning and recognition

Marta Palacios-Cuesta[1], Aitziber L. Cortajarena[2], Olga García[1]* and Juan Rodríguez-Hernández[1]*

[1] Department of Chemistry and Properties of Polymers, Instituto de Ciencia y Tecnología de Polímeros, (ICTP-CSIC), Juan de la Cierva 3, 28006 Madrid, Spain.

[2] Instituto Madrileño de Estudios Avanzados en Nanociencia (IMDEA-Nanociencia), Cantoblanco, 28049 Madrid, Spain & CNB-CSIC-IMDEA Nanociencia Associated Unit "Unidad de Nanobiotecnología".

Correspondence to:

Olga García (ogarcia@ictp.csic.es)

Juan Rodríguez-Hernández (rodriguez@ictp.csic.es)

Abstract

We report the preparation of different functional surface patterns based on the optimization of the photocrosslinking/degradation kinetics of polystyrene (PS) upon exposure to UV-light. We employed a PS-*b*-PGA (polystyrene-*block*-poly(L-glutamic acid)) block copolymer that will, in addition to the surface pattern, provide functionality. By using short irradiation times, PS can be initially crosslinked whereas an excess of the exposure time provokes the degradation of the material. As a result of the optimization of time of exposure, the use of an appropriate cover or the incorporation of an appropriate amount of absorbing active species (photoinitiator) different tailor made surface patterns can be obtained, from boxes to needles.

Moreover, in addition to the surface pattern we introduced changes on the chemical composition of the polystyrene using an amphiphilic block copolymer (for instance, we employ PS-*b*-PGA) that will provide functional surfaces with major advantages. In particular, the presence of carboxylic functional groups provides a unique opportunity to anchor, for instance polypeptide sequences. We describe the immobilization of polypeptide sequences in precise surface positions that allows the use of the surfaces for protein recognition purposes. The immobilization of the proteins evidences the success of the recognition and opens a new alternative for protein patterning on surfaces for many biotechnological and biomedical applications.

Introduction

The design of the surfaces requires the consideration of final use in order to obtain properties such as biocompatibility, adhesion, wear resistance, wettability or optical behavior among others. In order to adapt the material for a targeted purpose several surface modifications can be carried out including surface functionalization, modification of the crystallinity, creation of surface microdomains and morphology or variations on the roughness and topography [39-44]. In particular, from a chemical point of view several studies evidenced the significance of the control of both topography and functionality. An appropriate surface functionalization and patterning can lead to materials with adhesive [45-47] or lubricant [48, 50, 85], biocompatible [51] or antifouling [52, 53] or even superhydrophilic [54-58] or superhydrophobic properties [59].

Polystyrene is among the most extended commodity polymers and different approaches have been developed to control both the surface morphology and the functionality. PS has been patterned by hot embossing [60], breath figures [61-63], polymer dewetting on chemically patterned substrates [64, 65], by using soft-lithography to pattern silicon substrates grafted with polystyrene chains [66], by UV-laser radiation to produce micro-drilling [67] or by scanning electrochemical microscopy [68]. Patterning has been also obtained by dewetting in thin polymer films by spatially directed photocrosslinking [65]. The functionality in PS films has been modified either by chemical reactions [69] or upon exposure either to UV-light [70-72] or O_3 [73].

As a result of either/both surface functionalization or/and surface patterning steps the applications of the resulting materials are rather broad. For example, Knudsen et col.[74] proposed the use of polystyrene based resists as a cheaper alternative to other commercially available resists. Patterned polystyrene has been also extensively employed for biomedical purposes for instance in cell adhesion studies [68], the fabrication of medical devices able to measure the electrical activity of cells [67] or to improve the hemocompatibility [51].

In particular, the development of scaffolds with controlled surface properties and topography and the ability of patterning active biomolecules on the surfaces have a great interest in fields such as protein adhesion [86, 87], biosensors, cell attachment [88-90] diagnostic tools development or tissue engineering [91-93]. If we can combine a controlled topography and chemistry with specific biomolecules to provide functionality to the material surface we will have tools to generate sophisticated biomaterials for specific applications.

Besides the well-known requirements of biocompatibility or appropriate mechanical properties, the topography has been evidenced to play a key role on the applicability of the materials [94]. Since the outermost surface of the scaffolds is in contact with the cell, the properties of the surface will direct the interactions and, consequently, the cell adhesion. In this sense, several studies tackled the relation between the surface structure and the cell/protein adhesion [86, 87, 95-100]. Specific structures and topography of the material also provide advantages to the generation of arrays and define patterns of different active biomolecules and cells. For example, protein immobilization on solid surfaces is also crucial in the development of technologies such as miniaturization of sensing and diagnosis devices and biochemical assays [101-104]. The orientation of the immobilized biomolecule also needs to be controlled

in order to guarantee its functional properties. Therefore, oriented immobilization procedures should be used in combination with biomolecular patterning.

Herein we combine the use of photolithography with UV-light with the design of a polystyrene based amphiphilic block copolymer to simultaneously modify both structure and functionality of polystyrene based substrates and their use as platforms for protein patterning. We describe how UV-photolithography can be applied to obtain different structures using a single experimental setup and the same mask throughout the experiments as a result of the fine tuning of the photodegradation/crosslinking reactions [63, 75]. In addition, variations on the chemical composition will be achieved by using a block copolymer, more precisely, polystyrene-block-poly(glutamic acid) (PS-b-PGA). The carboxylic functional groups of the PGA side chains allowed us to chemically immobilize polypeptide sequences. This immobilization is carried out under conditions that preserve their biological activity in specific protein recognition processes in order to pattern proteins. Moreover, for this study we will employ modular TPR proteins and their peptide ligands provides the advantage of the potential design of different orthogonal recognition pairs for selective immobilization, because it has been shown that recognition function of TPR modules can be modified [105, 106].

Experimental section

Polystyrene (PS), Irgacure 651 (IRG 651) (Ciba®), and the rest of solvents were employed as received. Glasses with 0.15 mm thickness (Menzel-Glaser), microscope slides 1 mm thickness (Menzel-Glaser) and grids for transmission electron microscopy (copper, 25μm pitch). Ethyl(dimethylaminopropyl) carbodiimide (EDC), N-Hydroxysuccinimide (NHS), and TWEEN-20 were purchased from Sigma-Aldrich (St. Louis, MO, USA). Styrene was dried under CaH_2 and cryodistilled. γ-benzylester-L-glutamate N-carboxyanhydride was purchased from Isochem and recrystallized from ethylacetate/hexane before the polymerization. All other solvents were used as received unless otherwise specified.

The ^{1}H and ^{13}C NMR spectra were registered at room temperature in $CDCl_3$ solution in Varian INOVA-300. Chemical shifts are reported in parts per million (ppm) using as internal reference the peak of the trace of deuterated solvent (δ 7.26). Size exclusion chromatography (SEC) analyses were carried out on chromatographic system (Waters Division Millipore) equipped with a Waters model 410 refractive-index detector. Dimethylformamide (99.9%,

Aldrich) containing 0.1% of LiBr, was used as the eluent at a flow rate of 1 mL min^{-1} at 50 ºC. Styragel packed columns (HR2, HR3 and HR4, Waters Division Millipore) were used. Poly(methyl methacrylate) standards (Polymer Laboratories, Laboratories, Ltd.) between $2.4x10^6$ and $9.7x10^2$ g mol^{-1} were used to calibrate the columns. The molecular weights were estimated against poly(methyl methacrylate) standards.

Differential scanning calorimetry (DSC) measurements were carried out with a calorimeter (Perkin-Elmer DSC-7). Atomic force microscopy (AFM) measurements were conducted on a Multimode Nanoscope IVa, Digital Instrument/Veeco operated in tapping mode at room temperature under ambient conditions. Fluorescence microscopy assays were performed using a Leica DMRD, fluorescence microscope (Leica Microsystems, Wetzlar, Germany). Images are taken at different magnification using x20, x40 and x60 objectives and the corresponding set of filters for imaging: bright field, red fluorescence, and green fluorescence to monitor the immobilization of peptides and proteins.

Polystyrene-block-poly(L-glutamic acid) (PS_{49}-b-PGA_{17}) synthesis.

The synthesis of the diblock copolymers obtained combining both Atom Transfer Radical Polymerization (ATRP) and ring-opening polymerization of α-amino acid N-carboxyanhydrides has been already described elsewhere [107].

Film preparation

For the preparation of the thin films a 30 mg/mL solution of PS_{49}-*b*-PGA_{17} block copolymer in THF was spin coated onto glass covers at 2000 rpm during 1 min. These films were then irradiated under UV spot light irradiation from source Hamamatsu model lightningcure L8868 provided by an Hg-Xe lamp with 200W power. The incident light intensity was focused on the samples with an optic fiber at a constant distance of 5.5 cm using a TEM copper grid as a mask in contact with the solid polymer film. After irradiation the films were rinsed with THF in order to remove both degraded and non-crosslinked polymer.

Surface functionalization

The surface was functionalized using as coupling reagent EDC at 1 mg/mL and NHS 5mg/mL concentration in water (30 μL EDC + 30 μL NHS). After incubation of the surface

during 5 minutes with the EDC/NHS solution for carboxylate activation, 30 μL of the solution were removed and 30 μL of a 1mg/mL peptide solution with 0.1% (wt/v) of Tween-20 in water were added and mixed. The reaction was allowed to proceed overnight at room temperature. After reaction completion the surface was washed with water.

The surfaces were functionalized with two different peptide sequences using the previously described strategy. The first peptide employed was KKKGPKEK-Alexa546 which is a fluorescent labeled peptide. This first sequence will provide information about the immobilization step. The second sequence was a MEEVF peptide, a designed high affinity ligand for a specific tetratricopeptide protein (TPR) domain for the recognition experiments [108]. The TPR protein employed was TPR-MMY-VFP where VFP stands for Green Fluorescent Protein [109]. This protein was expressed and purified based on previously published protocols for His6-tagged TPR proteins [108, 110].

Functionalized surfaces with MEEVF peptide were incubated during 1 hour with 30 μM protein concentration (TPR-MMY-VFP) solution in TBST buffer (150 mM NaCl, 50 mM Tris pH 7.4, 0.1% Tween-20). After incubation the surface is thoroughly washed with the same buffer to remove non-specific absorbed protein molecules.

Results and discussion

The behavior of polystyrene upon exposure to UV-light has been extensively studied and is today well established [74, 77-81]. As schematically illustrated in Figure 1, the time of exposure, the presence or not of oxygen and the incorporation of a photoinitiator direct the mechanism followed during the UV irradiation. When the reaction is carried out under vacuum, without or with a low amount of oxygen and short irradiation times, polystyrene follows mainly the crosslinking path between different chains. On the contrary, in the presence of oxygen, by using longer irradiation times or using a photoinitiator β-scission reactions are favored thus leading either to degradation of the polymer chain or acting as a bridge between two polystyrene chains [82].

Taking into account these considerations, our group has recently evidenced that depending on the experimental conditions employed, either the crosslinking or the degradation, using deep UV irradiation we were able to construct robust and functional micropatterns, from

boxes to needles, on PS surfaces [111]. Based on these previously reported findings, herein we describe the employment of an amphiphilic block copolymer polystyrene-block-poly(glutamic acid) (PS_{49}-b-PGA_{17}) that will be either crosslinked or degraded thus leading to different surface patterns. A clear advantage is provided by the use of PGA block containing side chain carboxylic functional groups that can be employed to modify the surface composition by chemical reaction with antagonic functional groups. In this study the carboxylic groups will serve to anchor peptides by using the end-terminal amine functional group.

The PS_{49}-*b*-PGA_{17} thin films were prepared by spin coating from THF solutions (30 mg/mL). Spin coating allowed us to prepare films with controlled thicknesses of ~ 400nm as measured by AFM. The samples were irradiated at different times with a UV-light source at room temperature through a TEM copper grid used as a mask. As a consequence, we obtained areas either exposed or non-exposed to UV-light. After irradiation, the films were rinsed with THF, thus both degraded and non-crosslinked polymeric areas were dissolved and removed while the crosslinked regions of the film remain insoluble.

The irradiation of the films in contact to air was carried out at room temperature varying the exposure time between 1 - 3 hours. In Figure 2, are depicted the AFM images of the block copolymer films obtained upon irradiation at two different exposures times (1 and 3 hours) and subsequent rinsing. In addition, Figure 2 contains section profiles of the different surface patterns.

As observed in the AFM images of the samples, upon 1h of irradiation the films exhibit crosslinked polystyrene in the irradiated areas. After 3 hours, the areas directly exposed to UV-light are degraded as indicated by the decrease in height observed in the AFM images. Large irradiation times produce a complete degradation of these areas. This result is in good agreement with the results reported by Kaczmarek et al [75]. This group took advantage of the photodegradation of PS in a blend and selective removal of the photodegraded areas to induce changes in the final morphology of the film.

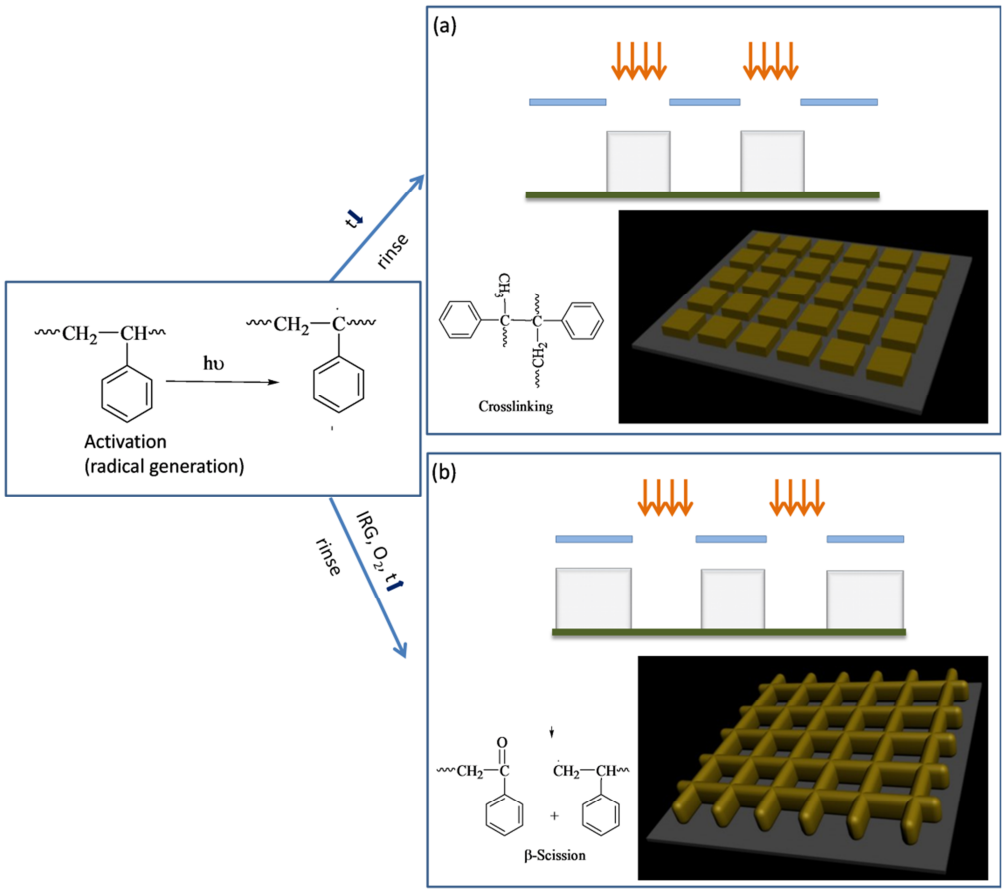

Figure 1. *Reactions accomplished by PS upon irradiation with UV light. Depending on the presence or absence of oxygen, the incorporation of a photoinitiator or varying the irradiation time, the reaction mechanism can follow two different reaction paths: a) crosslinking or b) β-scission reactions (degradation of the polymer chain). By using UV-irradiation, PS can have a crosslinked structure thus providing additional chemical and thermal stability to the film.*

More interestingly, whereas degradation is the main mechanism when the irradiation times increase, the non-directly exposed areas exhibit a different behavior. An increase of the irradiation time produces the crosslinking reaction initially at the edge of the exposed-non exposed areas and later in the center of the non-exposed areas. To the best of our knowledge, the radicals may diffuse into the non-exposed and start to react from the edge to the center of the exposed-non exposed areas. The consequence of this process is the formation of

complementary patterns as a result of the crosslinked polystyrene even if the film has not been exposed in these areas.

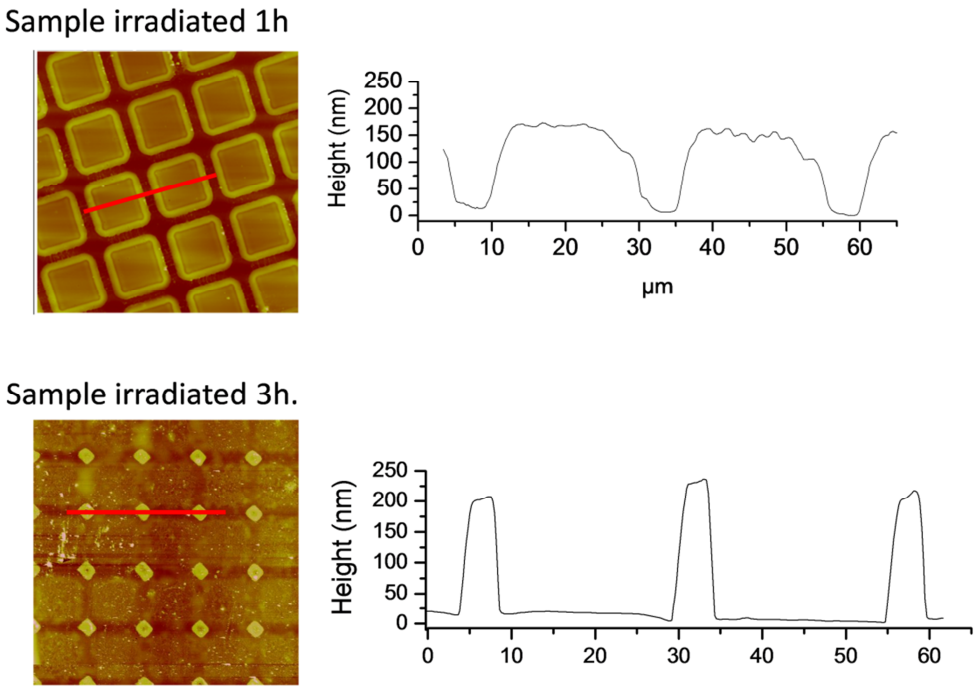

Figure 2. *AFM images in air of the microstructures formed by PS-b-PGA block copolymer at two different irradiation times (1h and 3h) using a 100% of light intensity. Whereas at low irradiation times the directly exposed areas were crosslinked (above), larger irradiation times produce the degradation of the exposed PS areas (below). Image size 120µm x 120µm.*

As a result of the combination of exposure time and either the use of an appropriate cover or the incorporation of a suitable amount of a photoinitiator different surface patterns can be tailor made [111]. In Figure 3 are illustrated the different patterns observed for the films by adjusting the exposure time. As mentioned above, short irradiation times up to 1h leads to crosslinked structures located in the directly exposed areas (Fig 3, Step 1). In this case, the non-exposed areas, that are protected by the mask, remained uncrosslinked and can be easily removed by rinsing with THF.

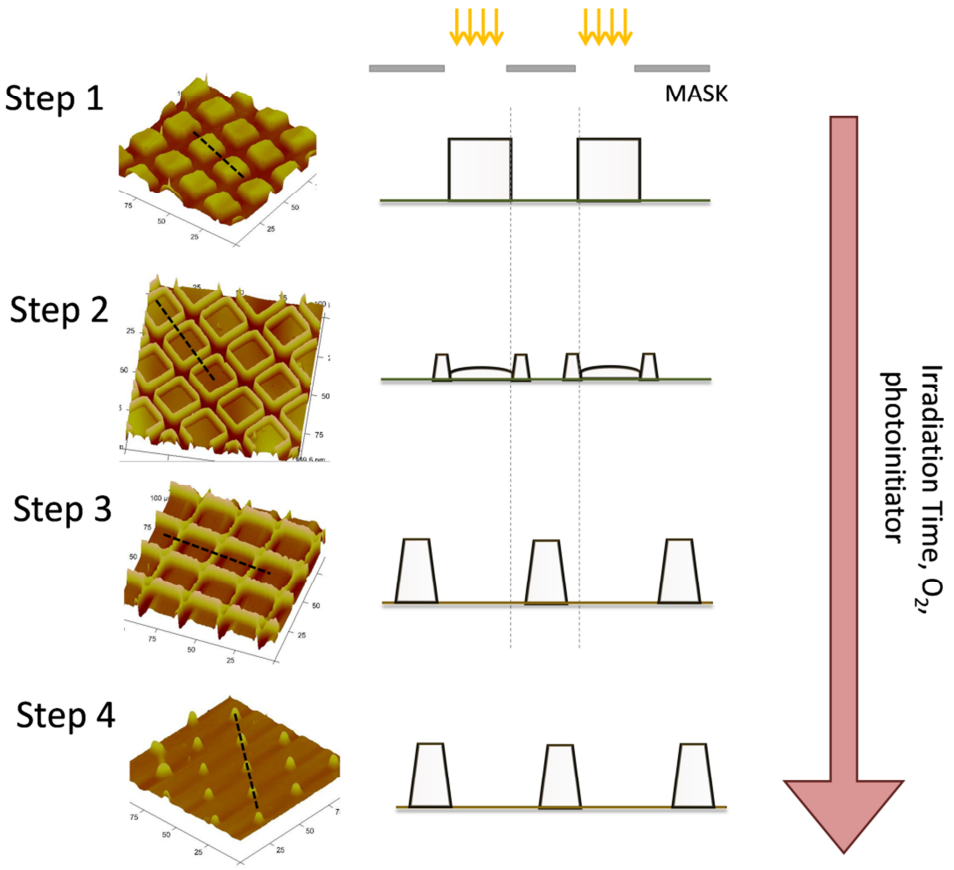

Figure 3. *AFM images of the diverse microstructures obtained by either crosslinking or degradation of the diblock copolymer films: Steps 1 to 4. These structures result from the variation of the exposure time (15, 30, 120 and 180 minutes, respectively), the use of a cover (glass) or incorporation of a photoinitiator.*

An increase of the exposure time increases equally the degradation kinetics. The areas directly exposed to the UV light partially degrade as evidenced by a decrease of the height (Step 2) in the AFM images. Apart from the degradation, at the edge of the exposed-non exposed areas we observed an increase of the crosslinking. The radicals created close to the light-shadow limits are able to diffuse and polymerize the non-exposed areas. The absence of direct light prevents from degradation thus leading to crosslinking. This observation is confirmed upon increase of either the irradiation time or the amount of photoinitiator that favors the total photooxidation of the directly irradiated regions (Step 3). Similarly to what has

been already observed in step 2, the non-exposed areas exhibit crosslinked polystyrene as a result of the radical diffusion and polymerization.

Finally, in step 4 not only the exposed areas but also the non-exposed areas suffered degradation. As a result, only the areas where the mesh pattern crosses remain crosslinked forming pillars with average sizes of ~ 5μm.

As we mentioned above, the surface patterns obtained have additionally functionality. In particular, carboxylic functional groups provided by the poly(L-glutamic acid) block. These groups can be employed, for instance, to anchor polypeptide sequences by using their amine terminus. In this contribution, we carried out two series of experiments (Figure 4). The first series of experiments were oriented to demonstrate the possibility of chemical reaction between the surface carboxylic functional groups and the amine groups of the polypeptide sequence. The polypeptide sequence used for these experiments is labeled with an Alexa fluorescent group that allowed us to monitor the success of the surface immobilization by using fluorescence spectroscopy. The second series of experiments contains two steps: immobilization of a MEEVF sequence and the recognition test with a tetratricopeptide protein (TPR) labeled with a Green Fluorescent Protein (VFP).

The covalent immobilization was carried out by using the EDC/NHS coupling protocol depicted in the experimental section. This reaction was performed in water overnight at room temperature. The films were washed extensively in order to remove absorbed polypeptide sequences. The fluorescent images of the surfaces irradiated at different times obtained after polypeptide coupling are depicted in Figure 5. The images clearly indicate the presence of fluorescent signal in the areas where the PS-*b*-PGA has been crosslinked. The fluorescent signal associated to the immobilization of the polypeptide sequence evidenced the success of the coupling reaction. Moreover, as a result of the variation exposure times that lead to different surface morphologies, have distinct immobilization patterns.

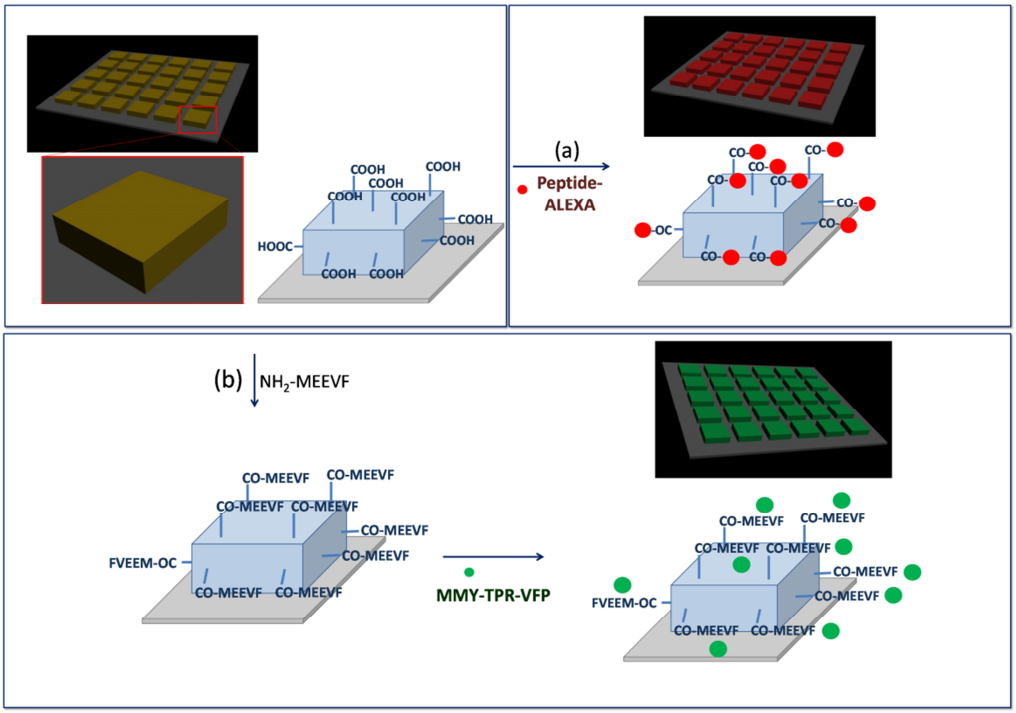

Figure 4. *Schematic representation of the strategy followed to immobilize polypeptide sequences and protein recognition experiments. (a) Immobilization of Alexa-polypeptide onto the crosslinked domains and (b) Immobilization of the NH_2-MEEVF peptide and recognition by MMY-TPR protein labeled with a Green Fluorescent Protein (VFP).*

The experiments carried out above evidenced the success of the coupling reaction and the possibility to selectively functionalize the areas in which PS-*b*-PGA is crosslinked. The next step concerns the evaluation of the recognition capabilities of the immobilized polypeptides. For this purpose, we selected a particular polypeptide sequence, more precisely MEEVF that is a designed peptide sequence with high affinity and specificity for the tetratricopeptide protein domain (TPR-MMY) [109, 112].

.

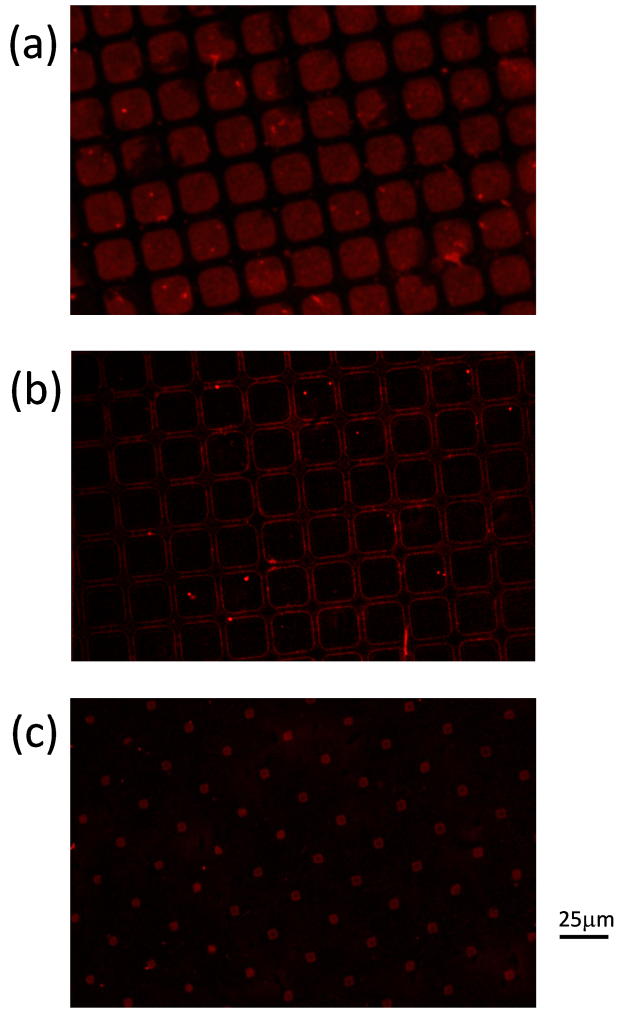

Figure 5. *Fluorescent images obtained upon surface immobilization of an Alexa labeled polypeptide onto the surface patterns. The immobilization was carried out by coupling the carboxylic acid functional groups of the films and the amine terminus of the fluorescent polypeptide. The surface patterns were obtained upon 1h of irradiation a), 2h b) and 3 hours c).*

The sequence was immobilized using the same protocol depicted above. Upon removal of the excess of MEEVF and extensive rinsing the films were submerged into a solution containing a TPR protein labeled with a green-emitting fluorescent protein (VPF). Figure 6 shows the fluorescent images of the films obtained upon chemical modification by covalent immobilization of the MEEVF sequence and consecutive recognition of the

fluorescent TPR protein. As a result of the interaction between the sequence covalently attached and the fluorescent TPR protein a particular protein patterning was observed directly related with the patterning obtained by irradiation of the PS-b-PGA films. A simple modification of the exposure time induces changes on the surface morphology that can produce different protein patterns. Additionally, the use of these modular TPR proteins and their peptide ligands provides the advantage of the potential design of different orthogonal recognition pairs for selective immobilization, because it has been shown that recognition function of TPR modules can be modified [105, 106]

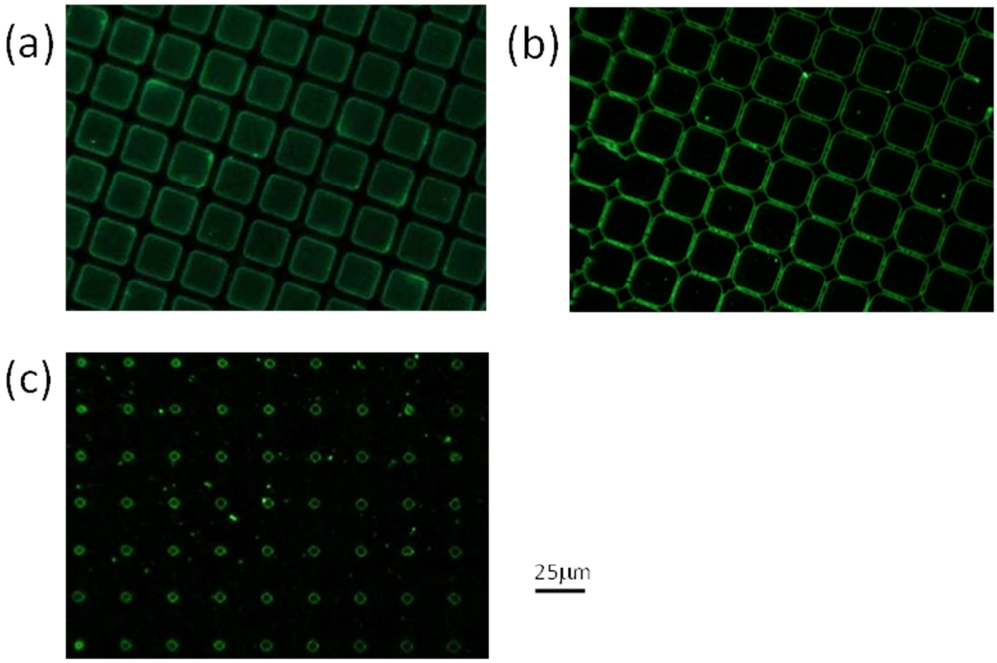

Figure 6. *Fluorescence microscopy images of the surfaces having different patterns upon recognition between the MEEVF modified surfaces and the fluorescently labeled TPR protein. The surface patterns were obtained upon 1h of irradiation a), 2h b) and 3 hours c).*

Conclusions

The results depicted above illustrated, by using a particular system, the large number of possibilities to construct surface patterns with precise functionality and the use of these platforms to immobilize bioactive molecules.

We developed an approach to create different patterns in a functionalized block copolymer, PS-b-PGA, samples by UV-light irradiation using a simple TEM-grid as a mask. We evidenced that short irradiation times tends to crosslink polystyrene blocks while longer irradiation times provokes the photodegradation. The simplicity of this approach and the possibilities to create a wide variety of surface patterns (depending on the experimental conditions: intensity and irradiation time, presence/absence of oxygen or photoinitiator, etc.) and functionalities (incorporated in the polystyrene chain) makes of this method an interesting alternative to other multistep approaches.

In addition, the possibility of using these substrates to immobilize active has been demonstrated, opening the door to the construction of protein arrays and pattern proteins at the micro-scale. For this purpose, we employed coupling reactions to form an amide bond between the carboxylic functional groups of the polymeric film and the amine end-terminus of the polypeptide. In particular, the coupling of a specific ligand peptide sequence in the active form allowed us to immobilize its partner protein by a biomolecular recognition process.

Acknowledgements;

The authors gratefully acknowledge support from the Consejo Superior de Investigaciones Científicas (CSIC). Equally, this work was financially supported by the Ministerio de Economía y Competitividad (MINECO) through MAT2011-22861 and MAT2009-12251. M. Palacios thanks the Ministerio de Education for the FPU fellowship. We would like to thank Sylvia Gutiérrez and staff members of the CNB-CSIC confocal microscopy facility for technical support. The plasmids encoding TPR-MMY-VFP protein and MEEVF peptide are gifts from Lynne Regan's group at MB&B Department at Yale University. This research is funded in part by the European Commission International Reintegration Grant (IRG-246688) (ALC) and AMAROUT-COFUND Europe Programme (ALC).

Artículo 4: *Patterning of individual Staphylococcus aureus bacteria onto photogenerated polymeric surface structures*

En este artículo se describe la fabricación de formaciones bacterianas ordenadas usando las técnicas fotolitográficas y de funcionalización descritas anteriormente en los artículos 2 y 3. En esta ocasión se ha utilizado un copolímero anfifílico de PS y poliácido acrílico que, como se demuestra a continuación, favorece la afinidad en la adhesión entre la bacteria y la superficie polimérica y, por tanto, su inmovilización. Así, se plantea este método como una alternativa eficaz y de bajo coste para la fabricación de estructuras funcionales submicrométicas. En este caso se ha aplicado a un tipo de bacteria, *Staphylococcus Aureus*, con la cual se consiguen realizar alineaciones de bacterias e incluso su inmovilización de forma individual, aun siendo un tipo de bacteria con gran tendencia a la agregación.

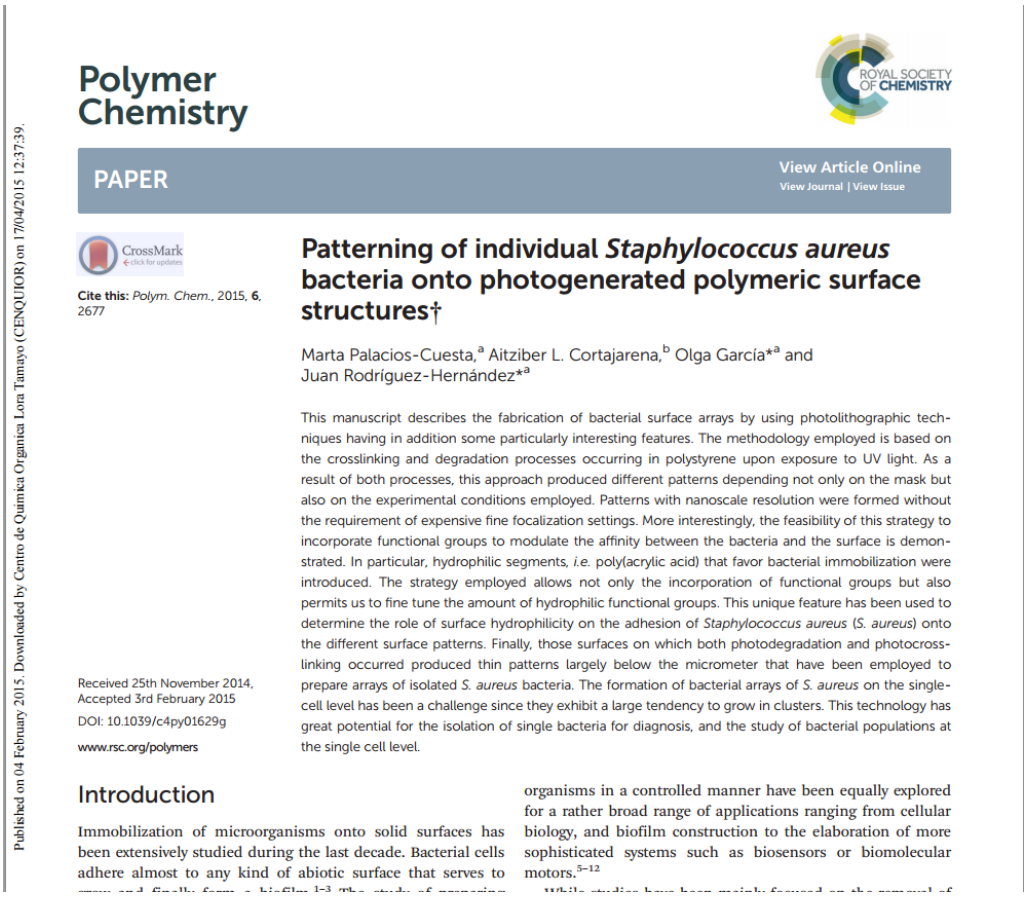

Polymer Chemistry

PAPER

View Article Online
View Journal | View Issue

CrossMark click for updates

Cite this: *Polym. Chem.*, 2015, **6**, 2677

Patterning of individual *Staphylococcus aureus* bacteria onto photogenerated polymeric surface structures†

Marta Palacios-Cuesta,[a] Aitziber L. Cortajarena,[b] Olga García*[a] and Juan Rodríguez-Hernández*[a]

This manuscript describes the fabrication of bacterial surface arrays by using photolithographic techniques having in addition some particularly interesting features. The methodology employed is based on the crosslinking and degradation processes occurring in polystyrene upon exposure to UV light. As a result of both processes, this approach produced different patterns depending not only on the mask but also on the experimental conditions employed. Patterns with nanoscale resolution were formed without the requirement of expensive fine focalization settings. More interestingly, the feasibility of this strategy to incorporate functional groups to modulate the affinity between the bacteria and the surface is demonstrated. In particular, hydrophilic segments, *i.e.* poly(acrylic acid) that favor bacterial immobilization were introduced. The strategy employed allows not only the incorporation of functional groups but also permits us to fine tune the amount of hydrophilic functional groups. This unique feature has been used to determine the role of surface hydrophilicity on the adhesion of *Staphylococcus aureus* (*S. aureus*) onto the different surface patterns. Finally, those surfaces on which both photodegradation and photocrosslinking occurred produced thin patterns largely below the micrometer that have been employed to prepare arrays of isolated *S. aureus* bacteria. The formation of bacterial arrays of *S. aureus* on the single-cell level has been a challenge since they exhibit a large tendency to grow in clusters. This technology has great potential for the isolation of single bacteria for diagnosis, and the study of bacterial populations at the single cell level.

Received 25th November 2014,
Accepted 3rd February 2015

DOI: 10.1039/c4py01629g

www.rsc.org/polymers

Introduction

Immobilization of microorganisms onto solid surfaces has been extensively studied during the last decade. Bacterial cells adhere almost to any kind of abiotic surface that serves to

organisms in a controlled manner have been equally explored for a rather broad range of applications ranging from cellular biology, and biofilm construction to the elaboration of more sophisticated systems such as biosensors or biomolecular motors.[5–12]

Patterning of individual *Staphylococcus aureus* bacteria onto photogenerated polymeric surface structures

Marta Palacios-Cuesta[1], Aitziber L. Cortajarena[2], Olga García[1]* and Juan Rodríguez-Hernández[1]*

[1] Department of Chemistry and Properties of Polymers, Instituto de Ciencia y Tecnología de Polímeros, (ICTP-CSIC), Juan de la Cierva 3, 28006 Madrid, Spain.

[2] Instituto Madrileño de Estudios Avanzados en Nanociencia (IMDEA-Nanociencia), Cantoblanco, 28049 Madrid, Spain & CNB-CSIC-IMDEA Nanociencia Associated Unit "Unidad de Nanobiotecnología".

Correspondence to:

Olga García (ogarcia@ictp.csic.es)

Juan Rodríguez-Hernández (rodriguez@ictp.csic.es)

Abstract

This manuscript describes the fabrication of bacterial surface arrays by using photolithographic techniques having in addition some particularly interesting features. The methodology employed is based on the crosslinking and degradation processes occurring in polystyrene upon exposure to UV light. As a result of both processes, this approach produced different patterns depending not only on the mask but also depending on the experimental conditions employed. Patterns with nanoscale resolution were formed without the requirement of expensive fine focalization settings. More interestingly, the feasibility of this strategy to incorporate functional groups to modulate the affinity between the bacteria and the surface is demonstrated. In particular, hydrophilic segments, i.e. poly(acrylic acid) that favor the bacterial immobilization were introduced. The strategy employed allowed not only the incorporation of functional groups but also permits to fine tune the amount of hydrophilic functional groups. This unique feature has been used to determine the role of the surface hydrophilicity on the adhesion of *Staphylococcus aureus* (*S. aureus*) onto the different surface patterns. Finally, those surfaces in which both the photodegradation and photocrosslinking occurred produced thin patterns largely below the micrometer that have been employed to prepare arrays of isolated *S. aureus* bacteria. The formation of bacterial arrays of S. aureus on the single-cell level has been a challenge since they exhibit a large tendency to grow in clusters. This technology has a great potential for the isolation of single bacteria for diagnosis, and the study of bacteria populations at the single cell level.

Introduction

The immobilization of microorganisms onto solid surfaces has been extensively studied during the last decade. Bacterial cells adhere almost to any kind of abiotic surface that serves to grow and finally form a biofilm [113-115]. The interest of preparing surfaces with either adherent or repellent properties towards microorganism has received an increasing interest for many different reasons. On the one hand, antifouling surfaces prepared using water repellent polymers or by anchoring antimicrobial compounds may prevent implants from contamination, reducing device-associated infections [116]. On the other hand, surfaces capable to immobilize and remove microorganisms in a controlled manner have been equally explored for a rather broad range of applications ranging from cellular biology, biofilm

construction to the elaboration of more sophisticated systems such as biosensors, or biomolecular motors [117-124].

Whereas studies have been mainly focused on the removal of bacteria from surfaces several groups have been during the last decade interested in the development of surfaces in which the microorganisms are distributed in a controlled manner. Bacterial microarrays on surfaces have the potential to be employed in the diagnostics of different diseases [125, 126] microbial ecology [127], genotoxin monitoring [128] and environmental monitoring[129] including the monitoring of heavy metals in the environment [130] or as assays of gene expression [131]. Patterned bacterial surfaces have been equally employed for to fabrication of in vitro model systems for fundamental studies of bacterial processes such as quorum sensing [129, 132-134] and horizontal gene transfer [135-137].

Precise immobilization of microorganisms and in particular bacteria onto surfaces have been achieved by using different fabrication approaches such as soft lithography [138], microcontact printing using micropattterned stamps [139, 140] or replication molding [122-124, 141] or different lithographic approaches including capillary lithography[142], electron-beam lithography [143], dip-pen nanolithography [122, 144] or photolithography[145, 146] or onto functional multilayers [147], inkjet printing. [148]

Typically, the above mentioned approaches succeeded in the immobilization of bacteria on micrometer size regions where, rather than isolated, the bacteria appeared to form aggregates. [141, 149] According to our knowledge, only few examples reported the controlled immobilization of single bacteria. [119, 150] The immobilization of isolated bacterial cell has been accomplished by using expensive approaches or time-consuming multistep procedures including dip-pen nanolithography [119], photolithography [151] or structural transformation by electrodeposition on patterned substrates. [152] and later Dufrêne and coworkers [153] employed an alternative and immobilized single bacterial cells onto Millipore filters with comparable sizes to the dimensions of the cell. In spite of the simple and inexpensive solution the last strategy is limited to the round shape features and the polydispersity of the pores.

Within this background, in this manuscript we describe the formation of different surface patterns by using a photolithographic based technique that do not require the use of high resolution masks or clean rooms to fabricate surface patterns with micrometer and

submicrometer resolution. The principle of this approach is based on the use of polystyrene (PS) as a polymer matrix of a blend. Polystyrene may undergo either crosslinking or degradation reactions depending on the UV-light irradiation conditions employed. More interestingly, as will be described in detail, radical diffusion between the exposed-non exposed areas permits to crosslink in this region with submicrometer precision. Moreover, as mentioned by Anselme *et al*. [154] photolithography has been typically limited to create topographical structures without the modification of the surface chemistry. Our approach allowed us to precise control the chemical functionality by using copolymers as additives in the PS polymer matrix. As will be described, the chemical functionality will favor the bacterial attachment. More precisely, an amphiphilic block copolymer with hydrophilic PAA groups that will enhance the contact with the bacteria was employed.

As a model bacterial strain to be immobilized *S. aureus*, a Gram positive bacteria that causes a broad number of infections in humans, being the leading cause of hospital acquired infections has been selected. In particular meticillin-resistant *S. aureus* (MRSA), a variant resistant to many antibiotics is an emerging threat to public health. *S. aureus* is spherical shaped bacterium (coccus) of about 1 micrometer diameter. *S. aureus* usually grow in grape-like clusters of several individuals [155] Therefore, the isolation of individual bacterium for identification and diagnostic purposes is of highly interest.

Experimental section

Polystyrene (PS), Irgacure 651 (IRG 651 - 2,2-dimethoxy-1,2-diphenylethan-1-one) (Ciba®), and the rest of solvents were employed as received. Glasses with 0.15 mm thickness (Menzel-Glaser) were employed as covers to limit the UV-light exposure. As a substrate microscope slides with a 1 mm thickness (Menzel-Glaser) were used The masks used for this study were copper grids typically used for transmission electron microscopy (using masks with different shaped features, composed of lines, hexagonal or squares and with variable pitch from 62 to 12.5μm pitch).

The synthesis of the block copolymers was achieved by either two consecutive controlled radical polymerization steps using ATRP (Polystyrene-*block*-poly(acrylic acid) (PS_{23}-*b*-PAA_{11}) and polystyrene-*b*-poly[poly(ethylene glycol) methyl ether methacrylate] (PS-*b*-PEGMA) or combining the controlled radical polymerization win the ring-opening

polymerization of N-carboxyanhydrides (Polystyrene-*b*-poly(L-glutamic acid) (PS-*b*-PGA), For a detailed description on the synthesis the reader is referred to the supporting information.

The ^{1}H and ^{13}C NMR spectra were registered at room temperature in $CDCl_3$ solution in Varian INOVA-300. Chemical shifts are reported in parts per million (ppm) using as internal reference the peak of the trace of deuterated solvent (δ 7.26). Size exclusion chromatography (SEC) analyses were carried out on chromatographic system (Waters Division Millipore) equipped with a Waters model 410 refractive-index detector. Dimethylformamide (99.9%, Aldrich) containing 0.1% of LiBr, was used as the eluent at a flow rate of 1 mL min^{-1} at 50 ºC. Styragel packed columns (HR2, HR3 and HR4, Waters Division Millipore) were used. Poly(methyl methacrylate) standards (Polymer Laboratories, Laboratories, Ltd.) between $2.4x10^{6}$ and $9.7x10^{2}$ g mol^{-1} were used to calibrate the columns. The molecular weights were estimated against these poly(methyl methacrylate) standards.

Atomic force microscopy (AFM) measurements were conducted on a Multimode Nanoscope IVa, Digital Instrument/Veeco operated in tapping mode at room temperature under ambient conditions. All the images are height images in which the clearer color corresponds to elevated areas whereas the darker color is related to deeper areas. Elevated areas result upon crosslinking since these areas are not removed upon rinsing. On the contrary, deeper areas correspond either to non-crosslinked or degraded areas.

For the preparation of the thin films a 30 mg mL^{-1} solution of PS homopolymer in THF was spin coated onto glass covers at 2000 rpm during 1 min. These films were then irradiated under UV spot light irradiation from source Hamamatsu model Lightningcure L8868 provided by an Hg-Xe lamp with 200W power. The incident light intensity was focused on the samples with an optic fiber placed at a constant distance of 5.5 cm with either 50% or 100% of the totalintensity of the lamp using a TEM copper grid as a mask, with different size and/or shape. After irradiation the films were rinsed with THF in order to remove both degraded and non-crosslinked polymer.

Bacterial adhesion tests

S. Aureus strain RN4220 carrying the plasmid pCN57 for Green fluorescent protein (GFP) expression (generous gift from Iñigo Lasa's Laboratory at Instituto de

Agrobiotecnología, UPNA-CSIC-Gobierno de Navarra) was grown overnight at 37ºC in Luria-Bertani (LB) media with erythromycin (10 μg/ml). The cells were centrifuged and washed three times in PBS buffer (150 mM NaCl, 50 mM Na-phosphate pH 7.4). The solution was adjusted to a cell concentration that corresponds to an optical density (OD) at 600 nm of 1.0 checked using an UV-*VIS* Varian Cary 50 spectrophotometer.

The different patterned polymeric surfaces were incubated for periods ranging from 1 to 4 hours with a bacterial suspension at OD = 1.0 in PBS buffer with 0.05 % Tween 20. After incubation the surfaces were washed with PBS three times during 15 minutes.

Bacteria adhesion was monitored by fluorescence microscopy using a Leica DMI-3000-B fluorescence microscope. Images were acquired using different magnifications (x10, x20, x40 and x63) and the corresponding set of filters for imaging green fluorescence and bright field. Also Scanning Transmission Electron Microscopy (STEM) images were taken using a FESEM apparatus HITACHI SU8000. Samples for STEM were previously immersed in Formalin 10% solution neutral buffered (Aldrich), washed first with water and then with water/ethanol solutions in increasing proportion up to 100% ethanol.

Results and discussion

Polystyrene (PS) is among the most extensively employed polymers due to their optical properties (transparency), the possibility to chemically modify its structure and polymerize with a broad amount of monomers or their easy processability. These characteristics have converted this material in a commonly used material among others in many biorelated applications such as in cell adhesion studies [68], the fabrication of medical devices able to measure the electrical activity of cells [67] or to improve the hemocompatibility. [51]

PS has been patterned by using different techniques including hot embossing [60], breath figures [61, 62, 156], polymer dewetting on chemically patterned substrates [64, 65], by using soft-lithography to pattern silicon substrates grafted with polystyrene chains [66], by UV-laser radiation to produce micro-drilling[67] or by scanning electrochemical microscopy. [68] In addition, polystyrene can be photocrosslinked/photodegraded by using UV light. The use of this approach has particular advantages. As has been depicted before the use of a single

mask allow us to prepare surfaces with variable surface patterns depending on the extent of photocrosslinking/photodegradation. As will be shown, the possibility to pattern at the interface between the exposed and non-exposed areas permits to achieve resolutions largely below the mask employed. Moreover, in contrast to such techniques as hot-embossing, the patterning can be carried out at room temperature so that the use of copolymers based on polystyrene that may degrade upon heating can be employed as additives.

Photocrosslinking has been typically carried out using different materials in order to create structured surfaces with more or less resolution but usually without paying special attention to their functionality [154]. Within this context, our group reported the use functional copolymers having styrene units and comonomers with either hydrophilic or hydrophobic functional groups to vary the surface chemical composition.[157, 158] In particular a large number of studies evidenced that surface hydrophilicity plays a key role on the protein immobilization and subsequent cell attachment. Herein, we will explore the possibility to modify the surface chemical composition and their role on the bacterial adhesion. For that purpose, in order to promote bacterial attachment on the photogenerated surface patterns an amphiphilic block copolymer was mixed with a polymer matrix (linear polystyrene). Thus, films composed by polystyrene (employed as reference), and an amphiphilic block copolymer (for instance, polystyrene-*block*-poly(acrylic acid) (PS_{23}-*b*-PAA_{11}) or blends of both components (Figure 1) were irradiated in order to produce different surface patterns.

The fabrication of different surface patterns that will serve as platforms to anchor the bacterial cells by UV-irradiation of the polystyrene based surfaces is schematically illustrated in Figure 2. In this particular case a square shaped mask (pitch 25 μm, bar 6 μm and hole 19 μm) has been employed. Equally, the AFM images obtained for each structure and their cross-sectional profiles are included. As depicted in Figure 2(A), at short irradiation times, the regions directly exposed are crosslinked as a consequence of the radical formation and interchain recombination. On the contrary, below the mask the polymer did not receive UV light and, therefore, did not crosslinked. Upon rinsing, the polymer below these areas could be completely removed. In this case, the pattern obtained is the negative of the mask.

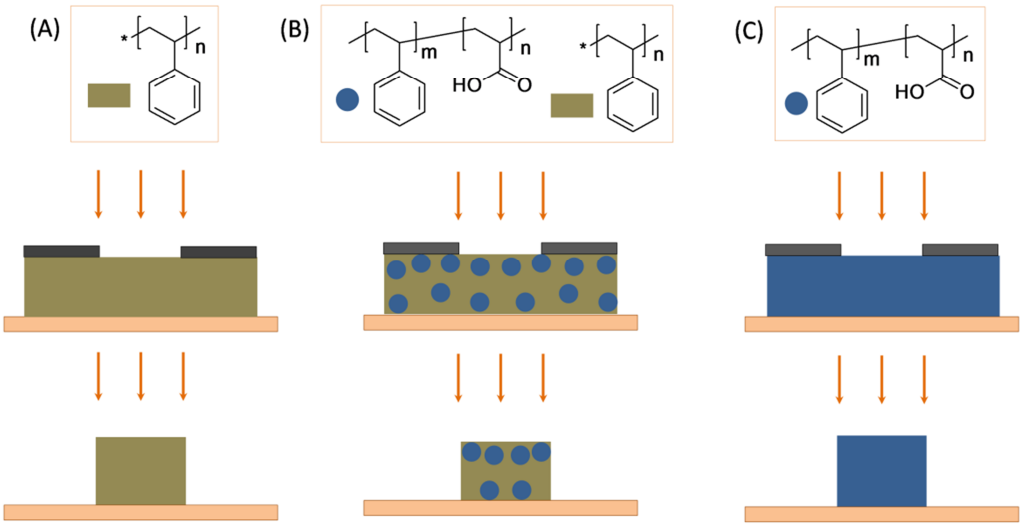

Figure 1. *Homopolymer (PS) and block copolymer (PS_{23}-b-PAA_{11}) employed in the preparation of the substrates with photogenerated patterns. (A) Polystyrene (PS), (B) blends of PS and an amphiphilic block copolymer PS_{23}-b-PAA_{11} and (C) films composed exclusively by the amphiphilic block copolymer.*

Upon longer irradiation times photodegradation appears to play a major role. In those samples that have been irradiated during longer times **(Figure 2(B))** it can be observed that at the interface between exposed/non-exposed areas, a thin region (from 200-300 nm on top up to 2 μm on their base) is formed by crosslinked polymer. According to our observations, in these regions placed at the limit between directly exposed/protected areas the radicals diffused from the exposed areas to the non-exposed producing the crosslinking of the polymer. Taking into account that polystyrene is in a glassy state at room temperature the diffusion is limited and therefore the pattern resolution is rather sharp. This is an interesting aspect since by using this approach different surface patterns with resolutions largely below the resolution provided by the mask employed can be obtained. More precisely, according to the AFM cross-sectional profiles of Figure 3 the half-path width observed is ~1.1 μm and the measured radius on top of the patterns ~200-300 nm.

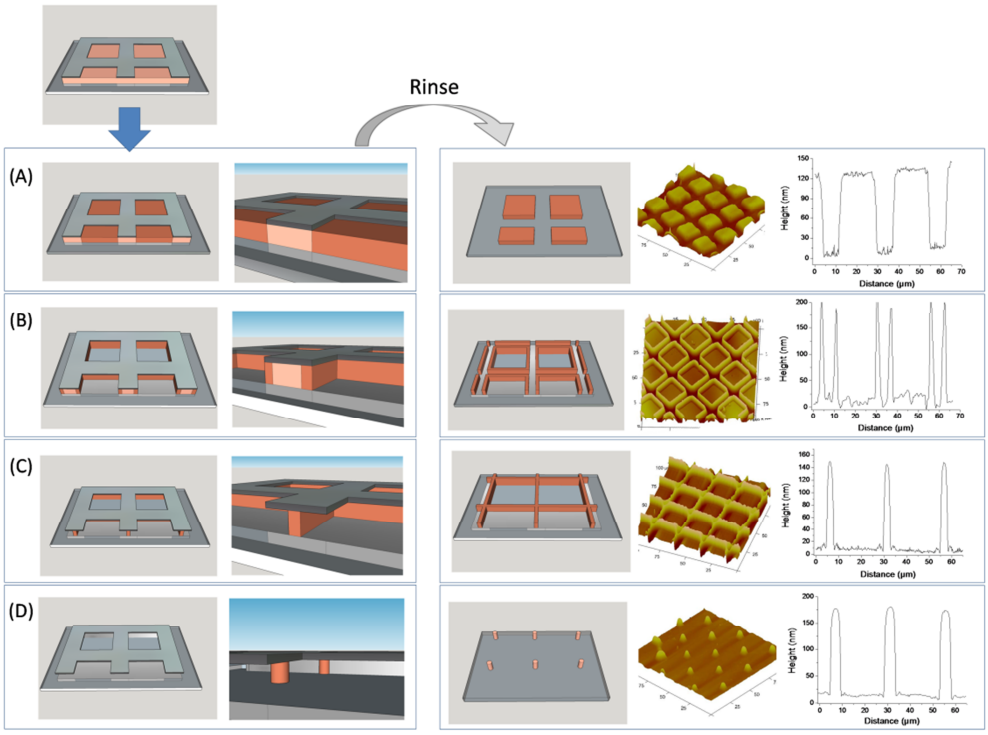

Figure 2. *Structures obtained as a function of the duration of the UV treatment. (A) Square-shaped pattern, (B) closed boxes, (C) crosshatched pattern and (D) micrometer size pillars.*

The radical diffusion towards the non-exposed areas is accompanied by the photodegradation. Thus, as depicted in Figure 2(C) the front crosslinked-degraded moves even below the mask. As a result, rather than open boxes the formation of a crosshatched pattern was observed. More interesting the half-path width for this particular structure is around 1.2 µm as measured by AFM. Finally, photodegradation progresses when using longer irradiations and, as observed in Figure 2(D) only the areas below the crossing points of the mask remained crosslinked. As a result, micrometer size pillars can be produced with a characteristic distance between them provided by the mask employed. In this study, the pillar spacing has been varied between 62 µm and 12,5 µm.

In summary, this approach has, thus, two interesting features: on the one hand, upon larger exposure, degradation of PS occurs as side reaction in those areas directly exposed to the UV irradiation. So that, in principle, it is possible to control the pattern by changing the

experimental conditions (time, UV intensity, etc.). Moreover, since crosslinking can be achieved at the exposed-non exposed interface and due to the low radical diffusion in this region the pattern resolution obtained improves the resolution of the mask employed.

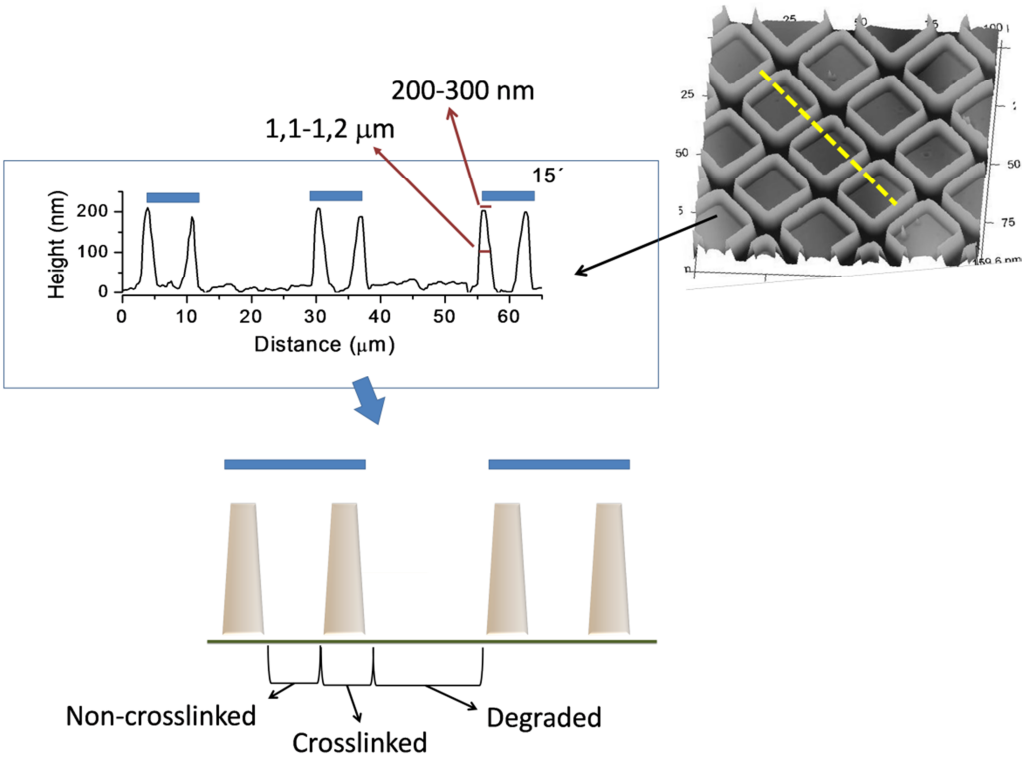

Figure 3. *Top: Cross-sectional profile and 3D AFM image of the open boxes structure with the dimensions on the half-height of the pattern (1.1-1.2 μm) and the diameter on the top of the pattern (~200-300 nm). Down: Model of the structure formed as a consequence of the complete photodegradation of the directly exposed areas and radical diffusion towards the non-exposed regions.*

Using these patterned and functional surfaces (taking advantage of the photocrosslinking/photodegradation of PS and simultaneously varying the surface functionality) the formation of bacterial arrays onto polymer surfaces was investigated. The combination of both aspects will allow us to study both the influence of the surface chemical composition that will be achieved by introducing hydrophilic poly(acrylic acid) groups as additives and how can the final polymer pattern direct the bacterial attachment. For that

purpose, polystyrene was either employed as unique component or partially combined with the block copolymers. Therefore, the hydrophilicity of the films can be varied depending on the amount of block copolymer introduced within the blend.

Films of the blends were prepared by spin coating from tetrahydrofurane (THF) solutions with a concentration of 30 mg mL^{-1}. Upon UV-light exposure and removal of both degraded and non-crosslinked areas by extensive rinsing, the patterned surface were incubated with *S. aureus* (employed as model bacteria). Bacterial solutions in physiological media were incubated for 1 hour and after thorough wash of the surface the bacteria immobilization was monitored by fluorescence microscopy.

The first series of experiments were carried out using different chemical functionalities in order to find those functional groups that favor the bacterial immobilization. We explored four different systems: (a) polystyrene, (b) polystyrene-*b*-poly(acrylic acid) (PS-*b*-PAA), (c) polystyrene-*b*-poly(L-glutamic acid) (PS-*b*-PGA) and (d) polystyrene-*b*-poly[poly(ethylene glycol) methyl ether methacrylate]) (PS-*b*-PEGMA) (Figure 4). The fluorescence images of the films evidenced that by using incubation conditions above depicted two materials, *i.e.* PS-*b*-PAA and PS-*b*-PGA exhibit a large amount of bacterial immobilization onto the patterns created by photocrosslinking (Figure 4b and 4c). These two systems exhibit carboxylic groups at the interface. Carboxylic groups at neutral pH values have negative charge at a consequence of the deprotonation of the acid group. In this situation we would expect that the repulsion between the carboxylic groups and the bacterial membrane would prevent the bacterial adhesion. On the contrary most probably due to the PBS buffer employed with physiological salt concentration the electrostatic repulsion is reduced and permits the bacterial cells to interact with the surface.

Upon finding the chemical functionality that favors the bacterial immobilization the following experiments were carried out by using the hydrophobic PS and a variable amount of PS_{23}-*b*-PAA_{11} block copolymer. On these surfaces, the immobilization of the bacteria was first attempted from a solution at an OD of 1.0 that corresponds to a concentration of about 1.5 10^9 cells mL^{-1}. As a result, whereas the pure polystyrene surfaces required at least 4 h of incubation to evidence the presence of *S. aureus* immobilized at the surface, the incorporation of an amphiphilic block copolymer PS_{23}-*b*-PAA_{11} significantly promote the bacterial adhesion for the substrates (results not shown here). As a consequence, incubation times as low as 1h

resulted in surfaces with a significant bacterial coverage. More interestingly, a gradual increase of the hydrophilicity (as a consequence of the higher amount of block copolymers in the blend) significantly modifies the affinity of the bacteria towards the interface.

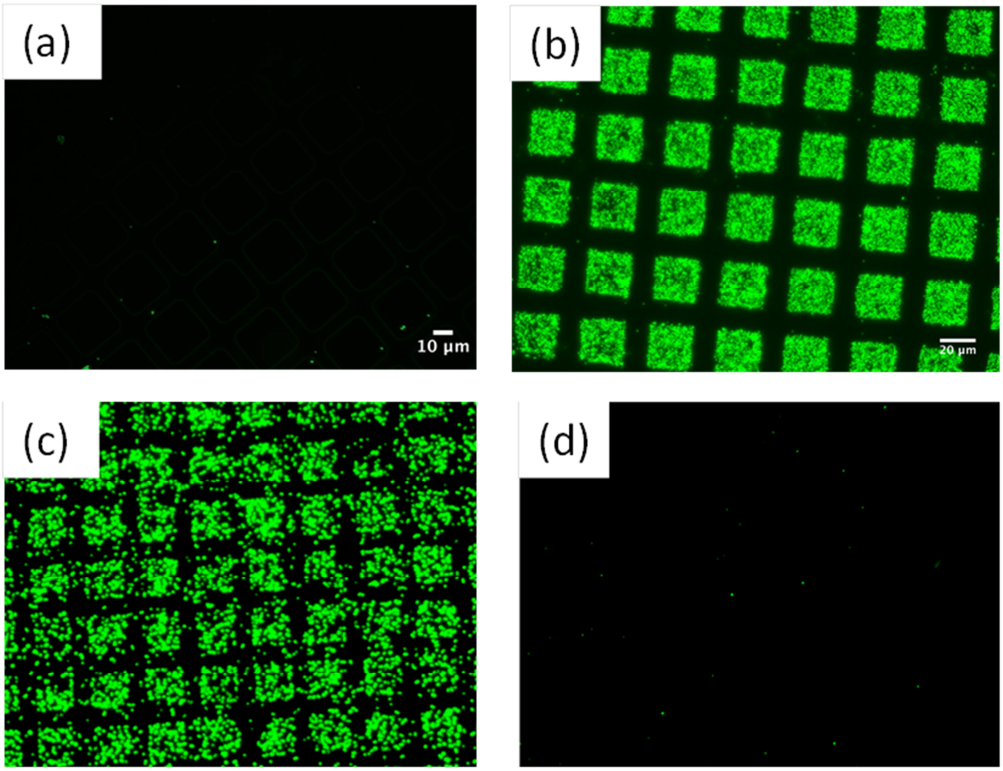

Figure 4. *Fluorescence images of the S. aureus adhesion onto square shaped patterns obtained from (a) Polystyrene (PS), (b) PS_{23}-b-PAA_{11}, (c) PS_{49}-b-PGA_{17} and (d) PS_{45}-co-$PEGMA_{34}$. (Scale bars: 10 µm).*

In Figure 5, are depicted the fluorescence and bright field images of patterned surfaces prepared from PS/PS_{23}-*b*-PAA_{11} blends with variable amount of PAA. An increase of the surface hydrophilicity is accompanied by an increase of the number of bacteria per motif. More precisely, whereas in the surface with no PAA isolated single bacteria in few of the motifs was observed, an increase to 25 wt% of block copolymer within the blend equally increases the number up to ~23±3 bacteria. Further increasing to 50 wt% of block copolymer leads to 32±2 bacteria per square. Finally, by using either 75 wt% of block copolymer or the pure block copolymer the number of bacteria immobilized is close to 41±4.

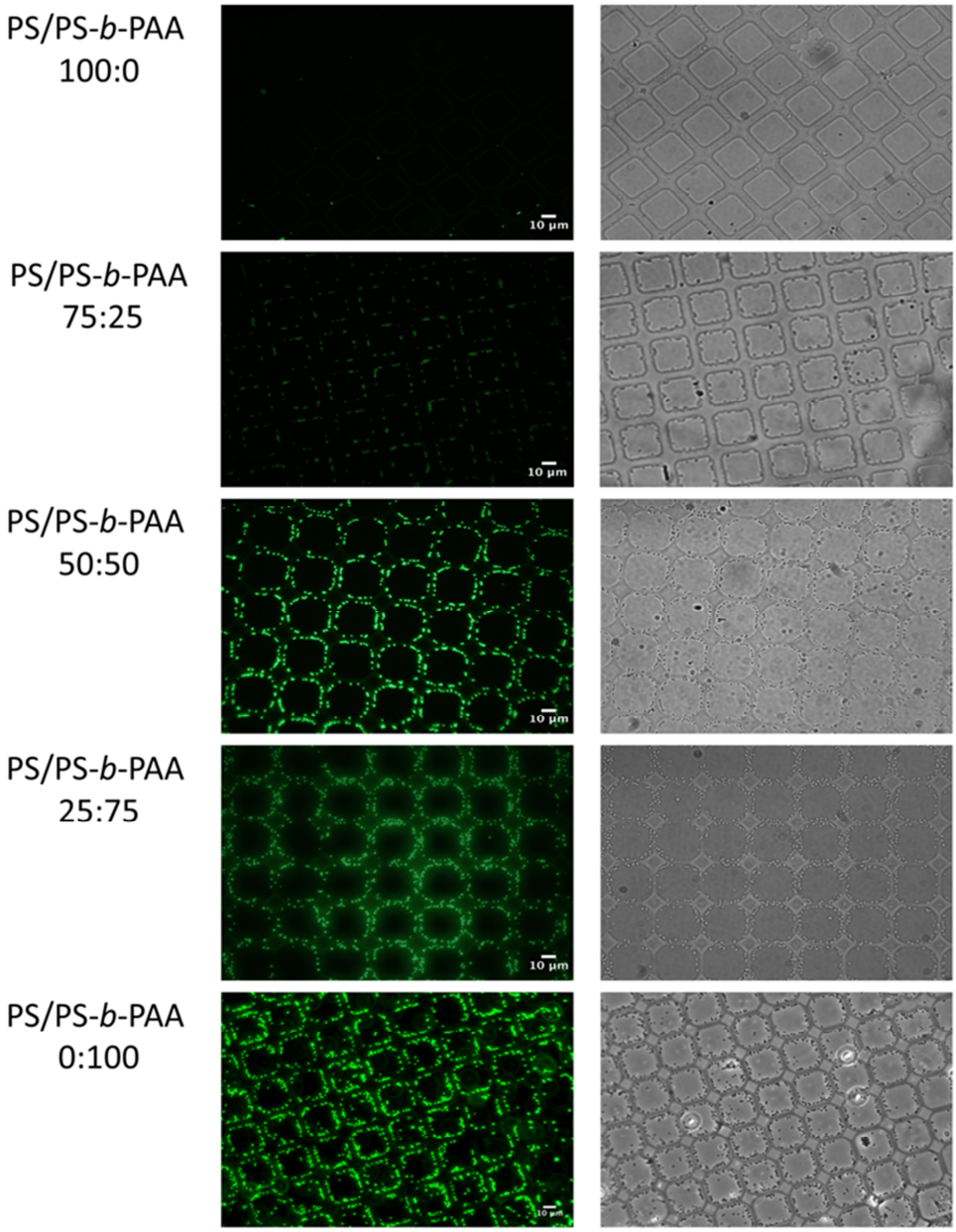

Figure 5. *Fluorescence (left) and bright-field (right) images of the S. aureus adhesion onto square shaped patterns obtained from blends of PS and PS_{23}-b-PAA_{11} with variable ratio between pure PS and pure PS_{23}-b-PAA_{11}. (Scale bar: 10 µm).*

As expected, the surface having a larger amount of hydrophilic PAA clearly favors the immobilization of *S. aureus* on the patterned surfaces. In order to extent the concept to other surface structures the crosslinking experiments were carried out using different masks composed of lines, hexagonal or squares shaped features with variable pitch on surfaces formed exclusively by the block copolymer. In Figure 6 are depicted both the modeled surfaces with the different patterns and the resulting fluorescence images of the surfaces upon bacterial immobilization. The fluorescence images clearly evidenced the selective immobilization of a large number of *S. aureus* on the surface areas formed by crosslinked polystyrene whereas almost none bacteria can be observed on the regions where the polymer has been degraded. The results are equally selective in the different patterned surfaces demonstrating that this is a general approach that can be used to generate different bacteria patterns by simply changing the mask used in the cross-linking process.

As described above, the use of different masks serve to produce different bacterial arrangements. In addition, the control over the photodegradation/photocrosslinking kinetics allowed us, equally, to obtain different surface patterns. In this concern, the changes of the bacterial distribution on patterned films prepared exclusively with the PS_{23}-*b*-PAA_{11} block copolymer and a unique mask depending on the pattern created at different irradiation times were evaluated. In Figure 7 are depicted the fluorescence images of the surfaces having different structural features upon immobilization of the bacterial cells. Figure 7 shows both the surface pattern and the subsequent bacterial arrays obtained upon immobilization of *S. aureus*. As expected, the photodegradation/photocrosslinking induced variations on the surface topography of the films from cubes (Figure 7A) to pillars (Figure 7D) producing, in addition, two intermediary structures i.e. open boxes (Figure 7B) and crosshatched patterns (Figure 7C). The immobilization occurs in all the cases selectively on the crosslinked areas as a consequence of the affinity between the bacterial cells and the hydrophilic carboxylic acid groups of the poly(acrylic acid) block.

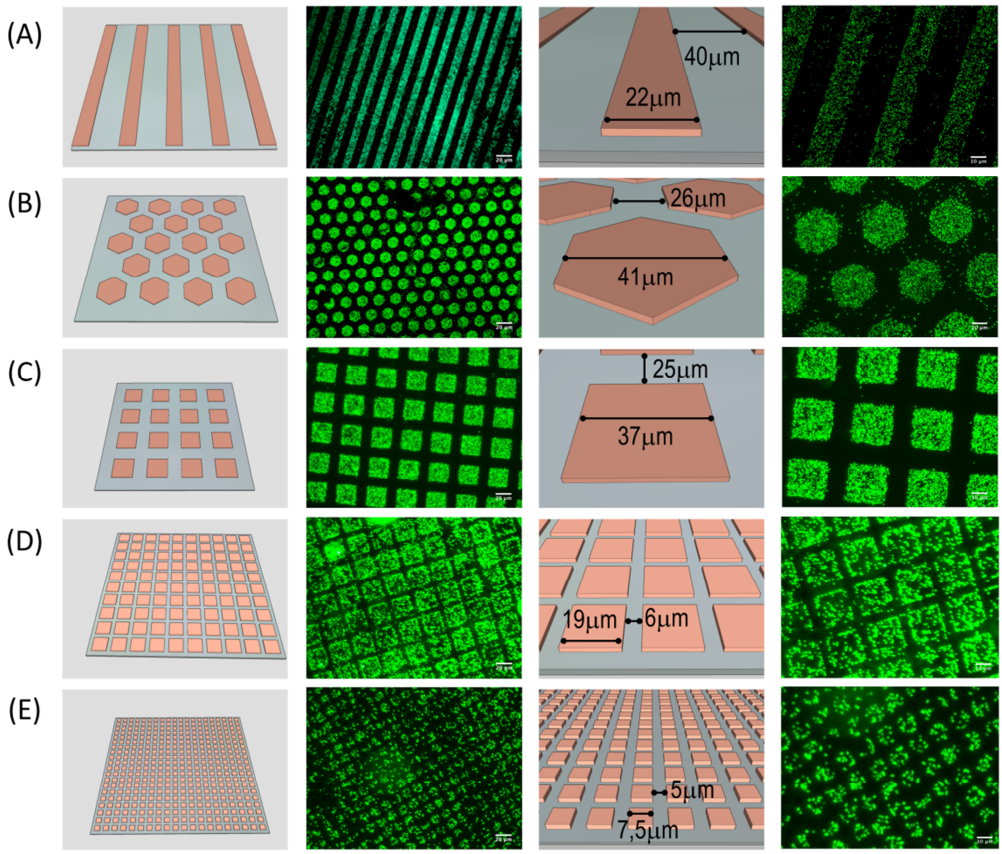

Figure 6. *Bacterial patterns obtained by crosslinking a PS_{23}-b-PAA_{11} block copolymer with UV light (365 nm) and subsequent exposure to a bacterial solution of S. aureus. (A) lines (thickness 22 µm), (B) hexagonal arrays (41x51 µm), (C), (D) and (E) square shaped patterns with decreasing pitch from 62 µm, 25 µm to 12.5 µm, respectively. The images in the left panel were acquired using a 20x amplification objective and in the right panel are shown close-up images of the same surfaces using a 40x amplification objective.*

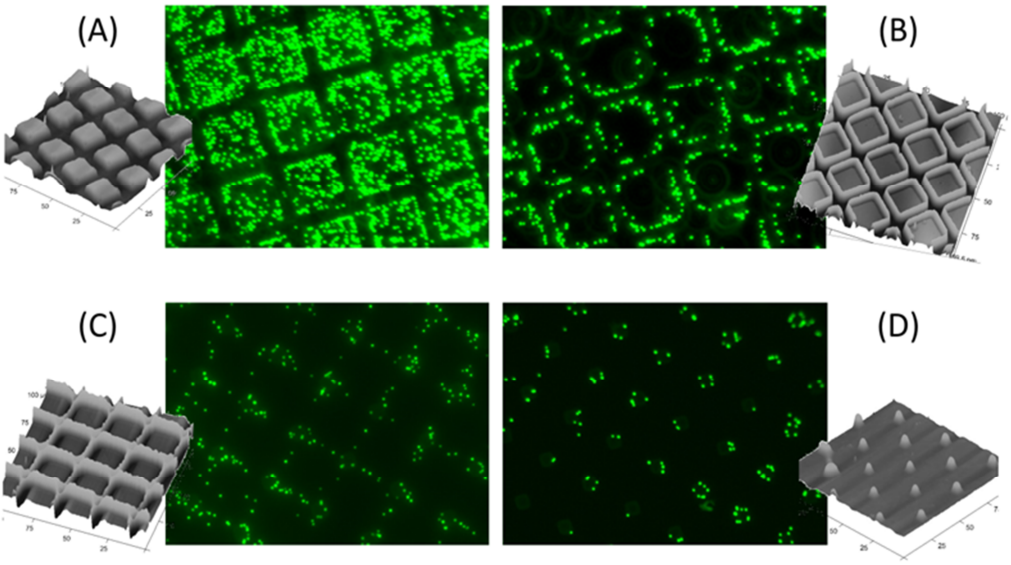

Figure 7. *Variation of the surface pattern and the subsequent bacterial distribution as a function of the treatment employed, i.e. the irradiation times under UV-light. (A) Square shaped distribution (treatment: 15 min UV exposure), (B) open boxes (treatment: 30 min UV exposure) (C) crosshatched pattern (treatment: 1h UV exposure) and (D) pillars (treatment: 2h min UV exposure). Mask: square shaped feature with 25 μm pitch.*

In addition to the precise control of the bacterial immobilization of the surface patterns one of the main objectives of this study is the immobilization of *S. aureus* cells to form single cell arrays. Previously reported literature focused on other types of bacteria such as *Escherichia coli* [123, 147] or *Pseudomonas aeruginosa* [144] while *S. aureus* in spite of their major role in multiple infection diseases has been somehow neglected. This is probably due to the large tendency of *S. aureus* to form aggregates that difficult their isolation and immobilization as single cells. [155, 159] In order to immobilize *S. aureus* as single entities the surface patterns created by crosslinking at the exposed-non exposed areas were employed. In these cases, due to the high resolution of the pattern (1μm and below) which is even below the dimension of the *S. aureus* diameter (~1 μm) we expect to anchor single cells on top of the micrometer/submicrometer size pattern. The resulting bacterial arrays obtained are depicted in Figure 8. On the top [(A), (B)] are depicted the surface patterns obtained with short UV-exposures and subsequent bacterial immobilization monitored by fluorescence microscopy (central panels) and by STEM (right panels). On the bottom [(C), (D) and (E)] the bacterial

arrays on different surface patterns generated by photocrosslinking on the edge (shadow-illuminated) areas of the mask. The A and Bpanels demonstrated the capability of the surface to immobilize *S. aureus* in different shapes. However, as has been already mentioned the bacteria are distributed forming large clusters on top of the pattern. On the contrary, the immobilization of *S. aureus* on the submicrometer patterns exhibits a different behavior. As can be observed in Figure 8 (C) and (D) the bacteria can be aligned on top of the patterned surface as a consequence of the large affinity between the bacteria and the hydrophilic PAA groups. As a consequence either corrals or lines of bacteria can be easily constructed. More interestingly, larger irradiation times using a square shaped mask leads to micrometer size pillars in which a single bacteria can be immobilized (Figure 8(E inset).

In summary, the simple approach depicted herein allows the formation of a large variety of surface patterns depending on the mask employed and the chemical composition of the polymer blend employed. Among others, as demonstrated herein this approach can be employed for the selective adhesion both of single bacteria in pillars and single bacteria alignment. One can envision many potential uses of these platforms. For example, the isolation of cluster growing bacteria can be applied for individual identification and diagnosis. The isolated positioning at the surface might be critical in the cases that are many variants of the same bacterial strain but only some associated with disease, such as in the antibiotic-resistant infections. Another broad field of application of these single cell array platforms concerns the study of different biological processes at the single cell level in a large bacteria population. Those studies have great relevance, for instance, to unravel biological stochastic processes, including gene expression because it has been shown that not even genetically identical cells behave the same. [160-163]

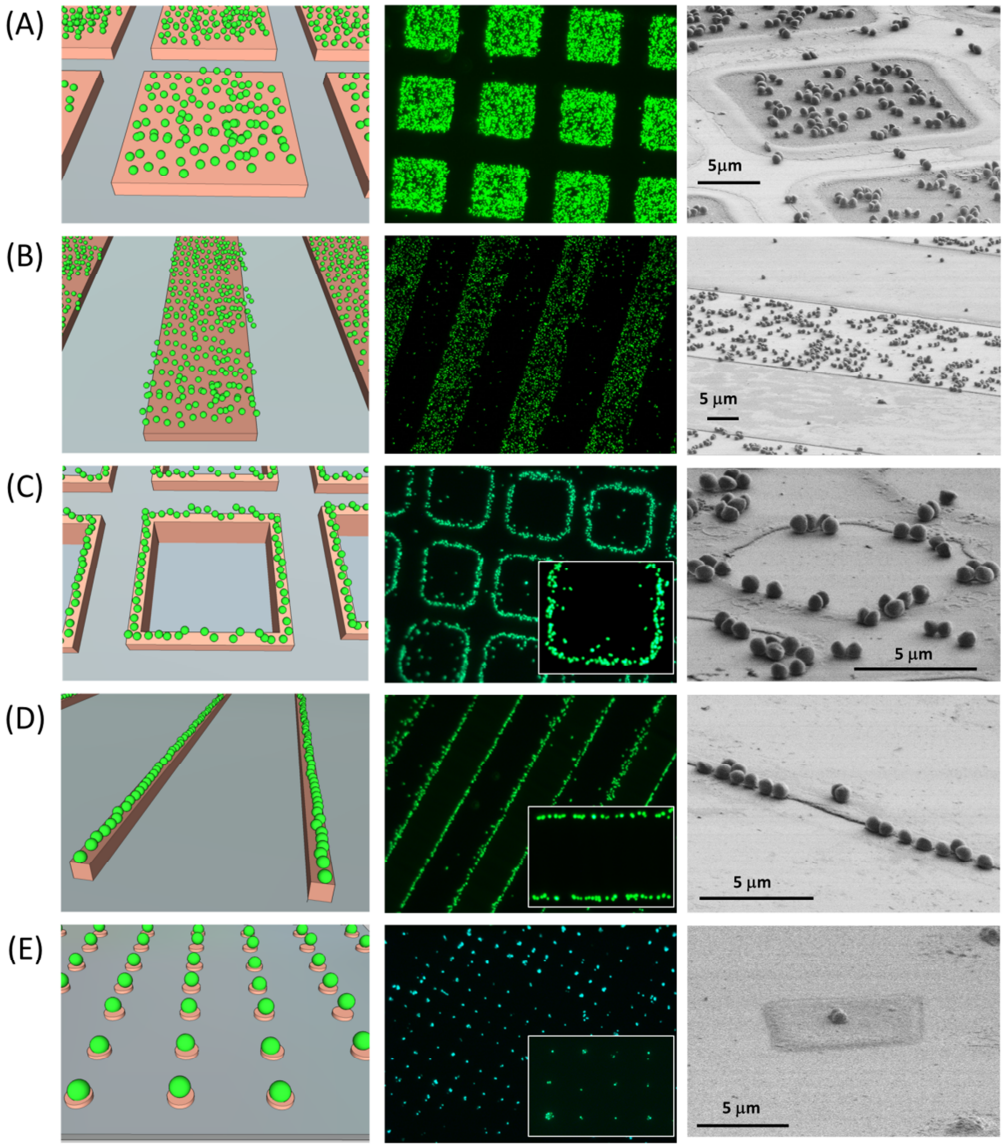

Figure 8. *Surface bacterial patterns generated using short irradiation times (panels, A and B) and upon longer irradiation where the directly exposed areas have been photodegraded (panels C, D and E). Masks employed (A and C) squares with a pitch of 25 µm, (B and D) lines with a width of 22 µm and (E) squares with a pitch of 12.5 µm. The fluorescence microscopy (central panels) and STEM (right panels) images show the selective immobilization of fluorescent S. aureus bacteria. C, D and E included an inset with a close-up image showing individual bacteria immobilization.*

Conclusions

The formation of bacterial surface arrays by using a photolithographic approach having some particular features has been described. First, the methodology employed permitted the incorporation of functional groups able to modify the affinity between the bacteria and the surface. Thus, the incorporation of hydrophilic segments, i.e. PAA favors the bacterial immobilization. Second, the amount of hydrophilic segment introduced can be finely tuned by preparing blends of the block copolymer and linear polystyrene. This unique feature has been employed to determine the role of the surface hydrophilicity on the adhesion of *S. aureus* onto the different surface patterns. More interestingly, the photolithographic approach employed produced different patterns not only depending on the mask employed but also depending on the experimental conditions applied. As a consequence, by using standard equipment without the requirement of expensive fine focalization settings lead to the formation of patterns with nanoscale resolution. The latter has been found to be crucial in order to prepare arrays of isolated bacteria as has been evidenced by using *S. aureus*. It has to be pointed out that the use of *S. aureus* has been up to know somehow neglected mainly due to their aggregation.

Acknowledgements

The authors gratefully acknowledge support from the Consejo Superior de Investigaciones Científicas (CSIC). Equally, this work was financially supported by the Ministerio de Economía y Competitividad (MINECO) through MAT2011-22861, MAT2013-47902-C2-1-R (JRH), and BIO2012-34835 (ALC). M. Palacios thanks the Ministerio de Education for the FPU fellowship. This research is funded in part by the European Commission International Reintegration Grant (IRG-246688) (ALC) and AMAROUT-COFUND Europe Programme (ALC).

Notes and references

[a] Department of Chemistry and Properties of Polymers, Instituto de Ciencia y Tecnología de Polímeros, (ICTP-CSIC), Juan de la Cierva 3, 28006-Madrid, Spain.

* To whom correspondence should be addressed. E-mail: ogarcia@ictp.csic.es and rodriguez@ictp.csic.es

[b] Instituto Madrileño de Estudios Avanzados en Nanociencia (IMDEA-Nanociencia), Cantoblanco, 28049 Madrid, Spain & CNB-CSIC-IMDEA Nanociencia Associated Unit "Unidad de Nanobiotecnología".

Supporting information for Polymer Chemistry manuscript:

Patterning of individual *Staphylococcus aureus* bacteria onto photogenerated polymeric surface structures

Marta Palacios-Cuesta[a], Aitziber L. Cortajarena[b], Olga García[a]* and Juan Rodríguez-Hernández[a]*.

[a] Department of Chemistry and Properties of Polymers, Instituto de Ciencia y Tecnología de Polímeros, (ICTP-CSIC), Juan de la Cierva 3, 28006-Madrid, Spain.

* To whom correspondence should be addressed. E-mail: ogarcia@ictp.csic.es and rodriguez@ictp.csic.es

[b] Instituto Madrileño de Estudios Avanzados en Nanociencia (IMDEA-Nanociencia), Cantoblanco, 28049 Madrid, Spain & CNB-CSIC-IMDEA Nanociencia Associated Unit "Unidad de Nanobiotecnología".

Synthesis of the block copolymers

2.1. Polystyrene-*b*-poly(acrylic acid) (PS-*b*-PAA) diblock copolymers

The diblock copolymers have been prepared by ATRP in two steps [76]:

Synthesis of a polystyrene (PS) macroinitiator by ATRP. All polymerizations were performed in Schlenk flasks previously flamed and dried under vacuum. ATRP was carried out

using the following stoichiometry [M]:[I]:[CuBr]:[L] = 250:1:1:2, where M = styrene, I = initiator (PhEBr) and L = ligand (bipy). The reactants were added under N_2. The reaction mixtures were then degassed by three freeze-pump-thaw cycles and placed in a thermostated oil bath at 110°C. After the polymerization, the mixtures were cooled to room temperature; the contents were diluted with dichloromethane (CH_2Cl_2) and passed through a neutral alumina column to remove the copper salt. After evaporation, the polymers were precipitated in ethanol, filtered, washed and dried under vacuum.

Synthesis of PS-b-PtBA by ATRP. The macroinitiator PS-Br and 5mL of degassed acetone were added to the mixture ([M]:[I]:[CuBr]:[L] = 400:1:1:1). Acetone enhanced the solubility of the CuBr/PMDETA complex. The *t*BA polymerizations were carried out at 65°C.

Hydrolysis of the PtBA block in the PS-b-PtBA copolymers. Copolymers were first dissolved in CH_2Cl_2. Trifluoroacetic acid (TFA) was then added (10 equivalent to *t*-butyl ester units), and the mixture was stirred at room temperature for 3 days. The deprotected polymers precipitated in the reaction media, were filtered and washed with CH_2Cl_2 and finally dried under vacuum.

2.2. Polystyrene-*b*-poly(L-glutamic acid) PS-*b*-PGA

The synthesis of these diblock copolymers was carried out in several steps. [164] First, styrene was polymerized by atom transfer radical polymerization (ATRP). By tuning adequately the conversion to values lower than 40% a large percentage of end-brominated polystyrene groups should be obtained. The end-terminal bromo group was easily modified into an amine function by reaction with 1,4-diaminoethane [107]. The amine modified PS was employed, in turn, as macroinitiator for the ring-opening polymerization of γ-benzylester-L-glutamate N-carboxyanhydride. Finally, deprotection under basic conditions ($KOH/H_2O/THF$) lead to the amphiphilic PS-b-PGA diblock copolymers. The block copolymers have been characterized by ^1H NMR spectroscopy and GPC both to evaluate the integrity of the structure and to determine the chemical composition.

2.3. Polystyrene-*b*-poly[poly(ethylene glycol) methyl ether methacrylate] PS-*b*-PEGMA

The amphiphilic block copolymer polystyrene-*b*-poly[poly(ethylene glycol) methyl ether methacrylate] (PS_{40}-*b*-$P(PEGMA300)_{48}$) (copolymer is labeled with the degree of polymerization of each block) and poly(2,3,4,5,6-pentafluorostyrene) ($P5FS_{21}$) were synthesized via atom transfer radical polymerization (ATRP) as previously reported [32] [165].

Illustrative images of the immobilization of bacterial cells onto PS-*b*-PGA and PS-*b*-PEGMA block copolymer films.

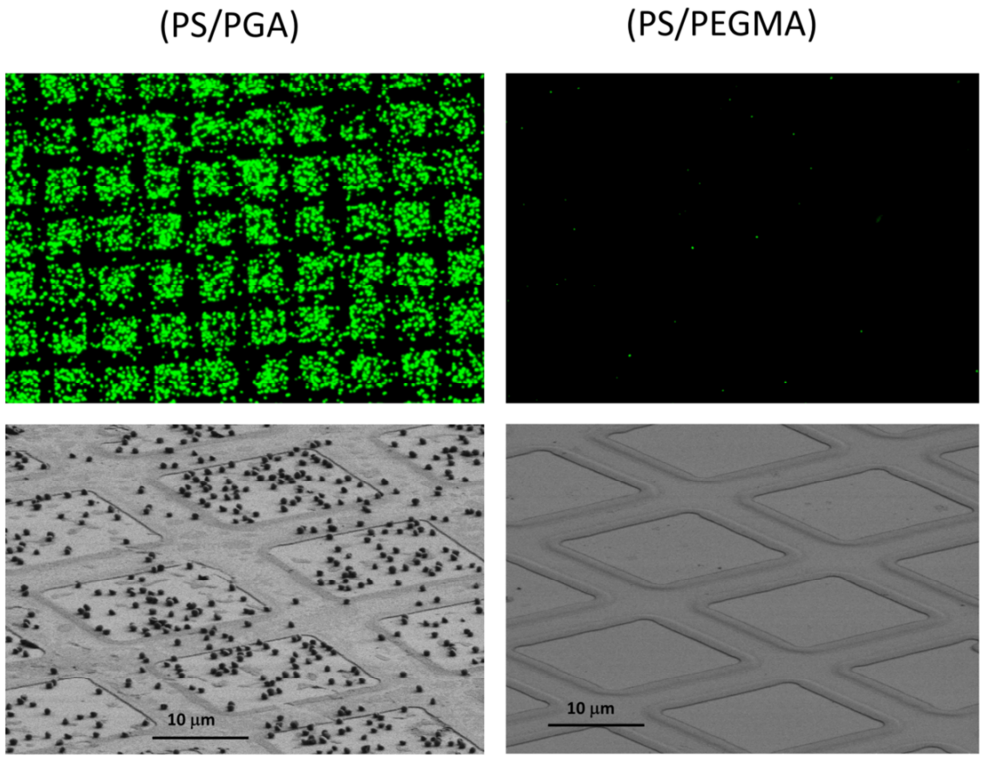

Figure S1. *Comparative bacterial adhesion between hydrophilic charged (PS-b-PGA) and uncharged (PS-b-PEGMA) block polymer surfaces. Up: fluorescence images of the surface upon bacterial immobilization. Down: Scanning electron microscopy images of the resulting surfaces.*

CAPÍTULO II.3: Bibliografía de la sección II

[1] D. Paretkar, M. Kamperman, A.S. Schneider, D. Martina, C. Creton, E. Arzt, Bioinspired pressure actuated adhesive system, *Materials Science and Engineering: C*, 31, **2011,** 1152-1159.

[2] X.J. Feng, L. Jiang, Design and Creation of Superwetting/Antiwetting Surfaces, *Advanced Materials*, 18, **2006,** 3063-3078.

[3] B. Cao, S. Yan, K. Zhang, Z. Song, T. Cao, X. Chen, L. Cui, J. Yin, A Poly(acrylic acid)-block-Poly(L-glutamic acid) Diblock Copolymer with Improved Cell Adhesion for Surface Modification, *Macromolecular Bioscience*, 11, **2011,** 970-977.

[4] K. Wulf, M. Teske, M. Löbler, F. Luderer, K.-P. Schmitz, K. Sternberg, Surface functionalization of poly(ε-caprolactone) improves its biocompatibility as scaffold material for bioartificial vessel prostheses, *Journal of Biomedical Materials Research Part B: Applied Biomaterials*, 98B, **2011,** 89-100.

[5] L.J. Hayes, Surface energy of fluorinated surfaces, *Journal of Fluorine Chemistry*, 8, **1976,** 69-88.

[6] M. Geissler, Y. Xia, Patterning: Principles and Some New Developments, *Advanced Materials*, 16, **2004,** 1249-1269.

[7] S.W. Lee, B.K. Oh, R.G. Sanedrin, K. Salaita, T. Fujigaya, C.A. Mirkin, Biologically Active Protein Nanoarrays Generated Using Parallel Dip-Pen Nanolithography, *Advanced Materials*, 18, **2006,** 1133-1136.

[8] N. Wu, W.B. Russel, Micro- and nano-patterns created via electrohydrodynamic instabilities, *Nano Today*, 4, **2009,** 180-192.

[9] H.-C. Kim, S.-M. Park, W.D. Hinsberg, Block Copolymer Based Nanostructures: Materials, Processes, and Applications to Electronics, *Chemical Reviews*, 110, **2009,** 146-177.

[10] S. Chauhan, F. Palmieri, R.T. Bonnecaze, C.G. Willson, Pinning at template feature edges for step and flash imprint lithography, *Journal of Applied Physics*, 106, **2009,** -.

[11] N. Gadegaard, D. McCloy, Direct stamp fabrication for NIL and hot embossing using HSQ, *Microelectronic Engineering*, 84, **2007,** 2785-2789.

[12] J. Park, J. Li, A. Han, Micro-macro hybrid soft-lithography master (MMHSM) fabrication for lab-on-a-chip applications, *Biomed Microdevices*, 12, **2010,** 345-351.

[13] B. Michel, A. Bernard, A. Bietsch, E. Delamarche, M. Geissler, D. Juncker, H. Kind, J.P. Renault, H. Rothuizen, H. Schmid, P. Schmidt-Winkel, R. Stutz, H. Wolf, Printing meets lithography: Soft approaches to high-resolution patterning, *IBM Journal of Research and Development*, 45, **2001,** 697-719.

[14] A.J.J.M. van Breemen, J.B.P.H. van der Putten, R. Cai, K. Reimann, A.W. Marsman, N. Willard, D.M. de Leeuw, G.H. Gelinck, Photocrosslinking of ferroelectric polymers and its application in three-dimensional memory arrays, *Applied Physics Letters*, 98, **2011,** -.

[15] W. Shi, Y. Lin, S. He, Y. Zhao, C. Li, M. Wei, D.G. Evans, X. Duan, Patterned fluorescence films with reversible thermal response based on the host-guest superarchitecture, *Journal of Materials Chemistry*, 21, **2011,** 11116-11122.

[16] H. Ito, Chemical Amplification Resists for Microlithography, in: Microlithography · Molecular Imprinting, Springer Berlin Heidelberg, 2005, pp. 37-245.

[17] M. Yamaguchi, K. Ikeda, M. Suzuki, A. Kiyohara, S.N. Kudoh, K. Shimizu, T. Taira, D. Ito, T. Uchida, K. Gohara, Cell Patterning Using a Template of Microstructured Organosilane Layer Fabricated by Vacuum Ultraviolet Light Lithography, *Langmuir*, 27, **2011,** 12521-12532.

[18] F. Xu, P. Datta, H. Wang, S. Gurung, M. Hashimoto, S. Wei, J. Goettert, R.L. McCarley, S.A. Soper, Polymer Microfluidic Chips with Integrated Waveguides for Reading Microarrays, *Analytical Chemistry*, 79, **2007,** 9007-9013.

[19] H. Qi, Y. Du, L. Wang, H. Kaji, H. Bae, A. Khademhosseini, Patterned Differentiation of Individual Embryoid Bodies in Spatially Organized 3D Hybrid Microgels, *Advanced Materials*, 22, **2010,** 5276-5281.

[20] E. Berndt, S. Behnke, A. Dannehl, A. Gajda, J. Wingender, M. Ulbricht, Functional coatings for anti-biofouling applications by surface segregation of block copolymer additives, *Polymer*, 51, **2010,** 5910-5920.

[21] H. Yokoyama, T. Miyamae, S. Han, T. Ishizone, K. Tanaka, A. Takahara, N. Torikai, Spontaneously Formed Hydrophilic Surfaces by Segregation of Block Copolymers with Water-Soluble Blocks, *Macromolecules*, 38, **2005,** 5180-5189.

[22] D.R. Iyengar, S.M. Perutz, C.-A. Dai, C.K. Ober, E.J. Kramer, Surface Segregation Studies of Fluorine-Containing Diblock Copolymers†, *Macromolecules*, 29, **1996,** 1229-1234.

[23] A. Bousquet, G. Pannier, E. Ibarboure, E. Papon, J. Rodríguez-Hernández, Control of the Surface Properties in Polymer Blends, *The Journal of Adhesion*, 83, **2007,** 335-349.

[24] D. Sundrani, S.B. Darling, S.J. Sibener, Hierarchical Assembly and Compliance of Aligned Nanoscale Polymer Cylinders in Confinement, *Langmuir*, 20, **2004,** 5091-5099.

[25] B. Gorzolnik, P. Mela, M. Moeller, Nano-structured micropatterns by combination of block copolymer self-assembly and UV photolithography, *Nanotechnology*, 17, **2006,** 5027.

[26] R.A. Segalman, H. Yokoyama, E.J. Kramer, Graphoepitaxy of Spherical Domain Block Copolymer Films, *Advanced Materials*, 13, **2001,** 1152-1155.

[27] Y. Xia, G.M. Whitesides, SOFT LITHOGRAPHY, *Annual Review of Materials Science*, 28, **1998,** 153-184.

[28] M.J. Fasolka, A.M. Mayes, BLOCK COPOLYMER THIN FILMS: Physics and Applications1, *Annual Review of Materials Research*, 31, **2001,** 323-355.

[29] M.A.S. Chong, Y.B. Zheng, H. Gao, L.K. Tan, Combinational template-assisted fabrication of hierarchically ordered nanowire arrays on substrates for device applications, *Applied Physics Letters*, 89, **2006,** -.

[30] N.J. Shirtcliffe, G. McHale, M.I. Newton, G. Chabrol, C.C. Perry, Dual-Scale Roughness Produces Unusually Water-Repellent Surfaces, *Advanced Materials*, 16, **2004,** 1929-1932.

[31] B. Zhao, W.J. Brittain, W. Zhou, S.Z.D. Cheng, Nanopattern Formation from Tethered PS-b-PMMA Brushes upon Treatment with Selective Solvents, *Journal of the American Chemical Society*, 122, **2000,** 2407-2408.

[32] A. Muñoz-Bonilla, E. Ibarboure, E. Papon, J. Rodriguez-Hernandez, Engineering polymer surfaces with variable chemistry and topography, *Journal of Polymer Science Part A: Polymer Chemistry*, 47, **2009,** 2262-2271.

[33] R. Sastre, M. Conde, J.L. Mateo, Photoinitiated bulk polymerization of lauryl acrylate by N-acetyl-4-nitro-1-naphthylamine in the presence of N,N-dimethylaniline, *Journal of Photochemistry and Photobiology A: Chemistry*, 44, **1988,** 111-122.

[34] N. Davidenko, O. Garcia, R. Sastre, O. GarcÃ-a, The efficiency of titanocene as photoinitiator in the polymerization of dental formulations, *Journal of biomaterials science. Polymer edition*, 14, **2003,** 733-746.

[35] C. Decker, A.D. Jenkins, Kinetic approach of oxygen inhibition in ultraviolet- and laser-induced polymerizations, *Macromolecules*, 18, **1985,** 1241-1244.

[36] J. Hutchison, A. Ledwith, Mechanisms and relative efficiencies in radical polymerization photoinitiated by benzoin, benzoin methyl ether and benzil, *Polymer*, 14, **1973,** 405-408.
[37] R. Mason, C.A. Jalbert, P.A.V. O'Rourke Muisener, J.T. Koberstein, J.F. Elman, T.E. Long, B.Z. Gunesin, Surface energy and surface composition of end-fluorinated polystyrene, *Advances in Colloid and Interface Science*, 94, **2001,** 1-19.
[38] J. Bico, U. Thiele, D. Quéré, Wetting of textured surfaces, *Colloids and Surfaces A: Physicochemical and Engineering Aspects*, 206, **2002,** 41-46.
[39] A. Ulman, Engineering surfaces, *CHEMTECH*, 25, **1995,** 22-28.
[40] Y.J. Hwang, S. Matthews, M. McCord, M. Bourham, Surface modification of organic polymer films treated in atmospheric plasmas, *Journal of the Electrochemical Society*, 151, **2004,** C495-C501.
[41] P. Fabbri, M. Messori, M. Montecchi, F. Pilati, R. Taurino, C. Tonelli, M. Toselli, Surface properties of fluorinated hybrid coatings, *Journal of Applied Polymer Science*, 102, **2006,** 1483-1488.
[42] E. Pamula, E. Dryzek, Structural changes in surface-modified polymers for medical applications, *Acta Physica Polonica A*, 113, **2008,** 1485-1493.
[43] J. Yang, Y. Mei, A.L. Hook, M. Taylor, A.J. Urquhart, S.R. Bogatyrev, R. Langer, D.G. Anderson, M.C. Davies, M.R. Alexander, Polymer surface functionalities that control human embryoid body cell adhesion revealed by high throughput surface characterization of combinatorial material microarrays, *Biomaterials*, 31, **2010,** 8827-8838.
[44] J.A. Barish, J.M. Goddard, Topographical and chemical characterization of polymer surfaces modified by physical and chemical processes, *Journal of Applied Polymer Science*, 120, **2011,** 2863-2871.
[45] R.A. Wolf, Plastic surface modification: Cleaning, adhesion and functionalization, in, 2011, pp. 851-854.
[46] I.L. Onder, A. Okudan, Functionalization of Polystyrene with Cyclic Anhydrides and their Spectroscopic, Adhesive and Corrosive Characterizations, *International polymer processing*, 27, **2012,** 270-276.
[47] S. Yuan, G. Xiong, A. Roguin, C. Choong, Immobilization of gelatin onto poly(Glycidyl Methacrylate)- grafted polycaprolactone substrates for improved cell-material interactions, *Biointerphases*, 7, **2012,** 1-12.
[48] C. Drummond, P. Richetti, J. Rodríguez-Hernández, S. Lecommandoux, Triblock copolymer lubricant films under shear: Effect of molecular cross-linking, *Journal of Adhesion*, 83, **2007,** 431-448.
[49] C. Drummond, G. Marinov, P. Richetti, Reinforcement of a surfactant boundary lubricant film by a hydrophilic - Hydrophilic diblock copolymer, *Langmuir*, 24, **2008,** 1560-1565.
[50] J.M. Lagleize, P. Richetti, C. Drummond, Effect of Surfactant Oligomerization Degree on Lubricant Properties of Mixed Surfactant-Diblock Copolymer Films, *Tribology letters*, 39, **2010,** 31-38.
[51] W.H. Kuo, M.J. Wang, C.W. Chang, T.C. Wei, J.Y. Lai, W.B. Tsai, C. Lee, Improvement of hemocompatibility on materials by photoimmobilization of poly(ethylene glycol), *Journal of Materials Chemistry*, 22, **2012,** 9991-9999.
[52] J.F. Briand, I. Djeridi, D. Jamet, S. Coupé, C. Bressy, M. Molmeret, B. Le Berre, F. Rimet, A. Bouchez, Y. Blache, Pioneer marine biofilms on artificial surfaces including antifouling coatings immersed in two contrasting French Mediterranean coast sites, *Biofouling*, 28, **2012,** 453-463.

[53] E. Patrucco, S. Ouasti, D.V. Cong, P. De Leonardis, A. Pollicino, S.P. Armes, M. Scandola, N. Tirelli, Surface-initiated ATRP modification of tissue culture substrates: Poly(glycerol monomethacrylate) as an antifouling surface, *Biomacromolecules*, 10, **2009,** 3130-3140.

[54] T. Bahners, L. Prager, S. Kriehn, J.S. Gutmann, Super-hydrophilic surfaces by photo-induced micro-folding, *Applied Surface Science*, **2012**.

[55] B. Cortese, H. Morgan, Controlling the wettability of hierarchically structured thermoplastics, *Langmuir*, 28, **2012,** 896-904.

[56] F. Kessler, S. Kühn, C. Radtke, D.E. Weibel, Controlling the surface wettability of poly(sulfone) films by UV-assisted treatment: Benefits in relation to plasma treatment, *Polymer International*, **2012**.

[57] M. Kobayashi, Y. Terayama, H. Yamaguchi, M. Terada, D. Murakami, K. Ishihara, A. Takahara, Wettability and antifouling behavior on the surfaces of superhydrophilic polymer brushes, *Langmuir*, 28, **2012,** 7212-7222.

[58] C.P. Stallard, K.A. McDonnell, O.D. Onayemi, J.P. O'Gara, D.P. Dowling, Evaluation of protein adsorption on atmospheric plasma deposited coatings exhibiting superhydrophilic to superhydrophobic properties, *Biointerphases*, 7, **2012,** 31.

[59] X.M. Li, D. Reinhoudt, M. Crego-Calama, What do we need for a superhydrophobic surface? A review on the recent progress in the preparation of superhydrophobic surfaces, *Chemical Society Reviews*, 36, **2007,** 1350-1368.

[60] M.R. Dusseiller, D. Schlaepfer, M. Koch, R. Kroschewski, M. Textor, An inverted microcontact printing method on topographically structured polystyrene chips for arrayed micro-3-D culturing of single cells, *Biomaterials*, 26, **2005,** 5917-5925.

[61] A.S. De León, A. Del Campo, M. Fernández-García, J. Rodríguez-Hernández, A. Muñoz-Bonilla, Hierarchically structured multifunctional porous interfaces through water templated self-assembly of ternary systems, *Langmuir*, 28, **2012,** 9778-9787.

[62] Y. Zheng, Y. Kubowaki, M. Kashiwagi, K. Miyazaki, Process optimization of preparing honeycomb-patterned polystyrene films by breath figure method, *Journal of Mechanical Science and Technology*, 25, **2011,** 33-36.

[63] L. Li, C. Chen, A. Zhang, X. Liu, K. Cui, J. Huang, Z. Ma, Z. Han, Fabrication of robust honeycomb polymer films: A facile photochemical cross-linking process, *Journal of Colloid and Interface Science*, 331, **2009,** 446-452.

[64] M. Ghezzi, S.C. Thickett, C. Neto, Early and intermediate stages of guided dewetting in polystyrene thin films, *Langmuir*, 28, **2012,** 10147-10151.

[65] G.T. Carroll, N.J. Turro, J.T. Koberstein, Patterning dewetting in thin polymer films by spatially directed photocrosslinking, *Journal of Colloid and Interface Science*, 351, **2010,** 556-560.

[66] I.W. Moran, J.R. Ell, K.R. Carter, Functionally decoupled soft lithography for patterning polymer brushes, *Small*, 7, **2011,** 2669-2674.

[67] W. Pfleging, M. Bruns, M. Przybylski, A. Welle, S. Wilson, Patterning of polystyrene by UV-laser radiation for the fabrication of devices for patch clamping, in, 2008.

[68] N. Ktari, P. Poncet, H. Sénéchal, L. Malaquin, F. Kanoufi, C. Combellas, Patterning of polystyrene by scanning electrochemical microscopy. Biological applications to cell adhesion, *Langmuir*, 26, **2010,** 17348-17356.

[69] A. del Prado, N. Briz, R. Navarro, M. Pérez, A. Gallardo, H. Reinecke, Transparent Polystyrene Substrates with Controllable Surface Chlorosulfonation: Stable, Versatile, and Water-Compatible Precursors for Functionalization, *Macromolecules*, 45, **2012,** 2648-2653.

[70] W. Song, X. Wang, H. Lu, N. Kawazoe, G. Chen, Exploring adipogenic differentiation of a single stem cell on poly(acrylic acid) and polystyrene micropatterns, *Soft Matter*, 8, **2012,** 8429-8437.

[71] W. Pfleging, M. Torge, M. Bruns, V. Trouillet, A. Welle, S. Wilson, Laser- and UV-assisted modification of polystyrene surfaces for control of protein adsorption and cell adhesion, *Applied Surface Science*, 255, **2009,** 5453-5457.

[72] P.S. Curti, M.R. De Moura, E. Radovanovic, A.F. Rubira, E.C. Muniz, R.A. Moliterno, Surface modification of polystyrene and poly(ethylene terephtalate) by grafting poly(N-isopropylacrylamide), *Journal of Materials Science: Materials in Medicine*, 13, **2002,** 1175-1180.

[73] S.M. Oliveira, W. Song, N.M. Alves, J.F. Mano, Chemical modification of bioinspired superhydrophobic polystyrene surfaces to control cell attachment/proliferation, *Soft Matter*, 7, **2011,** 8932-8941.

[74] D. Knudsen, B. Harnish, R. Toth, M. Yan, Creating microstructures on silicon wafers using UV-crosslinked polystyrene thin films, *Polymer Engineering and Science*, 49, **2009,** 945-948.

[75] H. Kaczmarek, Changes of polymer morphology caused by u.v. irradiation: 2. Surface destruction of polymer blends, *Polymer*, 37, **1996,** 547-553.

[76] A. Muñoz-Bonilla, A. Bousquet, E. Ibarboure, E. Papon, C. Labrugère, J. Rodríguez-Hernández, Fabrication and Superhydrophobic Behavior of Fluorinated Microspheres, *Langmuir*, 26, **2010,** 16775-16781.

[77] N. Grassie, N.A. Weir, The photooxidation of polymers. II. Photolysis of polystyrene, *Journal of Applied Polymer Science*, 9, **1965,** 975-986.

[78] L. O'Toole, R.D. Short, F.A. Bottino, A. Pollicino, A. Recca, The surface photo-oxidation of polystyrene: Part I-The application of ToF-SIMS to monitor changes in polymer chain length, *Polymer Degradation and Stability*, 38, **1992,** 147-154.

[79] S.I. Kuzina, A.I. Mikhailov, The photo-oxidation of polymers-1. Initiation of polystyrene photo-oxidation, *European Polymer Journal*, 29, **1993,** 1589-1594.

[80] J.F. Rabek, B. Ranby, STUDIES ON THE PHOTOOXIDATION MECHANISM OF POLYMERS - 2. THE ROLE OF QUINONES AS SENSITIZERS IN THE PHOTOOXIDATIVE DEGRADATION OF POLYSTYRENE, *J Polym Sci Part A-1 Polym Chem*, 12, **1974,** 295-306.

[81] M.D. Millan, J. Locklin, T. Fulghum, A. Baba, R.C. Advincula, Polymer thin film photodegradation and photochemical crosslinking: FT-IR imaging, evanescent waveguide spectroscopy, and QCM investigations, *Polymer*, 46, **2005,** 5556-5568.

[82] S.I. Kuzina, A.I. Mikhailov, Photo-oxidation of polymers 4. The dual mechanism of polystyrene photo-oxidation: A hydroperoxide and a photochain one, *European Polymer Journal*, 37, **2001,** 2319-2325.

[83] J.L. Gejo, N. Manoj, S. Sumalekshmy, H. Glieman, T. Schimmel, M. Wörner, A.M. Braun, Vacuum-ultraviolet photochemically initiated modification of polystyrene surfaces: Morphological changes and mechanistic investigations, *Photochemical and Photobiological Sciences*, 5, **2006,** 948-954.

[84] J. Kong, K.L. Yung, Y. Xu, W. Tian, Wettability transition of plasma-treated polystyrene micro/nano pillars-aligned patterns, *Express Polymer Letters*, 4, **2010,** 753-762.

[85] A. Bousquet, E. Ibarboure, C. Drummond, C. Labrugere, E. Papon, J. Rodriguez-Hernandez, Design of Stimuli-Responsive Surfaces Prepared by Surface Segregation of Polypeptide-b-polystyrene Diblock Copolymers, *Macromolecules*, 41, **2008,** 1053-1056.

[86] M.L. Cairns, B.J. Meenan, G.A. Burke, A.R. Boyd, Influence of surface topography on osteoblast response to fibronectin coated calcium phosphate thin films, *Colloids and Surfaces B: Biointerfaces*, 78, **2010,** 283-290.
[87] S. Tajima, J.S.F. Chu, S. Li, K. Komvopoulos, Differential regulation of endothelial cell adhesion, spreading, and cytoskeleton on low-density polyethylene by nanotopography and surface chemistry modification induced by argon plasma treatment, *Journal of Biomedical Materials Research Part A*, 84A, **2008,** 828-836.
[88] F.L. Yap, Y. Zhang, Assembly of polystyrene microspheres and its application in cell micropatterning, *Biomaterials*, 28, **2007,** 2328-2338.
[89] F.L. Yap, Y. Zhang, Protein and cell micropatterning and its integration with micro/nanoparticles assembly, *Biosensors and Bioelectronics*, 22, **2007,** 775-788.
[90] C.Y. Yang, T.C. Liao, H.H. Shuai, T.L. Shen, J.A. Yeh, C.M. Cheng, Micropatterning of mammalian cells on inorganic-based nanosponges, *Biomaterials*, 33, **2012,** 4988-4997.
[91] S. Sarkar, B.C. Isenberg, E. Hodis, J.B. Leach, T.A. Desai, J.Y. Wong, Fabrication of a layered microstructured polycaprolactone construct for 3-D tissue engineering, *Journal of Biomaterials Science, Polymer Edition*, 19, **2008,** 1347-1362.
[92] Y. Zhao, H. Zeng, J. Nam, S. Agarwal, Fabrication of skeletal muscle constructs by topographic activation of cell alignment, *Biotechnology and Bioengineering*, 102, **2009,** 624-631.
[93] I.E. Palamà, S. D'Amone, A.M. Coluccia, G. Gigli, Micropatterned polyelectrolyte nanofilms promote alignment and myogenic differentiation of C2C12 cells in standard growth media, *Biotechnology and Bioengineering*, **2012**.
[94] D. Geblinger, C. Zink, N.D. Spencer, L. Addadi, B. Geiger, Effects of surface microtopography on the assembly of the osteoclast resorption apparatus, *Journal of The Royal Society Interface*, **2011**.
[95] S. Zapotoczny, Stimuli responsive polymers for nanoengineering of biointerfaces, *Methods in molecular biology (Clifton, N.J.)*, 811, **2012,** 51-78.
[96] J.-J. Chen, H. Quoc-Phong, M.-J. Wang, Modulation of cell responses by creating surface submicron topography and amine functionalities, *Journal of Polymer Science Part B-Polymer Physics*, 50, **2012,** 484-491.
[97] X. Zhou, J. Shi, F. Zhang, J. Hu, X. Li, L. Wang, X. Ma, Y. Chen, Reversed cell imprinting, AFM imaging and adhesion analyses of cells on patterned surfaces, *Lab on a Chip*, 10, **2010,** 1182-1188.
[98] A.H.C. Poulsson, S.A. Mitchell, M.R. Davidson, A.J. Johnstone, N. Emmison, R.H. Bradley, Attachment of Human Primary Osteoblast Cells to Modified Polyethylene Surfaces, *Langmuir*, 25, **2009,** 3718-3727.
[99] B. Pidhatika, J. Möller, E.M. Benetti, R. Konradi, E. Rakhmatullina, A. Mühlebach, R. Zimmermann, C. Werner, V. Vogel, M. Textor, The role of the interplay between polymer architecture and bacterial surface properties on the microbial adhesion to polyoxazoline-based ultrathin films, *Biomaterials*, 31, **2010,** 9462-9472.
[100] M.M. Stevens, J.H. George, Exploring and engineering the cell surface interface, *Science*, 310, **2005,** 1135-1138.
[101] K.B. Lee, S.J. Park, C.A. Mirkin, J.C. Smith, M. Mrksich, Protein nanoarrays generated by dip-pen nanotithography, *Science*, 295, **2002,** 1702-1705.
[102] J.D. Hoff, L.J. Cheng, E. Meyhöfer, L.J. Guo, A.J. Hunt, Nanoscale protein patterning by imprint lithography, *Nano Letters*, 4, **2004,** 853-857.
[103] G.M. Whitesides, E. Ostuni, S. Takayama, X. Jiang, D.E. Ingber, Soft lithography in biology and biochemistry, in, 2001, pp. 335-373.

[104] T. Blättler, C. Huwiler, M. Ochsner, B. Städler, H. Solak, J. Vörös, H. Michelle Grandin, Nanopatterns with bioiogical functions, *Journal of Nanoscience and Nanotechnology*, 6, **2006,** 2237-2264.

[105] A.L. Cortajarena, T. Kajander, W.L. Pan, M.J. Cocco, L. Regan, Protein design to understand peptide ligand recognition by tetratricopeptide repeat proteins, *Protein Engineering Design & Selection*, 17, **2004,** 399-409.

[106] A.L. Cortajarena, T.Y. Liu, M. Hochstrasser, L. Regan, Designed Proteins To Modulate Cellular Networks, *Acs Chemical Biology*, 5, **2010,** 545-552.

[107] J. Babin, C. Leroy, S. Lecommandoux, R. Borsali, Y. Gnanou, D. Taton, Towards an easy access to amphiphilic rod-coil miktoarm star copolymers, *Chemical Communications*, **2005,** 1993-1995.

[108] T. Kajander, A.L. Cortajarena, L. Regan, Consensus design as a tool for engineering repeat proteins, *Methods in molecular biology (Clifton, N.J.)*, 340, **2006,** 151-170.

[109] R.P. Ilagan, E. Rhoades, D.F. Gruber, H.-T. Kao, V.A. Pieribone, L. Regan, A new bright green-emitting fluorescent protein - engineered monomeric and dimeric forms, *Febs Journal*, 277, **2010,** 1967-1978.

[110] M.E. Jackrel, R. Valverde, L. Regan, Redesign of a protein-peptide interaction; Characterization and applications, *Protein Science*, 18, **2009,** 762-774.

[111] M. Palacios, O. Garcia, J. Rodriguez-Hernandez, Constructing Robust and Functional Micropatterns on Polystyrene Surfaces by Using Deep UV Irradiation, *Langmuir : the ACS journal of surfaces and colloids*, 29, **2013,** 2756-2763.

[112] M.E. Jackrei, R. Valverde, L. Regan, Redesign of a protein-peptide interaction: Characterization and applications, *Protein Science*, 18, **2009,** 762-774.

[113] D. Alves, M.O. Pereira, Mini-review: Antimicrobial peptides and enzymes as promising candidates to functionalize biomaterial surfaces, *Biofouling*, 30, **2014,** 483-499.

[114] J. Hasan, R.J. Crawford, E.P. Lvanova, Antibacterial surfaces: the quest for a new generation of biomaterials, *Trends in Biotechnology*, 31, **2013,** 31-40.

[115] V. Nandakumar, S. Chittaranjan, V.M. Kurian, M. Doble, Characteristics of bacterial biofilm associated with implant material in clinical practice, *Polymer Journal*, 45, **2013,** 137-152.

[116] S.T. Reddy, K.K. Chung, C.J. McDaniel, R.O. Darouiche, J. Landman, A.B. Brennan, Micropatterned Surfaces for Reducing the Risk of Catheter-Associated Urinary Tract Infection: An In Vitro Study on the Effect of Sharklet Micropatterned Surfaces to Inhibit Bacterial Colonization and Migration of Uropathogenic Escherichia coli, *Journal of Endourology*, 25, **2011,** 1547-1552.

[117] K. Salaita, Y. Wang, C.A. Mirkin, Applications of dip-pen nanolithography, *Nature Nanotechnology*, 2, **2007,** 145-155.

[118] Y.-K. Kim, S.-R. Ryoo, S.-J. Kwack, D.-H. Min, Mass Spectrometry Assisted Lithography for the Patterning of Cell Adhesion Ligands on Self-Assembled Monolayers, *Angewandte Chemie-International Edition*, 48, **2009,** 3507-3511.

[119] A.I. Hochbaum, J. Aizenberg, Bacteria Pattern Spontaneously on Periodic Nanostructure Arrays, *Nano Letters*, 10, **2010,** 3717-3721.

[120] D.D. Doorneweerd, W.A. Henne, R.G. Reifenberger, P.S. Low, Selective Capture and Identification of Pathogenic Bacteria Using an Immobilized Siderophore, *Langmuir*, 26, **2010,** 15424-15429.

[121] F. Bai, R.W. Branch, D.V. Nicolau, Jr., T. Pilizota, B.C. Steel, P.K. Maini, R.M. Berry, Conformational Spread as a Mechanism for Cooperativity in the Bacterial Flagellar Switch, *Science*, 327, **2010,** 685-689.

[122] S. Rozhok, C.K.F. Shen, P.L.H. Littler, Z.F. Fan, C. Liu, C.A. Mirkin, R.C. Holz, Methods for fabricating microarrays of motile bacteria, *Small*, 1, **2005,** 445-451.

[123] S. Rozhok, Z. Fan, D. Nyamjav, C. Liu, C.A. Mirkin, R.C. Holz, Attachment of motile bacterial cells to prealigned holed microarrays, *Langmuir*, 22, **2006,** 11251-11254.
[124] B. Rowan, M.A. Wheeler, R.M. Crooks, Patterning bacteria within hyperbranched polymer film templates, *Langmuir*, 18, **2002,** 9914-9917.
[125] N.R. Thirumalapura, R.J. Morton, A. Ramachandran, J.R. Malayer, Lipopolysaccharide microarrays for the detection of antibodies, *Journal of Immunological Methods*, 298, **2005,** 73-81.
[126] N.R. Thirumalapura, A. Ramachandran, R.J. Morton, J.R. Malayer, Bacterial cell microarrays for the detection and characterization of antibodies against surface antigens, *Journal of Immunological Methods*, 309, **2006,** 48-54.
[127] C.-H. Choi, J.-H. Lee, T.-S. Hwang, C.-S. Lee, Y.-G. Kim, Y.-H. Yang, K.M. Huh, Preparation of bacteria microarray using selective patterning of polyelectrolyte multilayer and poly(ethylene glycol)-poly(lactide) diblock copolymer, *Macromolecular Research*, 18, **2010,** 254-259.
[128] Y. Kuang, I. Biran, D.R. Walt, Living bacterial cell array for genotoxin monitoring, *Analytical Chemistry*, 76, **2004,** 2902-2909.
[129] Z. Suo, R. Avci, X. Yang, D.W. Pascual, Efficient immobilization and patterning of live bacterial cells, *Langmuir*, 24, **2008,** 4161-4167.
[130] I. Biran, D.M. Rissin, E.Z. Ron, D.R. Walt, Optical imaging fiber-based live bacterial cell array biosensor, *Analytical Biochemistry*, 315, **2003,** 106-113.
[131] T.K. Van Dyk, E.J. DeRose, G.E. Gonye, LuxArray, a high-density, genomewide transcription analysis of Escherichia coli using bioluminescent reporter strains, *Journal of Bacteriology*, 183, **2001,** 5496-5505.
[132] M.B. Miller, B.L. Bassler, Quorum sensing in bacteria, *Annual Review of Microbiology*, 55, **2001,** 165-199.
[133] S. Raina, D. De Vizio, M. Odell, M. Clements, S. Vanhulle, T. Keshavarz, Microbial quorum sensing: a tool or a target for antimicrobial therapy?, *Biotechnology and Applied Biochemistry*, 54, **2009,** 65-84.
[134] B.A. Hense, C. Kuttler, J. Mueller, M. Rothballer, A. Hartmann, J.-U. Kreft, Opinion - Does efficiency sensing unify diffusion and quorum sensing?, *Nature Reviews Microbiology*, 5, **2007,** 230-239.
[135] C.M. Thomas, K.M. Nielsen, Mechanisms of, and barriers to, horizontal gene transfer between bacteria, *Nature Reviews Microbiology*, 3, **2005,** 711-721.
[136] S.J. Sorensen, M. Bailey, L.H. Hansen, N. Kroer, S. Wuertz, Studying plasmid horizontal transfer in situ: A critical review, *Nature Reviews Microbiology*, 3, **2005,** 700-710.
[137] B.V. Merkey, L.A. Lardon, J.M. Seoane, J.-U. Kreft, B.F. Smets, Growth dependence of conjugation explains limited plasmid invasion in biofilms: an individual-based modelling study, *Environmental Microbiology*, 13, **2011,** 2435-2452.
[138] A. Cerf, J.-C. Cau, C. Vieu, Controlled assembly of bacteria on chemical patterns using soft lithography, *Colloids and Surfaces B: Biointerfaces*, 65, **2008,** 285-291.
[139] D.B. Weibel, A. Lee, M. Mayer, S.F. Brady, D. Bruzewicz, J. Yang, W.R. DiLuzio, J. Clardy, G.M. Whitesides, Bacterial printing press that regenerates its ink: Contact-printing bacteria using hydrogel stamps, *Langmuir*, 21, **2005,** 6436-6442.
[140] Y.-j. Xie, H.-y. Yu, S.-y. Wang, Z.-k. Xu, Improvement of antifouling characteristics in a bioreactor of polypropylene microporous membrane by the adsorption of Tween 20, *Journal of Environmental Sciences-China*, 19, **2007,** 1461-1465.
[141] C.M. Costello, J.-U. Kreft, C.M. Thomas, D.M. Hammes, P. Bao, S.D. Evans, P.M. Mendes, Exploiting additive and subtractive patterning for spatially controlled and robust bacterial co-cultures, *Soft Matter*, 8, **2012,** 9147-9155.

[142] K.Y. Suh, A. Khademhosseini, P.J. Yoo, R. Langer, Patterning and separating infected bacteria using host-parasite and virus-antibody interactions, *Biomed Microdevices*, 6, **2004,** 223-229.

[143] P. Krsko, J.B. Kaplan, M. Libera, Spatially controlled bacterial adhesion using surface-patterned poly(ethylene glycol) hydrogels, *Acta Biomaterialia*, 5, **2009,** 589-596.

[144] D. Nyamjav, S. Rozhok, R.C. Holz, Immobilization of motile bacterial cells via dip-pen nanolithography, *Nanotechnology*, 21, **2010,** 6.

[145] P. Kim, A. Epstein, M. Khan, L. Zarzar, D. Lipomi, G. Whitesides, J. Aizenberg, Structural Transformation by Electrodeposition on Patterned Substrates (STEPS): A New Versatile Nanofabrication Method, *Nano letters*, 12, **2012,** 527-533.

[146] W.G. Koh, A. Revzin, A. Simonian, T. Reeves, M. Pishko, Control of mammalian cell and bacteria adhesion on substrates micropatterned with poly(ethylene glycol) hydrogels, *Biomed Microdevices*, 5, **2003,** 11-19.

[147] N.J. Lawrence, J.M. Wells-Kingsbury, M.M. Ihrig, T.E. Fangman, F. Namavar, C.L. Cheung, Controlling E. coli Adhesion on High-k Dielectric Bioceramics Films using Poly(amino acid) Multilayers, *Langmuir*, 28, **2012,** 4301-4308.

[148] T. Xu, S. Petridou, E.H. Lee, E.A. Roth, N.R. Vyavahare, J.J. Hickman, T. Boland, Construction of high-density bacterial colony arrays and patterns by the ink-jet method, *Biotechnology and Bioengineering*, 85, **2004,** 29-33.

[149] K. Kim, B.U. Lee, G.B. Hwang, J.H. Lee, S. Kim, Drop-on-Demand Patterning of Bacterial Cells Using Pulsed Jet Electrospraying, *Analytical Chemistry*, 82, **2010,** 2109-2112.

[150] J. Kim, Y.-H. Shin, S.-H. Yun, D.-S. Choi, J.-H. Nam, S.R. Kim, S.-K. Moon, B.H. Chung, J.-H. Lee, J.-H. Kim, K.-Y. Kim, K.-M. Kim, J.-H. Lim, Direct-Write Patterning of Bacterial Cells by Dip-Pen Nanolithography, *Journal of the American Chemical Society*, 134, **2012,** 16500-16503.

[151] L. Kailas, E.C. Ratcliffe, E.J. Hayhurst, M.G. Walker, S.J. Foster, J.K. Hobbs, Immobilizing live bacteria for AFM imaging of cellular processes, *Ultramicroscopy*, 109, **2009,** 775-780.

[152] S. Kasas, A. Ikai, A method for anchoring round shaped cells for atomic force microscope imaging, *Biophysical Journal*, 68, **1995,** 1678-1680.

[153] A. Beaussart, S. El-Kirat-Chatel, P. Herman, D. Alsteens, J. Mahillon, P. Hols, Yves F. Dufrêne, Single-Cell Force Spectroscopy of Probiotic Bacteria, *Biophysical Journal*, 104, 1886-1892.

[154] K. Anselme, P. Davidson, A.M. Popa, M. Giazzon, M. Liley, L. Ploux, The interaction of cells and bacteria with surfaces structured at the nanometre scale, *Acta Biomaterialia*, 6, **2010,** 3824-3846.

[155] T. Koyama, M. Yamada, M. Matsuhashi, FORMATION OF REGULAR PACKETS OF STAPHYLOCOCCUS-AUREUS CELLS, *Journal of Bacteriology*, 129, **1977,** 1518-1523.

[156] P. Vakuliuk, A. Burban, V. Konovalova, M. Bryk, M. Vortman, N. Klymenko, V. Shevchenko, Modified track membranes with antibacterial properties, *Desalination*, 235, **2009,** 160-169.

[157] M. Palacios, O. Garcia, J. Rodriguez-Hernandez, Constructing Robust and Functional Micropatterns on Polystyrene Surfaces by Using Deep UV Irradiation, *Langmuir*, 29, **2013,** 2756-2763.

[158] M. Palacios-Cuesta, A.L. Cortajarena, O. Garcia, J. Rodriguez-Hernandez, Versatile Functional Microstructured Polystyrene-Based Platforms for Protein Patterning and Recognition, *Biomacromolecules*, 14, **2013,** 3147-3154.

[159] D.H. Bergey, J.G. Holt, Bergey's Manual of Determinative Bacteriology, Williams & Wilkins, 1994.
[160] M.B. Elowitz, A.J. Levine, E.D. Siggia, P.S. Swain, Stochastic gene expression in a single cell, *Science*, 297, **2002,** 1183-1186.
[161] A. Raj, A. van Oudenaarden, Nature, Nurture, or Chance: Stochastic Gene Expression and Its Consequences, *Cell*, 135, **2008,** 216-226.
[162] B. Munsky, G. Neuert, A. van Oudenaarden, Using Gene Expression Noise to Understand Gene Regulation, *Science*, 336, **2012,** 183-187.
[163] A. Raj, S.A. Rifkin, E. Andersen, A. van Oudenaarden, Variability in gene expression underlies incomplete penetrance, *Nature*, 463, **2010,** 913-U984.
[164] I. Dimitrov, H. Schlaad, Synthesis of nearly monodisperse polystyrene-polypeptide block copolymers via polymerisation of N-carboxyanhydrides, *Chemical Communications*, **2003,** 2944-2945.
[165] A. Muñoz-Bonilla, A.M. van Herk, J.P.A. Heuts, Preparation of Hairy Particles and Antifouling Films Using Brush-Type Amphiphilic Block Copolymer Surfactants in Emulsion Polymerization, *Macromolecules*, 43, **2010,** 2721-2731.

SECCIÓN III: "Hot embossing" en superficies funcionales

SECCIÓN III:

HOT EMBOSSING EN SUPERFICIES FUNCIONALES

En esta sección III, como método alternativo a la fotopolimerización se ha evaluado la técnica de microimpresión en caliente o *"hot embossing"* para la estructuración de las superficies poliméricas. Este trabajo ha sido realizado durante una estancia en la Universidad de Glasgow en el grupo del Prof. N. Gadegaard. En este caso, la metodología se ha desarrollado utilizando esta técnica de estructuración, bien utilizando un único material y evaluando la capacidad de las películas poliméricas a estructurarse por microimpresión en caliente, o bien, incorporando estos copolímeros en mezclas poliméricas como aditivo para que posteriormente migren a la superficie por segregación superficial para su funcionalización.

Esta sección ha dado lugar al siguiente artículo científico:

CAPÍTULO III.1: *Hot embossing* en superficies funcionales

Artículo 5: *Direct micrometer patterning and functionalization of polymer blend surfaces by using hot embossing*

En este quinto artículo se describe una nueva metodología para la fabricación de superficies microestructuradas y funcionales utilizando, en este caso, el *hot embossing* como método de modificación de la topografía superficial. Como material base de fabricación, se ha utilizado el PMMA comercial, al que se le han incorporado diferentes porcentajes de copolímeros sintéticos funcionales de distinta naturaleza que, por técnicas de segregación superficial pueden migrar a la superficie modificándola. Así, gracias tanto a la topografía como a la composición química, se ha podido modificar la mojabilidad de las películas.

European Polymer Journal 59 (2014) 333–340

Contents lists available at ScienceDirect

European Polymer Journal

journal homepage: www.elsevier.com/locate/europolj

Direct micrometer patterning and functionalization of polymer blend surfaces by using hot embossing

Marta Palacios-Cuesta [a], Iskandar Vasiev [b], Nikolaj Gadegaard [b], Juan Rodríguez-Hernández [a,*], Olga García [a,*]

[a] Departamento de Química y Propiedades de Materiales Poliméricos, Instituto de Ciencia y Tecnología de Polímeros, (ICTP-CSIC), Juan de la Cierva 3, 28006 Madrid, Spain
[b] Division of Biomedical Engineering, School of Engineering, Rankine Building, University of Glasgow, Oakfield Avenue, Glasgow G12 8LT, UK

ARTICLE INFO

Article history:
Received 9 May 2014
Received in revised form 14 July 2014
Accepted 19 July 2014
Available online 4 August 2014

Keywords:
Surfaces
Polymer blends
Surface Segregation
Surface pattern
Hot embossing

ABSTRACT

Micrometer and submicrometer size features were prepared in poly(methyl methacrylate) based polymer blends by hot-embossing using a customized silicon master. The surface patterns were design to contain particular functionalities for wetting in combination by the additive included in the polymer blend. More precisely copolymers containing MMA units and either a hydrophobic fluorinated monomer or a hydrophilic monomer was incorporated in the polymer mixture prior to embossing. Surface segregation using the appropriated annealing conditions allowed us to vary the interfacial chemical composition. Thus, we demonstrate that the wettability of the surface can be varied as a function of both the low surface energy additive and the annealing carried out whilst maintaining the overall surface topography.

1. Introduction

The elaboration of functional microstructured interfaces is currently a centre of intensive research. The large variety of applications derive from these materials includ- recent years, many polymer-based microfabrication techniques [10] via microinjection molding [11,12], casting [4,13], and micro-hot embossing [14,15] have been developed. Among these approaches, micro-hot embossing consists on stamping a pattern into a polymer softened by

Direct micrometer patterning and functionalization of polymer blend surfaces by using hot embossing

Marta Palacios-Cuesta,[a] Iskandar Vasiev,[b] Nikolaj Gadegaard,[b] Juan Rodríguez-Hernández[a]*, Olga García[a]*

[a]Departamento de Química y Propiedades de Materiales Poliméricos, Instituto de Ciencia y Tecnología de Polímeros, (ICTP-CSIC), Juan de la Cierva 3, 28006-Madrid, Spain.

[b]Division of Biomedical Engineering, School of Engineering, Rankine Building, University of Glasgow, Oakfield Avenue, Glasgow-G12 8LT, UK.

Correspondence to:

Olga García (ogarcia@ictp.csic.es)

Juan Rodríguez-Hernández (rodriguez@ictp.csic.es)

Abstract

Micrometer and submicrometer size features were prepared in poly(methyl methacrylate) based polymer blends by hot-embossing using a customized silicon master. The surface patterns were design to contain particular functionalities for wetting in combination by the additive included in the polymer blend. More precisely copolymers containing MMA units and either a hydrophobic fluorinated monomer or a hydrophilic monomer was incorporated in the polymer mixture prior to embossing. Surface segregation using the appropriated annealing conditions allowed us to vary the interfacial chemical composition. Thus, we demonstrate that the wettability of the surface can be varied as a function of both the low surface energy additive and the annealing carried out whilest maintaining the overall surface topography.

Introduction

The elaboration of functional microstructured interfaces is currently a center of intensive research. The large variety of applications derive from these materials including biomedical purposes [1] such as (tissue engineering [2] or cell adhesion [3]), the elaboration of diffractive optical elements [4] or the design of superhydrophobic [5] surfaces among others.

The preparation of functional microstructured surface has been carried out using different approaches including: surface wrinkling or photolithography. As alternatives, techniques grouped under the name of “soft lithography” have been proposed for the development of nano- and micro-structured organic and inorganic matter [6-9]. In recent years, many polymer-based microfabrication techniques [10] via microinjection molding [11, 12], casting [4, 13], and micro-hot embossing [14, 15] have been developed. Among these approaches, micro-hot embossing consists on stamping a pattern into a polymer softened by raising the temperature of the polymer just above the glass transition temperature [10]. The stamp employed to induce the surface pattern at the polymer surface can be made using a variety of different techniques and can be carried out using high resolution working stamps [16]. Hot embossing has several advantages over the above mentioned techniques. By using hot-embossing the features can be located afterwards and a master can be reused several times to prepare samples, which helps minimize processing times, allows for automated mass-production and therefore enables costs to be reduced [17].

Hot embossing has been successfully employed for the fabrication of anti-reflective structures [18-20], microfluidic reactors [21], plastic chips, microfluidic chips and lab on a chip [22-24] and devices [25], for polymer replication [26], electrochemical sensors [27] or even to design microfluidic 3D cell culture platforms [28-30] that can direct the alignment and proliferation [31], among others [32-34]. However, until now the polymers employed for hot embossing have been limited to those commercially available [35-40]. In general, these polymers are hydrophobic in nature and the control of the wettability requires additional surface treatments. The surface modification techniques employed up to now in hot-embossed polymers typically resort either to plasma treatments [41, 42] or to the formation of self-assembled monolayers (SAMs) [43]. However, such treatments have been demonstrated to have a limited lifetime. In addition, plasma treatments requires the generation of surface radicals in spite of the partial surface degradation due to chain breaking.

Herein, we propose the design of an alternative to the above mentioned functionalization approaches in which we take advantage of the use of polymer blends composed of poly(methyl methacrylate) (PMMA) and a copolymer that contains either hydrophobic fluorinated functional groups [poly(methyl methacrylate-*co*-2,2,2-trifluoroethyl methacrylate)] or a copolymer with hydrophilic functional groups [poly(methyl methacrylate-*co*-acrylic acid)]. These blends will be employed as platforms to create surface microstructures with different patterns by using hot-embossing. Finally, the surface functional groups contained within the blend can be revealed at the interface by surface segregation/reorientation. As we will demonstrate, this methodology illustrated for a particular system (PMMA) offers the possibility to simultaneously vary the surface structure and the chemical composition.

Experimental Section

Materials

Commercial poly(methyl methacrylate) (PMMA-M_w=25000 g mol^{-1}, Polyscience). Methyl methacrylate (MMA) (Aldrich 99%) was washed three times first with a basic aqueous solution (10% NaOH) and then in water. Then, the resulting monomer was dried on anhydric magnesium sulfate, filtered and distilled. *Tert*-Butyl acrylate (*t*BuA), 2,2,2-trifluoroethyl methacrylate (TFMA) (Aldrich 99%), N,N,N',N'',N''-pentamethyldiethylenetriamine

(PMDETA) (Aldrich, 99%), copper (I) bromide (CuBr) (Aldrich 98%), ethyl-2-bromoisobutyrate (EBrIB) and the rest of solvents were employed as received. As supports, we used silicon wafers (Compart Technology).

Polymer Synthesis

The random copolymer of poly(methyl methacrylate-*co*-2,2,2-trifluoroethyl methacrylate) ($PMMA_x$-*co*-$TFMA_y$) was synthesized by Atom Transfer Radical Polymerization (ATRP). The polymerization was performed in *Schlenk* flasks previously flamed and dried under vacuum. ATRP was carried out using the following stoichiometry $[M_t]/[I]/[CuBr]/[L]$ 60:1:1:1 where $M_t = M_1 + M_2$; M_1= MMA, M_2= TFMA, I=Initiator (EBrIB), L=Ligand (PMDETA) in toluene. The reactants were added under N_2. The reaction mixture was degassed by three-pump-thaw cycles and placed in a thermostatic oil bath at 90^{o}C. After the polymerization, the mixture was cooled to room temperature, diluted with dichloromethane and passed through a neutral alumina column to remove the copper salt. After removing the solvent, the polymers were precipitated in hexane, washed and dried under vacuum.

Preparation of the copolymer poly(methyl methacrylate-*co*-acrylic acid) ($PMMA_x$-*co*-PAA_y): The polymerization was performed in *Schlenk* flasks previously flamed and dried under vacuum. ATRP was carried out using the following stoichiometry $[M_t]/[I]/[CuBr]/[L]$ 100:1:1:1 where $M_t = M_1 + M_2$; M_1= MMA, M_2= *t*BuA, I=Initiator (EBrIB), L=Ligand (PMDETA) in toluene. The reactants were added under N_2. The reaction mixture was degassed by three-pump-thaw cycles and placed in a thermostatic oil bath at 65^{o}C. After the polymerization, the mixture were cooled to room temperature, diluted with dichloromethane and passed through a neutral alumina column to remove the copper salt. After removing the solvent, the polymers were precipitated in cold hexane, washed and dried under vacuum. Finally, the *tert*-butyl groups were hydrolyzed to afford the carboxylic acid functional groups. For this purpose, the copolymers were first dissolved in dichloromethane. Trifluoroacetic acid (TFA) was then added (20 equivalents to *t*-butyl ester units), and the mixture was stirred at room temperature for 2 days. The deprotected polymers precipitated in the reaction media and were filtered, washed with dichloromethane, and finally dried under vacuum.

Hot-embossing

For the preparation of the PDMS master a mixture of Sylgard 184 (Dow Corning) was used in proportion 10:1 (base to curing agent). The mixture was stirred and was introduced over a silicon stamp with the negative pattern. Vacuum was applied before the sample was introduced in the oven at 90^{o}C for 2 hours. For the preparation of the hot-embossed samples, a polymer solution (200 mg mL^{-1}) in THF was spun coated onto silicon wafers and dried on a hot plate for 5 minutes to remove completely the solvent. The samples were pressed against a stamp (PDMS or silicon) with different patterns. In the initial experiments, the hot-embossing was carried out on an Obducat NIL machine (automatic control of temperature and pressure, PDMS and Si stamps were used). For the remainder of the experiments a manual hydraulic press, Specac, was used. For these experiments, only PDMS stamps were used. The samples were heated for 1 minute at 180^{o}C and a pressure of at 15 bars was applied for 5 minutes more while the temperature was maintained. A subsequent thermal annealing was carried out in order to favor the surface migration of the copolymers towards the interface. Depending on the polymer additive used, the annealing conditions were varied. In order to favor the surface enrichment of fluorinated groups, the hot-embossed films were annealed at 120^{o}C in vacuum for times ranging from 5 and 24 h. The films containing PMMA-*co*-PAA copolymer as additive were annealed at 100% humidity to enable migration of carboxylic acid groups to the surface. The hydrophilicity of the surfaces, in the case of PMMA-*co*-PAA, directly related with the chemical composition was characterized by contact angle measurements (before and after annealing). Also optical microscope images were taken in order to proof the integrity of the surfaces upon annealing.

Characterization

The ^{1}H- and ^{13}C-NMR spectra were registered at room temperature in $CDCl_3$ solution in a Varian INOVA-300. Chemical shifts are reported in parts per million (ppm) using as internal reference the peak of the trace of undeuterated solvent (δ 7.26). Size exclusion chromatography (SEC) analyses were carried out on chromatographic system (Waters Division Millipore) equipped with a Waters model 410 refractive-index detector. Dimethyl formamide (99.9%, Aldrich) containing 0.1% of LiBr, was used as the eluent at a flow rate of 1 mL min^{-1}

at 50°C. Styragel packed columns (HR2, HR3 and HR4, Waters Division Millipore) were used. The molecular weights were estimated against poly(methyl methacrylate) standards. Poly(methyl methacrylate) standards (Polymer Laboratories, Laboratories, Ltd.) between $2.4x10^6$ and $9.7x10^2$ g mol^{-1} were used to calibrate the columns.

Scanning electron microscopy (SEM) was used for surface structural and cross-sectional analysis. Micrographs were taken using a Philips XL30 with an acceleration voltage of 25 kV. The samples were coated with gold-palladium (80/20) prior to scanning.

Contact angles were measured with deionized water on a goniometer KSV theta (KSV instruments, Ltd., Finland) at room temperature. Water droplets (2µl) were placed on the films and a charged coupled device camera was used to capture the images of the water droplets for the determination of the contact angle. The experimental contact angle values were compared with those predicted by the Wenzel and Cassie-Baxter state models adapted for the two different situations. The Wenzel model assumes a complete wetting when a drop is placed on a rough surface. Whereas the Cassie-Baxter model is based on a situation in which the water droplet remains on the top of the pattern and air is trapped between the features. These models are represented by equations (1) and (2), respectively, where θ_i is the ideal contact angle on a flat surface, r is the roughness factor defined as the ratio of actual surface area divided by the projected area and f is the fraction of the projected wet area [5, 44].

$$\cos \theta_W = r \cos \theta_i \quad (1)$$

$$\cos \theta_{CB} = f (\cos \theta_i + 1) - 1 \quad (2)$$

Whereas the contact angle measurements of the surfaces containing the fluorinated copolymer were measured in pH neutral Millipore water, the contact angle values of the films of the blends prepared with PMMA-*co*-PAA were made with basic water (pH=9) to ensure the complete deprotonation of the carboxylic acid groups. As depicted in the literature the surface wettability of surfaces modified with carboxylic acid functional groups exhibit a remarkable dependence with the pH [45, 46].

Results and Discussion

Among others, two main factors have been identified to play a crucial role in the final surface properties and therefore have to be included in the design of a material for a targeted application: surface morphology and chemical composition [47-51]. Herein we propose an alternative to multistep patterning and functionalization procedures to vary both properties in a straightforward manner. For this purpose we studied blends composed of a linear PMMA and random and block copolymers employed as additives composed of methyl methacrylate and either a fluorinated monomer, i.e. poly(methyl methacrylate-*co*-2,2,2-trifluoroethyl methacrylate) (PMMA-*co*-PTFMA) or a monomer having carboxylic acid functional groups, i.e. poly(methyl methacrylate-*co*-acrylic acid) (PMMA-*co*-PAA). The inclusion within the PMMA matrix of a precise amount of functional additives will provide an interesting alternative to modify the surface composition. In effect, based on previous studies we will demonstrate how by surface segregation of the additives employed the surface composition and therefore the wettability by controlling the entropic [52, 53] and enthalpic factors [54] and the environment of exposure [55, 56]. In addition, as will be depicted below, surface segregation that provides a control over the surface chemical composition will be carried out on films with different surface patterns obtained by using hot embossing.

The copolymers employed as additives throughout this study were prepared by using controlled polymerization techniques. More precisely, atom transfer radical polymerization (ATRP) was used in order to obtain copolymers with controlled molecular weights and narrow polydispersity. The molecular characteristics of the copolymers employed for this study are summarized in table 1.

Table 1. *Molecular characteristics of the copolymers employed as additives for the blends. Whereas the molar composition was estimated by ^{1}H-NMR, the molecular weight and the polydispersity (PD) values included in this table were obtained by SEC.*

Copolymer	**Mn**	**PD**	**%PAA copolymer**	**%PTFMA copolymer**
$PMMA_{97}$-*co*-$PTFMA_{3}$	18700	1.06	-	3
$PMMA_{77}$-*co*-$PTFMA_{23}$	14000	1.16	-	23
$PMMA_{60}$-*co*-$PTFMA_{40}$	20000	1.07	-	40
$PMMA_{93}$-*co*-PAA_{7}	15700	1.09	7	-
$PMMA_{75}$-*co*-PAA_{25}	7500	1.20	25	-
$PMMA_{60}$-*co*-PAA_{40}	3500	1.20	40	-

Films from the blends composed of PMMA and either PMMA-*co*-PTFMA or PMMA-*co*-PAA were prepared by spin casting from concentrated solutions (200 mg mL^{-1}) in THF. The films were dried during 5 min at 115^{o}C to ensure the complete removal of the THF solvent prior to the hot-embossing.

The approach followed to carry out the hot-embossing on the blend films is illustrated in Figure 1. This involves a master (silicon or PDMS) being pressed for few minutes into the polymer film that has been heated above its glass transition temperature. The standard conditions employed were heated at 180^{o}C for 1 minute and 5 additional minutes applying a pressure of 15 bars. After that, the films were allowed to cool to room temperature. In this study, we have employed three different masters having circular features, lines or a hexagonal pattern. The masters are described by the pitch and the shape of the moieties. Illustrative SEM images of the film surfaces obtained upon hot embossing on the polymers blend films using the different PDMS stamps are depicted in Figure 2.

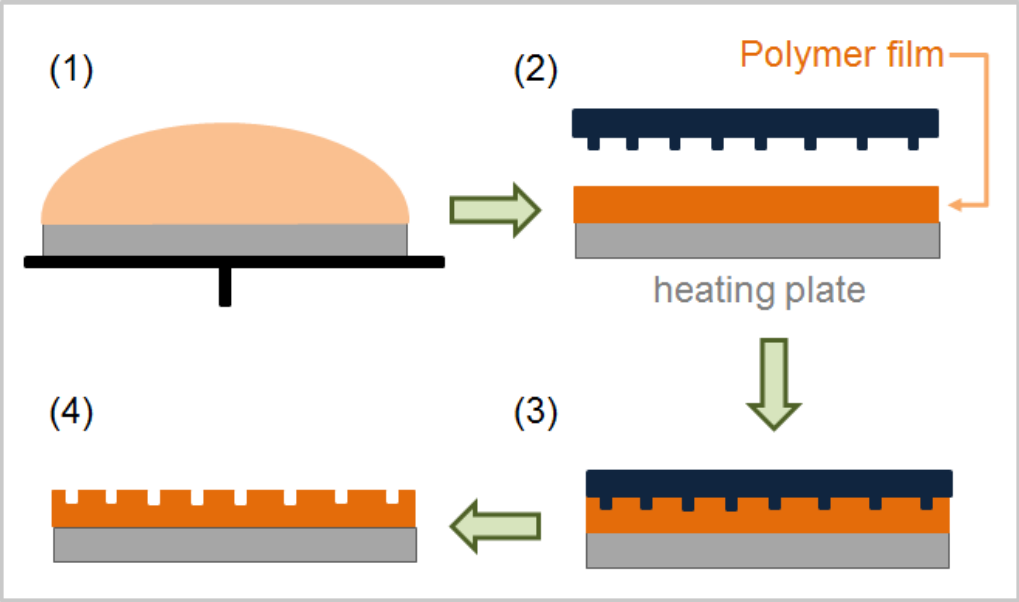

Figure 1: *Schematic representation of the steps to produce functional and microstructured polymer surface patterns by hot-embossing: The film was prepared by spin coating of a polymer blend solution in THF (1), the polymer films was heated above the Tg of the both PMMA and copolymers (2) and the master is pushed into the polymer film (3). Finally, the master is removed from the embossed polymer (4).*

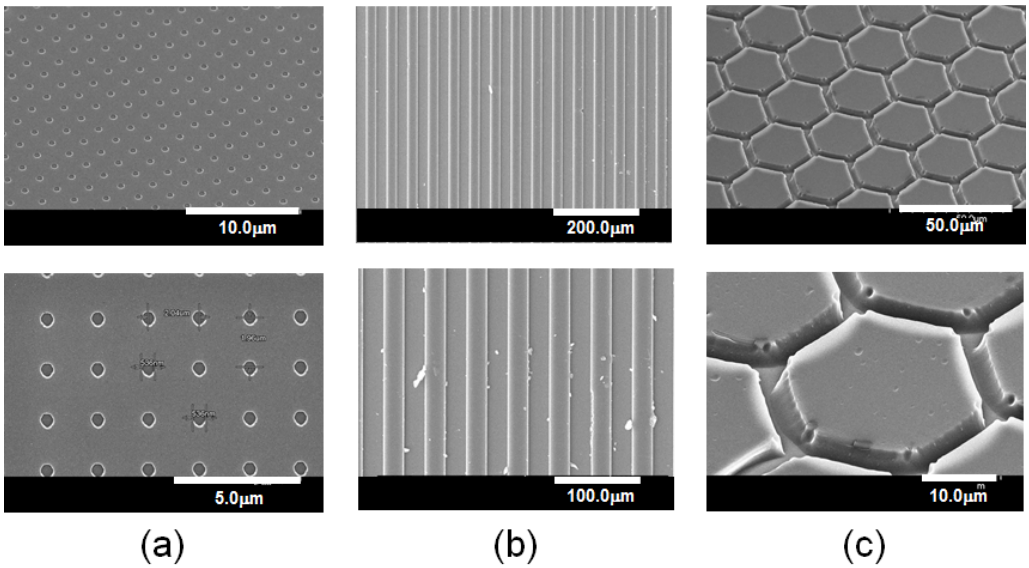

Figure 2: *Illustrative scanning electron microscopy images of the surface patterns obtained upon hot embossing in the polymer blends: (a) holes, (b) lines and (c) hexagonal morphology.*

The versatility of this approach is evidenced by the different surface patterns that can be obtained. The first stamp employed is composed of submicrometer regular pores with diameters of ~540 nm with a centre-to-centre spacing of 2 µm. The films of the blends were also embossed using lines with lateral dimensions of 25µm and hexagonal patterns with side lengths of 15 µm and 3 µm spacing between the hexagons.

The surface pattern plays a role on the surface wettability. In order to determine the effect of the pattern on the surface wettability we compared the contact angle measured directly after hot embossing of films having the same amount of additive prepared either by hot-embossing with a particular surface morphology or prepared by spin coating which are flat with a low roughness. In Figure 3, are summarized the contact angle values for a particular blend composed of a variable relative amount PMMA and the copolymer $PMMA_{97}$-*co*-$PTFMA_3$.

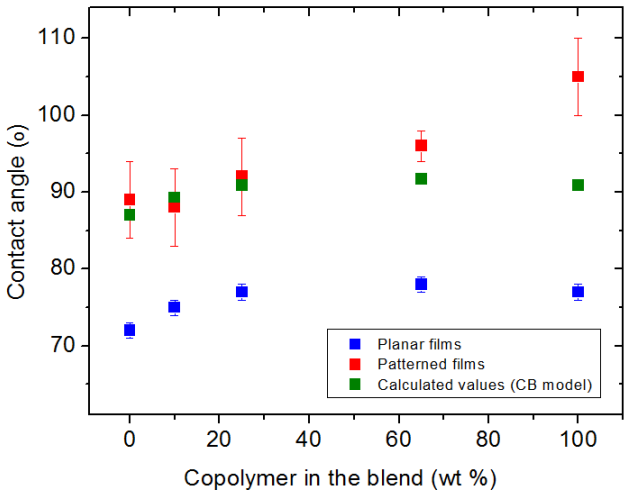

Figure 3: *Water contact angles measured for different blends using the copolymer $PMMA_{97}$-co-$PTFMA_3$ and PMMA on surfaces either prepared by spin coating (planar) or prepared by hot-embossing (case of hexagonal structured surfaces).*

By comparing the contact angles obtained for each particular blend composition it can be observed that the structured surfaces exhibit larger contact angles with differences ranging between 15^o and 29^o in average. This result evidencing the role of the surface structure allowed us to by combining structure and surface chemical composition finely tune the surface wettability. Moreover, an increasing amount of the fluorinated copolymer additive produces an additional increase of the hydrophobicity of the film. In effect, the water contact angle increases beyond what CB can justify. In principle two situations can explain this phenomenon. As depicted by Martines *et al.* [57] either the surface roughness or the pattern is driving additional fluorine groups to the surface.

The samples made from the hexagonal patterned stamp and containing the copolymer additive were annealed to either a water vapor or a dry environment. Exposure to either humid environment or dry air will favor or prevent the surface segregation of the copolymer towards the interface. Surface segregation will thus induce changes on the surface chemical composition. In Figure 4, is schematically shown the strategy employed to vary the surface chemical composition. The blends containing PMMA and PMMA-*co*-PAA were exposed to

water vapor in order to favor the surface reorganization and enrichment in polar groups. On the contrary, blends composed of PMMA and PMMA-*co*-PTFMA were annealed to air where the low surface energy fluorinated groups are expected to migrate to the interface. To follow the surface enrichment in the hydrophilic and the hydrophobic groups contact angle measurements were performed.

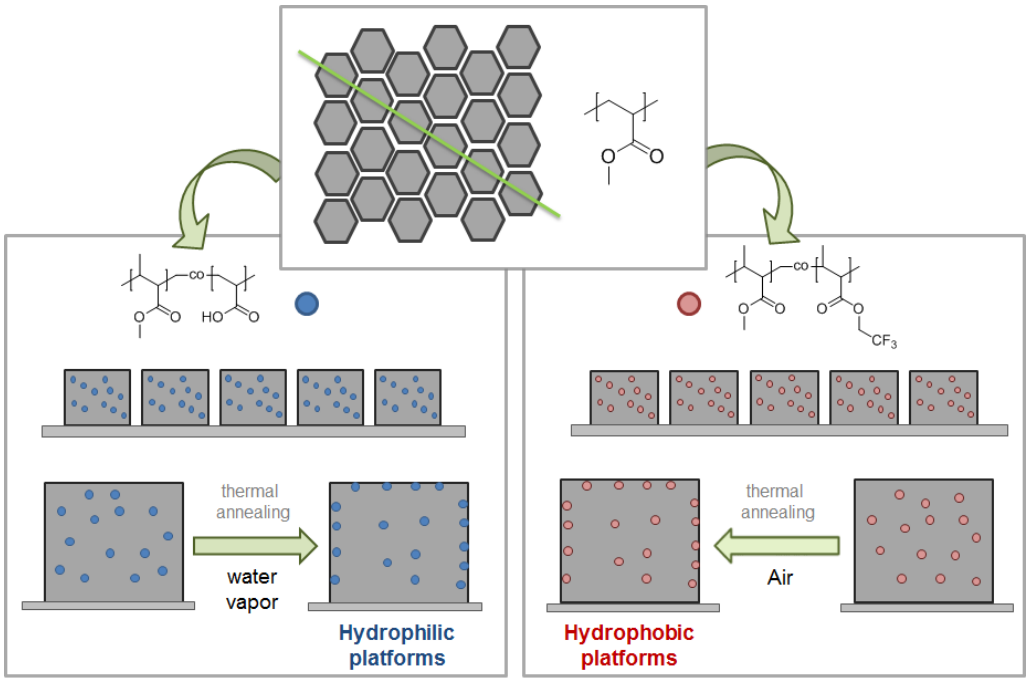

Figure 4: *Schematic illustrations of the polymer blends films obtained, the annealing conditions employed and the surface segregation process.*

Different blends were prepared varying either the amount of copolymer within the blend (between 100/0 wt% and 0/100 wt% in PMMA/copolymer) or the amount of either hydrophobic (TFMA) or hydrophilic (AA) monomer within the copolymer employed.

The major results obtained using blends of PMMA and PMMA-*co*-PTFMA are depicted in figures 5 and 6 upon thermal annealing at 120°C under vacuum at two different times: 5 and 24 hours. As observed in the graphs depicted in figure 5, the contact angle values increase after the thermal treatment of the blend that contains only 10% of fluorinated

copolymer from 88° to 97°. An increase of the hydrophobicity indicated that a change in the surface composition is produced [54, 58, 59]. For the case of the pure copolymer the contact angle observed remain constant independently of the annealing temperature and time around 105°. This value is higher than those observed for the polymer blend independently of the annealing time and evidenced the larger amount of fluorinated moieties at the surface in the pure copolymer film.

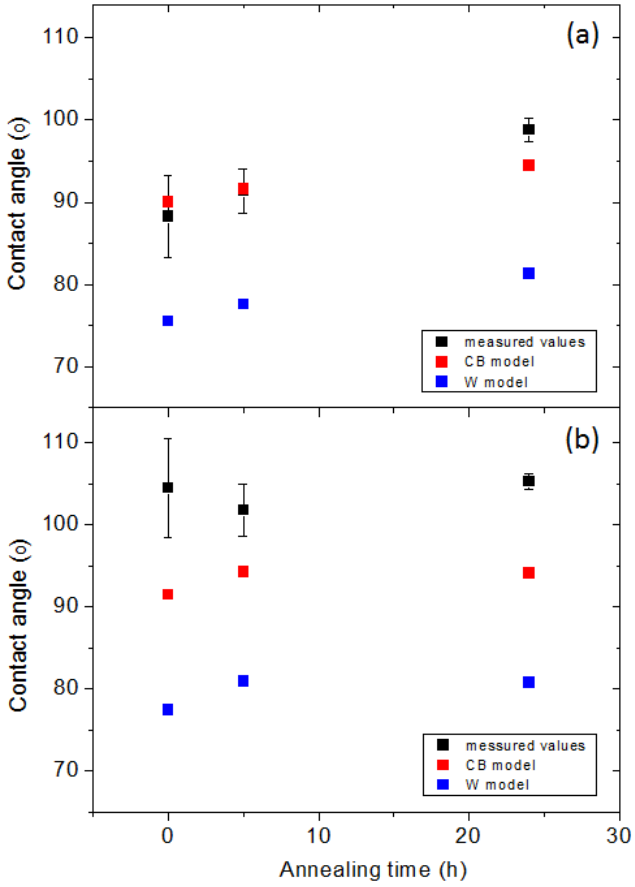

Figure 5: *Water contact angle values for films of the blends containing either (a) 10 wt% of $PMMA_{97}$-co-$PTFMA_3$ and 90 wt% of PMMA or (b) 100 wt% of $PMMA_{97}$-co-$PTFMA_3$ copolymer as a function of the annealing time. The calculated contact angle values using the Wenzel (W-blue points) and Cassie-Baxter (CB-red points) models are also included.*

In addition to the influence of the amount of copolymer within the blend and the annealing conditions on the surface wettability, blends of the copolymers with variable amount of fluorinated monomer ranging between 3 wt% and 40 wt% were also studied. In figure 6 are depicted the contact angle values observed for blend films with identical amount of copolymer 25 wt% but using the three different copolymers with variable fluorinated composition. In all the cases, annealing increases the contact angle values indicating the surface reorganization and migration of the hydrophobic fluoro functional groups towards the interface. Moreover the contact angle observed depended to some extent on the degree of fluorination of the copolymer employed. Upon annealing the blend using copolymer $PMMA_{97}$-*co*-$PTFMA_3$ has a contact angle of 105^o. An increase of the fluor content on the copolymer leads to an increase of the contact angle up to 110^o for blends using $PMMA_{77}$-*co*-$PTFMA_{23}$ and $PMMA_{60}$-co-$PTFMA_{40}$.

Figures 5 and 6 additionally include the contact angle values calculated using both the Wenzel (red points) and Cassie-Baxter (blue points) models in order to determine which model characterize the wettability of these surfaces. According to Figures 5 and 6 where the contact angles observed are close or above the values predicted for a Cassie-Baxter regime. The Wenzel model predicts contacts angles largely below the values measured for all the systems. This result indicates that the water droplets only wet the top of the surface independently of the amount of the copolymer employed or the monomer composition within the copolymer.

Whereas the incorporation within the blend of fluor containing copolymer decreases the surface wettability an increase of the hydrophilicity is expected by incorporation of hydrophilic functional groups such as carboxylic acids. Films from blends containing different proportions of commercial PMMA and a synthetic copolymer of PMMA-*co*-PAA were prepared by using copolymers having different proportion of AA: random copolymers (5, 11 and 40 mol%). In order to favor the surface migration of the copolymers towards the interface the samples were annealed at 90ºC and 100% humidity for 5 and 24 hours.

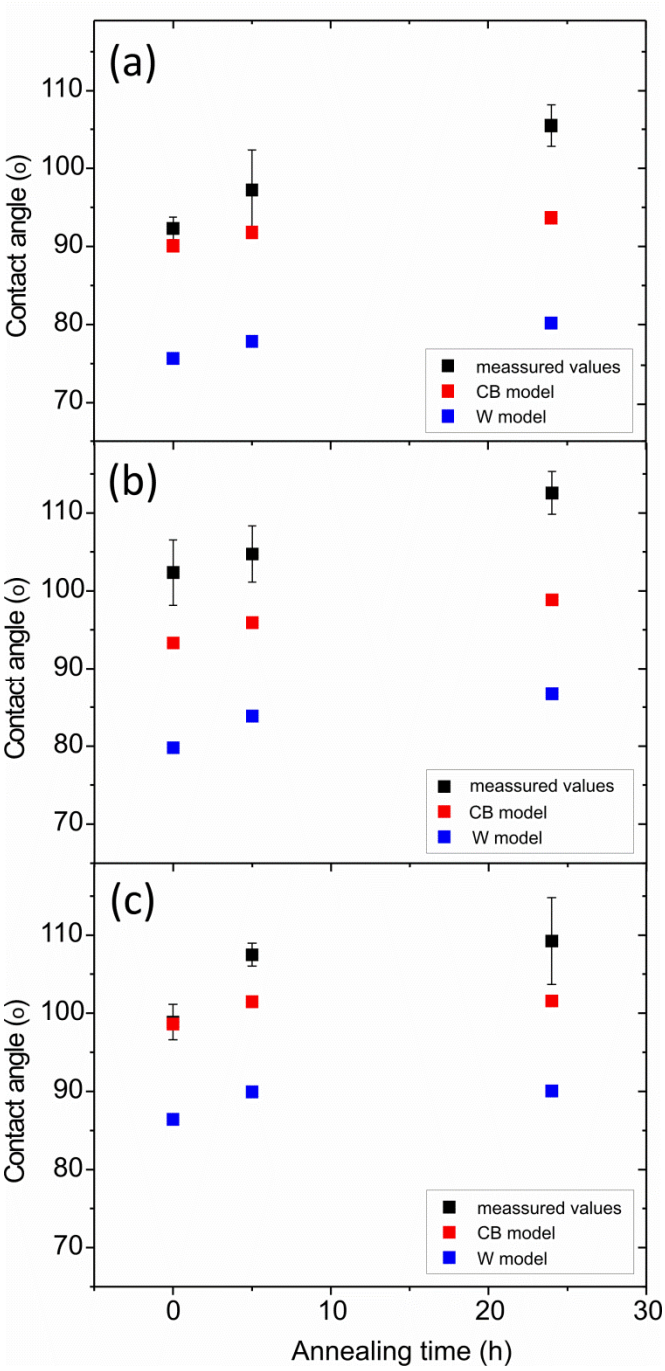

Figure 6: *Water contact angle values for films containing 25 wt% of the copolymers $PMMA_{97}$-co-$PTFMA_3$ (a), $PMMA_{77}$-co-$PTFMA_{23}$ (b) or $PMMA_{60}$-co-$PTFMA_{40}$ copolymer (c) and 75 wt% of PMMA as a function of the annealing time. The calculated contact angle values using the Wenzel (W-blue points) and Cassie-Baxter (CB-red points) models are also included.*

Films prepared using the copolymer $PMMA_{60}$-*co*-PAA_{40} were too unstable and contact angle measurements could not be carried out on these surfaces. The high content on hydrophilic polyacrylic acid enhances the solubility in water (Figure 7).

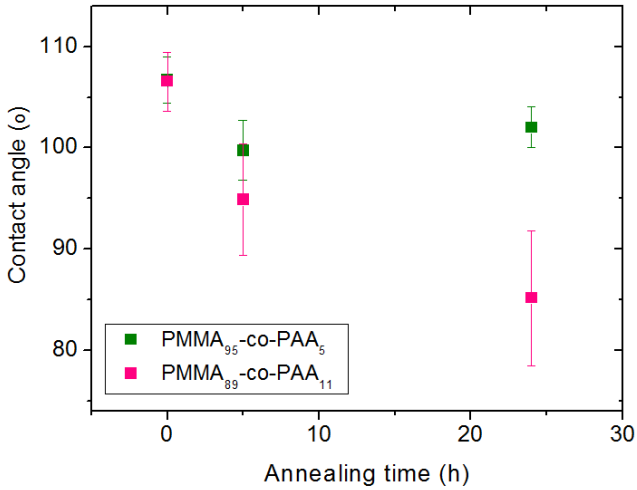

Figure 7: *Water contact angle values for films containing 25 wt% of the copolymers* $PMMA_{95}$-*co*-PAA_5 *or* $PMMA_{89}$-*co*-PAA_{11} *copolymer and 75 wt% of PMMA as a function of the annealing time.*

As a consequence the water droplet penetrates within the material bulk and disrupts the surface pattern. On the contrary, in the films prepared from the blends of the copolymers $PMMA_{95}$-*co*-PAA_5 and $PMMA_{89}$-*co*-PAA_{11} a decrease of the contact angle can be observed upon annealing in water vapor conditions. According to previous literature [59, 60] this effect is directly related to the surface enrichment on polar groups. In this particular case carboxylic acid functional groups contained within the copolymer tend to migrate to the polymer/water vapor interface.

Conclusions

Hot embossing has been employed to prepare different surface patterns with variable dimensions and shapes on poly(methyl methacrylate) based polymer blends. The blends were prepared using commercial PMMA and copolymers having different functional groups. By

using a hexagonal pattern we demonstrated the possibility of simultaneously modify the chemical composition. On the one hand, a poly(methyl methacrylate-*co*-2,2,2-trifluoroethyl methacrylate) (PMMA-*co*-PTFMA) containing low surface tension fluorinated monomer units. On the other hand a copolymer having acrylic acid monomer units, i.e. poly(methyl methacrylate-*co*-acrylic acid) (PMMA-*co*-PAA). The incorporation of such copolymers as additives and taking advantage of the surface segregation phenomenon we were able to modify simultaneously the surface topography and the chemical composition. The extent of hydrophilicity/hydrophobicity of the film surface was directly related with both the blend composition and the monomer composition of the copolymers employed.

Acknowledgements

The authors gratefully acknowledge support from the Agencia Estatal Consejo Superior de Investigaciones Científicas (CSIC). Equally, this work was financially supported by the Ministerio de Economia y Competitividad (MINECO) through MAT2011-22861 and MAT2009-12251. M. Palacios thanks the Ministerio de Education for the FPU fellowship. The Authors would like to thank EPSRC for funding I. Vasiev through a DTA award. We are grateful for the support and training provided by the JWNC technical staff for the microfabrication.

CAPÍTULO III.2: Bibliografía de la sección III

[1] V.N. Truskett, M.P.C. Watts, Trends in imprint lithography for biological applications, *Trends Biotechnol.*, 24, **2006,** 312-317.

[2] N. Gadegaard, E. Martines, M.O. Riehle, K. Seunarine, C.D.W. Wilkinson, Applications of nano-patterning to tissue engineering, *Microelectronic Engineering*, 83, **2006,** 1577-1581.

[3] J. Comelles, V. Hortigueela, J. Samitier, E. Martinez, Versatile Gradients of Covalently Bound Proteins on Microstructured Substrates, *Langmuir*, 28, **2012,** 13688-13697.

[4] M.T. Gale, Replication techniques for diffractive optical elements, *Microelectronic Engineering*, 34, **1997,** 321-339.

[5] E. Martines, K. Seunarine, H. Morgan, N. Gadegaard, C.D.W. Wilkinson, M.O. Riehle, Superhydrophobicity and superhydrophilicity of regular nanopatterns, *Nano Letters*, 5, **2005,** 2097-2103.

[6] A. Kumar, H.A. Biebuyck, G.M. Whitesides, Patterning Self-Assembled Monolayers: Applications in Materials Science, *Langmuir*, 10, **1994,** 1498-1511.

[7] Y. Xia, G.M. Whitesides, Soft Lithography, *Angewandte Chemie International Edition*, 37, **1998,** 550-575.

[8] B. Michel, A. Bernard, A. Bietsch, E. Delamarche, M. Geissler, D. Juncker, H. Kind, J.P. Renault, H. Rothuizen, H. Schmid, P. SchmidtWinkel, R. Stutz, H. Wolf, Printing meets lithography: Soft approaches to high-resolution patterning (vol 45, pg 697, 2001), *Ibm Journal of Research and Development*, 45, **2001,** 870-870.

[9] Y.N. Xia, G.M. Whitesides, Soft lithography, *Annual Review of Materials Science*, 28, **1998,** 153-184.

[10] M. Heckele, W.K. Schomburg, Review on micro molding of thermoplastic polymers, *Journal of Micromechanics and Microengineering*, 14, **2004,** R1-R14.

[11] R.M. McCormick, R.J. Nelson, M.G. AlonsoAmigo, J. Benvegnu, H.H. Hooper, Microchannel electrophoretic separations of DNA in injection-molded plastic substrates, *Analytical Chemistry*, 69, **1997,** 2626-2630.

[12] H. Pranov, H.K. Rasmussen, N.B. Larsen, N. Gadegaard, On the injection molding of nanostructured polymer surfaces, *Polymer Engineering & Science*, 46, **2006,** 160-171.

[13] D.C. Duffy, J.C. McDonald, O.J.A. Schueller, G.M. Whitesides, Rapid prototyping of microfluidic systems in poly(dimethylsiloxane), *Analytical Chemistry*, 70, **1998,** 4974-4984.

[14] M.U. Kopp, H.J. Crabtree, A. Manz, Developments in technology and applications of microsystems, *Current Opinion in Chemical Biology*, 1, **1997,** 410-419.

[15] H. Becker, W. Dietz, Microfluidic devices for mu-TAS applications fabricated by polymer hot embossing, in: A.B. Frazier, C.H. Ahn (Eds.) Microfluidic Devices and Systems, 1998, pp. 177-182.

[16] T. Glinsner, T. Veres, G. Kreindl, E. Roy, K. Morton, T. Wieser, C. Thanner, D. Treiblmayr, R. Miller, P. Lindner, Fully automated hot embossing processes utilizing high resolution working stamps, *Microelectronic Engineering*, 87, **2010,** 1037-1040.

[17] A. Mathur, S.S. Roy, M. Tweedie, S. Mukhopadhyay, S.K. Mitra, J.A. McLaughlin, Characterisation of PMMA microfluidic channels and devices fabricated by hot embossing and sealed by direct bonding, *Current Applied Physics*, 9, **2009,** 1199-1202.

[18] T.-F. Yao, P.-H. Wu, T.-M. Wu, C.-W. Cheng, S.-Y. Yang, Fabrication of anti-reflective structures using hot embossing with a stainless steel template irradiated by femtosecond laser, *Microelectronic Engineering*, 88, **2011,** 2908-2912.

[19] K.-S. Han, H. Lee, D. Kim, H. Lee, Fabrication of anti-reflection structure on protective layer of solar cells by hot-embossing method, *Solar Energy Materials and Solar Cells*, 93, **2009,** 1214-1224.
[20] C.-J. Ting, M.-C. Huang, H.-Y. Tsai, C.-P. Chou, C.-C. Fu, Low cost fabrication of the large-area anti-reflection films from polymer by nanoimprint/hot-embossing technology, *Nanotechnology*, 19, **2008**.
[21] J. Greener, W. Li, J. Ren, D. Voicu, V. Pakharenko, T. Tang, E. Kumacheva, Rapid, cost-efficient fabrication of microfluidic reactors in thermoplastic polymers by combining photolithography and hot embossing, *Lab on a Chip*, 10, **2010,** 522-524.
[22] M.-S. Huang, Y.-C. Chiang, S.-C. Lin, H.-C. Cheng, C.-F. Huang, Y.-K. Shen, Y. Lin, Fabrication of microfluidic chip using micro-hot embossing with micro electrical discharge machining mold, *Polymers for Advanced Technologies*, 23, **2012,** 57-64.
[23] D.K. Maurya, W.Y. Ng, K.A. Mahabadi, Y.N. Liang, I. Rodriguez, Fabrication of lab-on chip platforms by hot embossing and photo patterning, *Biotechnology journal*, 2, **2007,** 1381-1388.
[24] L.J. Kricka, P. Fortina, N.J. Panaro, P. Wilding, G. Alonso-Amigo, H. Becker, Fabrication of plastic microchips by hot embossing, *Lab on a Chip*, 2, **2002,** 1-4.
[25] S.R. Nugen, P.J. Asiello, A.J. Baeumner, Design and fabrication of a microfluidic device for near-single cell mRNA isolation using a copper hot embossing master, *Microsystem Technologies-Micro-and Nanosystems-Information Storage and Processing Systems*, 15, **2009,** 477-483.
[26] A. Kolew, D. Muench, K. Sikora, M. Worgull, Hot embossing of micro and sub-micro structured inserts for polymer replication, *Microsystem Technologies-Micro-and Nanosystems-Information Storage and Processing Systems*, 17, **2011,** 609-618.
[27] J. Kafka, N.B. Larsen, S. Skaarup, O. Geschke, Fabrication of an all-polymer electrochemical sensor by using a one-step hot embossing procedure, *Microelectronic Engineering*, 87, **2010,** 1239-1241.
[28] J.S. Jeon, S. Chung, R.D. Kamm, J.L. Charest, Hot embossing for fabrication of a microfluidic 3D cell culture platform, *Biomedical Microdevices*, 13, **2011,** 325-333.
[29] P. Schneider, C. Steitz, K.H. Schafer, C. Ziegler, Hot embossing of pyramidal micro-structures in PMMA for cell culture, *Phys. Status Solidi A-Appl. Mat.*, 206, **2009,** 501-507.
[30] J.L. Charest, L.E. Bryant, A.J. Garcia, W.P. King, Hot embossing for micropatterned cell substrates, *Biomaterials*, 25, **2004,** 4767-4775.
[31] L. Moroni, L.P. Lee, Micropatterned hot-embossed polymeric surfaces influence cell proliferation and alignment, *Journal of Biomedical Materials Research Part A*, 88A, **2009,** 644-653.
[32] S. Aukkaravittayapun, K.W. Tat, W. Hu, H.J. Lu, Flexible Transparent Conducting Film by Hot Embossing, in: J. Zhao, M. Kunieda, G. Yang, X.M. Yuan (Eds.) Advanced Precision Engineering, Trans Tech Publications Ltd, Stafa-Zurich, 2010, pp. 710-714.
[33] C.H. Wu, C.H. Lu, Fabrication of an LCD light guide plate using closed-die hot embossing, *Journal of Micromechanics and Microengineering*, 18, **2008**.
[34] X.C. Shan, T. Ikehara, Y. Murakoshi, R. Maeda, Applications of micro hot embossing for optical switch formation, *Sens. Actuator A-Phys.*, 119, **2005,** 433-440.
[35] Y. Murakoshi, X.C. Shan, T. Shimizu, R. Maeda, Hot embossing characteristics of PEEK compared to PC and PMMA, 2003.

[36] K. Hasui, I. Takagaki, O. Sugihara, N. Okamoto, Thermally stable grating comprised of silsesquioxane film fabricated with hot-embossing, in: J.G. Grote, T. Kaino (Eds.) Organic Photonic Materials and Devices V, 2003, pp. 355-365.
[37] J. Narasimhan, I. Papautsky, Rapid fabrication of hot embossing tools using PDMS, in: H. Becker, P. Woias (Eds.) Microfluidics, Biomems, and Medical Microsystems, 2003, pp. 110-119.
[38] S.Z. Qi, X.Z. Liu, S. Ford, J. Barrows, G. Thomas, K. Kelly, A. McCandless, K. Lian, J. Goettert, S.A. Soper, Microfluidic devices fabricated in poly(methyl methacrylate) using hot-embossing with integrated sampling capillary and fiber optics for fluorescence detection, *Lab on a Chip*, 2, **2002,** 88-95.
[39] H. Becker, U. Heim, I. Ieee, Silicon as tool material for polymer hot embossing, in: Mems '99: Twelfth Ieee International Conference on Micro Electro Mechanical Systems, Technical Digest, 1999, pp. 228-231.
[40] H. Becker, U. Heim, Polymer hot embossing with silicon master structures, *Sensors and Materials*, 11, **1999,** 297-304.
[41] H.T. Baytekin, T. Wirth, T. Gross, M. Sahre, W.E.S. Unger, J. Theisen, M. Schmidt, Surface analytical characterization of micro-fluidic devices hot embossed in polymer wafers: Surface chemistry and wettability, *Surface and Interface Analysis*, 42, **2010,** 1417-1431.
[42] H.T. Baytekin, T. Wirth, T. Gross, D. Treu, M. Sahre, J. Theisen, M. Schmidt, W.E.S. Unger, Determination of wettability of surface-modified hot-embossed polycarbonate wafers used in microfluidic device fabrication via XPS and ToF-SIMS, *Surface and Interface Analysis*, 40, **2008,** 358-363.
[43] H. Schift, L.J. Heyderman, C. Padeste, J. Gobrecht, Chemical nano-patterning using hot embossing lithography, *Microelectronic Engineering*, 61-2, **2002,** 423-428.
[44] A. Lafuma, D. Quéré, Superhydrophobic states, *Nature Materials*, 2, **2003,** 457-460.
[45] W. Van Camp, F.E. Du Prez, H. Alem, S. Demoustier-Champagne, N. Willet, G. Grancharov, A.-S. Duwez, Poly(acrylic acid) with disulfide bond for the elaboration of pH-responsive brush surfaces, *European Polymer Journal*, 46, **2010,** 195-201.
[46] J.R. Rasmussen, D.E. Bergbreiter, G.M. Whitesides, LOCATION AND MOBILITY OF FUNCTIONAL-GROUPS AT SURFACE OF OXIDIZED, LOW-DENSITY POLYETHYLENE FILM, *Journal of the American Chemical Society*, 99, **1977,** 4746-4756.
[47] F. Zhou, D. Li, Z.Q. Wu, B. Song, L. Yuan, H. Chen, Enhancing Specific Binding of L929 Fibroblasts: Effects of Multi-Scale Topography of GRGDY Peptide Modified Surfaces, *Macromol. Biosci.*, 12, **2012,** 1391-1400.
[48] T. Bahners, L. Prager, S. Kriehn, J.S. Gutmann, Super-hydrophilic surfaces by photo-induced micro-folding, *Applied Surface Science*, 259, **2012,** 847-852.
[49] B. Cortese, H. Morgan, Controlling the Wettability of Hierarchically Structured Thermoplastics, *Langmuir*, 28, **2012,** 896-904.
[50] C.P. Stallard, K.A. McDonnell, O.D. Onayemi, J.P. O'Gara, D.P. Dowling, Evaluation of Protein Adsorption on Atmospheric Plasma Deposited Coatings Exhibiting Superhydrophilic to Superhydrophobic Properties, *Biointerphases*, 7, **2012**.
[51] X.-M. Li, D. Reinhoudt, M. Crego-Calama, What do we need for a superhydrophobic surface? A review on the recent progress in the preparation of superhydrophobic surfaces, *Chemical Society Reviews*, 36, **2007,** 1350-1368.

[52] V.S. Minnikanti, L.A. Archer, Surface enrichment of branched polymers in linear hosts: Effect of asymmetry in intersegmental interactions and density gradients, *Journal of Chemical Physics*, 122, **2005**.
[53] M.D. Foster, C.C. Greenberg, D.M. Teale, C.M. Turner, S. Corona-Galvan, E. Cloutet, P.D. Butler, B. Hammouda, R.P. Quirk, Effective χ and surface segregation in blends of star and linear polystyrene, *Macromolecular Symposia*, 149, **2000,** 263-268.
[54] R. Mason, C.A. Jalbert, P. Muisener, J.T. Koberstein, J.F. Elman, T.E. Long, B.Z. Gunesin, Surface energy and surface composition of end-fluorinated polystyrene, *Advances in Colloid and Interface Science*, 94, **2001,** 1-19.
[55] I. Luzinov, S. Minko, V.V. Tsukruk, Adaptive and responsive surfaces through controlled reorganization of interfacial polymer layers, *Progress in Polymer Science*, 29, **2004,** 635-698.
[56] T.P. Russell, Surface-responsive materials, *Science*, 297, **2002,** 964-967.
[57] E. Martines, K. Seunarine, H. Morgan, N. Gadegaard, C.D.W. Wilkinson, M.O. Riehle, Air-Trapping on Biocompatible Nanopatterns, *Langmuir*, 22, **2006,** 11230-11233.
[58] P. Muisener, C.A. Jalbert, C.G. Yuan, J. Baetzold, R. Mason, D. Wong, Y.J. Kim, J.T. Koberstein, Measurement and modeling of end group concentration depth profiles for omega-fluorosilane polystyrene and its blends, *Macromolecules*, 36, **2003,** 2956-2966.
[59] J.T. Koberstein, Molecular design of functional polymer surfaces, *Journal of Polymer Science Part B-Polymer Physics*, 42, **2004,** 2942-2956.
[60] A. Bousquet, G. Pannier, E. Ibarboure, E. Papon, J. Rodriguez-Hernandez, Control of the surface properties in polymer blends, *Journal of Adhesion*, 83, **2007,** 335-349.

SECCIÓN IV: Arrugas en superficies funcionales

SECCIÓN IV:

ARRUGAS EN SUPERFICIES FUNCIONALES

En la sección IV se recoge la estructuración de materiales funcionales mediante la formación de arrugas en superficies poliméricas. Esta sección, a su vez, está dividida en tres capítulos: En el capítulo IV.1 se han preparado materiales funcionales reticulados con arrugas en su superficie a partir de monómeros que presentan alguna funcionalidad, mientras que en capítulo IV.2, se preparan estos materiales con superficies arrugadas a partir de mezclas de monómeros comerciales a los que se ha añadido un copolímero sintético (y funcional, en este caso) como carga. En el capítulo IV.3 se presenta, en primer lugar, la patente de invención a la que ha derivado este nuevo método de estructuración de superficies poliméricas y, en segundo lugar, la ampliación de esta misma patente cuando ha pasado a fase internacional PCT.

CAPÍTULO IV.1: Arrugas en superficies funcionales a partir de mezclas de monómeros funcionales

En esta ocasión la estructuración de las superficies poliméricas se ha realizado mediante la creación de arrugas superficiales, mientras que la química de estas superficies se ha variado gracias a la utilización de monómeros funcionales, hidrofóbicos o hidrofílicos.

El desarrollo de este trabajo ha dado lugar a un artículo de científico y a una patente, que se muestran a continuación:

Articulo 6: *Versatile approach for the fabrication of functional wrinkled polymer surfaces*

Se ha desarrollado un procedimiento novedoso de fabricación de arrugas en superficies funcionales. El procedimiento consiste, básicamente, en confinar una mezcla de monómeros (que pueden tener o no una determinada funcionalidad) que es irradiada con luz UV mientras se mantiene simultáneamente a una determinada temperatura constante. El estudio en profundidad de la influencia de las diferentes condiciones experimentales en la formación de las arrugas superficiales ha permitido conocer más en profundidad el proceso de formación de dichas arrugas. Es un proceso rápido, que se desarrolla en un solo paso y que permite obtener muestras estables en los que no existen restos de monómero sin reaccionar.

Langmuir

Article

pubs.acs.org/Langmuir

Versatile Approach for the Fabrication of Functional Wrinkled Polymer Surfaces

Marta Palacios-Cuesta,[†] Marta Liras,[†,§] Adolfo del Campo,[‡] Olga García,*[,†] and Juan Rodríguez-Hernández*[,†]

[†]Department of Chemistry and Properties of Polymers, Instituto de Ciencia y Tecnología de Polímeros (ICTP-CSIC), Juan de la Cierva 3, 28006 Madrid, Spain

[‡]Instituto de Cerámica y Vidrio (ICV-CSIC), Kelsen 5, 28049 Madrid, Spain

ABSTRACT: A simple and versatile approach to obtaining patterned surfaces via wrinkle formation with variable dimensions and functionality is described. The method consists of the simultaneous heating and irradiation with UV light of a photosensitive monomer solution confined between two substrates with variable spacer thicknesses. Under these conditions, the system is photo-cross-linked, producing a rapid volume contraction while capillary forces attempt to maintain the contact between the monomer mixture and the cover. As a result of these two interacting forces, surface wrinkles were formed. Several parameters play a key role in the formation and final characteristics (amplitude and period) of the wrinkles generated, including the formulation of the photosensitive solution (e.g., the composition of the monomer mixture) and preparation conditions (e.g., temperature employed, irradiation time, and film thickness). Finally, in addition, the possibility of modifying the surface chemical composition of these wrinkled surfaces was investigated. For this purpose, either hydrophilic or hydrophobic comonomers were included in the photosensitive mixture. The resulting surface chemical composition could be finely tuned as was demonstrated by significant variations in the wettability of the structured surfaces, between 56° and 104°, when hydrophilic and hydrophobic monomers were incorporated, respectively

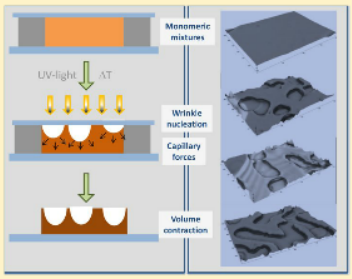

INTRODUCTION

Surface instabilities have received particular attention because they can be employed to pattern polymer surfaces and generate typically PDMS, as a substrate. During either mechanical stretching/compression or thermal expansion, a rigid layer (a metal,[38,39] a polymer layer,[28] or simple oxidation of the PDMS

Versatile approach for the fabrication of functional wrinkled polymer surfaces

*Marta Palacios-Cuesta,[a] Marta Liras,[a] Adolfo del Campo,[b] Olga García [a] * and Juan Rodríguez-Hernández [a] **

[a] Department of Chemistry and Properties of Polymers. Instituto de Ciencia y Tecnología de Polímeros, (ICTP-CSIC), Juan de la Cierva 3, 28006 Madrid, Spain.

[b] Instituto de Cerámica y Vidrio (ICV-CSIC). Kelsen 5, 28049-Madrid, Spain.

Correspondence to:

Olga García (ogarcia@ictp.csic.es)

Juan Rodríguez-Hernández (rodriguez@ictp.csic.es)

Abstract

A simple and versatile approach to obtain patterned surfaces via wrinkle formation with variable dimensions and functionality is described. The method consists of the simultaneous heating and irradiation with UV-light of a photosensitive monomer solution confined between two substrates with variable spacer thickness. Under these conditions the system is photocrosslinked producing a rapid volume contraction while capillary forces attempt to maintain the contact between the monomer mixture and the cover. As a result of these two interacting forces surface wrinkles were formed. Several parameters play a key role in the formation and final characteristics (amplitude and period) of the wrinkles generated, including the formulation of the photosensitive solution (e.g. the composition of the monomer mixture) and preparation conditions (e.g. temperature employed, irradiation time and film thickness). Finally, in addition the possibility to modify the surface chemical composition of these wrinkled surfaces was investigated. For this purpose either hydrophilic or hydrophobic comonomers were included in the photosensitive mixture. The resulting surface chemical composition could be finely tuned as was demonstrated by significant variations in the wettability of the structured surfaces, between 56º and 104º, when hydrophilic or hydrophobic monomers were incorporated, respectively.

Introduction

Surface instabilities have received a particular attention since they can be employed to pattern polymer surfaces and generate a variety of nano/micro structures. Surface instabilities produced in polymer films that have led to patterned surfaces include dewetting in thin films [1-8], phase separation of polymer blends or block copolymers, [9-11] the use of modified substrates [6, 12, 13], electric fields [14-18] or formation of surface wrinkles. [19-23] Whilst initially both buckling and wrinkling were considered as undesirable mechanical instabilities, the understanding of the mechanism of formation and the large amount of potential applications have stimulated interest in this particular approach to pattern polymer surfaces [24-27]. As examples, wrinkled surfaces have been employed to prepare electrodes for electroactive [28]/conductive [29] polymer actuators and anticorrosive coatings, [30] to produce high-performance electronics on rubber substrates, [31] and to produce surfaces with

controlled wettability for instance with superhydrophilic [22] or anisotropic wetting behavior on tunable surfaces [20]. More recently, in combination with surface nanopatterned substrates, anisotropic and hierarchically structured interfaces were obtained by Stafford and coworkers [27].

Although the formation of wrinkles on a polymer surface has been achieved by different approaches [32-37], in general the fabrication of this particular type of surface pattern is accomplished using a soft material with low elastic moduli, typically PDMS, as a substrate. During either mechanical stretching/compression or during thermal expansion, a rigid layer (a metal [38, 39], a polymer layer [28] or simple oxidation of the PDMS substrate [40, 41]) is deposited on the top of the material. Relaxation of the forces applied, [42] heating [43] or cooling to room temperature [38, 44] induce, upon buckling, the formation of surface wrinkles. The first method reported used the evaporation of aluminum on a flexible substrate to form a rigid layer [38]. The metal was spread on the thermally expanded PDMS layer (high temperature) that, upon cooling, contracts and induces the formation of wrinkles in the metallic layer. Other methods to obtain a rigid layer involve the oxidation of the PDMS film with UV-ozone or plasma treatment [40, 41]. Depending on the conditions employed and the oxidative method, microstructures with surface wrinkles from 150 nm to several hundreds of microns can be obtained. However, the different mechanical resistance of the layer deposited compared to the bulk limits the lifetime of the wrinkles and may induce cracking on the surface formed. Moreover, the chemical composition is limited to selected metals, oxides resulting from surface treatments or coatings with high modulus polymers.

As an alternative to the aforementioned examples, recently several groups have described the formation of wrinkled interfaces, replacing the PDMS substrate by other polymeric coatings such as hydrogels or photocrosslinkable systems.[45, 46] On the one hand, confinement of hydrogels has been demonstrated to induce surface deformations that may lead to surface instabilities and finally to wrinkle formation [35, 47-50]. In these homogeneously crosslinked materials, the presence of a rigid support is the responsible for the surface deformation. On the other hand, photocroslinkable systems are based on a vertical gradient in the crosslinking degree from the air/polymer to the polymer/support interface. Upon surface deformation, for instance by swelling, the interface buckles and form wrinkles. One of the most

recently described approaches to form wrinkled surfaces employs the irradiation in two steps of an acrylate mixture [51]. In order to create micro-structures, the sample is irradiated with a monochromatic excimer lamp with low penetration depth which polymerizes only the top layer of the photosensitive mixture. This gradually photopolymerized layer floats on the non-polymerized mixture, and due to the volume contraction superficial wrinkles are formed. In a second step designed to fix the structure, the system is treated using through-curing irradiation with, for instance, an Hg lamp. As an illustrative example, Crosby *et al*. [50] employed a mixture formed by acrylic monomers and a crosslinker and irradiated while applying a controlled oxygen flow on the top of the sample.

As mentioned above below, wrinkles prepared, for instance, using a PDMS substrate allows fine tuning of the wrinkle characteristics. However, variations in the chemical composition required the deposition of a functional layer. Equally, the micro-folded surfaces obtained from hydrogels or photocrosslinked materials has been employed using particular systems [52] of acrylic monomers [50]. These were carried out in two steps and the wrinkle dimensions seem to be difficult to control. In addition, the pattern completely changes by changing the formulation [51], or is limited to a particular system [53], wrinkle formation requires a large amount of non-crosslinked monomer, and the unreacted monomer partially remains in the polymer film and needs to be removed in order to prevent further side reactions.

In the present work we describe the elaboration of wrinkled surfaces with significant advantages over previous approaches [52, 54] based on the confinement of monomer mixtures between two interfaces varying the distance between them with a spacer. Firstly, by using simultaneous photocrosslinking and heating functional wrinkled interfaces with variable buckle dimensions (amplitude and period) depending on the monomer/crosslinking agent ratio and the spacer employed were prepared in a single straightforward step. In addition, in this case the reactive conversion is complete so that the presence of residual monomer, present in previously reported approaches, is avoided. Finally, monomer confinement between support and cover allowed the use of low boiling point monomers that would evaporate if other approaches were employed.

The mixture of a difunctional monomer (Ethylene glycol dimethacrylate -EGDMA- for the acrylates and divinylbenzene -DVB- for styrenics) with a linear monomer (Methyl methacrylate-MMA or Styrene-S) was employed. Firstly, we will describe the role of the temperature and thickness on the wrinkle formation. Subsequently, functional acrylates (2-hydroxyethyl methacrylate –HEMA and trifluoroethyl methacrylate -TFMA) or a styrene derivative monomer (pentafluorostyrene -5FS) were included with variable ratios to produce functional wrinkles with variable dimensions with the aim of simultaneously controlling the chemical composition. This allowed buckled surfaces with variable chemical composition to be generated depending on the initial monomer composition.

Experimental

Materials and methods

Methyl methacrylate (MMA) was washed three times with a basic aqueous solution (10% NaOH) and three additional times with water. Then, the resulting monomer was dried on anhydrous magnesium sulfate, filtered and distilled. Styrene (S) was dried under CaH_2 and distillated under reduced pressure. Ethylene glycol dimethacrylate (EGDMA), divinylbenzene (DVB), 2-(hydroxyethyl methacrylate) (HEMA), 2,2,2-trifluoroethyl methacrylate (TFMA), 2,3,4,5,6-pentafluorostyrene (5FS), all from Aldrich with the highest purity; Irgacure 651 (IRG 651), 2,2-dimethoxy-1,2-diphenylethan-1-one (Ciba), dichlorodimethylsilane (Aldrich 98.5%) and the rest of solvents were employed as received without further purification. Silicon wafers (Siegert Consulting e.k.) and 0.15 mm thickness glass covers (Menzel-Glaser) were employed as supports.

Infrared spectra were obtained using a Spectrum One FTIR spectrometer (Perkin-Elmer) fitted with a horizontal attenuated total reflectance (ATR) accessory under unforced conditions. The irradiated samples were placed in direct contact with the diamond crystal with no previous preparation. Spectra were collected at 8 cm^{-1} resolution co-adding 6 scans per spectrum.

Scanning electron microscopy (SEM) was used for surface structural and cross-sectional analysis. Micrographs were taken using a Philips XL30 with an acceleration voltage of 25 kV. The samples were coated with gold-palladium (80/20) prior to scanning. Cross sectional

profiles and 3D images of the wrinkled surfaces were characterized by using a Zeta-20 True Color 3D Optical Profiler from Zeta Instruments.

Methodology to prepare the wrinkles

Photosensitive mixtures contained variable amounts of a crosslinking agent, i.e. ethylene glycol dimethacrylate (EGDMA) for the methacrylic monomers and divinylbenzene (DVB) for the styrenics and the corresponding linear monomers. The methacrylic linear monomers employed throughout this study were methyl methacrylate (MMA), 2-hydroxyethyl methacrylate (HEMA) and 2,2,2-trifluoroethyl methacrylate (TFMA) in different ratios and were copolymerized with EGDMA. The styrenic monomers employed were styrene (S), and 2,3,4,5,6-pentafluorostyrene (5FS) and were copolymerized with DVB. In addition, a radical photoinitiator, IRG 651 (2 wt% respect to the total amount of monomers) was employed to start the polymerization process. The photopolymerization of the films was undertaken under UV spot light irradiation source using a Hamamatsu model Lightning Cure L8868 provided by an Hg-Xe lamp with 200 W power. To prepare the films, 2 x 2 cm silicon wafers with variable spacers (50-150 μm) were employed. A few drops of the photosensitive mixture were placed in the center of the wafer and covered by glass of 0.30 mm thickness. The samples were preheated on a hot plate and irradiated under constant heating. The incident light was focused on the samples with an optical fiber (distance sample to light was fixed at 8 cm) and the irradiation intensity was kept constant at 6150 mW/m^2 (measured by a Luzchem SPR-01 radiometer) throughout the experiments.

Initial tests were carried out varying the ratio of linear monomer *versus* crosslinking agent in order to optimize the wrinkle formation. The samples having additionally functional monomers were prepared using a constant ratio of linear monomers (i.e. both functional monomer and non-functional monomer) and crosslinking agent of 85/15 v/v%.

Results and discussion

Mechanism of wrinkle formation

The preparation of wrinkled topographies was carried out using the setup described in Scheme 1. The monofunctional monomer (MMA) was mixed with the crosslinking agent (Ethylene glycol dimethacrylate - EGDMA) and the photoinitiator (IRG 651), and the mixture was confined in a closed chamber. The liquid mixture was then simultaneously heated and irradiated using UV-light able to pass through the glass cover employed. After 4 minutes of irradiation the reaction was completed and the cover removed. The use of a cover avoids monomer evaporation thus assuring that the composition of the final material is identical to the feed composition. Moreover, a planar cover limits thickness variations over the sample and favors the homogeneity of the surface pattern. As a result of the simultaneous irradiation and photocrosslinking wrinkled structures such as the example in Scheme 1(B) were observed.

The approach illustrated in Scheme 1 has been extended to other monomers in order to demonstrate the versatility of this strategy. More precisely, Scheme 2 shows the chemical structures of monomers, crosslinking agents and photoinitiator employed throughout this study. We have explored two different families of monomers, i.e. acrylics and styrenics that may provide materials with different surface wettability, for example. In the EGDMA/MMA mixture the MMA was partially or totally substituted by a functional monomer: either hydrophilic (HEMA) or hydrophobic (TFMA). Equally for the DVB/S mixture the linear monomer, i.e. styrene was partially or totally replaced by HEMA or 5FS, which are hydrophilic and hydrophobic respectively.

However, before the variations in surface functionality were explored, the experimental conditions to perform the photopolymerizations were optimized. Initially, the photopolymerization reactions were undertaken at different temperatures, and the surface patterns were observed to change dramatically as a function of the temperature employed. The samples were irradiated with UV-light while maintaining the heating for 4 minutes. The micrometer size surface features formed using MMA (85 v/v%) and EGDMA (15 v/v%) using 2 wt% of IRG 651 as a photoinitiator are depicted in Figure 1(A). Whereas for temperatures from r.t. up to 70ºC no significant, or only partial, wrinkle formation was observed, at 100ºC

the formation of micrometer size wrinkles was quite homogenous over the entire film. It should be mentioned that in the case of styrene/DVB mixtures the temperature required to observe the formation of wrinkled interfaces was 140ºC. Indeed, the photopolymerization kinetics of S/DVB was slow in comparison to that for MMA/EGDMA and additional heating was required. It has to be mentioned at this point that the monomer conversion achieved is almost complete. According to analysis carried out by washing the films with organic solvents to extract residual monomer and further analysis by NMR confirmed the complete consumption of the monomers in the photocrosslinking reaction.

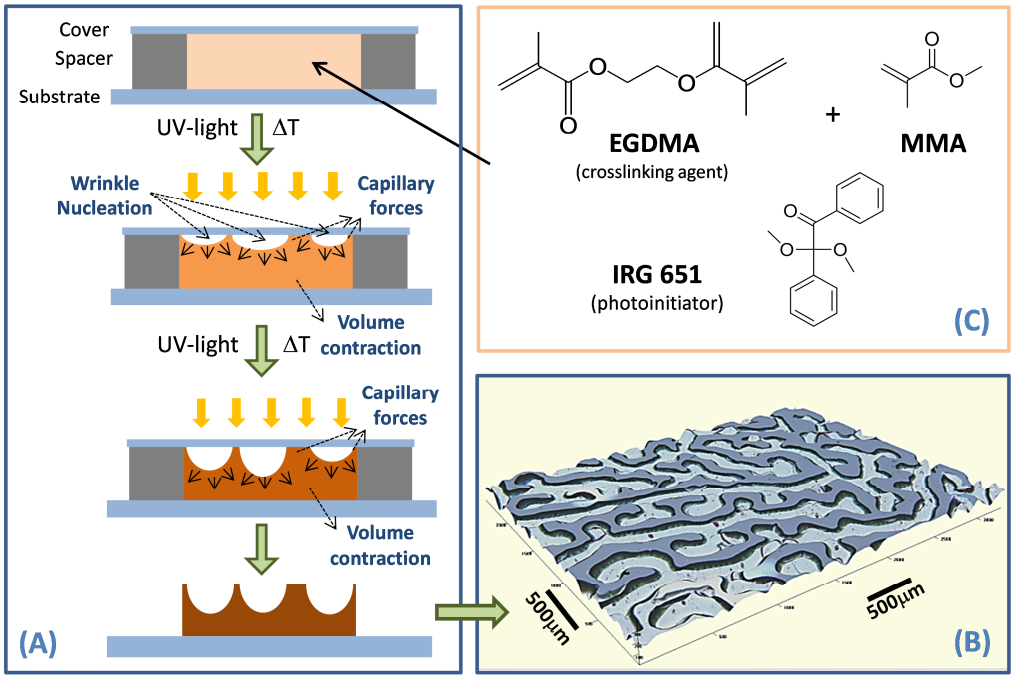

Scheme 1. *a) Illustration of the experimental procedure to fabricate wrinkled surfaces for MMA/EGDMA/IRG mixtures. The sample is irradiated and heated. During this process, volume contraction and capillary forces act simultaneously inducing the formation of wrinkled interfaces. b) The 3D image obtained by using an optical 3D optical profiler corresponds to photosensitive mixture c) contains 85 v/v% of monomer (MMA), 15 v/v % of crosslinking agent (EGDMA) and 2 wt% of photoinitiator (IRG 651).*

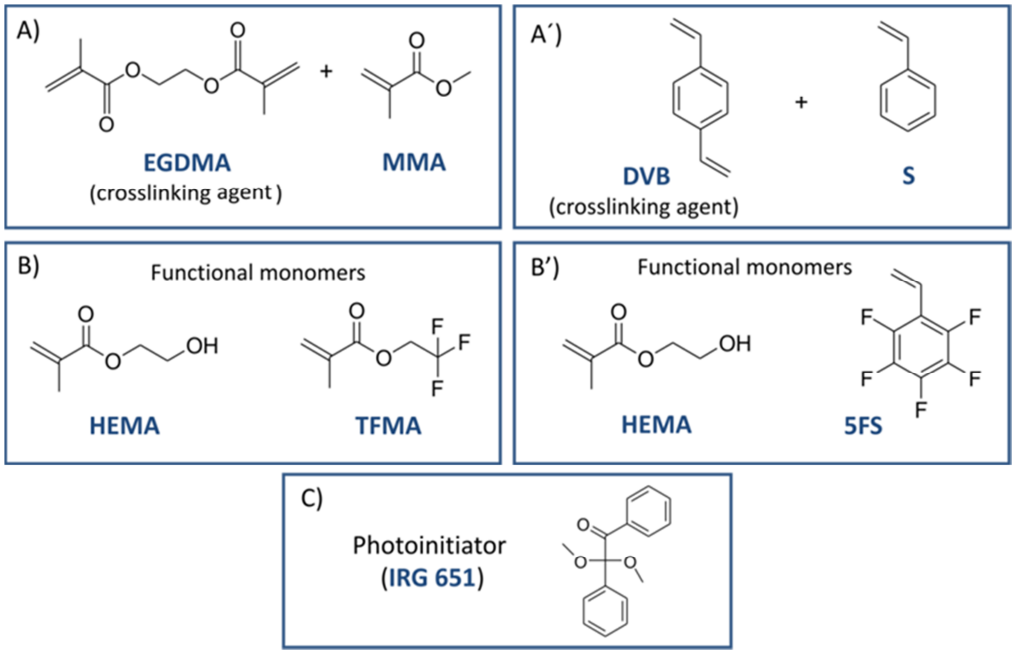

Scheme 2. *Chemical structures of the monomers, crosslinking agents and photoinitiator employed in this study. We explored two different families of monomers/crosslinking agent mixtures: a) methyl methacrylate/EGDMA and a´) styrene/DVB. Additionally the monomers MMA and S in the mixture have been partially or completely substituted with other functional monomers b or b´, respectively) in order to vary the chemical composition of the wrinkled interface.*

To obtain further information, complementary FTIR-ATR experiments were performed on the films prepared at different temperatures. Figure 1(B) shows the spectra from the films resulting from the photopolymerization, with those of both PMMA and EGDMA (with free double bonds) for comparison. A specific band can be identified at 812 cm^{-1} related to residual double bonds of the acrylic functionality (-CH=CH- twisting). At low temperatures, a relative large amount of residual double bonds is present in the film upon photopolymerization. Nevertheless, on increasing the temperature the -C=C- signal decreases while the -C-C- band observed at ~840 cm^{-1} is relatively more intense. We can thus conclude that increasing the temperature increases the effective crosslinking. The amount of residual -C=C- is reduced producing an increase of the volume contraction upon UV-irradiation. In addition, Figure 1(B)

exhibits the ratio of Band I and Band II as a function of the photocrosslinking temperature employed. This explains, at least to some extent, not only the formation of wrinkled interfaces but also why the formation of surface wrinkles was produced to a larger extent by carrying the reaction at higher temperatures.

According to the optical profiler images depicted in Figure 2, obtained at different reaction stages, wrinkle formation may occur as follows: The initial monomer mixture fills the volume between the covers. When the photopolymerization starts, as a consequence of the volume contraction, cavities with rather irregular dimensions are formed (Figure 2B). The polymerization continues and as a consequence of the volume contraction an enlargement of the cavities was observed (Figure 2C). As a result of this process, the cavities interconnect before the completion of the reaction and produce a completely wrinkled film.

According to these experimental observations, we can hypothesize that the wrinkle formation might be the result of the interplay between two different forces acting simultaneously. In Scheme 3 are depicted the 3D image of a wrinkled surfaces (A) and a cross-section of a particular wrinkle (B). The characteristic wrinkle profile also confirmed the presence of two different forces. On the one hand, the volume contraction resulting of the network construction during the crosslinking reaction produced the formation of cavities and enlarged them during the reaction. On the other hand, the attraction of the monomer molecules by the interface, i.e. capillary force, that maintain the contact between the solution and the interface. It has to be mention that the affinity of the monomer molecules by the cover is independent of the cover employed. Thus, the use of either hydrophilic or hydrophobic (obtained by silanization) covers exhibit similar wrinkle characteristics. This behavior, a priori unexpected, can be explained taking into account the chemical structure of the monomer units that possess both hydrophobic and hydrophilic functional groups and therefore are able to wet both types of interfaces.

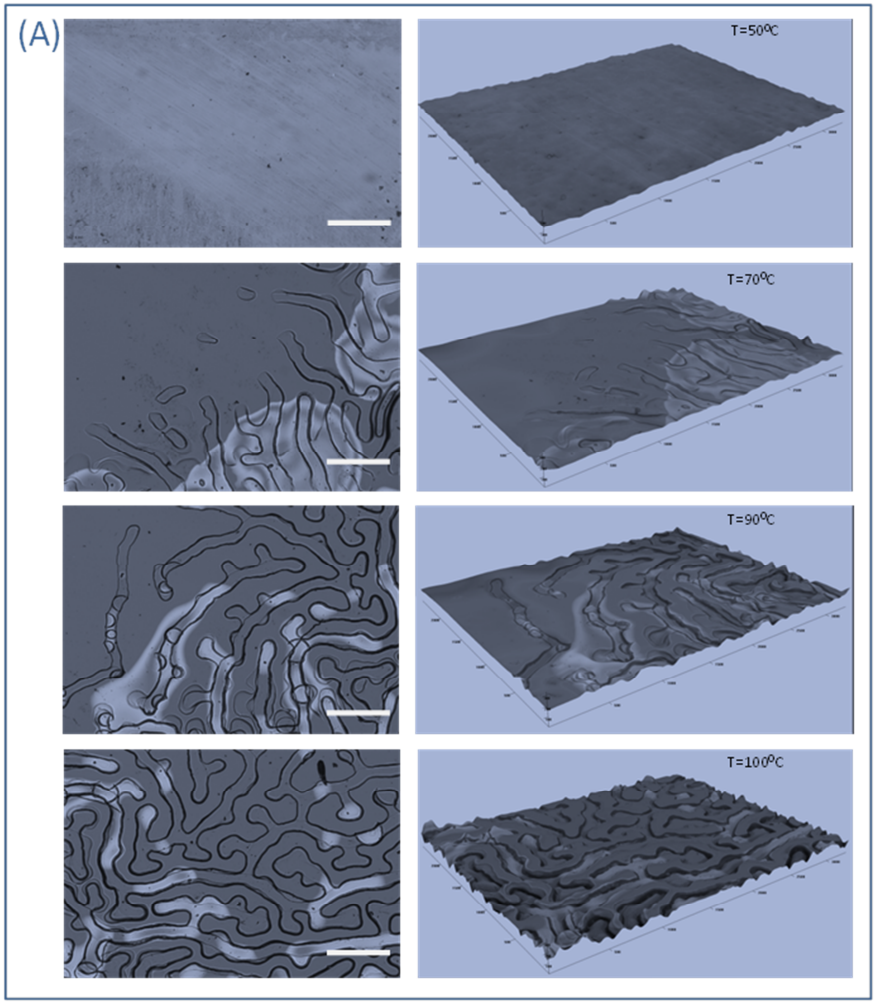
(A)
T=50ºC
T=70ºC
T=90ºC
T=100ºC

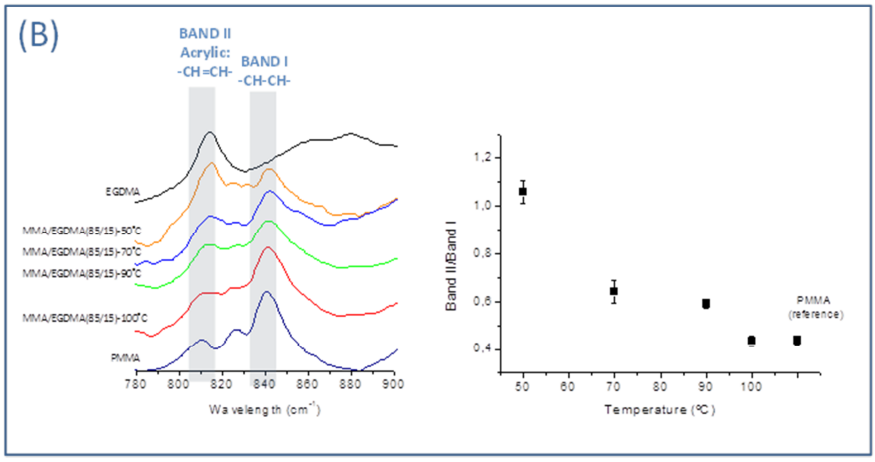
(B)
BAND II
Acrylic:
-CH=CH-
BAND I
-CH-CH-
EGDMA
MMA/EGDMA(85/15)-50ºC
MMA/EGDMA(85/15)-70ºC
MMA/EGDMA(85/15)-90ºC
MMA/EGDMA(85/15)-100ºC
PMMA
780
800
820
840
860
880
900
Wavelength (cm-1)
Band II/Band I
1,2
1,0
0,8
0,6
0,4
PMMA
(reference)
50
60
70
80
90
100
Temperature (ºC)

Figure 1. *a) Optical micrographs of the surface patterns formed by photocrosslinking of MMA/EGDMA (85/15) v/v% and 2 wt% of IRG 651 at different temperatures: 50ºC, 70ºC, 90ºC and 100ºC. The monomer mixture was allowed to reach the desired temperature prior to irradiation. Scale bar: 500 μm. b) Left: FTIR-ATR spectra of the crosslinked films obtained by simultaneous heating and UV irradiation of the monomer mixture MMA/EGDMA (85/15) v/v% at different temperatures. Right: Representation of the Band I/Band II ratio as a function of the photocrosslinking temperature employed.*

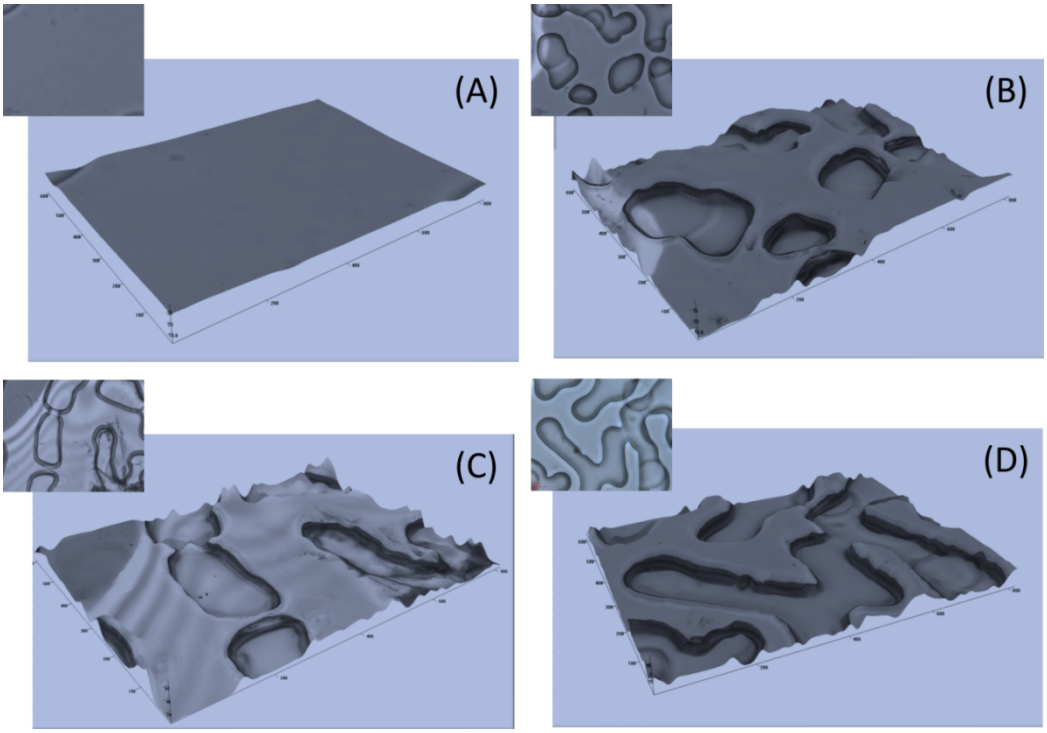

Figure 2. *Optical micrographs of the formation of wrinkles at different polymerization stages: a) initial monomer mixture, b) formation of nucleation points, c) extension of the nucleation and d) final formation of wrinkles.*

Whereas the mechanism and the equilibrium between the two forces which are directly related to the temperature drive the formation or not of the wrinkles, the experimental conditions employed for the film preparation clearly affect the wrinkle formation. In particular the role of the film thickness, controlled by the spacer employed, and the composition

MMA/EGDMA of the feed were explored. Figure 3 shows the SEM and optical images of the surface wrinkles obtained with variable v/v% of EGDMA (from 1 to 15 v/v%).

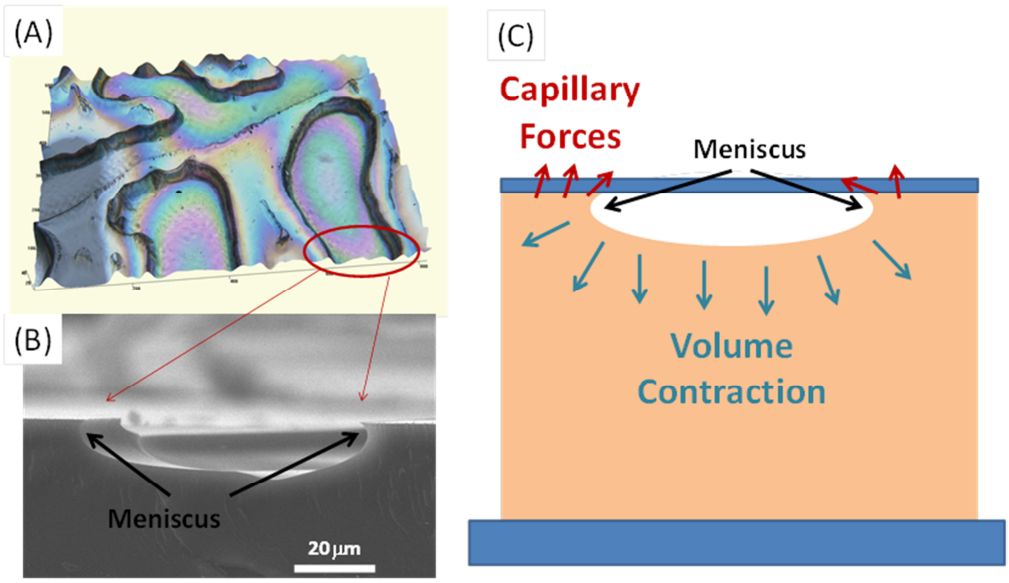

Scheme 3. *Illustration of the surface wrinkles obtained upon simultaneous heating/photocrosslinking and the forces involved in their formation.*

Wrinkles were observed for a particular spacer (50 □m) in samples with monomer composition with at least 5 v/v% of EGDMA. The volume contraction was rather low in the sample with only 1 v/v% and appeared to be insufficient to initiate the process. However, samples containing both 5 and 15 v/v% of EGDMA produced wrinkled interfaces. Moreover, whereas the wrinkle wavelength was similar in both cases we observed a higher density of wrinkles in the sample with more EGDMA. Therefore, the volume contraction observed is directly related to the amount of EGDMA employed, at least in the range described. However, the wrinkle formation in samples with higher EGDMA content did not exhibit significant variations in the wrinkle characteristics, such that we can anticipate that the amount of crosslinking agent available to react may reach a maximum value that could not be improved even by introducing a larger amount of crosslinking agent. This phenomenon is related to a dramatic decrease in the mobility by increasing the conversion, which reduces/limits the polymerization rate.

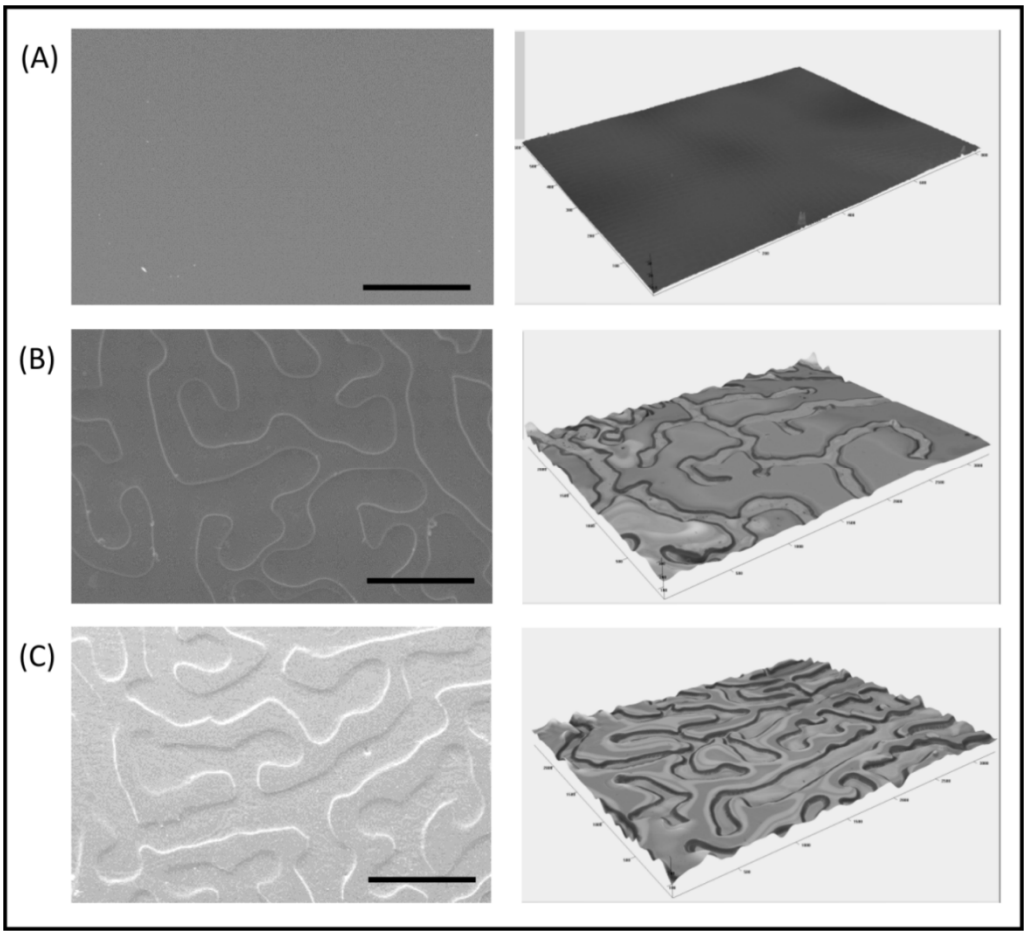

Figure 3. *SEM images and 3D optical micrographs of the surface patterns formed by photocrosslinking of variable MMA/EGDMA volume ratio a) 99/1, b) 95/5 and c) 85/15 but using a 50 μm spacer. All the experiments were photopolymerized with 2wt% of IRG 651 at 100ºC. Scale Bar: 500 μm.*

While the monomer composition above a certain amount of EGDMA for a particular thickness does not appear to significantly influence the pattern dimensions, the variation of the spacer thickness clearly affected the wrinkle size. As depicted in Figure 4, an increasing spacer size leads to larger average wrinkle periods. By using a 50 μm spacer, the wrinkle dimensions

remain in the range of 260-330 μm. For 100 μm spacers or 150 μm spacers average wrinkle dimensions between 460-580 μm and above 670 μm were obtained, respectively. At this point it should be mentioned that the formation of homogeneously distributed wrinkles requires a minimum amount of crosslinking agent. Thus, in order to form more homogeneous wrinkles when using larger spacers, higher amounts of crosslinking monomer are desirable. For example, when using a 100 μm spacer heterogeneous wrinkles with some planar areas were observed in samples containing less than 15 v% of crosslinking agent. When using 150 μm spacers, higher amounts of crosslinking agents were required in order to obtain more homogeneous surface patterns: For this particular system, 45 v% of EGDMA generates homogeneously distributed wrinkles. Thus, the optimum value of crosslinking agent necessary to produce homogeneously distributed wrinkles increases with spacer thickness.

In addition to the MMA/EGDMA combination, we have explored the formation of wrinkled interfaces to S/DVB. Similarly to what has been reported for the MMA/EGDMA system an increase of the film thickness induced the formation of larger wrinkles. Nevertheless, in contrast to the previous case, S/DVB forms wrinkles with similar homogeneity in any S to DVB ratios ranging from 5 to 45 v/v% of DVB.

Wrinkled surfaces are typically characterized both by the period and the amplitude of the wrinkles (depicted below). Whereas the wrinkled period (in both systems) appears to be directly connected with the film thickness and remains almost constant with the comonomer composition, the amplitude of the wrinkles prepared by simultaneous photopolymerization and heating exhibit a particular behavior. As depicted in Figure 4, low or high amounts of crosslinking agent produced wrinkles with low amplitudes typically below 5 μm. However, intermediate values of crosslinking (10 to 15 v/v% of crosslinking agent) produced wrinkles with larger amplitude with values up to 20 μm. This behavior that has been observed in both systems acrylics and styrenics occurs at different amounts of crosslinking agent. Whereas in the acrylic system the maximal amplitude appears in the samples having 10v% of crosslinking agent in the case of the styrenics the highest amplitude was observed in the samples having 15v% of crosslinking agent.

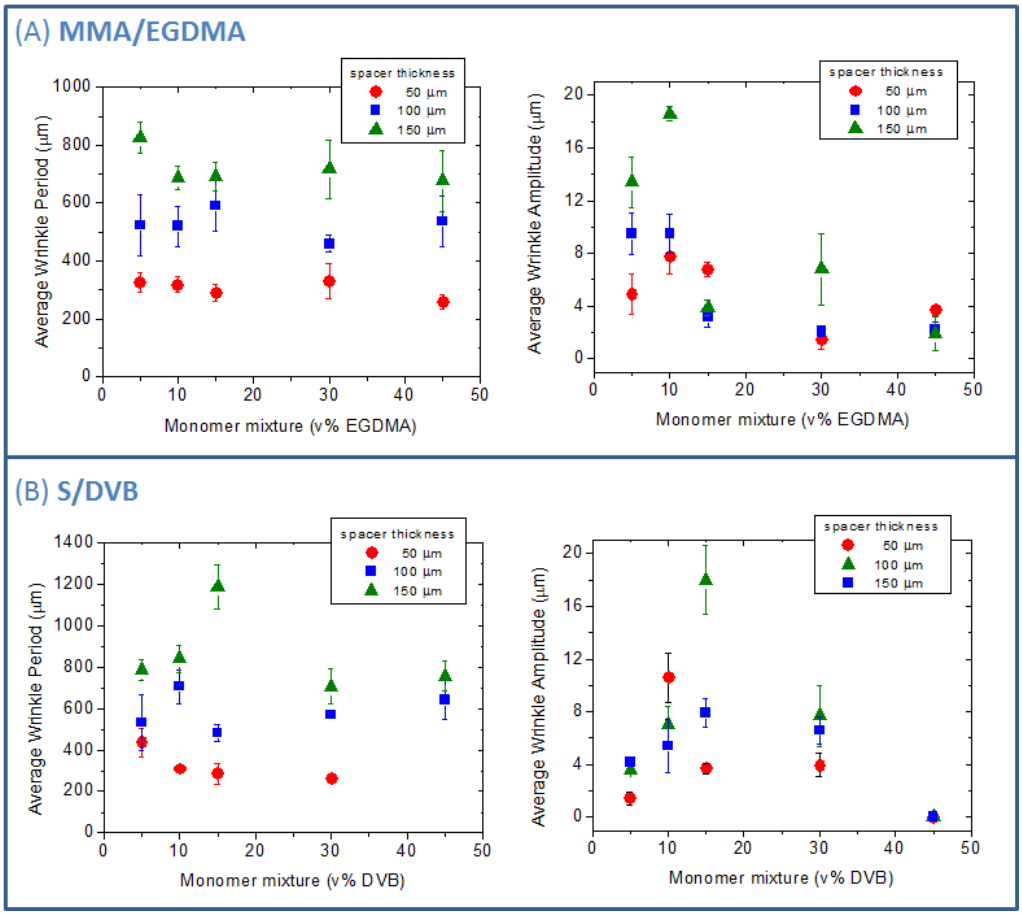

Figure 4. *Average wrinkle dimensions: wrinkle period (left) and wrinkle amplitude (right) measured for films obtained using different spacers from 50 to 150 µm. a) The monomer mixture employed (MMA/EGDMA) was varied from 5% to 45 v % of EGDMA. b) The monomer mixture employed (S/DVB) was varied from 5% to 45 v % of DVB. For these experiments undertaken at a temperature of 100ºC, a constant amount of 2 wt% of IRG 651 was employed.*

In view of these observations, we can conclude that depending on both the film thickness and the amount of crosslinking agent we can vary the main wrinkle features. Independently of the system employed MMA/EGDMA or S/DVB, the wrinkle characteristics amplitude and period could be varied between 2 to 20 µm and 200-250 µm up to 800 µm, respectively.

In addition to the control over the surface pattern dimensions, another crucial parameter in the design of polymer surfaces concerns the possibility to fine tune the surface chemical composition. This aspect has been up to now a limitation since it typically required additional functionalization steps for the case of wrinkled surfaces. The approach described herein for the preparation of buckled surfaces allowed us to modify the surface chemical composition by simply introducing a functional hydrophilic or hydrophobic comonomer within the photosensitive mixture.

In Scheme 4 is depicted the construction of wrinkled surfaces by introducing either a hydrophilic monomer, i.e. 2-hydroxyethyl methacrylate, HEMA (a) or a hydrophobic monomer i.e. 2,2,2-trifluoroethyl methacrylate, TFMA (b) in a MMA/EGDMA mixture. The incorporation of these two monomers replacing partially or totally the MMA component, did not alter or prevented the formation of wrinkles independently of the amount employed. On the contrary, the volume contraction that dictates the formation of the surface instabilities still being produced and wrinkles were observed in all cases when using the same experimental conditions. Additionally, as a result of the inclusion and the copolymerization of these two monomers within the network, the surface hydrophilicity dramatically changed. As observed in Figure 5 the incorporation of HEMA reduces the contact angle below 55º. On the contrary, the incorporation of TFMA increases the contact angle values measured up to 105º. These values clearly indicate the possibility to largely modulate the chemical composition and therefore the surface wettability of these buckled surfaces as a function of their monomer composition.

The gradual variation of the surface wettability as a function of the functional monomer incorporated in the photosensitive mixture measured by contact angle is evidenced in Figure 5 for both MMA/EGMA and S/DVB systems. Whereas the amount of crosslinking agent was maintained constant (15 v%), the amount of either the hydrophilic or the hydrophobic comonomer was varied by substitution of either MMA or S by the functional comonomer. The films measured were prepared using a 50μm spacer

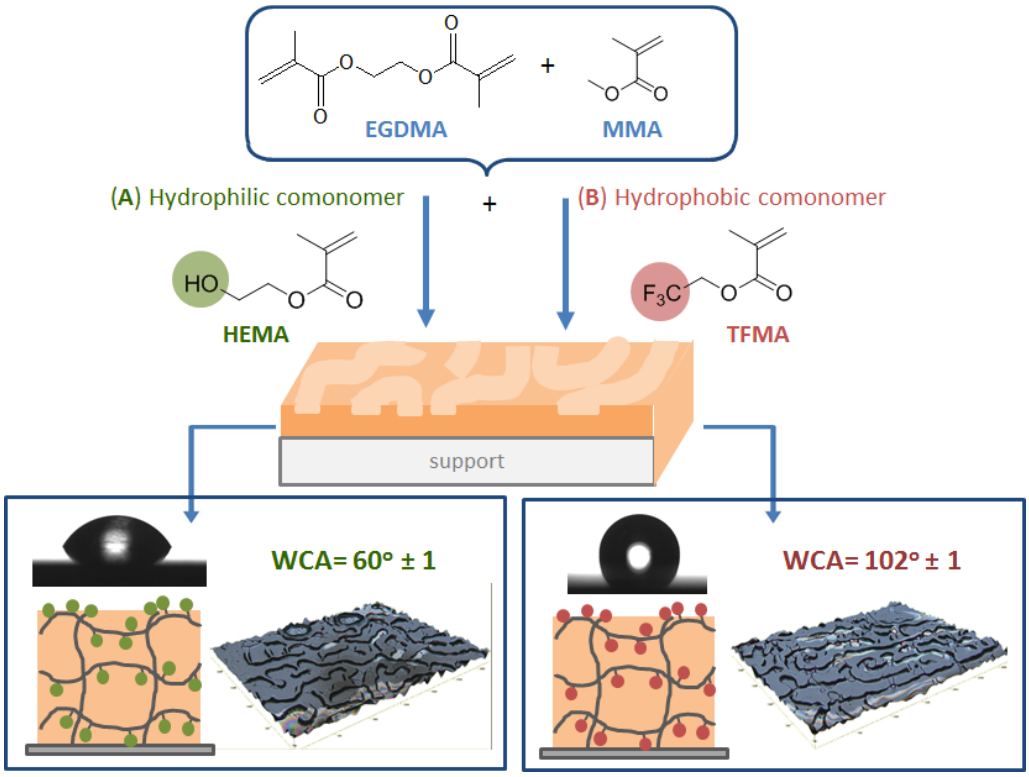

Scheme 4. *Illustration of the chemical structures of the networks formed upon photopolymerization of photosensitive mixtures containing additionally either HEMA or TFMA. Left: surface wrinkles produced HEMA/MMA/EGDMA (42.5/42.5/15) v/v/v %. Right: wrinkles produced from mixtures of TFMA/MMA/EGDMA (42.5/42.5/15) v/v/v %.*

In both cases the incorporation of and hydrophobic comonomer (either TFMA or 5FS) leaded to an increase in the hydrophobicity of the wrinkled surfaces raising to contact angles up to 105º in those samples with higher amount of hydrophobic monomer. On the contrary, the incorporation of hydrophilic moieties (HEMA in both cases) significantly reduced the contact angle from values above 80º-85º to contact angles below 55º. It has to be mentioned at this point that independently of the amount of HEMA introduced the large amount of EGDMA (15 v%) employed assured the material integrity and not detectable changes were observed on the wrinkled surface upon the water droplet deposition.

As a summary, the possibility to incorporate functional monomers within the photosensitive mixture allows us to fine tune the contact angle of the wrinkled interface. This result opens new ways to simultaneously control both topography and surface functionality in a single photopolymerization step.

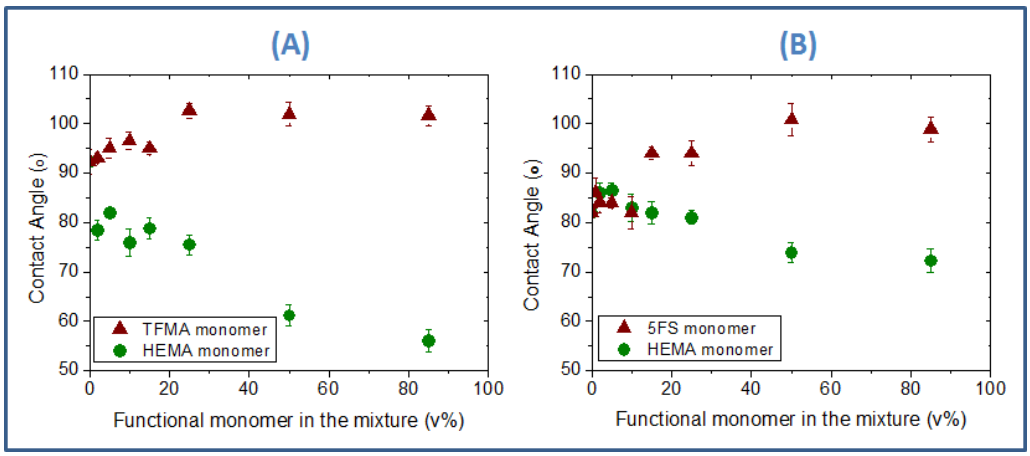

Figure 5. *Water contact angle values obtained for wrinkled surfaces having variable chemical composition. a) MMA/EGDMA system in which a variable amount from 0 to 85 v% of either TFMA or HEMA has been incorporated substituting MMA while maintaining the EGDMA amount constant to 15 v%. b) S/DVB system in which a variable amount from 0 to 85 v% of either 5FS or HEMA has been incorporated to substitute S while maintaining the amount of DVB constant to 15v%.*

Conclusions

Herein we report a straightforward approach to develop patterned surface by wrinkle formation as a consequence of the shrinking produced upon crosslinking of a monomer (MMA or S) with a crosslinking agent (EGDMA or DVB). From this basic concept, i.e. heating and photocrosslinking in confined films, wrinkles were obtained in which their characteristics could be varied by changing the amount of the crosslinking agent and/or the film thickness. Moreover, as evidenced the surface chemical composition can be finely tuned incorporation of a functional monomer within the monomeric photosensitive mixture.

The structure obtained is stable both to solvents and temperature as a consequence of the formation of a covalent 3D network. The system of the elaboration of highly stable wrinkled surfaces described here is the starting point for further developments. This appears to be interesting for technological exploitation in the development of materials with controlled adhesion, friction and wetting while keeping thermal and chemical stability provided by the crosslinked structure. In addition, the process is carried out in one step, at short times and do not require particular equipment what make it profitable at industrial scale. Compared with other techniques, with this method there is no risk of residual monomers in the final product enabling its use in biological applications like cell templates for tissue engineering or also as coatings in aeronautics and construction.

Acknoledgements

This work was financially supported by the Ministerio de Economía y Competitividad (MINECO) (Projects MAT2010-17016 and MAT2011-22861). M. Palacios-Cuesta gratefully acknowledges her FPU fellowship (Ministerio de Educación, Cultura y Deporte - MECD).

AUTHOR INFORMATION

Corresponding Authors

Olga García* (ogarcia@ictp.csic.es) and Juan Rodríguez-Hernández* (rodriguez@ictp.csic.es)

* Department of Chemistry and Properties of Polymers. Instituto de Ciencia y Tecnología de Polímeros, (ICTP-CSIC), Juan de la Cierva 3, 28006 Madrid, Spain.

Present Addresses

Marta Liras: Department of Synthesis, Structure and Properties of Organic Compounds

Instituto de Química Orgánica General (IQOG-CSIC), Juan de la Cierva 3, 28006 Madrid, Spain.

CAPÍTULO IV.2: Arrugas en superficies funcionales a partir de mezclas monoméricas con incorporación de copolímeros funcionales como carga.

Como en el capítulo IV.1, las modificaciones de topografía de la superficie se llevan a cabo por la creación de arrugas superficiales durante el proceso de fotopolimerizacion. Sin embardo,en este caso, la variación de la composición química superficial se ha conseguido gracias a la incorporación como aditivos, de copolímeros funcionales, tanto hidrofóbicos o hidrofílicos, en las mezclas de polimerización.

Articulo 7: *Fabrication of Functional Wrinkled Interfaces from Polymer Blends: Role of the Surface Functionality on the Bacterial Adhesion*

Utilizando el mismo procedimiento de creación de arrugas superficiales descrito en el artículo 6 de esta Tesis (donde se fabrican arrugas a partir de la irradiación UV y a temperatura constante de mezclas de monómeros), se han añadido copolímeros funcionales como cargas a las mezclas fotosensibles, lo que ha permitido funcionalizar dichas superficies arrugadas. La incorporación dentro del material de un copolímero funcional ha permitido variar la composición química de la superficie mientras se mantiene la estructura de la misma. Por último, se ha ensayado la aplicabilidad de este tipo de microestructuras funcionales, donde la hidrofobicidad de las mismas juega un papel crucial en la adhesión específica de la superficie bacteriana de *Staphylococcus Aureus*.

Polymers **2014**, *6*, 2845-2861; doi:10.3390/polym6112845

OPEN ACCESS

polymers

ISSN 2073-4360

www.mdpi.com/journal/polymers

Article

Fabrication of Functional Wrinkled Interfaces from Polymer Blends: Role of the Surface Functionality on the Bacterial Adhesion

Marta Palacios-Cuesta [1], Aitziber L. Cortajarena [2], Olga García [1,*] and Juan Rodríguez-Hernández [1,*]

[1] Department of Chemistry and Properties of Polymers, Instituto de Ciencia y Tecnología de Polímeros-Consejo Superior de Investigaciones Científicas (ICTP-CSIC), Juan de la Cierva 3, 28006 Madrid, Spain; E-Mail: mpalacios@ictp.csic.es

[2] Instituto Madrileño de Estudios Avanzados en Nanociencia (IMDEA-Nanociencia), Cantoblanco, 28049 Madrid, Spain; E-Mail: aitziber.lopezcortajarena@imdea.org

* Authors to whom correspondence should be addressed; E-Mails: ogarcia@ictp.csic.es (O.G.); rodriguez@ictp.csic.es (J.R.-H.); Tel.: +34-912-587-560 (O.G. & J.R.-H.); Fax: +34-915-644-853 (O.G. & J.R.-H.).

External Editor: Lloyd Robeson

Received: 22 September 2014; in revised form: 27 October 2014 / Accepted: 31 October 2014 / Published: 14 November 2014

Fabrication of Functional Wrinkled Interfaces from Polymer Blends: Role of the Surface Functionality on the Bacterial Adhesion

Marta Palacios-Cuesta [1], Aitziber L. Cortajarena [2], Olga García [1,*] and Juan Rodríguez-Hernández [1,*]

[1] Department of Chemistry and Properties of Polymers, Instituto de Ciencia y Tecnología de Polímeros (ICTP-CSIC), Juan de la Cierva 3, 28006 Madrid, Spain; E-Mail: mpalacios@ictp.csic.es

[2] Instituto Madrileño de Estudios Avanzados en Nanociencia (IMDEA-Nanociencia), Cantoblanco, 28049 Madrid, E-Mail: aitziber.lopezcortajarena@imdea.org

***** Authors to whom correspondence should be addressed; E-Mails: ogarcia@ictp.csic.es (O.G.); rodriguez@ictp.csic.es (J.R.-H.); Tel.: +34-912-587-560; Fax: +34-915-644-853.

Abstract

The generation of nano-microstructured surfaces is a current challenge in polymer science. The fabrication of such surfaces has been accomplished mainly following two different alternatives *i.e.*, by adapting techniques, such as molding (embossing) or nano/microimprinting, or by developing novel techniques including laser ablation, soft lithography or laser scanning. Surface instabilities have been recently highlighted as a promising alternative to induce surface features. In particular, wrinkles have been extensively explored for this purpose. Herein, we describe the preparation of wrinkled interfaces by confining a photosensitive monomeric mixture composed of monofunctional monomer and a crosslinking agent within a substrate and a cover. The wrinkle characteristics can be controlled by the monomer mixture and the experimental conditions employed for the photopolymerization. More interestingly, incorporation within the material of a functional copolymer allowed us to vary the surface chemical composition while maintaining the surface structure. For that purpose we incorporated either a fluorinated copolymer that enhanced the surface hydrophobicity of the wrinkled interface or an acrylic acid containing copolymer that increased the hydrophilicity of the wrinkled surface. Finally, the role of the hydrophobicity on the bacterial surface adhesion will be tested by using *Staphylococcus aureus*.

Introduction

Surface instabilities caused by different forces (mechanical, spinodal dewetting, electric field, and thermal gradient) have received particular attention since they can derive in a variety of surface nano/micro structures. Surfaces instabilities used to pattern polymer surfaces have been reported in literature and include the use of modified substrates [6, 12, 13], electric fields [14-18], dewetting in thin films [1-7] or phase separation of polymer blends or block copolymers [9-11, 55].

A particularly extended approach to pattern polymer surfaces concerns the use of mechanically induced wrinkled morphologies [19-23]. This strategy alone or combined with other patterning technologies has been employed to produce different surface patterns with

multiple applications. Wrinkled interfaces have been, for instance, employed in the preparation of polymer actuators and anticorrosive coatings [30], electroactive [28]/conductive [29] to produce high-performance electronics on rubber substrates [31], and to produce surfaces with controlled wettability, for instance with superhydrophilic [22] or anisotropic wetting behavior on tunable surfaces [20, 27].

Several strategies have been successfully employed to produce wrinkled interfaces [32-37] including the formation of a rigid layer on a pre-stretched soft film or the gradient polymerization on hydrogels. In effect, the most extended strategy resorts to the use of soft materials with low elastic modulus that can be easily mechanically stretched/compressed. Upon stretching, a rigid layer is either deposited on top of the surface [28, 38, 39] or created by chemical modification [40, 41]. Finally, upon removal of the mechanical force the rigid layer at the surface buckles and finally forms surface wrinkles. However, this strategy has several drawbacks including the formation of cracks at the surface as a consequence of the different mechanical resistance of the layer deposited compared to the bulk. In addition, even with the recent studies on the formation of multilayers on these structures the chemistry of such surfaces is restrained to particular metals, oxides resulting of surface treatments or particular high modulus polymers.

Interested in this type of surface patterns, other alternatives have been developed in order to improve the above mentioned drawbacks. In these systems, instead of a soft elastic foundation, photopolymerizable monomers are typically employed. Thus, on the one hand, wrinkles have been obtained from confined hydrogels [35, 47-50]. On the other hand, several groups reported the formation of buckling on systems in which the density of crosslinking exhibits a vertical gradient through the film [50, 51].

Even if, up to now, the latter has been employed only with acrylic monomers this method offers novel chemical possibilities that were limited in the previous approaches. Nevertheless, although with great potential this strategy to fabricate wrinkled surfaces still has remaining issues. These include the need of two distinct steps to be carried out, the precision of

the formulation employed that largely affects the final pattern or the presence of residual monomer that must be removed.

In this manuscript, we describe a novel approach to produce wrinkled surfaces. Our strategy relies on the confinement of a phocrosslinkable monomeric mixture between two interfaces with a controlled distance between the two provided by a spacer. We will describe the formation of wrinkled surfaces based on simultaneous heating and UV-irradiation. As will be reported, we employed a mixture of monofunctional (Methyl methacrylate: MMA) and difunctional monomer (Ethylene glycol dimethacrylate: EGDMA) in different proportions to produce wrinkles with variable dimensions. More interestingly, we design the photosensitive mixture to include a variable amount of a functional copolymer additive that will modify the chemical composition of the surface. The functional copolymers employed comprise either hydrophilic moieties (acrylic acid groups: AA) or hydrophobic functional groups (trifluoroethyl methacrylate: TFMA) to produce functional wrinkles with variable chemical composition. The possibility to incorporate polymeric additives offers unique alternatives to chemically fine-tune the interfacial properties of the wrinkled surface. More interestingly, as a proof of concept we will explore the bacterial adhesion of *Staphylococcus aureus* on the functionalized surfaces as a function of the hydrophilicity of the wrinkled interface.

Results and Discussion

The fabrication of the surface wrinkles was carried out using the experimental setup described in Figure 1A. A photosensitive mixture was confined between two glass slides and simultaneously heated and irradiated with UV-light. This specific setup avoids the monomer evaporation (low boiling point of the component employed) thus permitting the use of a large variety of monomers and assures simultaneously that the composition of the final material is identical to the feed composition. Moreover, a planar cover will limit the thickness variations over the sample.

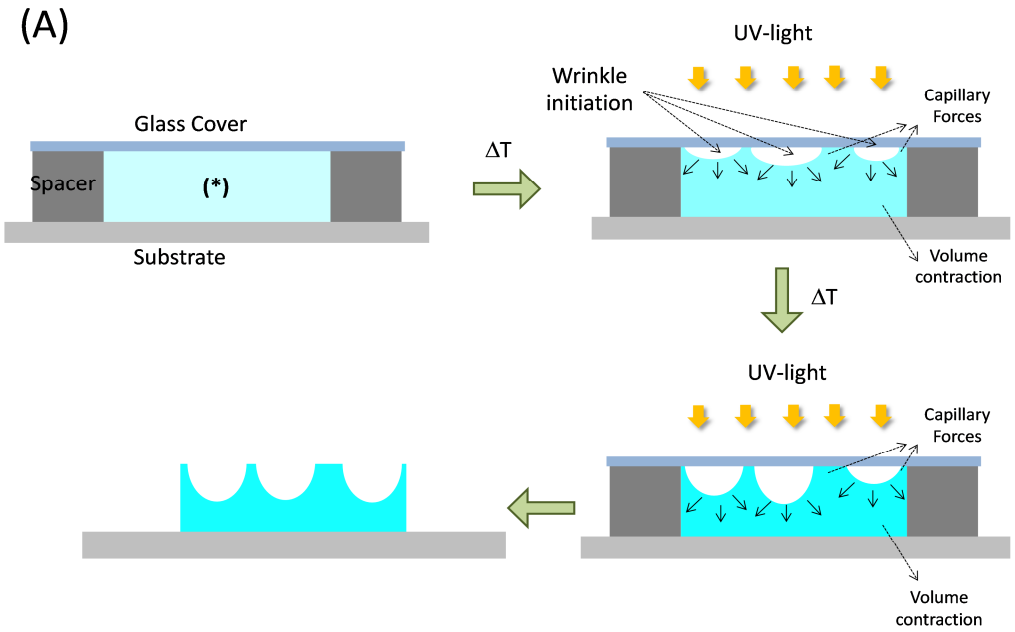
(A)
Glass Cover
Spacer
(*)
Substrate
ΔT
UV-light
Wrinkle initiation
Capillary Forces
Volume contraction
ΔT
UV-light
Capillary Forces
Volume contraction

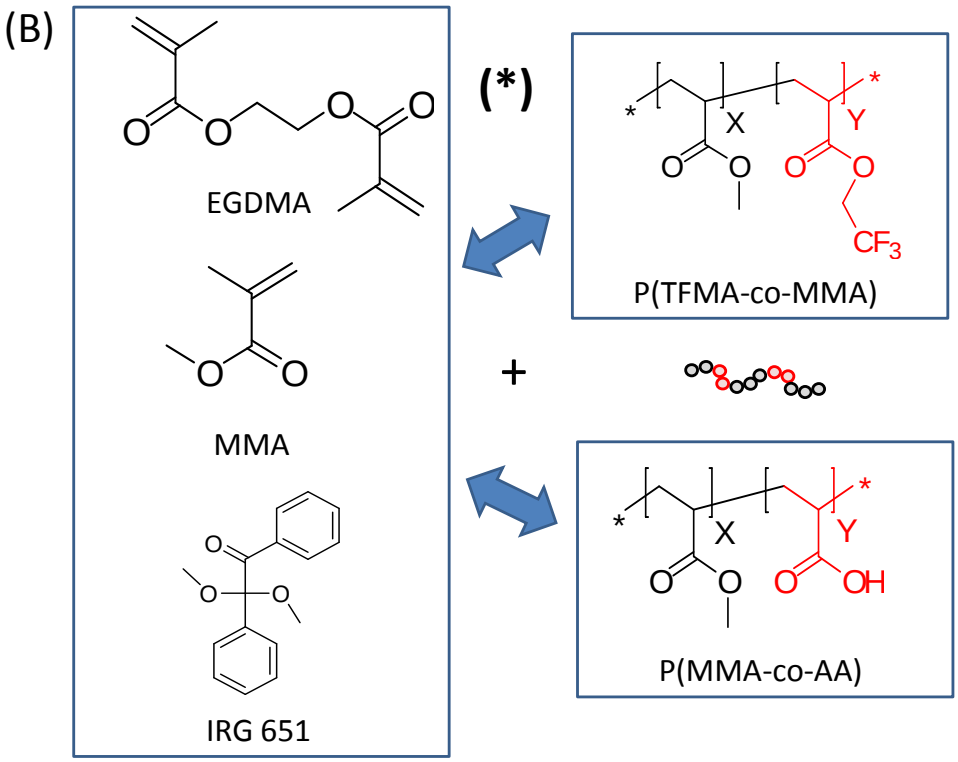
(B)
EGDMA
MMA
IRG 651
(*)
+
P(TFMA-co-MMA)
P(MMA-co-AA)

Figure 1. *a) Schematic illustration of the experimental procedure to fabricate wrinkled surfaces. A confined photosensitive mixture is irradiated and heated at the same time. During this process volume contraction and capillary forces act simultaneously, inducing the formation of wrinkled interfaces; b) Photosensitive mixture employed comprising EGDMA (Ethylene glycol dimethacrylate), MMA (Methyl methacrylate) and IRG651. In addition, the monomer mixture contains either a double hydrophobic copolymer [P(TFMA-co-MMA)] or an amphiphilic copolymer [P(MMA-co-AA)] in order to provide functionality upon surface segregation.*

In particular, the photosensitive mixture employed in this study is composed of a monofunctional monomer (MMA), a crosslinking agent (ethylene glycol dimethacrylate: EGDMA) and a photoinitiator (IRG 651). Initial experiments were conducted using this mixture with variable amounts of MMA and EGDMA to proof the concept. In those experiments, the liquid mixture was irradiated using UV-light able to traverse the cover employed during four minutes of irradiation. It has to be mentioned that, as will be depicted later, wrinkle formation requires simultaneous heating of the photocrosslinkable mixture in order to increase the reaction kinetics.

As depicted in Figure 2, initial experiments were carried out at different temperatures. The 3D optical profiler images show the variation of the surface structure as a function of the temperature employed. In addition, the films resulting of these experiments were characterized by FTIR-ATR (attenuated total reflectance Fourier transform infrared spectroscopy) in order to establish a correlation between the surface patterns observed and the extent of the photocrosslinking reaction. For comparative purposes, also included in Figure 2 are the FTIR-ATR spectra of the homopolymers obtained from MMA (PMMA) and EGDMA (PEGDMA). A particular signal, identified at 812 cm^{-1} relative to residual double bonds of the acrylic functionality ($–CH_2=CH–$ twisting) can be employed to follow the photocrosslinking. In addition, a –C–C– band can be observed at ~840 cm^{-1}.

From the IR (Infrared) spectra of Figure 2 obtained from the films photopolymerized at room temperature a large amount of unreacted double bonds can be easily distinguished.

This clearly indicated that the reaction was not completed in the period of time employed (~4 min). Longer photopolymerization times carried out also at room temperature did not produce the formation of a wrinkled surface in spite of a clear reduction of the residual double bonds due to the photochemical reaction progress. Upon increasing the temperature, the –C=C– signal gradually decreased while the –C–C– band was in comparison larger (observed at ~840 cm^{-1}) for the same reaction time. This indicates both a significant increase of the reaction kinetics and that the crosslinking reaction occurs to a larger extent. By comparison with the 3D profile images of the surfaces we observed that an increase of the reaction temperature up to 80 °C initiates the wrinkle formation whereas at 100 °C the film exhibits a rather regular wrinkled pattern at the surface.

The optimal experimental conditions to obtain a rather homogeneous wrinkle formation were further analyzed by varying both the UV-light intensity employed or the amount of photoinitiator (in this case Irgacure) introduced in the mixture. In the first case a decrease of the light intensity below 50% leaded to the formation of rather irregular wrinkles with some planar surface areas. Using light intensities above 75% produced surfaces with randomly distributed wrinkles homogeneous covered. As an excess of light exposure may not be required, the rest of the experiments were carried out at 75% light intensity.

We equally explored the influence of the photoinitiator concentration on the wrinkle formation. For this purpose, we varied the amount of Irgacure employed between 0.5 and 5 wt% while maintaining 75% of light intensity and a temperature of 100 °C. In this series of experiments we observed that 0.5 wt% of Irgacure provide heterogeneous surfaces with only partial formation of wrinkles. An increasing amount of Irgacure was then added in following samples and the results indicated that the minimum amount of Irgacure required to produced homogeneous wrinkles was 2 wt%. Larger amounts of photoinitiator also produced wrinkled surface. However, herein for the following experiments we employed 2 wt% in order to prepare the functional microwrinkled films.

Thus, the formation of wrinkled surface requires fast reactions. According to our experiments we can propose the mechanism of formation shown in Figure 1A. Before the

photopolymerization started, the volume comprised between the substrate and the glass cover was filled by the monomer mixture. When the photopolymerization starts, an initial wrinkle formation appears as a consequence of the volume contraction forming cavities while the rest of the film due to capillarity remains in contact with the glass cover. The polymerization continues and the volume contraction induces the enlargement of the cavities. As a result of this process, the cavities interconnect before the completion of the reaction and produce a completely wrinkled film.

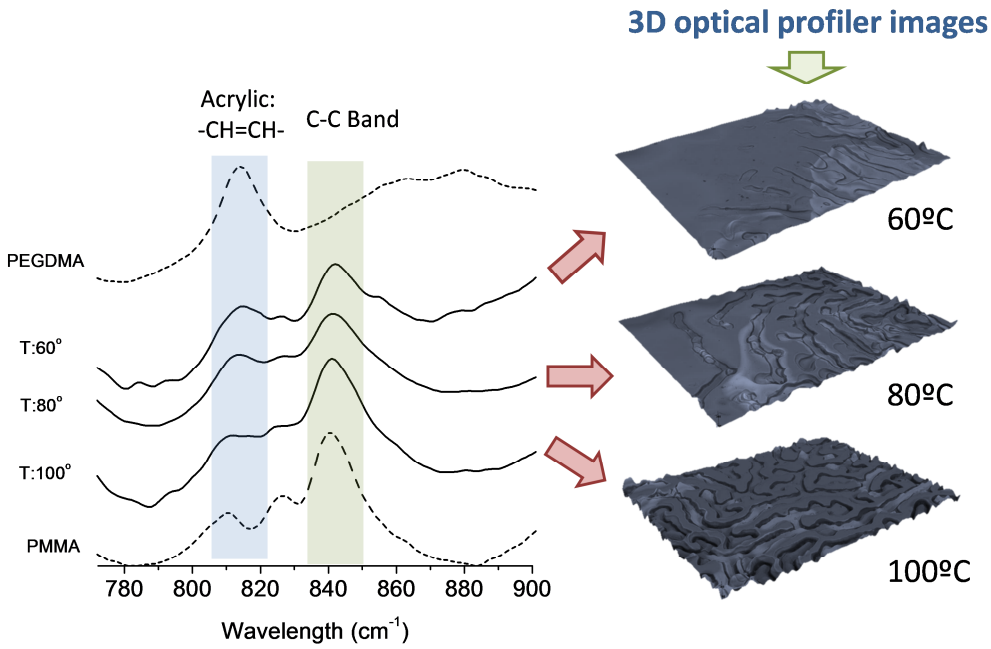

Figure 2. *FTIR-ATR spectra of the crosslinked films obtained by simultaneous heating and UV irradiation of the monomer mixture and the resulting 3D images of the surface patterns formed by photocrosslinking. The photosensitive mixture employed was MMA/EGDMA (85/15) v/v% and 2 wt% of IRG 651. The irradiation experiments were carried out at three different temperatures: 60, 80 and 100 °C, using a spacer of 50 μm.*

The approach illustrated in Figure 1A, has been later employed with photosensitive mixtures containing functional copolymers as additives with the aim of producing

simultaneously microstructured and functional surfaces in the polymer blends. In particular, we have explored two different additives, a double hydrophobic copolymer: P(TFMA-*co*-MMA) or an amphiphilic copolymer: P(MMA-*co*-AA).

As depicted above, wrinkle formation largely relies on the experimental conditions employed for the film preparation. In order to get further insight into the role of the latter on the formation of structured surfaces, preliminary studies were carried out without adding the copolymer. On the one hand, film thickness can be controlled by the spacer that is employed. On the other hand, the relative composition of MMA/EGDMA of the photosensitive mixture on the final surface morphology was then analyzed. From these initial experiments we found that the formation of wrinkles for a particular spacer (50 μm) was observed in samples with monomer composition with at least 5 *v*/*v*% of EGDMA. The volume contraction is rather low in the sample having only 1*v*/*v*% and appears to be insufficient to initiate the nucleation process. However, samples containing both 5 and 15 *v*/*v*% of EGDMA produce wrinkled interfaces. In addition, whereas the monomer composition for a particular thickness does not appeared to influence the pattern dimensions, variations on the spacer play an important role. An increasing spacer leads to larger average wrinkle periods. For either, 100 μm spacers or 150 μm spacers average wrinkle dimensions between 460 and 580 μm and above 670 μm were obtained respectively. Within this context we selected the use of 50 μm spacer with a relative ratio MMA/EGDMA of 85/15 *v*/*v*%.

As an illustrative example, in Figure 3 is depicted the optical profiler images on the surfaces prepared incorporating 2, 5, 10 and 20 wt% of functional copolymer within the photosensitive mixture. Remaining in this range of copolymer employed (2–20 wt%), the wrinkle periodicity remains in a region between 280 and 360 μm whereas to height varies between 7 and 14 μm.

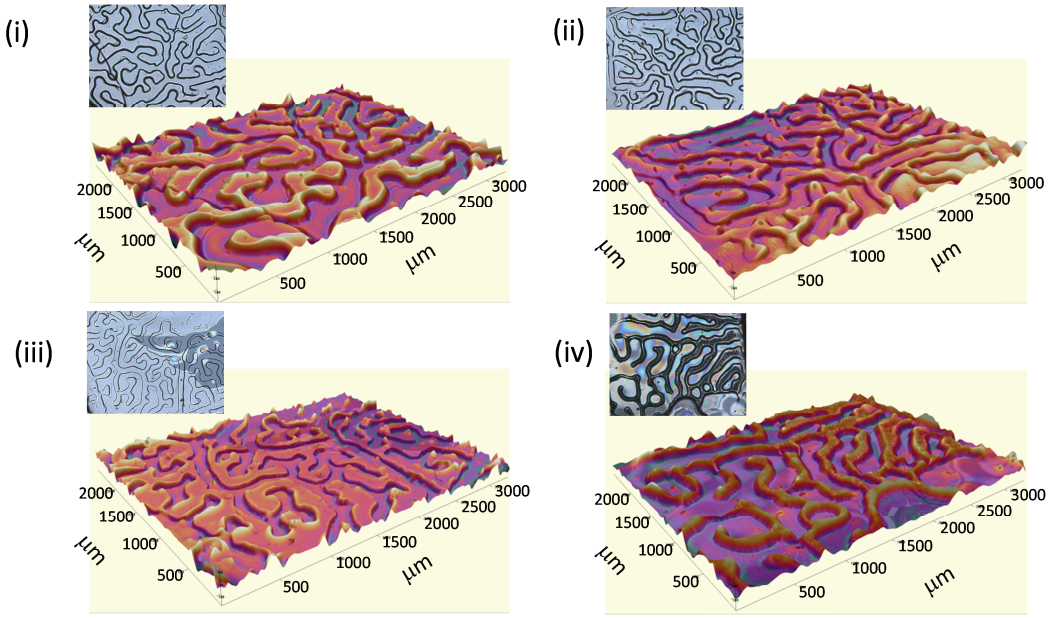

Figure 3. *3D images of the wrinkled surfaces prepared form blends having* ***(i)*** *2,* ***(ii)*** *5,* ***(iii)*** *10, and* ***(iv)*** *20 wt% of copolymer P(TFMA-co-MMA). Inset: Optical images of the surfaces.*

Wettability of the Functional Wrinkled Surfaces

Thus, in principle, the incorporation of functional copolymer did not alter the wrinkle formation. However, as they are designed with either hydrophobic or hydrophilic functional groups the surface wettability should be affected. The contact angle of the wrinkled surface prepared using either the hydrophilic or the hydrophobic copolymers as additive are depicted in Figure 4.

In addition, in Figures 4 the values obtained by using the Wenzel state model are equally plotted (see supporting information of further details). The Wenzel model assumes a complete wetting when a drop is placed on a rough surface. The model is represented by Equations (1) where θ_i is the ideal contact angle on a flat surface, *r* is the roughness factor defined as the ratio of actual surface area divided by the projected area [44]:

$$\cos\theta_w = r \cdot \cos\theta_i \quad (1)$$

The incorporation of P(MMA-*co*-AA) increased the surface wettability of the films, and the decrease of the measured contact angle is directly related to the amount of copolymer incorporated in the photosensitive mixture. On the contrary, hydrophobic trifluoro-functional groups decreased the surface wettability and provided contact angles above 90°. In addition, in Figure 4 are included the contact angle values measured for both flat surfaces obtained by spin coating. Independently of the surface structure, the tendency exhibited is similar. Thus, surfaces prepared with the acrylic acid (AA) containing copolymer decreased the contact angle values while the copolymer having trifluoroethyl methacrylate (TFMA) units increased the hydrophobicity of the surface. Nevertheless, significant differences were observed between the samples with or without wrinkles. Wrinkled interfaces appeared to enlarge the tendency observed for flat surfaces. Thus, whereas the planar surfaces prepared with P(MMA-*co*-AA) as additive slightly decreased the contact angles down to ~75°, the wrinkled surfaces reduced the measured contact angles up to ~55°. On the contrary, the incorporation of the fluorinated additive significantly reduced the surface wettability. Whereas in the flat films a slight increase of the contact angle from ~72° to ~78° was observed, the structuration further improved the hydrophobicity of the interface. By incorporation of 20 wt% of copolymer the contact angle increased from ~78° observed in flat films and up to ~92° measured in the wrinkled surfaces with the same composition.

More interestingly, as observed in Figure 4 the values obtained for the wrinkled surfaces independently of the chemical composition are in good agreement with the contact angle values calculated by using the Wenzel model. This wetting model allows us to affirm that the surface is wetted both on top and at the bottom of the wrinkles.

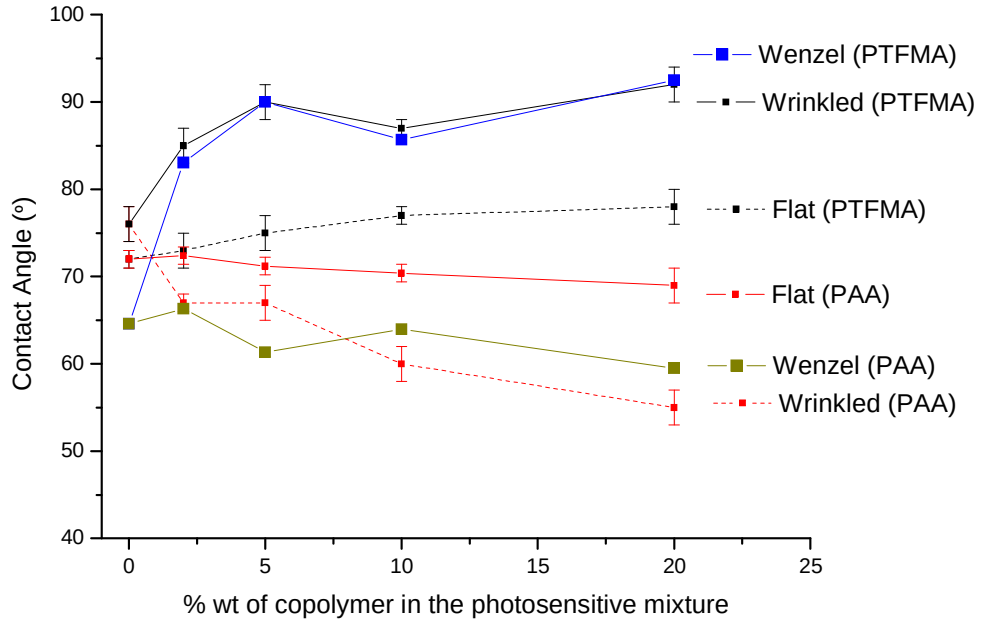

Figure 4. *Variation of the contact angle as a function of the wt% of functional copolymer incorporated within the photosensitive mixture. Whereas PAA refers to the copolymer P(MMA-co-AA) introduced, PTFMA refers to the P(TFMA-co-MMA). Flat refers to planar surfaces, wrinkled to the surfaces with wrinkled interfaces and Wenzel to the contact angle values calculated using the Wenzel model.*

As described above, the setup of the wrinkle fabrication requires a cover in order both to prevent monomer evaporation during the irradiation step and simultaneously to avoid film irregularities. However, the hydrophilicity of the glass cover significantly affects the interfacial migration of the additive and therefore the contact angle observed. The contact angle values measured for wrinkled interfaces prepared using a hydrophilic glass cover and a silanized (hydrophobic) glass cover and blends with the hydrophobic additive P(TFMA-*co*-MMA) are represented in Figure 5. As expected, the contact angle values observed for the wrinkled interfaces prepared using a silanized glass cover are higher than those measured for wrinkled surfaces prepared using a hydrophilic cover. As illustrated in Figure 5, before the film rigidifies

as a consequence of the crosslinking reaction the additive with a larger affinity by the hydrophobic silanized cover migrates towards this surface and enriched the interface in fluorinated copolymer.

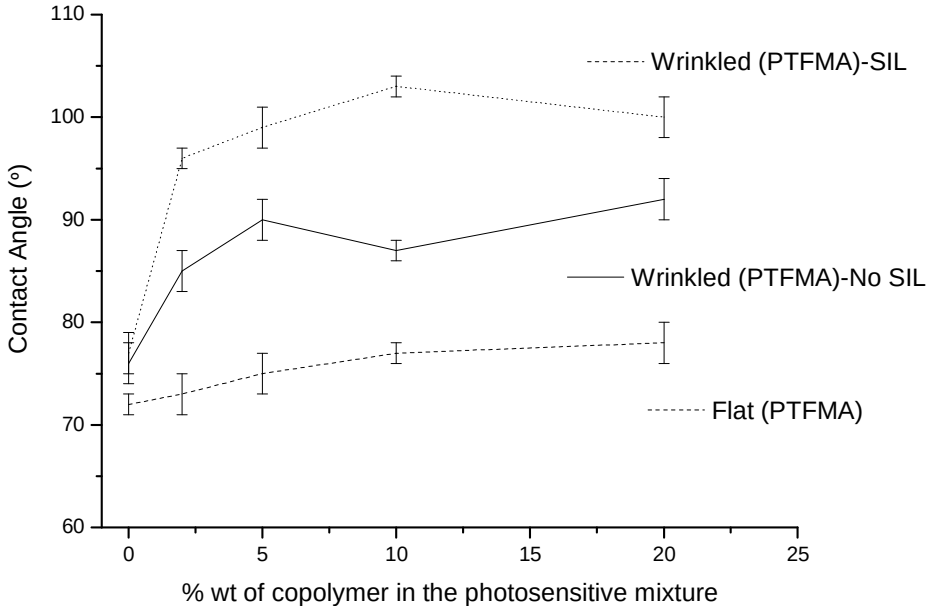

Figure 5. *Variation of the contact angle as a function of the wt% of P(TFMA-co-MMA) copolymer incorporated within the photosensitive mixture prepared using either silanized glass covers (SIL) or cleaned glass covers (No SIL).*

Bacterial Assays on the Functional and Wrinkled Surfaces

As demonstrated above both the formation of a wrinkled surface and the presence of either hydrophilic or hydrophobic functional groups at the interface as a result of the segregation of the functional copolymer affected the surface wettability. The hydrophilicity/hydrophobicity of polymer surfaces is related with the final application of the material. Herein, as a proof of concept we explored the bacterial adhesion onto these wrinkled surfaces depending on the surface chemical composition. For that purpose, we incubated *S.*

aureus onto wrinkled surfaces prepared using two different glass covers and formed form blends of either the hydrophilic or the hydrophobic copolymer.

On the one hand, we prepared wrinkled surfaces from blends having 20 wt% of P(MMA-*co*-AA) copolymer using a hydrophilic cover (cleaned using Ultraviolet Ozone (UVO) treatments). The hydrophilic interface will induce the segregation of the hydrophilic PAA groups towards the interface. On the other hand, blends of the photosensitive monomers and 20 wt% of P(MMA-*co*-TFMA) were prepared using a silanized glass cover. In this case the fluorinated groups of the copolymer are expected to migrate to the polymer/glass interface.

Bacterial attachment is directly related, at least during the early stages, with the hydrophilicity and structure of the contact surface. In general, hydrophilic surfaces enhance the affinity of bacteria for these surfaces and favor the bacterial immobilization, whereas hydrophobic interfaces repel the adhesion of microorganisms. Based on this initial hypothesis we explored the immobilization of *S. aureus* labelled with green fluorescent protein that allowed for their detection using fluorescence microscopy in both hydrophilic and hydrophobic surfaces upon 1 h of incubation. The resulting bright field and fluorescence images are depicted in Figure 6. More precisely we explored the bacterial adhesion onto wrinkled surfaces prepared using the hydrophobic copolymer (i and ii) and the amphiphilic copolymer (iii and iv) using either a silanized cover (ii and iv) or a hydrophilic (UVO cleaned) cover (i and iii). As anticipated, independently of the copolymer employed, the surfaces prepared using the hydrophobic copolymer and a silanized interface did not exhibit bacterial adhesion upon 1 h of incubation. In the case of the wrinkles prepared using P(MMA-*co*-TFMA) the presence of trifluoro-groups prevented the attachment of *S. aureus* on the surface (Figure 6i). In the case of P(MMA-*co*-AA), the hydrophilic groups are depleted from the surfaces in order to reduce the thermodynamically unfavorable contact with the hydrophobic cover (Figure 6iii). As a result, the surface chemical composition is mainly composed of PMMA that appears (at least under the experimental conditions employed) to avoid bacterial adhesion. Similar behavior was observed in those wrinkled films prepared using P(MMA-*co*-AA) and a cleaned (hydrophilic) cover (Figure 6ii). In this case, the hydrophobic groups of the TFMA units may direct the

migration of the additive towards the bulk of the film. Thus, the surface may have similar surface composition as the previous case.

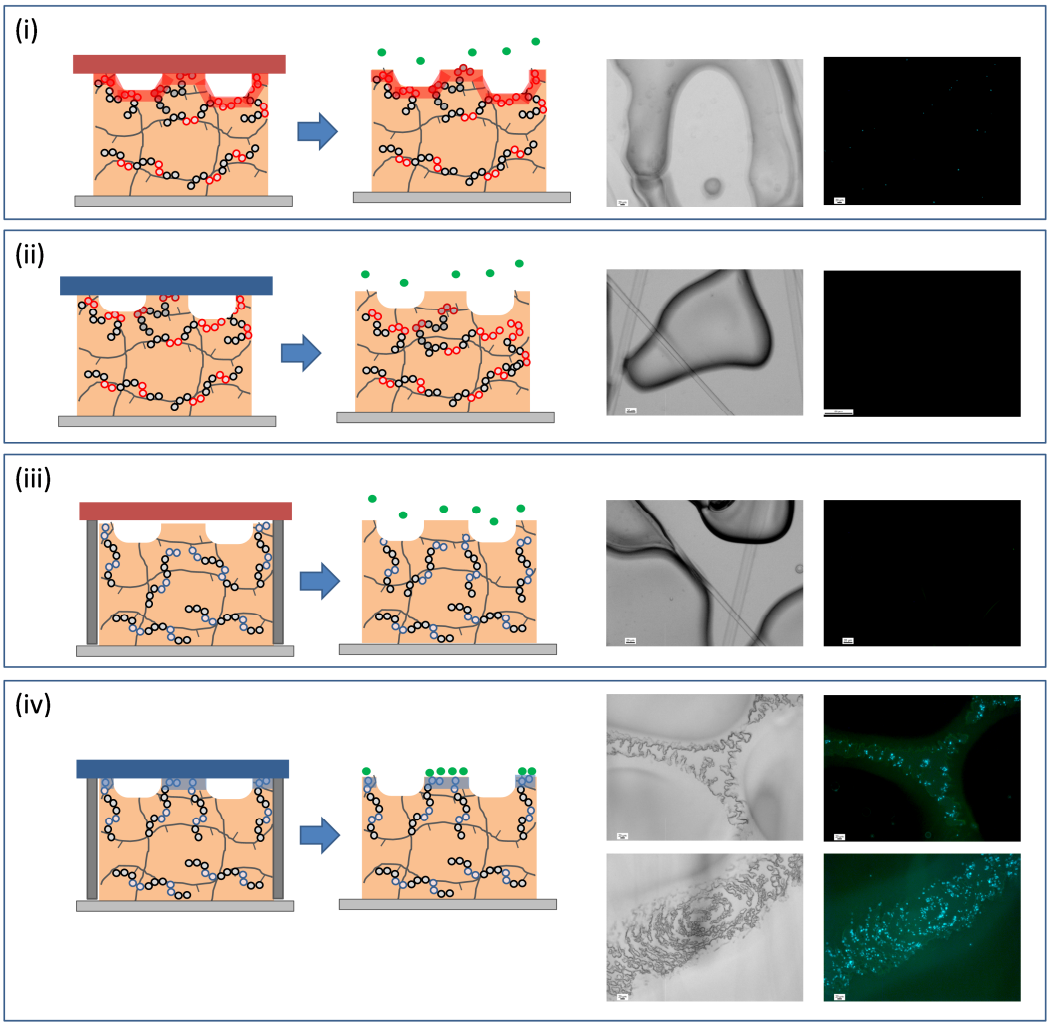

Figure 6. *Immobilization of S. aureus onto wrinkled surfaces with the copolymers either P(MMA-co-TFMA) (**i** and **ii**) or P(MMA-co-AA) (**iii** and **iv**). Wrinkled surfaces with P(MMA-co-TFMA) were prepared using either a hydrophobic (silanized glass covers: SIL) **(i)** or a hydrophilic cover (cleaned glass covers: No SIL) **(ii).** Equally, wrinkled surfaces with P(MMA-co-AA) were prepared using either a hydrophobic **(iii)** or a hydrophilic cover **(iv)**.*

The wrinkled surfaces prepared by using the hydrophilic copolymer and a cleaned glass cover exhibit a different behavior (Figure 6iv). In this case, bacterial attachment occurs as demonstrated by the presence of fluorescent dots in the fluorescent images. More interestingly, the bacterial adhesion did not occur homogeneously on the surface. This bacterial immobilization occurs on top of the wrinkles that correspond to those areas where the films are in contact with the glass cover. In these areas, the hydrophilic glass cover directs the surface enrichment in copolymer and forms rather hydrophilic areas.

On the contrary, those areas forming the valley of the wrinkles did not exhibit any bacterial adhesion. In this case, the hydrophilic glass interface remains apart and the polymer is in contact to vacuum/air present and the hydrophilic functional groups of the copolymer remain embedded within the material. In summary, the presence of different functional groups at the wrinkle interface produces materials with either antifouling/adhesive properties towards bacteria.

Materials and Methods

Methyl methacrylate (MMA) (Aldrich, St. Louis, MO, USA 99%) was washed three times with a basic aqueous solution (10% NaOH) and then washed three times with water. Then, the resulting monomer was dried on anhydrous magnesium sulfate, filtered and distilled. Ethylene glycol dimethacrylate (EGDMA) (Aldrich 99%), Irgacure 651 (IRG 651: 2,2-dimethoxy-1,2-diphenylethan-1-one) (Ciba, basel, Switzeland), dichlorodimethylsilane (Aldrich 98.5%) *tert*-Butyl acrylate (tBuA), 2,2,2-trifluoroethyl methacrylate (TFMA) (Aldrich 99%), *N*,*N*,*N*',*N*'',*N*''-pentamethyldiethylenetriamine (PMDETA) (Aldrich, 99%), copper(I) bromide (CuBr) (Aldrich 98%), ethyl-2-bromoisobutyrate (EBrIB) and the rest of solvents were employed as received without further purification. Silicon wafers (Siegert Consulting e.k., Aachen, Germany) and 0.15 mm thickness glass covers (Menzel-Glaser, Braunschweig, Germany) were employed as supports.

Infrared spectra were obtained using a Spectrum One FT-IR (Fourier transform infrared) spectrometer (Perkin-Elmer, Waltham, MA, USA) fitted with an attenuated total

reflectance (ATR) accessory under unforced conditions. The irradiated samples were placed in direct contact with the diamond crystal with no previous preparation. Measurements were collected at 8 cm^{-1} resolution and co-adding 6 scans per spectrum.

Water contact angles (CA) were measured using a KSV Theta goniometer from Attension (Stockholm, Sweden). The volume of the droplets was controlled to be approximately 2.0 μL and a charge coupled device camera was used to capture the images of the water droplets for the determination of the contact angles. In addition to the measured contact angles, the predicted contact angle values were calculated using the Wenzel model [45]:

$$\cos\theta_w = r \cdot \cos\theta_y \quad (2)$$

where r is the roughness ratio calculated from the expression:

$$r = 1 + S_{dr}/100 \quad (3)$$

S_{dr} (area factor) corresponds to the ratio between the interfacial and the projected areas and was directly obtained from the 3D Optical profiler software.

Scanning electron microscopy (SEM) was used for surface structural and cross-sectional analysis. Micrographs were taken using a Philips XL30 (Amsterdam, The Netherlands) with an acceleration voltage of 25 kV. The samples were coated with gold-palladium (80/20) prior to scanning.

Cross sectional profiles and 3D images of the wrinkled surfaces were achieved by using a Zeta-20 True Color 3D Optical Profiler from Zeta Instruments (San Jose, CA, USA).

Synthesis of the Copolymers

- *Poly(methyl methacrylate-co-2,2,2-trifluoroethyl methacrylate)*

A random copolymer of poly(methyl methacrylate-*co*-2,2,2-trifluoroethyl methacrylate) (P(MMA_{77}-*co*-$TFMA_{23}$)) (*i.e.*, 77 mol% of MMA and 23 mol% of TFMA) was synthesized by Atom Transfer Radical Polymerization (ATRP) in order to obtain low polydispersity and controlled chain length. The polymerization was performed in *Schlenk* flasks previously flamed and dried under vacuum. It was carried out using the following stoichiometry [M1]/[M2]/[I]/[CuBr]/[L] = 48:12:1:1:1, where M1 = MMA, M2 = TFMA, I = EBrIB, L = PMDETA in toluene. The reaction mixture was degassed by three-pump-thaw cycles and placed in a thermostatic oil bath at 90 °C; after the polymerization, the mixtures were cooled to room temperature; the contents were diluted with dichloromethane and passed through a neutral alumina column to remove the copper salt. After removing the solvent, the polymers were precipitated in hexane, washed and dried under vacuum. (M_n: 11,318 g/mol; Polydispersity (PD): 1.10).

- *Poly(methyl methacrylate-co-acrylic acid)*

Preparation of the copolymer poly(methyl methacrylate-*co*-acrylic acid) ($PMMA_{80}$-*co*-PAA_{20}). The polymerization was performed in *Schlenk* flasks previously flamed and dried under vacuum. ATRP was carried out using the following stoichiometry [M_t]/[I]/[CuBr]/[L] = 100:1:1:1 where M_t = M1 + M2; M1 = MMA, M2 = tBuA, I = Initiator (EBrIB), L = Ligand (PMDETA) in toluene. The reactants were added under N_2. The reaction mixture was degassed by three-pump-thaw cycles and placed in a thermostatic oil bath at 65 °C. After the polymerization, the mixture were cooled to room temperature, diluted with dichloromethane and passed through a neutral alumina column to remove the copper salt. After removing the solvent, the polymers were precipitated in cold hexane, washed and dried under vacuum. Finally, the *tert*-butyl groups were hydrolyzed to afford the carboxylic acid functional groups. For this purpose, the copolymers were first dissolved in dichloromethane (CH_2Cl_2). Trifluoroacetic acid (TFA) was then added (20 equivalents to *t*-butyl ester units), and the

mixture was stirred at room temperature for two days. The deprotected polymers precipitated in the reaction media and were filtered, washed with CH_2Cl_2, and finally dried under vacuum. (Mn: 8123 g/mol; PD: 1.25)

Methodology to Prepare the Wrinkles

Photosensitive mixtures were obtained from variable monomeric mixtures of a crosslinking agent, ethylene glycol dimethacrylate (EGDMA), and a linear monomer, methyl methacrylate (MMA). In addition, a radical photoinitiator, IRG 651 (2 wt% respect to the total amount of monomers) was employed to start the polymerization process. IRG 651 has two UV/Vis absorption peaks at 250 and 340 nm. A variable amount of copolymer comprised between 2 and 20 wt% of either P(MMA-*co*-AA) or P(MMA-*co*-FTMA) was added to control the surface chemical composition. To prepare the films, 2 cm × 2 cm silicon wafers with variable spacers (50–150 μm) were employed. A few drops of the photosensitive mixture were placed in the center of the wafer and covered by a glass of 0.30 mm thickness. The samples were preheated and irradiated while the heating was kept constant. The photopolymerization of the films has been done under UV spot light irradiation source using a Hamamatsu model lightning cure L8868 (Hamamatsu, Japan) provided by Hg–Xe lamp with 200 W power. The irradiation intensity was kept constant throughout the experiments and focused on the samples with an optic fiber at a constant distance of 8 cm. The incident light intensity was maintained constant for all experiments at 6150 mW/m^2, measured by a Luzchem radiometer SPR-01 (Ottawa Ontario, Canada) (75% of the lamp capacity). Initial tests were carried out varying the ratio linear monomer *versus* crosslinking agent in order to optimize the wrinkle formation. The samples having additionally functional monomers were prepared using a constant ratio of linear monomers (*i.e.*, both functional monomer and non-functional monomer) and crosslinking agent of 85/15 *v*/*v*%.

For the treatment of the glass covers to obtain hydrophobic surface a silanization process was carried out, where the glass is submerged in a dichlorodimethylsilane solution for one minute. After the treatment, the films were rinsed with a mixture ethanol/water and ethyl

acetate. On the other hand, to obtain a clean hydrophilic surface, the glass covers were exposed to ozone by using a UV-cleaner lamp for 15 min.

Bacterial Immobilization Tests

S. aureus strain RN4220 carrying the plasmid pCN57 for green fluorescent protein (GFP) expression (generous gift from Iñigo Lasa's Laboratory at Instituto de Agrobiotecnología, Universidad Politécnica de Navarra (UPNA-CSIC-Gobierno de Navarra) was grown overnight at 37 °C in Luria-Bertani (LB) media with erythromycin (10 μg/ml). The cells were centrifuged and washed three times in PBS (phosphate buffered saline) buffer (150 mM NaCl, 50 mM Na-phosphate pH 7.4). The solution was adjusted to a cell concentration that corresponds to an optical density (OD) at 600 nm of 1.0 using an UV-VIS Varian (Palo Alto, CA, USA) Cary 50 spectrophotometer.

The different patterned polymeric surfaces were incubated for 1 hour with a bacterial suspension at OD = 1.0 in PBS buffer with 0.05% Tween 20. After incubation the surfaces were washed with PBS three times during 15 min.

Bacteria immobilization was monitored by fluorescence microscopy using a Leica (Wetzlar, Germany) DMI-3000-B fluorescence microscope. Images were acquired using ×20 magnification and the corresponding set of filters for imaging green fluorescence and bright field.

Conclusions

In this contribution we described the preparation of wrinkled interfaces based on surface instabilities generated during a photocrosslinking process. In comparison with previously reported procedures, where wrinkles have been obtained upon surface treatment of a particular material (typically PDMS (Polydimethylsiloxane)) or by gradual crosslinking of polymer gels, wrinkled interfaces were obtained by confining a photosensitive monomeric mixture composed of monofunctional monomer and a crosslinking agent within a substrate and a cover. We described how, by using this approach, the wrinkle characteristics can be

controlled by the monomer mixture, the spacer employed or the temperature of the photopolymerization.

More interestingly, the designed fabrication approach allowed, by blending, the incorporation within the material of a functional copolymer that permitted the variation of the surface chemical composition while maintaining the surface structure. For that purpose we incorporated either a fluorinated copolymer that enhanced the surface hydrophobicity of the wrinkled interface, or an acrylic acid containing copolymer that increased the hydrophilicity of the wrinkled surface.

In view of the application of such structured interfaces, we evaluated the role of the surface chemistry depending on the functional copolymer employed and the hydrophobicity of the interface on the bacterial adhesion using *S. aureus*. As a result, for the conditions employed the wrinkled surfaces prepared using fluorinated copolymer behave as anti-adhesive surfaces whereas the surfaces prepared with the hydrophilic copolymer promote the bacterial adhesion in those areas where the film is in contact with the glass cover. Moreover, as the surface chemistry depends on the environment of exposure, the proposed wrinkled surfaces are excellent candidates to design materials with tunable surface properties.

Acknowledgements

The authors gratefully acknowledge support from the Agencia Estatal Consejo Superior de Investigaciones Científicas (CSIC). Equally, this work was financially supported by the Ministerio de Economia y Competitividad (MINECO) through MAT2011-22861, MAT2013-47902-C2-1-R and MAT2009-12251. Marta Palacios-Cuesta thanks the Ministerio de Education for the FPU fellowship.

Author Contributions

Marta Palacios-Cuesta, Olga García and Juan Rodríguez-Hernández are experts in the surface structuration and functionalization of polymeric surfaces. In particular, they have been

involved in the preparation of the wrinkled surfaces by using UV-light and the fabrication of the functional copolymers employed as additives.

Aitziber L. Cortajarena has been involved in the immobilization of bacteria onto the surfaces by optimizing the experimental conditions for this particular system.

CAPÍTULO IV.3: Patente

PROCEDIMIENTO DE OBTENCIÓN DE MATERIALES POLIMÉRICOS CON SUPERFICIES ESTRUCTURADAS, LOS MATERIALES ASÍ OBTENIDOS Y SUS APLICACIONES

Justificante de presentación electrónica de solicitud de patente

Este documento es un justificante de que se ha recibido una solicitud española de patente por vía electrónica, utilizando la conexión segura de la O.E.P.M. Asimismo, se le ha asignado de forma automática un número de solicitud y una fecha de recepción, conforme al artículo 14.3 del Reglamento para la ejecución de la Ley 11/1986, de 20 de marzo, de Patentes. La fecha de presentación de la solicitud de acuerdo con el art. 22 de la Ley de Patentes, le será comunicada posteriormente.

Número de solicitud:	P201231928
Fecha de recepción:	12 diciembre 2012, 11:52 (CET)
Oficina receptora:	OEPM Madrid
Su referencia:	648
Solicitante:	CONSEJO SUPERIOR DE INVESTIGACIONES CIENTÍFICAS (CSIC)

RESUMEN

Se describe un procedimiento para la obtención de superficies estructuradas mediante la formación controlada de arrugas de dimensiones variables. El método se basa en la irradiación con luz y calentamiento simultáneo de una disolución fotosensible. La obtención de las estructuras superficiales se lleva a cabo en pocos minutos. Además, este método permite la incorporación de distintos monómeros funcionales y de copolímeros y/o cargas como aditivos en la mezcla inicial que pueden dotar a la superficie de funcionalidad sin necesidad de etapas adicionales de funcionalización.

TITULO

PROCEDIMIENTO DE OBTENCIÓN DE MATERIALES POLIMÉRICOS CON SUPERFICIES ESTRUCTURADAS, LOS MATERIALES ASÍ OBTENIDOS Y SUS APLICACIONES

SECTOR DE LA TÉCNICA

La presente invención puede ser aplicada a diversos campos que pueden ir desde los recubrimientos de distintos materiales al campo de los biomateriales. Además de controlar la topografía superficial, se pueden obtener superficies químicamente funcionalizadas. Las aplicaciones de este tipo de superficies con mojabilidad controlada incluyen los recubrimientos para cristales, textiles o pinturas autolimpiables y superficies antiadherentes o antibacterianas. También permitiría su utilización en procesos en los que se precisa un control de la adhesión/fricción. En los campos de la optoelectrónica y de la óptica, las superficies con arrugas controladas pueden ser aplicadas en sensores y son potencialmente interesantes para la fabricación de dispositivos delgados y flexibles como transistores y diodos. Asimismo, si las estructuras generadas poseen tamaños entorno a la longitud de onda de la luz se podrían obtener propiedades reflectactes/antireflectantes y, por tanto, podrían ser utilizadas para otras aplicaciones ópticas como paneles solares, lentes o espejos entre otros.

ESTADO DE LA TÉCNICA

Hay numerosas propiedades en los materiales poliméricos como la adhesividad, la mojabilidad o la biocompatibilidad, que dependen casi en exclusiva de su superficie. En ocasiones, por tanto, la adaptación de un material a una determinada aplicación requiere del diseño de su superficie. Así, aparte de las propiedades mecánicas del material, para adaptarlo y adecuarlo a su uso final, se debe considerar a que medio va estar expuesto, es decir, tener en cuenta la interfase. Son dos los factores que juegan un papel fundamental en las propiedades finales de la superficie de un material: la funcionalidad y la estructura.

La primera requiere, normalmente, tratamientos químicos o físicos que modifican la parte más superficial del material. La segunda se realiza mediante distintos métodos de

fabricación que se pueden agrupar en dos grandes familias: Las técnicas "*bottom-up*" y "*top-down*". La combinación de ambos aspectos requiere varias etapas y procesos de larga duración.

La unión estructura y funcionalidad dentro del mismo material requiere, por tanto, la consecución de etapas de funcionalización con etapas de estructuración en procesos, por tanto, multietapa, largos y a menudo costosos.

La formación de arrugas superficiales se han ido desarrollando durante la década pasada (A. Schweikart, A. Fery, *Microchim Acta*, 165, 249, 2009). La gran mayoría de los métodos de formación de arrugas superficiales se basan en la utilización de sistemas bicapa; En las que una de las capas suele ser un material flexible (habitualmente polidimetilsiloxano (PDMS)) y sobre ésta, se deposita una delgada capa de un material más rígido (película metálica, capa inorgánica o polimérica) que como requerimiento inicial debe poseer un módulo de Young mucho más grande que el del PDMS. El primer método descrito consistió en la evaporación de aluminio sobre el material flexible. La cobertura de metal se realiza sobre las películas poliméricas de PDMS una vez expandidas térmicamente, que, al volverse a enfriar a temperatura ambiente, se contraen formando arrugas en la capa superior metálica.

Otro método empleado para la obtención de esta capa superior rígida es mediante la oxidación de la propia película de PDMS (con corriente de UV-ozono o con plasma). Para llevar a cabo este procedimiento se utilizan máquinas de estiramiento mecánico para las películas de PDMS en vez de hacerlo térmicamente. Aunque este método tiene la ventaja de utilizar un único material y no necesita la utilización de metales, la capa superior tiene la limitación de ser muy frágil, por lo que estas muestras sufren frecuentemente craqueos.

La utilización como capa rígida de coberturas de carácter polimérico es posterior. Se han descrito sistemas como poliestireno sobre PDMS expandido o multicapas de polielectrolitos con el módulo de Young muy superior al PDMS. Dependiendo de cada método, se pueden crear microestructuras de arrugas superficiales que van desde los 150 nm hasta los cientos de micras.

La complejidad de estas metodologías y la necesidad de utilizar soportes flexibles han limitado, en gran medida, su desarrollo industrial. Hasta ahora, sólo dos grupos de

investigación han publicado recientemente la preparación de arrugas mediante la utilización de reacciones de fotopolimerización para dos sistemas concretos y utilizando montajes experimentales muy diferentes al descrito en esta patente.

El primero de los métodos descritos, consiste en la irradiación UV en dos pasos de una mezcla de acrilatos, (R. Schubert, T. Scherzer, M. Hinkefuss, B. Marquardt, J. Vogel, M. R. Buchmeiser, *Surf. Coat. Technol.*, 203, 1844, 2009) donde, en primer lugar, se irradia con una lámpara de excímero, luz monocromática de Xenón (<230 nm) con baja penetración en acrilatos (<500 nm), que polimeriza sólo la capa superior de la disolución fotosensible. Esta capa polimeriza gradualmente a lo largo de su espesor y queda flotando sobre las capas inferiores, en disolución, aún no polimerizadas. De esta manera consiguen formar las arrugas superficialmente. Para congelar este cambio estructural se realiza una segunda irradiación con una lámpara de mercurio, con mayor poder de penetración, que acaba polimerizando la totalidad de la película en todo su espesor.

El segundo método descrito, desarrollado por J. Crosby y colaboradores, plantea la creación de arrugas a partir de la irradiación UV de disoluciones acrílicas, de mezclas de monómeros acrílicos mono- y poli-funcionales, sometidas superficialmente a una corriente de oxígeno controlada (D. Chandra, A. J. Crosby, *Adv. Mater.*, 23, 3441, 2011). En este caso, el proceso de fotopolimerización se ve impedido en las capas superiores puesto que los radicales iniciadores se quenchean por el oxígeno y la polimerización en esta capa más superficial no ocurre. Por otro lado, el resto de la mezcla no curada superficialmente es capaz de hinchar la película inferior generando tensiones que provocan la generación de las arrugas en la película. Éste método tiene la desventaja principal de que, aunque se produce en un sólo paso, son necesarios 20 minutos tras la irradiación para que se produzca el hinchamiento de las capas inferiores por parte de la disolución no polimerizada. Además, presenta el inconveniente de que el monómero sin polimerizar quedaría dentro de la película final, con los consiguientes problemas de reactividad o de segregación al exterior, haciendo que este tipo de materiales que no están totalmente polimerizados presenten serios problemas para su aplicación en cierto tipo de usos, por ejemplo, en aplicaciones de tipo biológico o medioambiental (debido a problemas de toxicidad).

DESCRIPCIÓN DE LA INVENCIÓN

La presente invención se basa en que los inventores han observado que es posible la obtención de materiales poliméricos con superficies estructuradas mediante la formación de arrugas superficiales partiendo de disoluciones fotosensibles formadas por mezclas de monónomero/s, entrecruzante, y fotoiniciador en una cavidad cerrada y aplicando una etapa de calentamiento simultánea a la irradiación UV como sistema fotopolimerizador, aunque también se puede llevar a cabo una etapa previa de calentamiento. Son materiales reticulados, es decir, con una alta estabilidad térmica y química.

Las arrugas se producen superficialmente durante la reacción de fotopolimerización y su tamaño (tanto la anchura como la profundidad) puede ser controlado variando factores externos como el porcentaje de monómero entrecruzante añadido (donde se pueden obtener arrugas con anchuras que van desde las 100 hasta las 720 micras) o variando el tamaño del espaciador empleado y, por lo tanto, el espesor de la película fotosensible irradiada (obteniéndose arrugas con anchuras que van desde las 100 hasta las 720 micras y con profundidades variables de 4 a 15 micras).

A diferencia de los anteriores procedimientos descritos, el procedimiento de la invención parte de disoluciones monoméricas fotosensibles, se ha comprobado que aparte de los sistemas formados por monómeros acrilícos y metacrílicos se puede extender su uso a monómeros de otra naturaleza como, por ejemplo, los vinílicos (estireno), y se desarrolla en una cavidad cerrada aplicando simultáneamente calor durante el proceso de fotopolimerización. Este procedimiento permite, además, un ahorro de tiempo ya que las arrugas superficiales se producen simultáneamente con la polimerización en pocos minutos. El sistema experimental se desarrolla de un solo paso, en tan solo unos pocos minutos y, además, no requiere el empleo de equipos complejos o de alto precio.

A esto se añade el hecho de que estos monómeros pueden incluir alguna funcionalidad o incluso es posible incorporar otros componentes en la disolución fotosensible de partida que modifique las propiedades superficiales de la película final. Teniendo en cuenta todas estas consideraciones, las aplicaciones potenciales de este nuevo método son numerosas.

Además de lo mencionado anteriormente, presenta otras ventajas que incluyen la posibilidad de obtención de dibujos superficiales desde 100 µm hasta centenas de micras y que optimizan los problemas asociados al empleo de otras metodologías de estructuración superficial convencionales, como es la fotolitografía, para conseguir la estructuración de grandes áreas.

Así, un objeto de la invención lo constituye un procedimiento de obtención de materiales con superficies estructuradas con arrugas, en adelante procedimiento de la invención, caracterizado porque comprende las siguientes etapas:

a) preparación de una disolución fotosensible en una cámara cerrada con una cubierta superior transparente que permita la irradiación, y

b) calentamiento e irradiación con luz simultáneas de dicha disolución.

Un objeto de la invención lo constituye el procedimiento de la invención donde la preparación de la disolución de a) se lleva a cabo de la siguiente manera:

i. Colocación de un espaciador sobre un soporte (tapa inferior), donde el soporte puede ser un soporte rígido como un vidrio o un sustrato de silicio así como una superficie flexible, mientras que el espaciador puede ser de espesor variable en función de las necesidades de anchura del material a obtener y para la tapa superior se puede utilizar cualquier material que deje pasar la luz, como por ejemplo un vidrio (Figura 1).
ii. Vertido sobre el soporte de a) de la disolución fotosensible en la cámara formada,
iii. Colocación de una tapa superior sobre la disolución, y
iv. Fijación de las tapas con algún sistema de presión para mantener la dimensionalidad (Figura 1) y la estanqueidad del sistema.

Durante la reacción de fotopolimerización de la lámina se producen las arrugas superficiales. Transcurrida la fotopolimerización (4-6 minutos para los sistemas concretos utilizados para asegurarse de una polimerización total) se retira el vidrio superior.

Otro objeto particular lo constituye el procedimiento de la invención donde la irradiación del sistema con luz ultravioleta se realiza durante un tiempo comprendido entre 5 segundos y 10 minutos, preferentemente entre 4 minutos y 6 minutos.

Otro objeto particular lo constituye el procedimiento de la invención donde se incluye un precalentamiento previo al proceso de irradiación y calentamiento simultáneos. Una realización particular lo constituye el procedimiento de la invención donde la etapa de precalentamiento tiene una duración comprendida entre 0 segundos y 10 minutos, preferentemente entre 30 segundos y 60 segundos.

La disolución fotosensible de la invención está formada por una mezcla que comprende un monónomero/s fotosensibles, un agente entrecruzante y un fotoiniciador. En un ejemplo de realización particular el fotoiniciador es un compuesto químico capaz de absorber la luz, UV o Visible, y transformarla en energía química generando especies reactivas, radicales libres, que actúan como iniciadores de la polimerización (N. Arsu; *J. Eng. Nat. Sci.*, sigma-1, 1-20, 2006). En los ejemplos de realización se ha utilizado Irgacure 651, pero cualquier otro fotoiniciador capaz de absorber la luz UV o incluso en el visible podría igualmente ser utilizado.

Una realización particular de la invención lo constituye el procedimiento de la invención donde el monómero funcional de la disolución fotosensible pertenece al grupo siguiente, a título ilustrativo y no limitativo: monómeros metacrílicos, acrílicos y vinílicos.

Un objeto particular de la invención lo constituye el procedimiento de la invención donde el agente entrecruzante que se puede utilizar es un monómero con dos (caso del dimetacrilato de etilenglicol (EGDMA)) o más puntos de entrecruzamiento [caso del triacrilato de pentaeritritol (PETA) o del tetraacrilato de pentaeritritol (PETRA)].

Mediante el procedimiento de la invención la anchura y/o la profundidad de la arruga se puede controlar variando el porcentaje de monómero entrecruzante y/o el tamaño del espaciador empleado, donde los tamaños de las anchuras obtenidas están comprendidos entre 100 y 720 micras y las profundidades de las mismas pueden estar comprendidas en el intervalo de 4-15 micras. (Tabla I)

Ya que muchas de las propiedades finales en las superficies poliméricas dependen tanto de la estructuración de la superficie, como de la funcionalización química de ésta, se han utilizado también en las disoluciones fotosensibles de partida monómeros/copolímeros con algún grupo funcional en su estructura que modifique las propiedades químicas superficiales de la película final. Otra realización particular de la invención lo constituye el procedimiento de la invención donde el grupo funcional puede ser tanto de carácter hidrófobo como hidrófilo, creándose, de este modo, un amplio abanico de posibilidades en cuanto a composición se refiere. El control de la composición superficial, es decir de la funcionalidad, permite dotar al material de propiedades adicionales. La funcionalidad puede hacer que materiales químicamente inertes puedan, una vez funcionalizados adecuadamente, ser utilizados como adhesivos, catalizadores, materiales biocompatibles, etc. Además los grupos funcionales pueden servir como punto de anclaje de otras moléculas que pueden tener interés tanto biológico como en otras áreas.

TABLA 1.- *Diferentes tamaños de arrugas superficiales obtenidos para distintas composiciones de monómero y agente entrecruzante. Además se incluyen los espaciadores utilizados para la realización.*

AGENTE ENTRECRUZANTE DIFUNCIONAL (%)	ESPACIADOR (μm)	AMPLITUD DE LA ARRUGA (μm) (media)	PROFUNDIDAD (μm) (media)
15	50	290	11
	100	510	10
	150	690	14
30	100	240	8
	150	720	4
45	150	720	10

Otra realización particular de la invención lo constituye el procedimiento de la invención donde el grupo funcional presenta cargas sólidas en las disoluciones fotosensibles. El término “cargas sólidas” utilizado en la presente invención se refiere a compuestos de distinta naturaleza, por ejemplo, orgánica, inorgánica o metálica, que contienen algún grupo funcional en su estructura o en su superficie y que pueden igualmente modificar la composición química superficial o influir en las propiedades finales del compuesto mejorándolas o creando nuevas propiedades, por ejemplo, térmicas, mecánicas, conductoras, fotosensibles, etc.).

Otro objeto de la invención lo constituye un material estructurado con arrugas superficiales obtenido por el procedimiento de la invención, en adelante material estructurado de la invención.

El procedimiento de la invención permite obtener materiales con superficies con mojabilidad y rugosidad controlada. Este nuevo método de creación de arrugas superficiales es simple y económico.

Por último, otro objeto de la presente invención lo constituye el uso del material estructurado de la invención:

- como recubrimientos para, a título ilustrativo y sin carácter limitativo, cristales, textiles o pinturas autolimpiables y superficies antiadherentes o antibacterianas.
- para procesos en los que se precisa un control de la adhesión/fricción.
- para la fabricación de sensores y de dispositivos delgados y flexibles como transistores y diodos, o
- como material reflectacte/antireflectante, y
- más concretamente, para otras aplicaciones ópticas como paneles solares, lentes o espejos, entre otros.

A lo largo de la descripción y las reivindicaciones, la palabra "comprende" y sus variantes no pretenden excluir otras características técnicas, aditivos, componentes o pasos. Para los expertos en la materia, otros objetos, ventajas y características de la invención se desprenderán en parte de la descripción y en parte de la práctica de la invención. Los siguientes

ejemplos se proporcionan a modo de ilustración, y no se pretende que sean limitativos de la presente invención.

DESCRIPCION DE LAS FIGURAS

Figura 1.- Esquema experimental utilizado para la fabricación de las arrugas superficiales de la invención. Se distingue la etapa 1, o etapa de precalentamiento, donde la muestra se calienta a la temperatura de ebullición del monómero, y la etapa 2, donde se irradia con luz UV, manteniendo esta temperatura constante. **a)** Cubierta de vidrio **b)** Espaciador con espesor variable **c)** Soporte (en este caso oblea de silicio) **d)** Disolución fotosensible, formada por: monómero lineal, monómero entrecruzante, fotoiniciador y carga (en algunos casos), e) Fuente de calor, f) fuente de irradiación UV.

Figura 2.-Micrografía de un material de naturaleza metacrílica obtenido de acuerdo al procedimiento de la invención. Micrografía SEM de las arrugas superficiales formadas a partir de una disolución fotosensible con composición MMA (metacrilato de metilo) : EGDMA (dimetacrilato de etilenglicol) 85:15 v/v% y 2%p en IRG 651 (Irgacure 651) utilizando un espaciador de 50 micras, utilizando calentamiento e irradiación de manera simultánea.

Figura 3.- Micrografía de un material de naturaleza metacrílica obtenido de acuerdo al procedimiento de la invención. a) Micrografía SEM (microscopía electrónica de barrido) de las arrugas superficiales formadas a partir de una disolución fotosensible con composición MMA:EGDMA 85:15 v/v% y 2%p en IRG 651 utilizando un espaciador de 50 micras. **b)** Micrografía SEM de la sección donde se aprecia la profundidad de las arrugas superficiales.

Figura 4.- Micrografía de un material de naturaleza no metacrílica obtenido de acuerdo al procedimiento de la invención. a) Micrografía SEM de las arrugas superficiales formadas a partir de una disolución fotosensible con composición PS: DVB 85:15 v/v% y 2%p en IRG 651 utilizando un espaciador de 50 micras. **b)** Micrografía SEM de la sección donde se aprecia la profundidad de las arrugas superficiales.

Figura 5.- Micrografía de un material de naturaleza metacrílica con cargas integradas obtenido de acuerdo al procedimiento de la invención. a) Micrografía SEM de las arrugas superficiales formadas a partir de una disolución fotosensible con composición MMA:EGDMA 85:15 v/v%, 10%p de copolímero PMMA-co-PTFMA (poli(metacrilato de metilo)-co-(polimetacrilato de 2,2,2,-trifluorometilo)) y 2%p en IRG 651 utilizando un espaciador de 50 micras. **b)** Micrografía SEM de la sección donde se aprecia la profundidad de las arrugas superficiales.

Figura 6.- Micrografía de un material de naturaleza metacrílica con funcionalidades obtenido de acuerdo al procedimiento de la invención. a) Micrografía SEM de las arrugas superficiales formadas con una disolución fotosensible con composición TFMA:EGDMA (metacrilato de 2,2,2,-trifluorometilo:dimetacrilato de etilenglicol) 85:15 v/v% y 2%p en IRG 651 utilizando un espaciador de 50 micras. **b)** Micrografía de la sección para el análisis de la profundidad de las arrugas.

EJEMPLOS DE REALIZACIÓN DE LA INVENCIÓN

Como ejemplos representativos de los materiales objeto de esta patente a continuación se describe la obtención de estas superficies con arrugas superficiales.

Ejemplo 1.- Obtención de superficies con arrugas superficiales en sistemas metacrílicos aplicando calor e irradiando simultáneamente. (Figura 2)

Sobre un sustrato de silicio de 2 cm de largo por 2 de ancho, se coloca un espaciador de 50 micras de espesor. En la cavidad que se forma entre el espaciador y el sustrato se vierte la disolución fotosensible formada por: Metacrilato de metilo (MMA), dimetacrilato de Etilenglicol (EGDMA) (Aldrich 99%), en proporción 85:15 v/v y a la que se ha añadido un 2%p, respecto a la cantidad total de monómeros, de Irgacure 651 (IRG 651)(2,2-dimetoxi-1,2-difenilentan-1-ona) (Ciba) como fotoiniciador.

El metacrilato de metilo (MMA) utilizado y previamente purificado se obtiene de la siguiente manera: el MMA (Aldrich 99%) se lava tres veces con una disolución acuosa básica

(10% NaOH) y después con agua. El monómero resultante se seca sobre sulfato magnésico, se filtra y se destila.

Esta disolución se tapa con dos coberturas de vidrio (2 x 0.15 mm de espesor) (Menzel-Glaser) y se cierra con pinzas de presión, tipo "clip", para mantener la dimensionalidad de la película.

La muestra se coloca sobre una placa calefactora a 100ºC y simultáneamente se comienza a irradiar con una lámpara UV durante otros cuatro minutos para que se produzca la fotopolimerización, mientras se mantiene la temperatura constante. Para las irradiaciones se ha utilizado un sistema de irradiación Hamamatsu modelo Ligthnincure L8868 equipada con una lámpara de xenón-mercurio de 200 W de potencia. La intensidad de luz se ha mantenido constante durante todos los experimentos (al 75% de la potencia total de la lámpara) y la luz se ha focalizado sobre las muestras con una fibra óptica emplazada a 8 cm de altura respecto a la muestra. La luz incidente se mantiene constante a 6150 mW/m^2, medida con un radiómetro marca Luzchem modelo SPR-01.

Una vez irradiadas las muestras, se separan las cubiertas de vidrio.

Las muestras se caracterizan usando un espectrómetro FTIR-ATR. Las muestras sólidas se colocan en contacto directo con el cristal de diamante del equipo sin preparación previa. La microscopía electrónica de barrido (SEM) se utilizó para el análisis de las microestructuras superficiales obtenidas. (Figura 2).

Ejemplo 2.- Obtención de superficies con arrugas superficiales en sistemas metacrílicos con anchuras y profundidad controladas por el espesor del espaciador. (Figura 3)

Sobre un sustrato de silicio de 2 cm de largo por 2 de ancho, se coloca un espaciador de espesor variable (50, 100 ó 150 micras). En la cavidad que se forma entre el espaciador y el sustrato se vierte la disolución fotosensible formada por: metacrilato de metilo (MMA), dimetacrilato de Etilenglicol (EGDMA) (Aldrich 99%), en proporción 85:15 v/v y a la que se

ha añadido un 2%p, respecto a la cantidad total de monómeros, de Irgacure 651 (IRG 651)(2,2-dimetoxi-1,2-difenilentan-1-ona) (Ciba) como fotoiniciador.

Esta disolución se tapa con dos coberturas de vidrio (2 x 0.15 mm de espesor) (Menzel-Glaser) y se cierra con pinzas de presión, tipo "clip", para mantener la dimensionalidad de la película.

La muestra se coloca sobre una placa calefactora a 100ºC durante un minuto y pasado este tiempo se comienza a irradiar con una lámpara UV durante otros cuatro minutos para que se produzca la fotopolimerización, mientras se mantiene la temperatura constante. Para las irradiaciones se ha utilizado un sistema de irradiación Hamamatsu modelo Ligthnincure L8868 equipada con una lámpara de xenón-mercurio de 200 W de potencia. La intensidad de luz se ha mantenido constante durante todos los experimentos (al 75% de la potencia total de la lámpara) y la luz se ha focalizado sobre las muestras con una fibra óptica emplazada a 8 cm de altura respecto a la muestra. La luz incidente se mantiene constante a 6150 mW/m^2, medida con un radiómetro marca Luzchem modelo SPR-01.

Una vez irradiadas las muestras, se separan las cubiertas de vidrio.

Las muestras se caracterizan usando un espectrómetro FTIR-ATR. Las muestras sólidas se colocan en contacto directo con el cristal de diamante del equipo sin preparación previa. La microscopía electrónica de barrido (SEM) se utilizó para el análisis de las microestructuras superficiales obtenidas y la medición de las profundidades alcanzadas a partir de los cortes transversales de las muestras.

Tal y como se muestra en la Figura 2 con este método experimental se forman arrugas superficiales cuya anchura y profundidad varía dependiendo del espesor del espaciador utilizado. Estos datos se muestran en la Tabla 1I.

TABLA 1I.- *Diferentes tamaños de arrugas superficiales obtenidos para distintos tamaños de espaciador. La disolución de partida utilizada en todos ellos ha sido de MMA: EGDMA 85:15 v/v + 2%p IRG 651*.

ESPACIADOR (μm)	AMPLITUD DE LA ARRUGA (μm) (media)	PROFUNDIDAD (μm) (media)
50	290	10
100	590	10
150	690	14

Ejemplo 3.- Extensión del empleo de este método a otros sistemas de naturaleza no metacrílica: Obtención de sistemas vinílicos. (Figura 4).

Sobre un sustrato de silicio de 2 cm de largo por 2 de ancho, se coloca un espaciador de 50 micras de espesor. En la cavidad que se forma entre el espaciador y el sustrato se introduce la disolución fotosensible formada por: Estireno (ST) (Aldrich 99%) Divinilbenzeno (DVB) (Aldrich 99%) en proporción 85:15 v/v% y a la que se añade un 2%p, respecto a la cantidad total de monómeros presentes en la mezcla, de Irgacure 651 (IRG 651) (2,2-dimetoxi-1,2-difenilentan-1-ona) (Ciba) como fotoiniciador.

Esta disolución se tapa con una cubierta de vidrio (2 x 0.15 mm de espesor) (Menzel-Glaser) y se cierra con pinzas de presión tipo “clip”, para mantener la dimensionalidad de la película.

La muestra se coloca sobre una placa calefactora a 140 ºC durante un minuto y pasado este tiempo se irradia con una lámpara UV durante otros seis minutos para que se produzca la fotopolimerización, manteniendo constante la temperatura de la muestra. El método de irradiación es idéntico al descrito en el ejemplo 2.

En la Figura 3 se muestran las micrografías superficiales de muestras con composición PS:DVB 85:15 v/v% + 2%p IRG 651.

Ejemplo 4.- Extensión del empleo de este método a otros sistemas con cargas integradas: Introducción de un copolímero al azar poli(metacrilato de metilo-co-metacrilato de 2,2,2-trifluoroetilo)(PMMA-co-PTFMA) sintetizado por ATRP como aditivo funcional en la mezcla fotosensible (Figura 5).

Sobre un sustrato de silicio de 2 cm de largo por 2 de ancho, se coloca un espaciador de 50 micras de espesor. En la cavidad que se forma entre el espaciador y el sustrato se introduce la disolución fotosensible formada por: Metacrilato de metilo (MMA) purificado según el procedimiento descrito en el ejemplo 1, Etilenglicol dimetacrilato (EGDMA) en proporción 85:15 v/v%, a la que se añade un 2%p de Irgacure 651 (IRG 651) (2,2-dimetoxi-1,2-difenilentan-1-ona) como fotoiniciador y 10%p respecto al peso total de monómeros del copolímero poli(metacrilato de metilo-co-2,2,2-metacrilato de trifluoroetilo).(M. Palacios-Cuesta, M. Liras, C: Labrugère, J. Rodríguez-Hernández, O. Garcia J. Polym. Sci. Part A: Polym. Chem. 2012, 50, 4902-4910).

Esta disolución se tapa con una cubierta de vidrio (2 x 0.15 mm de espesor) (Menzel-Glaser) y se cierra con pinzas de presión tipo “clip”, para mantener la dimensionalidad de la película. La muestra se coloca sobre una placa calefactora a 100ºC durante un minuto y pasado este tiempo se irradia con una lámpara UV durante otros cuatro minutos para que se produzca la fotopolimerización, manteniendo constante la temperatura de la muestra a 100ºC.

El método de irradiación es idéntico al descrito en el Ejemplo 2.

Ejemplo 5.- Extensión del empleo de este método a otros sistemas con monómeros que poseen grupos con alguna funcionalidad: Creación de arrugas superficiales con el monómero fluorado 2,2,2-metacrilato de trifluoroetilo (TFMA) en la disolución fotosensible. (Figura 6)

Sobre un sustrato de silicio de 2 cm de largo por 2 de ancho, se coloca un espaciador de 50 micras. En la cavidad que se forma entre el espaciador y el sustrato se vierte la disolución fotosensible formada por: 2,2,2-metacrilato de trifluoroetilo (TFMA) (Aldrich 99%), Etilenglicol dimetacrilato (EGDMA) (Aldrich 99%) en proporción 85:15 v/v y a la que

se añade un 2%p de Irgacure 651 (IRG 651) (2,2-dimetoxi-1,2-difenilentan-1-ona)(Ciba)como fotoiniciador. Estos productos se utilizan sin purificación previa.

Esta disolución se tapa con una cobertura de vidrio (2 x 0.15 mm de espesor) (Menzel-Glaser) y se cierra con pinzas de presión tipo “clip”, para mantener la dimensionalidad de la película. La muestra se coloca sobre una placa calefactora a 100ºC durante un minuto y pasado este tiempo se irradia con una lámpara UV durante otros cuatro minutos para que se produzca la fotopolimerización. El método de irradiación es idéntico al descrito en el ejemplo 2 de este mismo documento.

REIVINDICACIONES

1. Procedimiento de obtención de materiales poliméricos con superficies estructuradas con la formación de arrugas caracterizado porque comprende los siguientes pasos:

    a) preparación de una disolución fotosensible en una cámara cerrada con una cubierta superior transparente que permita la irradiación, y

    b) Calentamiento e irradiación con luz simultáneas de dicha disolución.

2. Procedimiento según la reivindicación 1 caracterizado porque se incluye una etapa de calentamiento de la disolución fotosensible previa a la etapa b).

3. Procedimiento según reivindicación 2 caracterizado porque la etapa de precalentamiento tiene una duración comprendida entre 0 segundos y 10 minutos, preferentemente entre 30 segundos y 60 segundos.

4. Procedimiento según reivindicaciones 1 a la 3 caracterizado porque la etapa de irradiación se realiza con luz ultravioleta.

5. Procedimiento según reivindicación 1 a la 4 caracterizado porque la irradiación del sistema con luz ultravioleta se realiza durante un tiempo comprendido entre 5 segundos y 10 minutos, preferentemente entre 4 minutos y 6 minutos.

6. Procedimiento según reivindicación 1 a la 5 caracterizado porque la disolución fotosensible comprende una mezcla de un monómero fotosensible, un agente entrecruzante y un fotoiniciador.

7. Procedimiento según reivindicación 6 caracterizado porque el monómero fotosensible puede ser del tipo vinílico, acrílico y/o metacrílico.

8. Procedimiento según reivindicación 7 caracterizado porque el monómero fotosensible pueden tener un grupo funcional en su estructura.

9. Procedimiento según reivindicación 8 caracterizado porque el grupo funcional puede ser hidrófobo y/o hidrófilo.

10. Procedimiento según reivindicación 8 a la 9 caracterizado porque el grupo funcional presenta cargas sólidas.

11. Procedimiento según reivindicacion caracterizado porque el agente entrecruzante es un monómero con dos o más puntos de entrecruzamiento.

12. Procedimiento según la reivindicación 1 caracterizado porque la preparación de la película de a) se lleva a cabo de la siguiente manera:

    a) colocación de un espaciador sobre un soporte (tapa inferior),

    b) vertido sobre el soporte de a) de la disolución fotosensible en la cámara formada,

    c) colocación de una tapa superior sobre la disolución, y

d) fijación de las tapas con algún sistema de presión para mantener la dimensionalidad (Figura 1) y la estanqueidad del sistema.

13. Procedimiento según la reivindicación 12 caracterizado porque el soporte es de vidrio o bien un sustrato de silicio.

14. Material estructurado con arrugas en superficie obtenido por el procedimiento según una cualquiera de las reivindicaciones anteriores.

15. Uso del material estructurado según la reivindicación 12 para la fabricación de: recubrimientos para cristales, textiles o pinturas autolimpiables y superficies antiadherentes o antibacterianas, en procesos en los que se precisa un control de la adhesión/fricción, sensores, dispositivos delgados y flexibles como transistores y diodos, materiales reflectantes/anti-reflectantes y para otras aplicaciones ópticas como paneles solares, lentes o espejos.

. FIGURAS

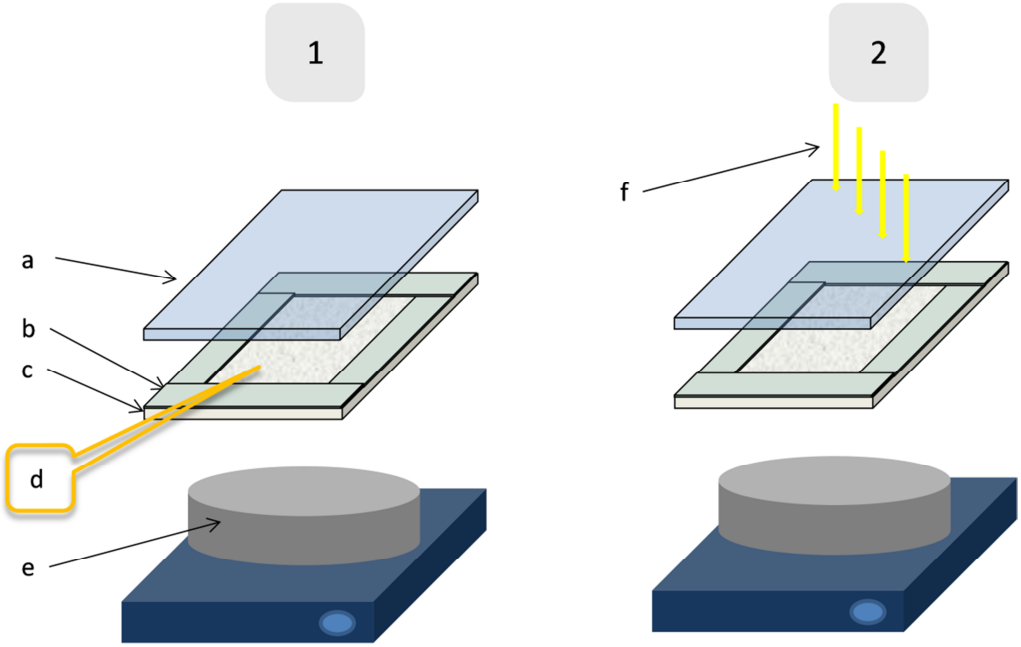

Figura 1

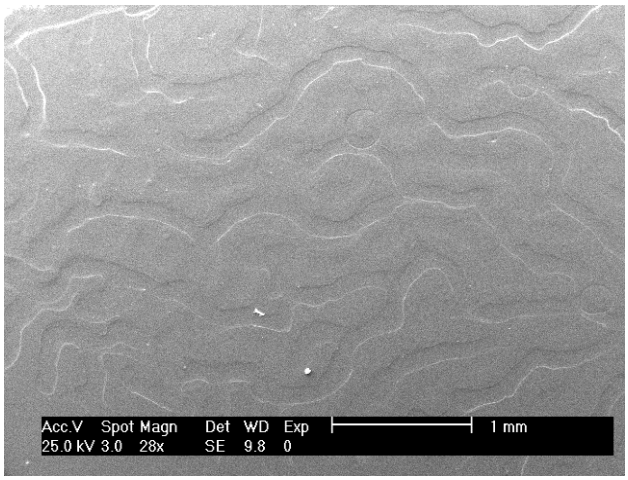

Figura 2

A **B**

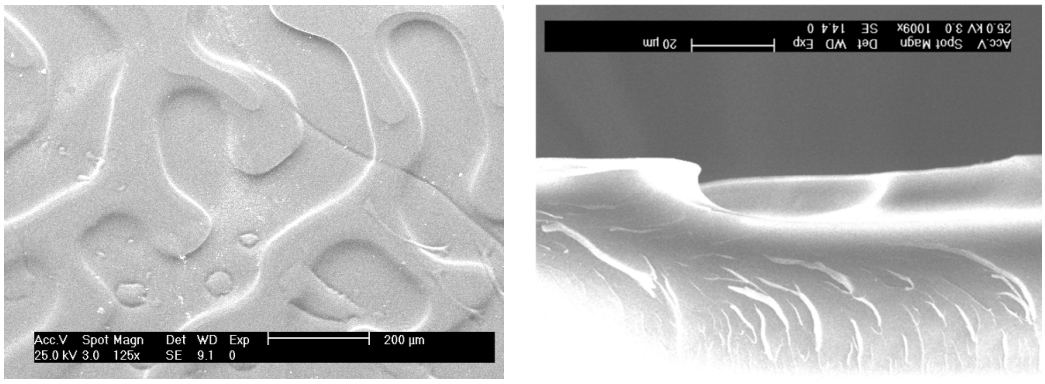

Figura 3

A **B**

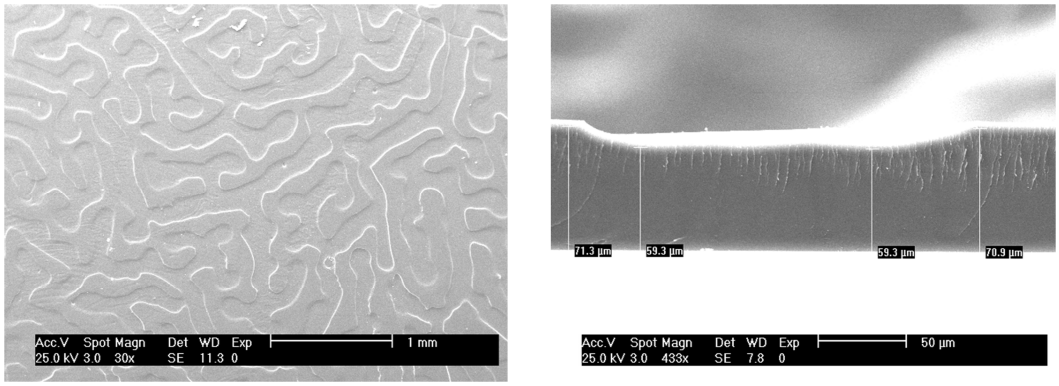

Figura 4

A **B**

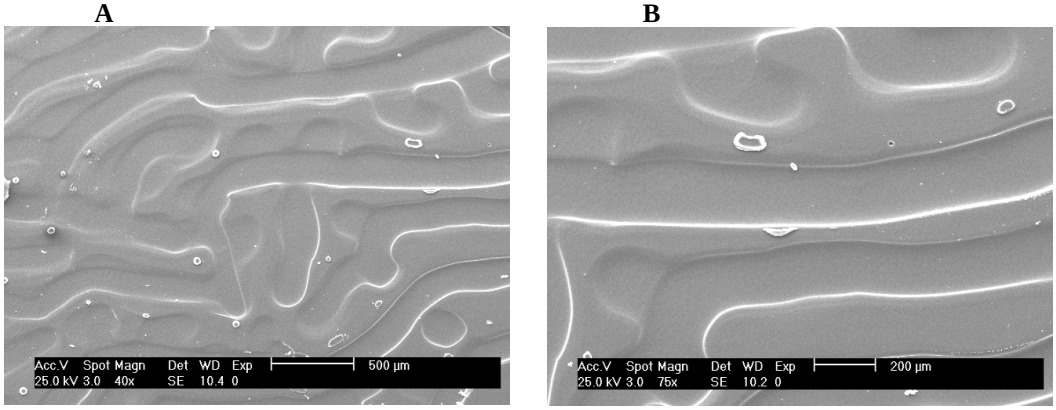

Figura 5

A **B**

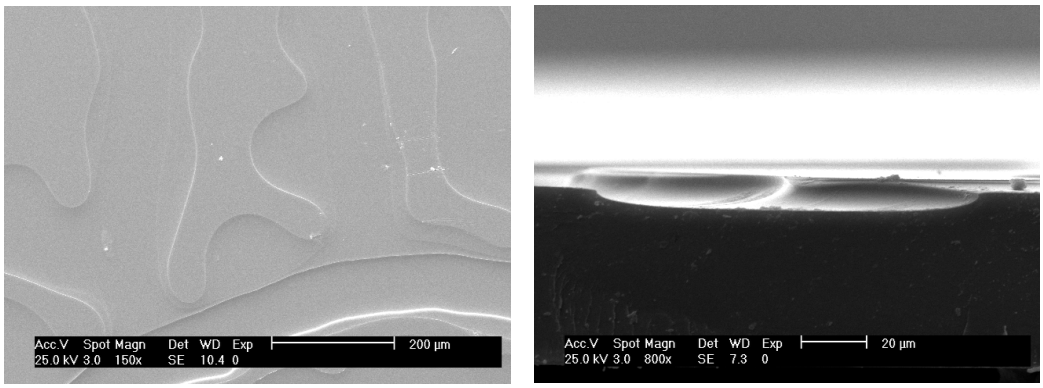
Acc.V Spot Magn Det WD Exp
25.0 kV 3.0 150x SE 10.4 0
200 µm
Acc.V Spot Magn Det WD Exp
25.0 kV 3.0 800x SE 7.3 0
20 µm

Figura 6

PASO A FASE PATENTE INTERNACIONAL PCT:

PROCEDIMIENTO DE OBTENCIÓN DE MATERIALES POLIMÉRICOS CON SUPERFICIES ESTRUCTURADAS, LOS MATERIALES ASÍ OBTENIDOS Y SUS APLICACIONES

TRATADO DE COOPERACIÓN EN MATERIA DE PATENTES
NOTIFICACIÓN DE LA RECEPCIÓN DE LOS DOCUMENTOS QUE CONSTITUYEN SUPUESTAMENTE UNA SOLICITUD INTERNACIONAL PRESENTADA DE FORMA ELECTRÓNICA.
(Instrucciones Administrativas del PCT, Parte Séptima)

1.-Se notifica al solicitante que la Oficina Receptora ha recibido en la fecha de recepción indicada más abajo, los documentos que supuestamente constituyen una solicitud internacional.
2.-Se llama la atención del solicitante sobre el hecho de que la Oficina Receptora no ha comprobado aún si estos documentos satisfacen las condiciones del art. 11.1, es decir, si cumple los requisitos para que le sea atribuida una fecha de presentación internacional. En cuanto la Oficina Receptora haya comprobado los documentos, avisará al solicitante.
3.-El número de la supuesta solicitud internacional indicado más abajo ha sido otorgado automáticamente a estos documentos. Se invita al solicitante a mencionar este número en toda la correspondencia con la Oficina Receptora.

Número de presentación	300111751
Solicitud Número PCT	PCT/ES2013/070871
Fecha de recepción	12 diciembre 2013

RESUMEN

Se describe un procedimiento para la obtención de superficies estructuradas mediante la formación controlada de arrugas de dimensiones variables. El método se basa en la irradiación con luz y calentamiento simultáneo de una disolución fotosensible. La obtención de las estructuras superficiales se lleva a cabo en pocos minutos. Además, este método permite la incorporación de distintos monómeros funcionales y de copolímeros y/o cargas como aditivos

en la mezcla inicial que pueden dotar a la superficie de funcionalidad sin necesidad de etapas adicionales de funcionalización.

SECTOR DE LA TÉCNICA

La presente invención puede ser aplicada a diversos campos que pueden ir desde los recubrimientos de distintos materiales al campo de los biomateriales. Además de controlar la topografía superficial, se pueden obtener superficies químicamente funcionalizadas. Las aplicaciones de este tipo de superficies con mojabilidad controlada incluyen los recubrimientos para cristales, textiles o pinturas autolimpiables y superficies antiadherentes o antibacterianas. También permitiría su utilización en procesos en los que se precisa un control de la adhesión/fricción. En los campos de la optoelectrónica y de la óptica, las superficies con arrugas controladas pueden ser aplicadas en sensores y son potencialmente interesantes para la fabricación de dispositivos delgados y flexibles como transistores y diodos. Asimismo, si las estructuras generadas poseen tamaños entorno a la longitud de onda de la luz se podrían obtener propiedades reflectactes/antireflectantes y, por tanto, podrían ser utilizadas para otras aplicaciones ópticas como paneles solares, lentes o espejos entre otros.

ESTADO DE LA TÉCNICA

Hay numerosas propiedades en los materiales poliméricos como la adhesividad, la mojabilidad o la biocompatibilidad, que dependen casi en exclusiva de su superficie. En ocasiones, por tanto, la adaptación de un material a una determinada aplicación requiere del diseño de su superficie. Así, aparte de las propiedades mecánicas del material, para adaptarlo y adecuarlo a su uso final, se debe considerar a que medio va estar expuesto, es decir, tener en cuenta la interfase. Son dos los factores que juegan un papel fundamental en las propiedades finales de la superficie de un material: la funcionalidad y la estructura.

La primera requiere, normalmente, tratamientos químicos o físicos que modifican la parte más superficial del material. La segunda se realiza mediante distintos métodos de fabricación que se pueden agrupar en dos grandes familias: Las técnicas "*bottom-up*" y "*top-down*". La combinación de ambos aspectos requiere varias etapas y procesos de larga duración.

La unión estructura y funcionalidad dentro del mismo material requiere, por tanto, la consecución de etapas de funcionalización con etapas de estructuración en procesos, por tanto, multietapa, largos y a menudo costosos.

La formación de arrugas superficiales se han ido desarrollando durante la década pasada (A. Schweikart, A. Fery, *Microchim Acta,* 165, 249, 2009). La gran mayoría de los métodos de formación de arrugas superficiales se basan en la utilización de sistemas bicapa; En las que una de las capas suele ser un material flexible (habitualmente polidimetilsiloxano (PDMS)) y sobre ésta, se deposita una delgada capa de un material más rígido (película metálica, capa inorgánica o polimérica) que como requerimiento inicial debe poseer un módulo de Young mucho más grande que el del PDMS. El primer método descrito consistió en la evaporación de aluminio sobre el material flexible. La cobertura de metal se realiza sobre las películas poliméricas de PDMS una vez expandidas térmicamente, que, al volverse a enfriar a temperatura ambiente, se contraen formando arrugas en la capa superior metálica.

Otro método empleado para la obtención de esta capa superior rígida es mediante la oxidación de la propia película de PDMS (con corriente de UV-ozono o con plasma). Para llevar a cabo este procedimiento se utilizan máquinas de estiramiento mecánico para las películas de PDMS en vez de hacerlo térmicamente. Aunque este método tiene la ventaja de utilizar un único material y no necesita la utilización de metales, la capa superior tiene la limitación de ser muy frágil, por lo que estas muestras sufren frecuentemente craqueos.

La utilización como capa rígida de coberturas de carácter polimérico es posterior. Se han descrito sistemas como poliestireno sobre PDMS expandido o multicapas de polielectrolitos con el módulo de Young muy superior al PDMS. Dependiendo de cada método, se pueden crear microestructuras de arrugas superficiales que van desde los 150 nm hasta los cientos de micras.

La complejidad de estas metodologías y la necesidad de utilizar soportes flexibles han limitado, en gran medida, su desarrollo industrial. Hasta ahora, sólo dos grupos de investigación han publicado recientemente la preparación de arrugas mediante la utilización de reacciones de fotopolimerización para dos sistemas concretos y utilizando montajes experimentales muy diferentes al descrito en esta patente.

El primero de los métodos descritos, consiste en la irradiación UV en dos pasos de una mezcla de acrilatos, (R. Schubert, T. Scherzer, M. Hinkefuss, B. Marquardt, J. Vogel, M. R. Buchmeiser, *Surf. Coat. Technol.*, 203, 1844, 2009) donde, en primer lugar, se irradia con una lámpara de excímero, luz monocromática de Xenón (<230 nm) con baja penetración en acrilatos (<500 nm), que polimeriza sólo la capa superior de la disolución fotosensible. Esta capa polimeriza gradualmente a lo largo de su espesor y queda flotando sobre las capas inferiores, en disolución, aún no polimerizadas. De esta manera consiguen formar las arrugas superficialmente. Para congelar este cambio estructural se realiza una segunda irradiación con una lámpara de mercurio, con mayor poder de penetración, que acaba polimerizando la totalidad de la película en todo su espesor.

El segundo método descrito, desarrollado por J. Crosby y colaboradores, plantea la creación de arrugas a partir de la irradiación UV de disoluciones acrílicas, de mezclas de monómeros acrílicos mono- y poli-funcionales, sometidas superficialmente a una corriente de oxígeno controlada (D. Chandra, A. J. Crosby, *Adv. Mater.*, 23, 3441, 2011). En este caso, el proceso de fotopolimerización se ve impedido en las capas superiores puesto que los radicales iniciadores se quenchean por el oxígeno y la polimerización en esta capa más superficial no ocurre. Por otro lado, el resto de la mezcla no curada superficialmente es capaz de hinchar la película inferior generando tensiones que provocan la generación de las arrugas en la película. Éste método tiene la desventaja principal de que, aunque se produce en un sólo paso, son necesarios 20 minutos tras la irradiación para que se produzca el hinchamiento de las capas inferiores por parte de la disolución no polimerizada. Además, presenta el inconveniente de que el monómero sin polimerizar quedaría dentro de la película final, con los consiguientes problemas de reactividad o de segregación al exterior, haciendo que este tipo de materiales que no están totalmente polimerizados presenten serios problemas para su aplicación en cierto tipo de usos, por ejemplo, en aplicaciones de tipo biológico o medioambiental (debido a problemas de toxicidad).

DESCRIPCIÓN DE LA INVENCIÓN

La presente invención se basa en que los inventores han observado que es posible la obtención de materiales poliméricos con superficies estructuradas mediante la formación de arrugas superficiales partiendo de disoluciones fotosensibles formadas por mezclas de monónomero/s, entrecruzante, y fotoiniciador en una cavidad aplicando una etapa de calentamiento que puede ser simultánea a la irradiación UV como sistema fotopolimerizador, aunque también se puede llevar a cabo una etapa previa adicional de calentamiento. Son materiales reticulados, es decir, con una alta estabilidad térmica y química.

Las arrugas se producen superficialmente durante la reacción de fotopolimerización y su tamaño (tanto la anchura como la profundidad) puede ser controlado variando factores externos como el porcentaje de monómero entrecruzante añadido (donde se pueden obtener arrugas con anchuras que van desde las 10 hasta las 720 micras) o variando el tamaño del espaciador empleado y, por lo tanto, el espesor de la película fotosensible irradiada (obteniéndose arrugas con anchuras que van desde las 10 hasta las 720 micras y con profundidades variables de 4 a 25 micras).

A diferencia de los anteriores procedimientos descritos, el procedimiento de la invención parte de disoluciones monoméricas fotosensibles, se ha comprobado que aparte de los sistemas formados por monómeros acrílicos y metacrílicos se puede extender su uso a monómeros de otra naturaleza como, por ejemplo, los vinílicos (estireno) y los monómeros tipo epoxi (poliéteres cíclicos) y se desarrolla en una cavidad irradiando, aunque puede realizarse aplicando simultáneamente calor durante el proceso de fotopolimerización. Este procedimiento permite, además, un ahorro de tiempo ya que las arrugas superficiales se producen simultáneamente con la polimerización en pocos minutos. El sistema experimental se desarrolla de un solo paso, en tan solo unos pocos minutos y, además, no requiere el empleo de equipos complejos o de alto precio.

A esto se añade el hecho de que estos monómeros pueden incluir alguna funcionalidad o incluso es posible incorporar otros componentes en la disolución fotosensible de partida que modifique las propiedades superficiales de la película final. Teniendo en cuenta todas estas consideraciones, las aplicaciones potenciales de este nuevo método son numerosas.

Además de lo mencionado anteriormente, presenta otras ventajas que incluyen la posibilidad de obtención de dibujos superficiales desde 10 micras hasta centenas de micras y que optimizan los problemas asociados al empleo de otras metodologías de estructuración superficial convencionales, como es la fotolitografía, para conseguir la estructuración de grandes áreas.

Así, un objeto de la invención lo constituye un procedimiento de obtención de materiales poliméricos con superficies estructuradas con arrugas, en adelante procedimiento de la invención, caracterizado porque comprende las siguientes etapas:

a) preparación de una disolución fotosensible en una cámara abierta sin tapa o cerrada con una cubierta superior transparente que permita la irradiación y

b) irradiación con luz de dicha disolución.

La cámara puede estar cerrada con una tapa o cubierta superior transparente o abierta, sin esa tapa.

La irradiación puede realizarse con calentamiento simultáneo

Un objeto de la invención lo constituye el procedimiento de la invención donde la preparación de la disolución de a) se lleva a cabo de la siguiente manera:

v. colocación de un espaciador sobre un soporte (tapa inferior), donde el soporte puede ser un soporte rígido como un vidrio o un sustrato de silicio así como una superficie flexible, mientras que el espaciador puede ser de espesor variable en función de las necesidades de anchura del material a obtener y para la tapa superior se puede utilizar cualquier material que deje pasar la luz, como por ejemplo un vidrio (Figura 1).

vi. vertido sobre el soporte de a) de la disolución fotosensible en la cámara formada,

vii. colocación de una tapa superior sobre la disolución, y

viii. fijación de las tapas con algún sistema de presión para mantener la dimensionalidad (Figura 1) y la estanqueidad del sistema.

Otro objeto particular lo constituye el procedimiento de la invención donde se incluye un precalentamiento previo al proceso de irradiación, este precalentamiento puede ser realizado antes que el calentamiento simultáneo al proceso de irradiación o independiente de éste o realizarse aunque no se caliente posteriormente. Una realización particular lo constituye el procedimiento de la invención donde la etapa de precalentamiento tiene una duración comprendida entre 0 segundos y 10 minutos, preferentemente entre 30 segundos y 60 segundos.

Durante la reacción de fotopolimerización de la lámina se producen las arrugas superficiales. Transcurrida la fotopolimerización (2-6 minutos para los sistemas concretos utilizados para asegurarse de una polimerización total) se retira la tapa superior en el caso de que sea requerida.

Otro objeto particular lo constituye el procedimiento de la invención donde la irradiación del sistema con luz ultravioleta se realiza durante un tiempo comprendido entre 5 segundos y 10 minutos, preferentemente entre 2 minutos y 6 minutos.

La disolución fotosensible de la invención está formada por una mezcla que comprende un monónomero/s fotosensibles, un agente entrecruzante y un fotoiniciador. En un ejemplo de realización particular el fotoiniciador es un compuesto químico capaz de absorber la luz, UV o Visible, y transformarla en energía química generando especies reactivas (como por ejemplo radicales libres o especies iónicas), que actúan como iniciadores de la polimerización (N. Arsu; *J. Eng. Nat. Sci*., sigma-1, 1-20, 2006). En los ejemplos de realización se ha utilizado Irgacure 651 o TSH, pero cualquier otro fotoiniciador capaz de absorber la luz UV o incluso en el visible podría igualmente ser utilizado.

Una realización particular de la invención lo constituye el procedimiento de la invención donde el monómero funcional de la disolución fotosensible pertenece al grupo

siguiente, a título ilustrativo y no limitativo: monómeros metacrílicos, acrílicos, vinílicos y tipo epoxis.

Un objeto particular de la invención lo constituye el procedimiento de la invención donde el agente entrecruzante que se puede utilizar es un monómero con dos (caso del dimetacrilato de etilenglicol (EGDMA)) o más puntos de entrecruzamiento [caso del triacrilato de pentaeritritol (PETA) o del tetraacrilato de pentaeritritol (PETRA)].

Mediante el procedimiento de la invención la anchura y/o la profundidad de la arruga se puede controlar variando el porcentaje de monómero entrecruzante y/o el tamaño del espaciador empleado, donde los tamaños de las anchuras obtenidas están comprendidos entre 10 y 720 micras y las profundidades de las mismas pueden estar comprendidas en el intervalo de 4-25 micras. (Tabla I).

TABLA I.- *Diferentes tamaños de arrugas superficiales obtenidos para distintas composiciones de monómero y agente entrecruzante. Además se incluyen los espaciadores utilizados para la realización.*

AGENTE ENTRECRUZANTE DIFUNCIONAL (%)	ESPACIADOR (µm)	AMPLITUD DE LA ARRUGA (µm) (media)	PROFUNDIDAD (µm) (media)
15	50	290	11
	100	510	10
	150	690	14
30	100	240	8
	150	720	4
45	150	720	10

Ya que muchas de las propiedades finales en las superficies poliméricas dependen tanto de la estructuración de la superficie, como de la funcionalización química de ésta, se han utilizado también en las disoluciones fotosensibles de partida monómeros/copolímeros con algún grupo funcional en su estructura que modifique las propiedades químicas superficiales de la película final. Otra realización particular de la invención lo constituye el procedimiento de la invención donde el grupo funcional puede ser tanto de carácter hidrófobo como hidrófilo, creándose, de este modo, un amplio abanico de posibilidades en cuanto a composición se refiere. El control de la composición superficial, es decir de la funcionalidad, permite dotar al material de propiedades adicionales. La funcionalidad puede hacer que materiales químicamente inertes puedan, una vez funcionalizados adecuadamente, ser utilizados como adhesivos, catalizadores, materiales biocompatibles, etc. Además los grupos funcionales pueden servir como punto de anclaje de otras moléculas que pueden tener interés tanto biológico como en otras áreas.

Otra realización particular de la invención lo constituye el procedimiento de la invención donde la funcionalidad viene determinada por la adición de cargas sólidas añadidas inicialmente en las disoluciones fotosensibles. El término “cargas sólidas” utilizado en la presente invención se refiere a compuestos de distinta naturaleza, por ejemplo, orgánicas (copolímeros funcionalizados, grafeno, nanotubos de carbono, fibras de vidrio), inorgánicas (POSS, sílice, aerosil) o metálicas (nanopartículas magnéticas, de oro, plata o quantum dots), que contienen algún grupo funcional en su estructura o en su superficie y que pueden igualmente modificar la composición química superficial o influir en las propiedades finales del compuesto mejorándolas o creando nuevas propiedades, por ejemplo, térmicas, mecánicas, conductoras, fotosensibles, etc.

Otro objeto de la invención lo constituye un material estructurado con arrugas superficiales obtenido por el procedimiento de la invención, en adelante material estructurado de la invención.

El procedimiento de la invención permite obtener materiales con superficies con mojabilidad y rugosidad controlada. Este nuevo método de creación de arrugas superficiales es simple y económico.

Por último, otro objeto de la presente invención lo constituye el uso del material estructurado de la invención:

- como recubrimientos para, a título ilustrativo y sin carácter limitativo, cristales, textiles o pinturas autolimpiables y superficies antiadherentes o antibacterianas.

- para procesos en los que se precisa un control de la adhesión/fricción.

- para la fabricación de sensores y de dispositivos delgados y flexibles como transistores y diodos, o

- como material reflectacte/antireflectante,

- para la obtención de superficies conductoras o aumentar la rigidez de la superficie y

- más concretamente, para otras aplicaciones ópticas como paneles solares, lentes o espejos, entre otros.

A lo largo de la descripción y las reivindicaciones, la palabra "comprende" y sus variantes no pretenden excluir otras características técnicas, aditivos, componentes o pasos. Para los expertos en la materia, otros objetos, ventajas y características de la invención se desprenderán en parte de la descripción y en parte de la práctica de la invención. Los siguientes ejemplos se proporcionan a modo de ilustración, y no se pretende que sean limitativos de la presente invención.

DESCRIPCION DE LAS FIGURAS

Figura 1.- Esquema experimental utilizado para la fabricación de las arrugas superficiales . Se distingue la etapa 1, o etapa de precalentamiento, donde la muestra se calienta a la temperatura de ebullición del monómero, y la etapa 2, donde se irradia con luz UV: a) Cubierta de vidrio (opcional en el caso de utilizar una tapa superior) b) Espaciador con espesor variable c) Soporte (en este caso oblea de silicio) d) Disolución fotosensible, formada

por: monómero lineal, monómero entrecruzante, fotoiniciador y carga (en algunos casos), e) Fuente de calor (opcional), f) fuente de irradiación UV.

Figura 2.-Micrografía de un material de naturaleza metacrílica obtenido de acuerdo al procedimiento de la invención. Micrografía SEM de las arrugas superficiales formadas a partir de una disolución fotosensible con composición MMA (metacrilato de metilo) : EGDMA (dimetacrilato de etilenglicol) 85/15 v/v% y 2%p en IRG651 (Irgacure 651) utilizando un espaciador de 50 micras, utilizando calentamiento e irradiación de manera simultánea.

Figura 3.- Micrografía de un material de naturaleza metacrílica obtenido de acuerdo al procedimiento de la invención. A) Micrografía SEM (microscopía electrónica de barrido) de las arrugas superficiales formadas a partir de una disolución fotosensible con composición MMA:EGDMA 85/15 v/v% y 2%p en IRG 651 utilizando un espaciador de 50 micras. **B)** Micrografía SEM de la sección donde se aprecia la profundidad de las arrugas superficiales.

Figura 4.- Micrografía de un material de naturaleza no metacrílica obtenido de acuerdo al procedimiento de la invención. A) Micrografía SEM de las arrugas superficiales formadas a partir de una disolución fotosensible con composición PS: DVB 85/15 v/v% y 2%p en IRG 651 utilizando un espaciador de 50 micras. **B)** Micrografía SEM de la sección donde se aprecia la profundidad de las arrugas superficiales.

Figura 5.- Micrografía de un material de naturaleza metacrílica con cargas integradas obtenido de acuerdo al procedimiento de la invención. A) Micrografía SEM de las arrugas superficiales formadas a partir de una disolución fotosensible con composición MMA/EGDMA 85/15 v/v%, 10%p de copolímero PMMA-co-PTFMA [poli(metacrilato de metilo)-co-(polimetacrilato de 2,2,2,-trifluorometilo)] y 2%p en IRG 651 utilizando un espaciador de 50 micras. **B)** Micrografía SEM de la sección donde se aprecia la profundidad de las arrugas superficiales.

Figura 6.- Micrografía de un material de naturaleza metacrílica con funcionalidades obtenido de acuerdo al procedimiento de la invención. A) Micrografía

SEM de las arrugas superficiales formadas con una disolución fotosensible con composición TFMA/EGDMA (metacrilato de 2,2,2,-trifluorometilo/dimetacrilato de etilenglicol) 85/15 v/v% y 2%p en IRG 651 utilizando un espaciador de 50 micras. **B)** Micrografía de la sección para el análisis de la profundidad de las arrugas.

Figura 7.- Micrografías de un material de naturaleza epoxi obtenido de acuerdo al procedimiento de la invención. Micrografías SEM de las arrugas superficiales (arriba) y sus cortes (abajo) formadas a partir de una disolución fotosensible con composición ECH y 2%p en TSH utilizando tres espaciadores distintos de (**A**) 50, (**B**) 100 y (**C**) 150 micras, y realizando calentamiento e irradiación de manera simultánea.

Figura 8.-Micrografía de un material de naturaleza epoxi obtenido de acuerdo al procedimiento de la invención. Micrografía SEM de (**A**) las arrugas superficiales y (**B**) su corte formadas a partir de una disolución fotosensible con composición ECH, 2%p en TSH y 0,2% de POSS utilizando un espaciador de 50 micras, realizando calentamiento e irradiación de manera simultánea.

EJEMPLOS DE REALIZACIÓN DE LA INVENCIÓN

Como ejemplos representativos de los materiales objeto de esta patente a continuación se describe la obtención de estas superficies con arrugas superficiales.

Ejemplo 1.- Obtención de superficies con arrugas superficiales en sistemas metacrílicos aplicando calor e irradiando simultáneamente. (Figura 2)

Sobre un sustrato de silicio de 2 cm de largo por 2 cm de ancho, se coloca un espaciador de 50 micras de espesor. En la cavidad que se forma entre el espaciador y el sustrato se vierte la disolución fotosensible formada por: Metacrilato de metilo (MMA), dimetacrilato de Etilenglicol (EGDMA) (Aldrich 99%), en proporción 85/15 v/v y a la que se ha añadido un 2%p, respecto a la cantidad total de monómeros, de Irgacure 651 (IRG 651) (2,2-dimetoxi-1,2-difenilentan-1-ona) (Ciba) como fotoiniciador.

El metacrilato de metilo (MMA) utilizado y previamente purificado se obtiene de la siguiente manera: el MMA (Aldrich 99%) se lava tres veces con una disolución acuosa básica (10% NaOH) y después con agua. El monómero resultante se seca sobre sulfato magnésico, se filtra y se destila.

Esta disolución se tapa con dos coberturas de vidrio (2 x 0.15 mm de espesor) (Menzel-Glaser) y se cierra con pinzas de presión, tipo "clip", para mantener la dimensionalidad de la película.

La muestra se coloca sobre una placa calefactora a 100ºC y simultáneamente se comienza a irradiar con una lámpara UV durante otros cuatro minutos para que se produzca la fotopolimerización, mientras se mantiene la temperatura constante. Para las irradiaciones se ha utilizado un sistema de irradiación Hamamatsu modelo Ligthnincure L8868 equipada con una lámpara de xenón-mercurio de 200 W de potencia. La intensidad de luz se ha mantenido constante durante todos los experimentos (al 75% de la potencia total de la lámpara aunque no es limitativo, funciona a intensidades menores y hasta el 100% de la potencia) y la luz se ha focalizado sobre las muestras con una fibra óptica emplazada a 8 cm de altura respecto a la muestra. La luz incidente se mantiene constante a 6150 mW/m^2, medida con un radiómetro marca Luzchem modelo SPR-01.

Una vez irradiadas las muestras, se separan las cubiertas de vidrio.

Las muestras se caracterizan usando un espectrómetro infrarrojo por transformada de Fourier FTIR-ATR. Las muestras sólidas se colocan en contacto directo con el cristal de diamante del equipo sin preparación previa. La microscopía electrónica de barrido (SEM) se utilizó para el análisis de las microestructuras superficiales obtenidas. (Figura 2).

Ejemplo 2.- Obtención de superficies con arrugas superficiales en sistemas metacrílicos con anchuras y profundidad controladas por el espesor del espaciador. (Figura 3).

Sobre un sustrato de silicio de 2 cm de largo por 2 cm de ancho, se coloca un espaciador de espesor variable (50, 100 ó 150 micras). En la cavidad que se forma entre el

espaciador y el sustrato se vierte la disolución fotosensible formada por: metacrilato de metilo (MMA), dimetacrilato de Etilenglicol (EGDMA) (Aldrich 99%), en proporción 85/15 v/v y a la que se ha añadido un 2%p, respecto a la cantidad total de monómeros, de Irgacure 651 (IRG 651)(2,2-dimetoxi-1,2-difenilentan-1-ona) (Ciba) como fotoiniciador.

Esta disolución se tapa con dos coberturas de vidrio (2 x 0.15 mm de espesor) (Menzel-Glaser) y se cierra con pinzas de presión, tipo "clip", para mantener la dimensionalidad de la película.

La muestra se coloca sobre una placa calefactora a 100ºC durante un minuto y pasado este tiempo se comienza a irradiar con una lámpara UV durante otros cuatro minutos para que se produzca la fotopolimerización, mientras se mantiene la temperatura constante. Para las irradiaciones se ha utilizado un sistema de irradiación Hamamatsu modelo Ligthnincure L8868 equipada con una lámpara de xenón-mercurio de 200 W de potencia. La intensidad de luz se ha mantenido constante durante todos los experimentos (al 75% de la potencia total de la lámpara, aunque no es limitativo, también funciona a intensidades menores y hasta el 100% de la potencia) y la luz se ha focalizado sobre las muestras con una fibra óptica emplazada a 8 cm de altura respecto a la muestra. La luz incidente se mantiene constante a 6150 mW/m^2, medida con un radiómetro marca Luzchem modelo SPR-01.

Una vez irradiadas las muestras, se separan las cubiertas de vidrio.

Las muestras se caracterizan usando un espectrómetro FTIR-ATR. Las muestras sólidas se colocan en contacto directo con el cristal de diamante del equipo sin preparación previa. La microscopía electrónica de barrido (SEM) se utilizó para el análisis de las microestructuras superficiales obtenidas y la medición de las profundidades alcanzadas a partir de los cortes transversales de las muestras.

Tal y como se muestra en la Figura 2 con este método experimental se forman arrugas superficiales cuya anchura y profundidad varía dependiendo del espesor del espaciador utilizado. Estos datos se muestran en la Tabla II.

TABLA II.- *Diferentes tamaños de arrugas superficiales obtenidos para distintos tamaños de espaciador. La disolución de partida utilizada en todos ellos ha sido de MMA: EGDMA 85:15 v/v + 2%p IRG 651.*

ESPACIADOR (µm)	AMPLITUD DE LA ARRUGA (µm) (media)	PROFUNDIDAD (µm)(media)
50	290	10
100	590	10
150	690	14

Ejemplo 3.- Extensión del empleo de este método a otros sistemas de naturaleza no metacrílica: Obtención de sistemas vinílicos. (Figura 4).

Sobre un sustrato de silicio de 2 cm de largo por 2 cm de ancho, se coloca un espaciador de 50 micras de espesor. En la cavidad que se forma entre el espaciador y el sustrato se introduce la disolución fotosensible formada por: Estireno (ST) (Aldrich 99%) Divinilbenzeno (DVB) (Aldrich 99%) en proporción 85/15 v/v% y a la que se añade un 2%p, respecto a la cantidad total de monómeros presentes en la mezcla, de Irgacure 651 (IRG 651) (2,2-dimetoxi-1,2-difenilentan-1-ona) (Ciba) como fotoiniciador.

Esta disolución se tapa con una cubierta de vidrio (2 x 0.15 mm de espesor) (Menzel-Glaser) y se cierra con pinzas de presión tipo “clip”, para mantener la dimensionalidad de la película.

La muestra se coloca sobre una placa calefactora a 140 ºC durante un minuto y pasado este tiempo se irradia con una lámpara UV durante otros seis minutos para que se produzca la fotopolimerización, manteniendo constante la temperatura de la muestra. El método de irradiación es idéntico al descrito en el Ejemplo 2.

En la Figura 3 se muestran las micrografías superficiales de muestras con composición PS/DVB 85/15 v/v% + 2%p IRG 651.

Ejemplo 4.- Extensión del empleo de este método a otros sistemas con cargas integradas: Introducción de un copolímero al azar poli(metacrilato de metilo-co-metacrilato de 2,2,2-trifluoroetilo) (PMMA-co-PTFMA) sintetizado por ATRP como aditivo funcional en la mezcla fotosensible (Figura 5).

Sobre un sustrato de silicio de 2 cm de largo por 2 cm de ancho, se coloca un espaciador de 50 micras de espesor. En la cavidad que se forma entre el espaciador y el sustrato se introduce la disolución fotosensible formada por: Metacrilato de metilo (MMA) purificado según el procedimiento descrito en el ejemplo 1, Etilenglicol dimetacrilato (EGDMA) en proporción 85/15 v/v%, a la que se añade un 2%p de Irgacure 651 (IRG 651) (2,2-dimetoxi-1,2-difenilentan-1-ona) como fotoiniciador y 10%p respecto al peso total de monómeros del copolímero poli(metacrilato de metilo-co-2,2,2-metacrilato de trifluoroetilo).(M. Palacios-Cuesta, M. Liras, C: Labrugère, J. Rodríguez-Hernández, O. Garcia J. Polym. Sci. Part A: Polym. Chem. 2012, 50, 4902-4910).

Esta disolución se tapa con una cubierta de vidrio (2 x 0.15 mm de espesor) (Menzel-Glaser) y se cierra con pinzas de presión tipo “clip”, para mantener la dimensionalidad de la película. La muestra se coloca sobre una placa calefactora a 100ºC durante un minuto y pasado este tiempo se irradia con una lámpara UV durante otros cuatro minutos para que se produzca la fotopolimerización, manteniendo constante la temperatura de la muestra a 100ºC.

El método de irradiación es idéntico al descrito en el Ejemplo 2.

Ejemplo 5.- Extensión del empleo de este método a otros sistemas con monómeros que poseen grupos con alguna funcionalidad: Creación de arrugas superficiales con el monómero fluorado 2,2,2-metacrilato de trifluoroetilo (TFMA) en la disolución fotosensible. (Figura 6).

Sobre un sustrato de silicio de 2 cm de largo por 2 de ancho, se coloca un espaciador de 50 micras. En la cavidad que se forma entre el espaciador y el sustrato se vierte la

disolución fotosensible formada por: 2,2,2-metacrilato de trifluoroetilo (TFMA) (Aldrich 99%), Etilenglicol dimetacrilato (EGDMA) (Aldrich 99%) en proporción 85/15 v/v y a la que se añade un 2%p de Irgacure 651 (IRG 651) (2,2-dimetoxi-1,2-difenilentan-1-ona) (Ciba) como fotoiniciador. Estos productos se utilizan sin purificación previa.

Esta disolución se tapa con una cobertura de vidrio (2 x 0.15 mm de espesor) (Menzel-Glaser) y se cierra con pinzas de presión tipo "clip", para mantener la dimensionalidad de la película. La muestra se coloca sobre una placa calefactora a 100ºC durante un minuto y pasado este tiempo se irradia con una lámpara UV durante otros cuatro minutos para que se produzca la fotopolimerización. El método de irradiación es idéntico al descrito en el Ejemplo 2.

Ejemplo 6.- Obtención de superficies con arrugas superficiales en sistemas epoxi con anchuras y profundidad controladas por el espesor del espaciador en cavidad sin tapa superior sin calentamiento simultáneo a la irradiación. (Figura 7)

Sobre un sustrato de vidrio de 2 cm de largo por 2 cm de ancho, se coloca un espaciador de espesor variable (50, 100 ó 150 micras). En la cavidad que se forma entre el espaciador y el sustrato se vierte la disolución fotosensible formada por: 3,4-epoxycyclohexylmethyl-3',4'-epoxicyclohexane carboxylate (ECH: CAS: 407208), al que se ha añadido un 2%p de TSH (mezcla de sales de hexafluoro-antimoniato de Triarilsulfonio Triarylsulfonium hexafluoro-antimonate salts mixed CAS: 109037-75-4) como fotoiniciador.

La muestra se deja expuesta al aire y se coloca sobre una placa calefactora con temperatura entre la temperatura ambiente y 100ºC durante un minuto (si no se calienta la muestra se observa la formación de arrugas regulares también fotopolimerizando manteniendo la temperatura ambiente durante todo el proceso) y pasado este tiempo se comienza a irradiar con una lámpara UV durante otros dos minutos para que se produzca la fotopolimerización, mientras se mantiene la temperatura constante. Para las irradiaciones se ha utilizado un sistema de irradiación Hamamatsu modelo Ligthnincure L8868 equipada con una lámpara de xenón-mercurio de 200 W de potencia. La intensidad de luz se ha mantenido constante durante todos los experimentos (al 100% de la potencia total de la lámpara, aunque también ha funcionado con menor intensidad la luz), y se ha focalizado sobre las muestras con una fibra óptica emplazada a 5 cm de altura respecto a la muestra, aunque ha funcionado desde 1 a 10 cm

La microscopía electrónica de barrido (SEM) se utilizó para el análisis de las microestructuras superficiales obtenidas y la medición de las profundidades alcanzadas a partir de los cortes transversales de las muestras.

Tal y como se muestra en la Figura 7 con este método experimental se forman arrugas superficiales cuya anchura y profundidad varía dependiendo del espesor del espaciador utilizado. Estos datos se muestran en la Tabla III.

TABLA III.- *Diferentes tamaños (amplitud y profundidad) de arrugas superficiales obtenidos para distintos tamaños de espaciador. La disolución de partida utilizada en todos ellos ha sido de ECH + 2%p TSH.*

ESPACIADOR (µm)	AMPLITUD DE LA ARRUGA (µm) (media)	PROFUNDIDAD (µm)(media)
50	290 ± 20	11 ± 1
100	425 ± 25	22 ± 2
150	546 ± 50	18 ± 1

Ejemplo 7.- Extensión del empleo de este método a otros sistemas epoxi con cargas integradas: Introducción de un MethacrylIsobutyl POSS (POSS) en la mezcla fotosensible (Figura 8).

Sobre un sustrato de vidrio de 2 cm de largo por 2 de ancho, se coloca un espaciador de 50 micras de espesor. En la cavidad que se forma entre el espaciador y el sustrato se vierte la disolución fotosensible formada por ECH, al que se ha añadido un 2%p respecto a la cantidad total de TSH como fotoiniciador y 0,5%p de POSS.

La muestra se coloca sobre una placa calefactora a 100ºC durante un minuto (también se obtienen arrugas de dimensionalidad regular a temperatura ambiente sin necesidad de aplicar ningún calentamiento durante todo el proceso) y pasado este tiempo se irradia con una lámpara

UV (al 100% de la potencia total de la lámpara, aunque no es limitativo, también funciona a intensidades menores) y focalizando sobre las muestras con una fibra óptica emplazada a 5 cm de altura respecto a la muestra (aunque funciona también para entre 1 y 10 cm) durante otros dos minutos para que se produzca la fotopolimerización, manteniendo constante la temperatura de la muestra desde temperatura ambiente hasta 100ºC.

El método de irradiación es idéntico al descrito en el Ejemplo 6.

Dimensiones de las arrugas obtenidas: longitud: 276 ± 15 micras, Profundidad: 12 ± 1 micras.

Se ha comprobado que también se obtienen arrugas utilizando otras cargas en proporción similar como grafeno o nanotubos de carbono entre 0.1 y 2%.

REIVINDICACIONES

1. Procedimiento de obtención de materiales poliméricos con superficies estructuradas con la formación de arrugas, caracterizado por que comprende los siguientes pasos:

    a) preparación de una disolución fotosensible en una cámara abierta sin tapa o cerrada con una cubierta superior transparente que permita la irradiación

    b) irradiación con luz de dicha disolución.

2. Procedimiento según la reivindicación 1, caracterizado por que la preparación de la película de la etapa a) se hace con una cubierta superior transparente.

3. Procedimiento según la reivindicación 1, caracterizado por que la preparación de la película de la etapa a) se hace sin poner una tapa.

4. Procedimiento según cualesquiera de las reivindicaciones 1 a 3, caracterizado por que la preparación de la película de la etapa b) se hace con calentamiento simultáneo a la irradiación.

5. Procedimiento según cualesquiera de las reivindicaciones 1 a 4, caracterizado por que se incluye una etapa de calentamiento de la disolución fotosensible previa a la etapa b).

6. Procedimiento según reivindicación 5, caracterizado por que la etapa de precalentamiento tiene una duración comprendida entre 0 segundos y 10 minutos, preferentemente entre 30 segundos y 60 segundos.

7. Procedimiento según cualesquiera de las reivindicaciones 1 a la 6, caracterizado por que la etapa de irradiación se realiza con luz ultravioleta.

8. Procedimiento según cualesquiera de las reivindicaciones 1 a la 7, caracterizado por que la irradiación del sistema con luz ultravioleta se realiza durante un tiempo comprendido entre 5 segundos y 10 minutos, preferentemente entre 2 minutos y 6 minutos.

9. Procedimiento según cualesquiera de las reivindicaciones 1 a la 8, caracterizado por que la disolución fotosensible comprende una mezcla de un monómero, un agente entrecruzante y un iniciador fotosensible.

10. Procedimiento según la reivindicación 9, caracterizado por que el monómero puede ser del tipo vinílico, acrílico y/o metacrílico.

11. Procedimiento según la reivindicación 10, caracterizado por que el monómero puede ser del tipo epoxi.

12. Procedimiento según cualesquiera de las reivindicaciones 9 a 11, caracterizado por que el monómero pueden tener un grupo funcional en su estructura.

13. Procedimiento según la reivindicación 12, caracterizado por que el grupo funcional puede ser hidrófobo y/o hidrófilo.

14. Procedimiento según cualesquiera de las reivindicaciones 12 a 13, caracterizado por que el grupo funcional presenta cargas sólidas.

15. Procedimiento según la reivindicación 12, caracterizado porque las cargas sólidas son orgánicas, incluyendo, copolímeros funcionalizados, grafeno, nanotubos de carbono; inorgánicas como POSS; y/o metálicas como nanopartículas magnéticas, de oro, de plata o quantum dots.

16. Procedimiento según cualesquiera de las reivindicaciones 9 a 15, caracterizado por que el agente entrecruzante es un monómero con dos o más puntos de entrecruzamiento.

17. Procedimiento según cualesquiera de las reivindicaciones 1 a 16, caracterizado por que la preparación de la película de la etapa a) se lleva a cabo de la siguiente manera:

    i. colocación de un espaciador sobre un soporte (tapa inferior),

    ii. vertido sobre el soporte de la etapa a) de la disolución fotosensible en la cámara formada,

    iii. colocación de una tapa superior sobre la disolución, y

    iv. fijación de las tapas con algún sistema de presión para mantener la dimensionalidad y la estanqueidad del sistema.

18. Material estructurado con arrugas en superficie obtenido por el procedimiento según una cualquiera de las reivindicaciones anteriores.

19. Uso del material estructurado según la reivindicación 18, para la fabricación de: recubrimientos para cristales, textiles o pinturas autolimpiables y superficies antiadherentes o antibacterianas, en procesos en los que se precisa un control de la adhesión/fricción, sensores, dispositivos delgados y flexibles como transistores y diodos, materiales reflectantes/anti-reflectantes, para la obtención de superficies conductoras o aumentar la rigidez de la superficie y para otras aplicaciones ópticas como paneles solares, lentes o espejos.

FIGURAS

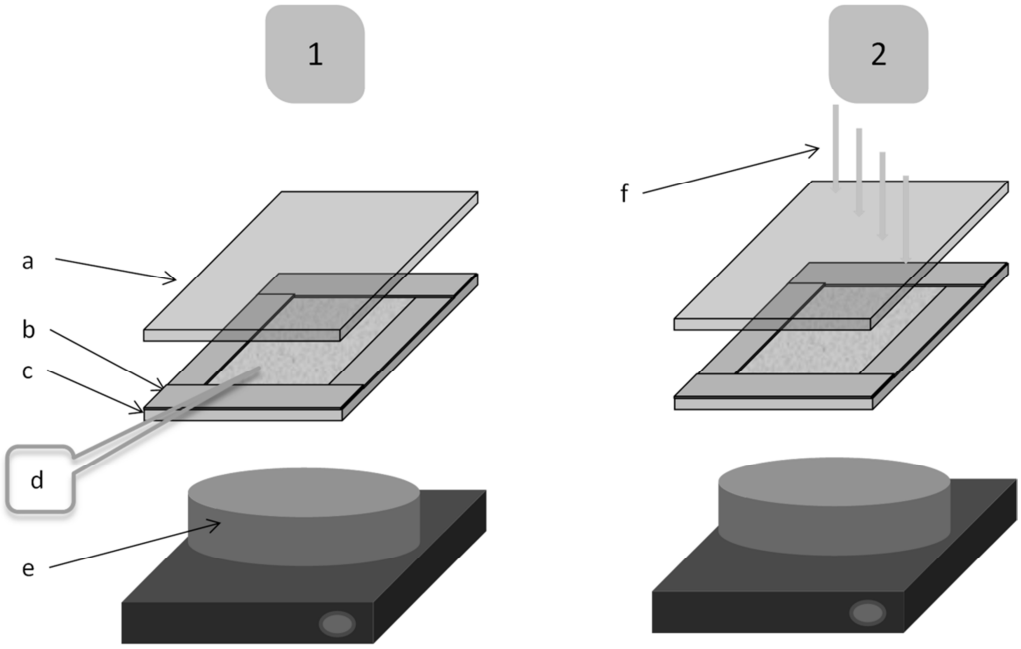

Figura 1

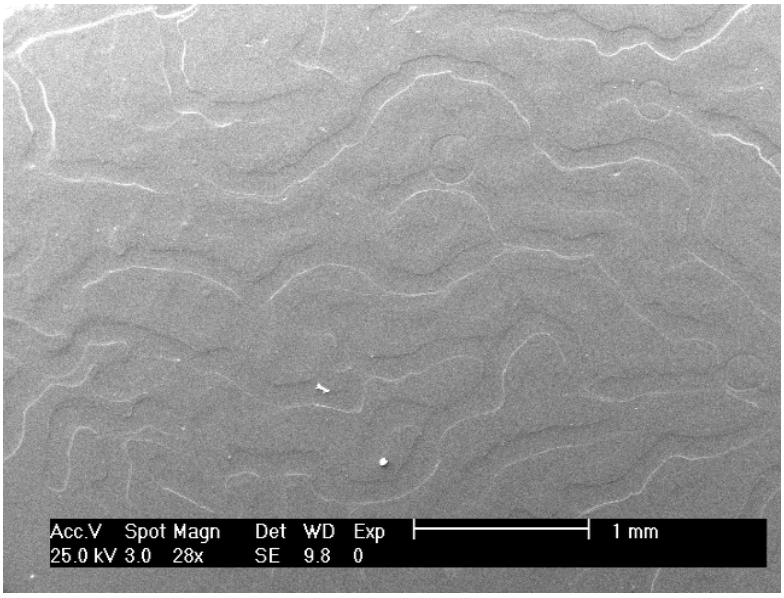

Figura 2

A **B**

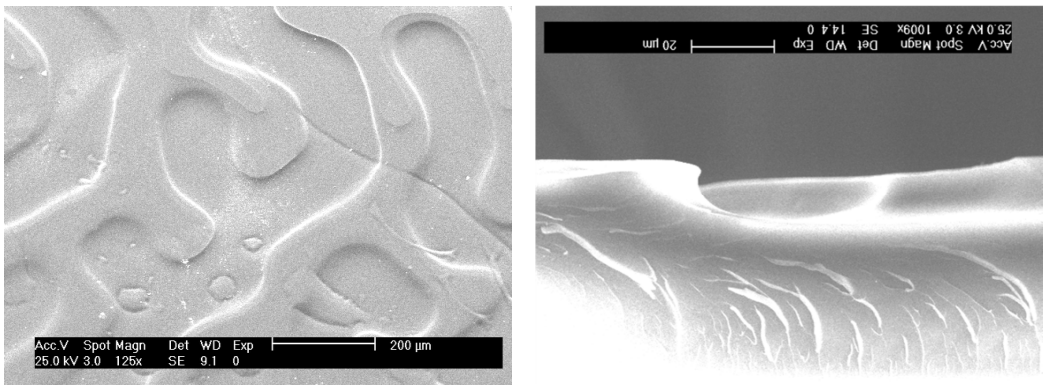

Figura 3

A **B**

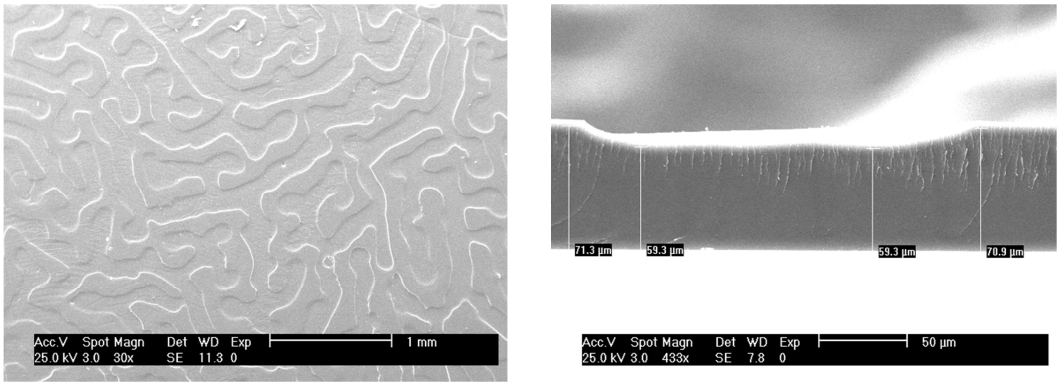

Figura 4

A **B**

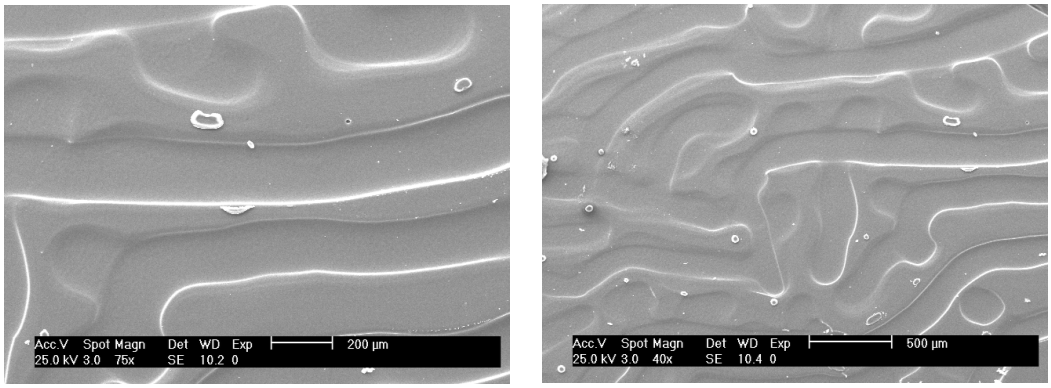

Figura 5

A **B**

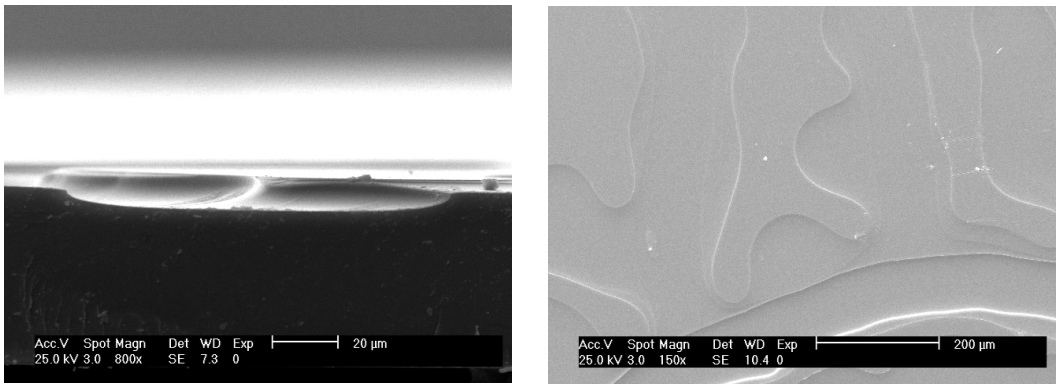

Figura 6

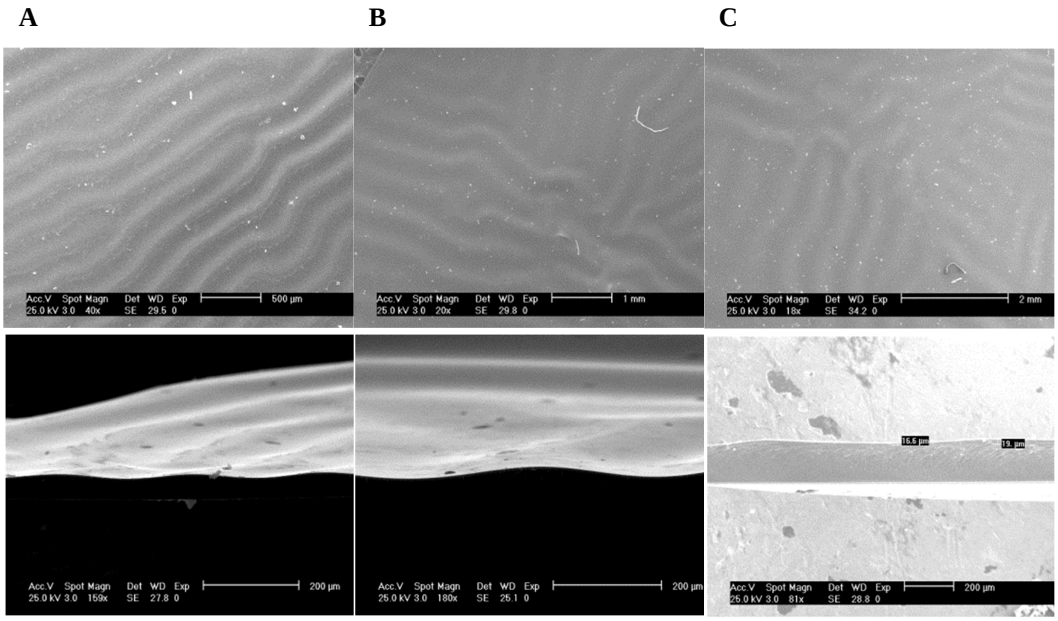

Figura 7

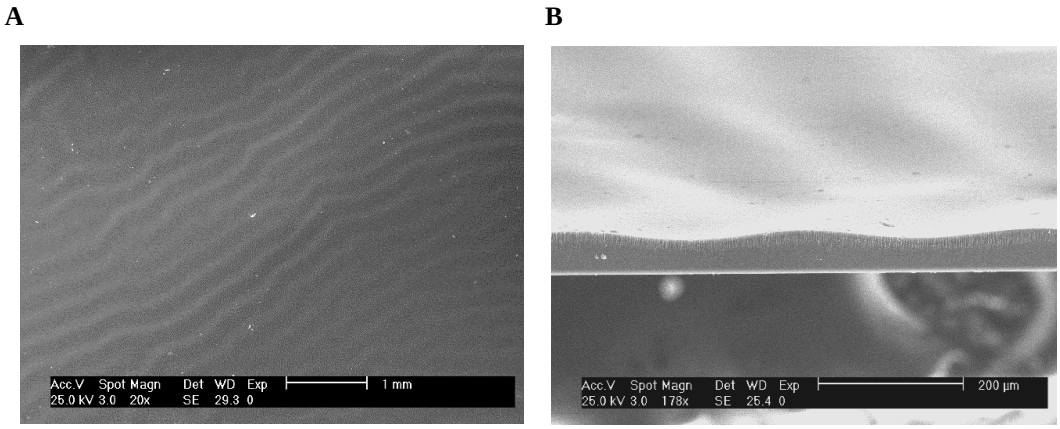

Figura 8

CAPÍTULO IV.4: Bibliografía del capítulo IV

[1] A. Hens, K. Mondal, D. Bandyopadhyay, Self-organized pathways to nanopatterns exploiting the instabilities of ultrathin confined bilayers, *Physical Review E*, 87, **2013**.
[2] H.-D. Koh, Y.J. Park, S.-J. Jeong, Y.-N. Kwon, I.T. Han, M.-J. Kim, Location-controlled parallel and vertical orientation by dewetting-induced block copolymer directed self-assembly, *Journal of Materials Chemistry C*, 1, **2013,** 4020-4024.
[3] S.Y. Choi, C. Lee, J.W. Lee, C. Park, S.H. Kim, Dewetting-Induced Hierarchical Patterns in Block Copolymer Films, *Macromolecules*, 45, **2012,** 1492-1498.
[4] R.A. Farrell, N. Kehagias, M.T. Shaw, V. Reboud, M. Zelsmann, J.D. Holmes, C.M.S. Torres, M.A. Morris, Surface-Directed Dewetting of a Block Copolymer for Fabricating Highly Uniform Nanostructured Microdroplets and Concentric Nanorings, *Acs Nano*, 5, **2011,** 1073-1085.
[5] H. Park, T.P. Russell, S. Park, Spatial control of dewetting: Highly ordered Teflon nanospheres, *Journal of Colloid and Interface Science*, 348, **2010,** 416-423.
[6] A.M. Higgins, R.A.L. Jones, Anisotropic spinodal dewetting as a route to self-assembly of patterned surfaces, *Nature*, 404, **2000,** 476-478.
[7] A.S. Padmakar, K. Kargupta, A. Sharma, Instability and dewetting of evaporating thin water films on partially and completely wettable substrates, *Journal of Chemical Physics*, 110, **1999,** 1735-1744.
[8] M. Ramanathan, S.B. Darling, Mesoscale morphologies in polymer thin films, *Progress in Polymer Science*, 36, **2011,** 793-812.
[9] H. Wang, R.J. Composto, Thin film polymer blends undergoing phase separation and wetting: Identification of early, intermediate, and late stages, *Journal of Chemical Physics*, 113, **2000,** 10386-10397.
[10] M. Boltau, S. Walheim, J. Mlynek, G. Krausch, U. Steiner, Surface-induced structure formation of polymer blends on patterned substrates, *Nature*, 391, **1998,** 877-879.
[11] L. Kielhorn, M. Muthukumar, Spinodal decomposition of symmetric diblock copolymer homopolymer blends at the Lifshitz point, *Journal of Chemical Physics*, 110, **1999,** 4079-4089.
[12] P. Cyganik, A. Bernasik, A. Budkowski, B. Bergues, K. Kowalski, J. Rysz, J. Lekki, M. Lekka, Phase decomposition in polymer blend films cast on substrates patterned with self-assembled monolayers, *Vacuum*, 63, **2001,** 307-313.
[13] K. Kargupta, A. Sharma, Morphological self-organization by dewetting in thin films on chemically patterned substrates, *Journal of Chemical Physics*, 116, **2002,** 3042-3051.
[14] N. Wu, L.F. Pease, III, W.B. Russel, Toward large-scale alignment of electrohydrodynamic patterning of thin polymer films, *Advanced Functional Materials*, 16, **2006,** 1992-1999.
[15] N. Wu, L.F. Pease, W.B. Russel, Electric-field-induced patterns in thin polymer films: Weakly nonlinear and fully nonlinear evolution, *Langmuir*, 21, **2005,** 12290-12302.
[16] L.F. Pease, W.B. Russel, Limitations on length scales for electrostatically induced submicrometer pillars and holes, *Langmuir*, 20, **2004,** 795-804.
[17] L.F. Pease, W.B. Russel, Electrostatically induced submicron patterning of thin perfect and leaky dielectric films: A generalized linear stability analysis, *Journal of Chemical Physics*, 118, **2003,** 3790-3803.
[18] L.F. Pease, W.B. Russel, Linear stability analysis of thin leaky dielectric films subjected to electric fields, *Journal of Non-Newtonian Fluid Mechanics*, 102, **2002,** 233-250.

[19] A.F. Miller, Exploiting wrinkle formation, *Science*, 317, **2007,** 605-606.
[20] J.Y. Chung, J.P. Youngblood, C.M. Stafford, Anisotropic wetting on tunable micro-wrinkled surfaces, *Soft Matter*, 3, **2007,** 1163-1169.
[21] E.P. Chan, E.J. Smith, R.C. Hayward, A.J. Crosby, Surface wrinkles for smart adhesion, *Advanced Materials*, 20, **2008,** 711-716.
[22] T. Bahners, L. Prager, S. Kriehn, J.S. Gutmann, Super-hydrophilic surfaces by photo-induced micro-folding, *Applied Surface Science*, 259, **2012,** 847-852.
[23] S.F. Ahmed, G.H. Rho, K.R. Lee, A. Vaziri, M.W. Moon, High aspect ratio wrinkles on a soft polymer, *Soft Matter*, 6, **2010,** 5709-5714.
[24] J.Y. Chung, A.J. Nolte, C.M. Stafford, Surface Wrinkling: A Versatile Platform for Measuring Thin-Film Properties, *Advanced Materials*, 23, **2011,** 349-368.
[25] C.-M. Chen, S. Yang, Wrinkling instabilities in polymer films and their applications, *Polymer International*, 61, **2012,** 1041-1047.
[26] Y. Gan, X. Jiang, J. Yin, Self-Wrinkling Patterned Surface of Photocuring Coating Induced by the Fluorinated POSS Containing Thiol Groups (F-POSS-SH) as the Reactive Nanoadditive, *Macromolecules*, 45, **2012,** 7520-7526.
[27] J.-H. Lee, H.W. Ro, R. Huang, P. Lemaillet, T.A. Germer, C.L. Soles, C.M. Stafford, Anisotropic, Hierarchical Surface Patterns via Surface Wrinkling of Nanopatterned Polymer Films, *Nano Letters*, 12, **2012,** 5995-5999.
[28] M. Watanabe, H. Shirai, T. Hirai, Wrinkled polypyrrole electrode for electroactive polymer actuators, *Journal of Applied Physics*, 92, **2002,** 4631-4637.
[29] F. Greco, T. Fujie, L. Ricotti, S. Taccola, B. Mazzolai, V. Mattoli, Microwrinkled conducting polymer interface for anisotropic multicellular alignment, *ACS applied materials & interfaces*, 5, **2013,** 573-584.
[30] C.-W. Peng, K.-C. Chang, C.-J. Weng, M.-C. Lai, C.-H. Hsu, S.-C. Hsu, S.-Y. Li, Y. Wei, J.-M. Yeh, UV-curable nanocasting technique to prepare bio-mimetic super-hydrophobic non-fluorinated polymeric surfaces for advanced anticorrosive coatings, *Polymer Chemistry*, 4, **2013,** 926-932.
[31] D.Y. Khang, H. Jiang, Y. Huang, J.A. Rogers, A stretchable form of single-crystal silicon for high-performance electronics on rubber subtrates, *Science*, 311, **2006,** 208-212.
[32] P. Gruner, M. Arlt, T. Fuhrmann-Lieker, Surface Wrinkling Induced by Photofluidization of Low Molecular Azo Glasses, *Chemphyschem*, 14, **2013,** 424-430.
[33] N. Lambricht, T. Pardoen, S. Yunus, Giant stretchability of thin gold films on rough elastomeric substrates, *Acta Materialia*, 61, **2013,** 540-547.
[34] M. Ramanathan, B.S. Lokitz, J.M. Messman, C.M. Stafford, S.M. Kilbey, II, Spontaneous wrinkling in azlactone-based functional polymer thin films in 2D and 3D geometries for guided nanopatterning, *Journal of Materials Chemistry C*, 1, **2013,** 2097-2101.
[35] Z. Wu, N. Bouklas, R. Huang, Swell-induced surface instability of hydrogel layers with material properties varying in thickness direction, *International Journal of Solids and Structures*, 50, **2013,** 578-587.
[36] Z. Chen, Y.Y. Kim, S. Krishnaswamy, Anisotropic wrinkle formation on shape memory polymer substrates, *Journal of Applied Physics*, 112, **2012**.
[37] Y.-C. Chen, A.J. Crosby, Wrinkling of inhomogeneously strained thin polymer films, *Soft Matter*, 9, **2013,** 43-47.
[38] N. Bowden, S. Brittain, A.G. Evans, J.W. Hutchinson, G.M. Whitesides, Spontaneous formation of ordered structures in thin films of metals supported on an elastomeric polymer, *Nature*, 393, **1998,** 146-149.

[39] W.T.S. Huck, N. Bowden, P. Onck, T. Pardoen, J.W. Hutchinson, G.M. Whitesides, Ordering of spontaneously formed buckles on planar surfaces, *Langmuir*, 16, **2000,** 3497-3501.
[40] N. Bowden, W.T.S. Huck, K.E. Paul, G.M. Whitesides, The controlled formation of ordered, sinusoidal structures by plasma oxidation of an elastomeric polymer, *Applied Physics Letters*, 75, **1999,** 2557-2559.
[41] D.B.H. Chua, H.T. Ng, S.F.Y. Li, Spontaneous formation of complex and ordered structures on oxygen-plasma-treated elastomeric polydimethylsiloxane, *Applied Physics Letters*, 76, **2000,** 721-723.
[42] R.C. Hedden, H. Saxena, C. Cohen, Mechanical properties and swelling behavior of end-linked poly(diethylsiloxane) networks, *Macromolecules*, 33, **2000,** 8676-8684.
[43] T. Okayasu, H.L. Zhang, D.G. Bucknal, G. Andrew, D. Briggs, Spontaneous formation of ordered lateral patterns in polymer thin-film structures, *Advanced Functional Materials*, 14, **2004,** 1081-1088.
[44] E.P. Chan, K.A. Page, S.H. Im, D.L. Patton, R. Huang, C.M. Stafford, Viscoelastic properties of confined polymer films measured via thermal wrinkling, *Soft Matter*, 5, **2009,** 4638-4641.
[45] V. Trujillo, J. Kim, R.C. Hayward, Creasing instability of surface-attached hydrogels, *Soft Matter*, 4, **2008,** 564-569.
[46] M. Guvendiren, S. Yang, J.A. Burdick, Swelling-Induced Surface Patterns in Hydrogels with Gradient Crosslinking Density, *Advanced Functional Materials*, 19, **2009,** 3038-3045.
[47] T. Tanaka, S.T. Sun, Y. Hirokawa, S. Katayama, J. Kucera, Y. Hirose, T. Amiya, MECHANICAL INSTABILITY OF GELS AT THE PHASE-TRANSITION, *Nature*, 325, **1987,** 796-798.
[48] E.S. Matsuo, T. Tanaka, PATTERNS IN SHRINKING GELS, *Nature*, 358, **1992,** 482-485.
[49] Z.B. Hu, Y.Y. Chen, C.J. Wang, Y.D. Zheng, Y. Li, Polymer gels with engineered environmentally responsive surface patterns, *Nature*, 393, **1998,** 149-152.
[50] D. Chandra, A.J. Crosby, Self-wrinkling of UV-cured polymer films, *Advanced Materials*, 23, **2011,** 3441-3445.
[51] R. Schubert, T. Scherzer, M. Hinkefuss, B. Marquardt, J. Vogel, M.R. Buchmeiser, VUV-induced micro-folding of acrylate-based coatings. 1. Real-time methods for the determination of the micro-folding kinetics, *Surface and Coatings Technology*, 203, **2009,** 1844-1849.
[52] J.G. Gaillard, C. Hendrus, B.D. Vogt, Tunable Wrinkle and Crease Surface Morphologies from Photoinitiated Polymerization of Furfuryl Alcohol, *Langmuir*, 29, **2013,** 15083-15089.
[53] J.M. Torres, C.M. Stafford, B.D. Vogt, Photoinitator surface segregation induced instabilities from polymerization of a liquid coating on a rigid substrate, *Soft Matter*, 8, **2012,** 5225-5232.
[54] M. Palacios Cuesta, O. Garcia, J. Rodriguez-Hernandez, Method of surface structuration in one single step by controlled wrinkle formation P201231928, in, Spain, 2012.
[55] L. Kielhorn, M. Muthukumar, Phase separation of polymer blend films near patterned surfaces, *Journal of Chemical Physics*, 111, **1999,** 2259-2269.

SECCIÓN V: Conclusiones

Conclusiones

1.- Se ha desarrollado una nueva estrategia para la fabricación de superficies funcionales microestructuradas por combinación simultánea de fotolitografía y segregación superficial. La metodología se basa en la irradiación con luz UV de mezclas fotosensibles que contienen monómero/s met/acrílicos comerciales, agentes entrecruzantes y un fotoiniciador; además de la incorporación de diferentes copolímeros fluorados sintetizados previamente por ATRP. La composición superficial final puede ser modificada variando diversos factores como las condiciones medioambientales o la concentración del copolímero fluorado añadido a la mezcla y su naturaleza. Se consiguen así cambios en la mojabilidad de las películas obtenidas variando tanto la composición superficial como su microestructura.

2.- Se ha descrito un nuevo procedimiento para la obtención de superficies microestructuradas en películas delgadas de naturaleza estirénica basado en procesos fotolitográficos. Modulando adecuadamente las condiciones experimentales aplicadas a este tipo de materiales poliméricos se puede controlar la fotorespuesta de los filmes a la irradiación UV, principalmente procesos de fotoentrecruzamiento y fotodegradación, y generar estructuras con patrones definidos en su superficie. Se ha comprobado cómo tiempos cortos de irradiación favorecen el fotoentrecruzamiento del material, mientras que tiempos largos de exposición tienden a fotodegradarlo. De forma que utilizando siempre el mismo montaje experimental y empleando, en todos los casos, exactamente la misma fotomáscara pero aplicando únicamente diferentes condiciones experimentales como: la cantidad de fotoiniciador, el tiempo de exposición a la luz, la naturaleza de la cubierta de la muestra empleada y/o la intensidad de la luz irradiada, se consigue la creación controlada de diversas estructuras superficiales: estructura tipo caja cerrada, caja abierta, red o agujas. Además, y gracias, a esta metodología se consiguen alcanzar altas resoluciones en tamaño, estructuras que llegan a tener un tamaño de hasta 25 veces menor que el dibujo de la máscara utilizada para la fotolitografía. En último término mencionar que la estructura superficial obtenida consigue ejercer una notable influencia en la mojabilidad superficial de los filmes.

El procedimiento citado en el punto 2 ha resultado ser muy versátil y asimismo útil en la aplicación a otros sistemas poliméricos, que manteniendo la misma naturaleza poliestirénica

poseen, además, distinta funcionalidad; es decir, se han desarrollado nuevos copolímeros funcionales que presentan fotorespuesta muy similar a la del PS simple. Estos copolímeros funcionales han sido sintetizados por polimerización controlada (ATRP) y están formados por bloques de poliestireno y bloques que contienen otros grupos funcionales: bien grupos fluorados (de naturaleza hidrofóbica), o bien con grupos de poliácido glutámico o poliácido acrílico (de naturaleza hidrofílica). Estos copolímeros se han utilizado, asimismo, para desarrollar diferentes aplicaciones:

2a.-Se han desarrollado sistemas con mojabilidad variable. Se ha comprobado como la variación de esta propiedad en las superficies obtenidas depende no sólo del tipo de estructuras generadas en la superficie, sino también de cambios introducidos en la química superficial.

2b.- La preparación de superficies microestructuradas siguiendo el procedimiento del punto 2 empleando, en este caso, un copolímero de bloque de poliestireno y poliácido glutámico permite desarrollar nuevos sistemas útiles para el reconocimiento de proteínas. Gracias a la presencia de los grupos carboxílicos en superficie se consigue el anclaje de secuencias polipeptídicas a la misma, que quedan inmovilizadas sólo en posiciones específicas de la superficie.

2c.- En último lugar, se han fabricado microestructuras siguiendo el método del punto 2 a partir de un copolímero de bloque de poliestireno y poliácido acrílico. Este grupo funcional promueve la adhesión de las paredes celulares de la bacteria *Staphylococcus Aureus*. Se ha conseguido la adhesión selectiva de esta bacteria sólo en determinadas zonas de la superficie y se llega a alcanzar tanto la alineación de las mismas como su aislamiento sobre las estructuras fabricadas, a pesar de que la citada bacteria posee una alta tendencia a estar en estado de agregación unas con otras.

3.-En esta tesis también se ha descrito un nuevo método para fabricar microestructuras funcionales aplicando la técnica de *hot embossing* en mezclas de PMMA que incluyen copolímeros de naturaleza metacrílica que además contienen unidades con distinta funcionalidad (hidrofóbicas ó hidrofílicas), sintetizados previamente por ATRP y que, por

posterior segregación superficial, pueden migrar a la superficie aplicando diferentes condiciones medioambientales y modificando, así, sus propiedades finales, entre ellas la mojabilidad. Se ha comprobado nuevamente como esta propiedad depende tanto de la estructura como de la funcionalidad de la superficie generada.

4.- Se presenta una nueva metodología para la creación de arrugas superficiales que permite la creación de superficies rugosas partiendo de disoluciones fotosensibles, formadas por mezclas de monónomero/s, entrecruzante, y un fotoiniciador al ser irradiados con luz UV en un espacio confinado, mientras se aplica simultáneamente una temperatura constante al sistema. Los sistemas desarrollados incluyen disoluciones de monómeros de naturaleza tanto metacrílica, acrílica como estirénica. Se han utilizado para preparar las formulaciones fotosensibles monómeros que contengan algún grupo funcional en su estructura que modifique las propiedades químicas superficiales de la película final. Estos grupos pueden ser tanto de carácter hidrófobo como hidrófilo, creándose, de este modo, un amplio abanico de posibilidades en cuanto a composición y propiedades finales se refiere. Por último, con este nuevo método que permite la creación de arrugas también es posible la introducción de cargas sólidas en las disoluciones fotosensibles (aerosiles, nanotubos de carbono, etc.).

Summary/Resumen

SUMMARY

A wide number of applications in polymeric materials depend, almost in exclusively, on its surface. For this reason, the design and control of the polymer surface of a particular material is essential to be able to adapt the polymeric materials to the requirements of a precise application. The control of the structure and functionality of interfaces, can occur simultaneously, and allow us to develop materials with superhydrophobic, superhydrophilic, biocompatible, adhesive or antifouling properties, just to mention few of them.

In this PhD Thesis, alternative strategies to fabricate interfaces with both controlled topography and interfacial chemical composition are developed. For that purpose, we aim to simplify the fabrication process. Thus, the strategies depicted in this work resort to straightforward technologies which can be carried out using affordable technical equipment and at economic level. The alternatives for the fabrication of functional and structured interfaces employed in this thesis are described in different sections as a function of the methodology selected:

SECTION II: PHOTOLITHOGRAPHY AND FUNCTIONAL SURFACES.

- CHAPTER II.1: Photolithography using monomers and surface segregation.

In this chapter, the use of photolithography to obtain microstructured surfaces is described. This approach has been already employed for similar purposes in the past. However, our approach involves the irradiation of a photosensitive mixture through a photomask and the surface segregation of one of the compounds of the mixture (carrier of a functional group) to the surface. The photosensitive mixtures used had the following components: a monofunctional monomer (typically methacrylic monomer such as methyl methacrylate, MMA), a crosslinking agent (Ethylenglycol dimethacrylate, EGDMA), a photoinitiator (Irgacure 651) and, finally, a fluorinated copolymer. The latter was previously synthetized by using controlled radical polymerization, i.e. ATRP (methacrylate-co-2,2,2-trifluoroethyl methacrylate, p(MMA-*co*-TFMA)).

Upon irradiation of these through a photomask the areas exposed to UV-light were crosslinked and the microstructure formed according to the shape of the photomask employed. More interestingly, at the same time, the fluorinated copolymer migrated to the surface of the sample when the photosensitive solution is covered by a silanized glass. As a result, an enrichment of the surface with fluorine atoms is observed. These chemical changes are traduced in variations of the surface properties that were evaluated measuring the contact angle and with XPS measures of the surfaces.

The method developed here presents the advantage of its versatility since it can be used with a wide variety of systems and photosensitive formulations. Moreover, we can produce functional and structured interfaces in one single step, thus, saving time and cost in view of their industrial application.

- CHAPTER II.2: Photolithography from PS films.

In this chapter, the method to create different surface structures (squares, boxes, lines, needles, etc) onto spun coated PS films, using photolithography, is detailed. The generation of the surface structures is obtained as a result of photodegradation/photocrosslinling processes observed in PS under UV light exposure. Short irradiation times produced the crosslinking of the directly exposed areas. However, an increase of the irradiation time degrade these areas, the radicals diffuse into the non-exposed and produced variable surface patterns. Since the diffusion is limited, the surface structures exhibit a better pattern resolution than the mask employed. Using photolithographic processes and only one kind of mask the surface structure can be varied exclusively by optimizing the experimental conditions (time of irradiation, sample cover, amount of photoinitiator, oxygen in the sample).

Once, the experimental conditions were optimized in PS films, the study was extended to different functional blocks copolymers. These were designed to have a polystyrene block and either a hydrophobic block (formed by fluorinated groups) or a hydrophilic block (poly(L-glutamic acid) or poly(acrylic acid)).

The functional and microstructured surfaces were employed for two different applications. On the one hand, we explored the immobilization of proteins able to interact in

biorecognition processes. On the other hand, the bacterial adhesion on surfaces with variable both structure and functionality was studied. For the first application, the patterns were fabricated using a block copolymer of PS and poly(L-glutamic acid). The carboxylic acid groups were used to anchor polypeptide sequences using the amine terminal group. The immobilized sequences were selected to act in recognition processes with TPR proteins. Equally, the microstructures made of mixtures of PS and a block copolymer of polystyrene and polyacrylic acid were made in order to study the specific adhesion of the *Staphylococcus Aureus* bacteria onto the patterns. As a result of this process and based on the submicrometer resolution achieved it was possible to prepare arrays of bacteria, by align them or even to isolate them individually.

SECTION III: HOT EMBOSSING IN FUNCTIONAL SURFACES

The work described in this section was carried out at Glasgow University in a predoctoral stay during the Thesis. As an alternative to photoirradiation processes herein we proposed the fabrication of functional microstructures by hot embossing. In addition, surface segregation of the functional copolymers was employed to modify the surface chemical composition, as has been carried out for the previous approaches. Mixtures of PMMA and statistical copolymers, having either fluorinated or carboxylic acid moieties, (previously synthetized by ATRP) were used, to fabricate the microstructured interfaces.

The obtained results verify again how the surface properties, and especially the wettability, depend on both the surface chemistry and topography. It can be noticed how the contact angle increases if the proportion of fluorinated copolymer in the polymeric mixture increases, and also increases if the film was microstructured. It can be noticed how the contact angle rises even more after the heating of the sample, due to the migration of fluorinated atoms (with low superficial energy) to the surface. On the contrary, when experiments were carried out with PAA copolymers, the contact angle values decrease both with the increasing of PAA percentage in the initial polymer blend and during surface segregation process carried out in an humid environment.

SECTION IV: WRINKLES AND FUNCTIONAL SURFACES

- CHAPTER IV.1: Wrinkles and functionalized surfaces from functional monomers.

In this chapter a new procedure to obtain structured surfaces by the formation of controlled-size wrinkles has been described. This method is based on the UV irradiation and simultaneous heating of a photosensitive solution in a confined space. We described how, by varying experimental parameter such as spacing or amount of crosslinking agent we can vary both the surface topography and the chemical composition of the surface wrinkles. The process occurs in few minutes and in one single step, using monomers with different functionalities. Moreover we investigated the mechanism of the wrinkles formation. We concluded that, upon irradiation, the system crosslinked producing a fast volume contraction, while capillary forces try to maintain the contact between the monomeric mixture and the glass cover. As a result of these competitive processes we observed the formation of interfacial wrinkles.

The methodology proposed to fabricate wrinkles is versatile. First of all, we demonstrated that it can be carried out using solutions with different components (functional monomers, copolymers). Equally, wrinkles were obtained using methacrylic, acrylic, or styrenic monomers, and more recently we evidenced that this method can be extrapolated to other systems with different nature, as epoxy. Furthermore, this new method for the creation of wrinkles in a surface can be also used for the introduction of solid charges in the initial photosensitive mixtures (silica particles, carbon nanotubes, nanoparticles, etc).

- CHAPTER IV.2: Wrinkles and functionalized surfaces from the introduction of functional synthetized copolymers

Once the period and amplitude of the wrinkles and its functionalization using different monomers (functional and non-functional) was optimized (it was described in the previous chapter), the possibility of varying the chemical composition introducing a functional copolymer as an additive, or a charge in the photosensitive, mixture was studied. In this case

both a fluorinated copolymer (PTFMA) and another one with PAA groups were included. Variable proportions were tried in order to understand the role of the incorporation of a solid charge on the wrinkle parameters. The main purpose of this work is to evidence if there are differences at the surface level in terms of surface composition between the areas directly in contact with the cover and those forming the valleys of the wrinkles. To evidence this and based on our previous findings in the role of the bacterial adhesion onto PAA surfaces we incubated the surfaces with bacteria. The essays with bacteria (*S. Aureus*) were carried out supporting the fact that the bacterial adhesion is related with hydrophilicity. On the one hand, adhesion is not observed in PTFMA copolymer samples. On the other hand, in the wrinkled surfaces having PAA, the bacterial adhesion selectively occurs in the top of the wrinkles, thus evidencing a variable surface composition.

RESUMEN

Un gran número de las propiedades que presentan los materiales poliméricos dependen, casi en exclusiva, de su superficie. Para éstas, es independiente de cómo sea el interior del material y su aplicabilidad sólo se va a ver afectada por las capas más externas del material, las últimas micras superficiales. Por todo ello, el diseño y el control de estas superficies resulta hoy en día imprescindible para poder adaptar los materiales poliméricos a los requerimientos necesarios en determinadas aplicaciones. Estas adaptaciones pueden conllevar desde la funcionalización de las superficies, la modificación de su cristalinidad, la creación de microdominios o incluso variaciones de la rugosidad y de la topografía. El control de la estructuración de una superficie y de la funcionalización de ésta, que pueden ser procesos simultáneos, permite desarrollar nuevos materiales con propiedades superhidrofóbicas, superhidrofílicas, biocompatibles, adhesivas, lubricantes o *antifouling*, entre otras.

En esta Tesis Doctoral se han desarrollado métodos alternativos que nos han permitido modificar la topografía de superficies poliméricas a la vez que se han generado superficies con grupos funcionales. Las metodologías desarrolladas, tanto de funcionalización como de modificación de la topografía superficial, además han sido adaptadas de manera que puedan ser fácilmente implantables a nivel industrial, tanto a nivel técnico como económico.

Cada uno de los métodos optimizados o desarrollados es descrito en cada una de las secciones siguientes:

SECCIÓN II: FOTOLITOGRAFÍA Y SUPERFICIES FUNCIONALES

- **CAPÍTULO II.1: Fotolitografía a partir de monómeros y segregación superficial**

En este capítulo se ha descrito el desarrollo de una nueva metodología para la obtención de superficies funcionales microestructuradas combinando, de manera simultánea, la irradiación UV de una mezcla fotosensible a través de una fotomáscara con la segregación

superficial de uno de los componentes de la mezcla (portador de un grupo funcional) a la superficie.

Se han preparado mezclas que contienen un monómero metacrílico (metacrilato de metilo, MMA), un agente entrecruzante (dimetacrilato de etilenglicol, EGDMA), un fotoiniciador (Irgacure 651) y un copolímero fluorado sintetizado por ATRP, el metacrilato-*co*-2,2,2-trifluoroetil metacrilato [p(MMA-*co*-TFMA)] que contiene un 23%mol del monómero fluorado.

La irradiación con luz UV de estas mezclas a través de una fotomáscara genera la microestructura superficial, mientras que, al mismo tiempo, el copolímero fluorado migra hacia la superficie del vidrio, si éste está silanizado, enriqueciendo la superficie polimérica con átomos de flúor y modificando las propiedades de la misma. Estos cambios se han evaluado midiendo el ángulo de contacto y por medidas de XPS de las superficies.

El método aquí desarrollado presenta una gran versatilidad, ya que puede ser utilizado con una amplia variedad de sistemas o formulaciones fotosensibles, con la ventaja de que esta metodología se desarrolla de forma eficiente y en un solo paso, con el consecuente ahorro de tiempo y de costes de fabricación.

- CAPÍTULO II.2: Fotolitografía a partir de películas de PS

En este capítulo se detalla cómo es posible crear diferentes tipos de estructuras superficiales (cuadrados, cajas, líneas, agujas, etc.) sobre láminas delgadas de poliestireno (PS) mediante la aplicación de procesos de fotolitografía. La generación de este tipo de estructuras superficiales tan variadas se consigue gracias a los procesos de fotodegradación/fotoentrecruzamiento que es capaz de experimentar el PS bajo irradiación UV. Así, mediante procesos de fotolitografía, empleando un único tipo de máscara y variando únicamente las condiciones experimentales del proceso (tiempo de irradiación, cubierta de la muestra, oxígeno en la muestra, cantidad de fotoiniciador) se han podido llegar a generar

diferentes estructuras superficiales submicrométricas, alcanzado resoluciones de hasta 25 veces más pequeñas que el tamaño de la máscara empleada.

Una vez se han optimizado las condiciones experimentales necesarias en cada caso para obtener los diferentes tipos de estructuras descritas en los filmes de PS, se ha extendido su aplicación a filmes formados a partir de copolímeros de bloque que contienen bloques con distinta funcionalidad mientras siguen manteniendo su naturaleza poliestirénica: bien grupos fluorados (de naturaleza hidrofóbica), o bien grupos de poliácido glutámico o poliácido acrílico (de naturaleza hidrofílica).

Posteriormente, la fabricación de los patrones utilizando un copolímero de bloque de PS con un bloque poli(ácido L-glutámico) ha permitido anclar a las superficies secuencias polipeptídicas a través de sus grupos amina, de manera que este método se puede emplear como un nuevo método para el reconocimiento de proteínas, tal y como se ha descrito en la presente Tesis.

Por último, se han fabricado microestructuras sobre un copolímero de bloque de poliestireno y poliácido acrílico para promover la adhesión específica de bacterias *Staphylococcus Aureus* sobre los patrones formados en superficie gracias a la presencia de este grupo funcional. Así, se consigue alinear las bacterias o incluso aislarlas de una en una, aun siendo la *Staphylococcus Aureus* una bacteria que presenta con gran tendencia a la agregación.

SECCIÓN III: HOT EMBOSSING EN SUPERFICIES FUNCIONALES

En esta sección, cuyo trabajo experimental se ha llevado a cabo durante una estancia predoctoral realizada en la Universidad de Glasgow, se explica un nuevo método para fabricar microestructuras funcionales aplicando la técnica de impresión en caliente (*hot embossing)* seguida de la segregación superficial de copolímeros funcionales presentes en la muestra. Se han utilizado mezclas de PMMA con copolímeros de naturaleza metacrílica, sintetizados previamente por ATRP, que contienen unidades con distinta funcionalidad.

Los resultados obtenidos han permitido constatar, una vez más, como las propiedades superficiales y, en especial, la mojabilidad dependen tanto de la química superficial como de la topografía. Se ha observado como el ángulo de contacto aumenta con la proporción de copolímero fluorado añadido a la mezcla polimérica y se incrementa todavía más, si la película ha sido microestructurada. Tras el tratamiento de calentamiento al aire de las muestras, se ha observado como el ángulo de contacto aumenta incluso más, debido a la migración de los átomos de flúor, de baja energía superficial, hacia la superficie. En el estudio de los copolímeros con grupos de ácido acrílico (PAA) ocurre justo lo contrario: descenso de los valores de ángulo de contacto tanto al aumentar el porcentaje de PAA como al llevar a cabo la segregación superfical (en este caso en ambiente húmedo).

SECCIÓN IV: ARRUGAS Y SUPERFICIES FUNCIONALES

- CAPÍTULO IV.1: Arrugas y superficies funcionalizadas a partir de monómeros funcionales.

En este capítulo se ha descrito el desarrollo de un nuevo procedimiento para la obtención de superficies estructuradas mediante la formación controlada de arrugas en superficie de dimensiones variables. El método se basa en la irradiación con luz UV y calentamiento simultáneo de una disolución fotosensible confinada en un espacio definido que permite, en pocos minutos y simultáneamente, controlar la topografía superficial y la composición química, utilizando monómeros con distinta funcionalidad. Bajo estas condiciones de irradiación, el sistema se entrecruza produciendo una rápida contracción de volumen mientras las fuerzas capilares intentan mantener el contacto entre la mezcla monomérica y la cubierta de vidrio.

El método aquí desarrollado para la formación de arrugas funcionales ha resultado ser muy versátil, puesto que puede aplicarse en disoluciones de muy distinta naturaleza química. Hasta el momento, se ha aplicado en disoluciones de monómeros de naturaleza tanto metacrílica, acrílica como estirénica, aunque la utilización del método podría extrapolarse a sistemas de distinta naturaleza, por ejemplo epoxídica.

- CAPÍTULO IV.2: Arrugas funcionalizadas a partir de la introducción de polímeros funcionales de síntesis.

Una vez se han optimizado el período y amplitud de las arrugas, ajustando las condiciones experimentales, y la funcionalización de éstas usando monómeros de diferente naturaleza (descrito en el capítulo anterior), se ha explorado la posibilidad de variar la composición química de la superficie introduciendo un copolímero funcional como aditivo o carga en la mezcla fotosensible. En este caso, se han incorporado proporciones variables tanto un copolímero fluorado (PTFMA) como otro que contiene grupos de poliácido acrílico (AA) consiguiendo así modular el período de las arrugas que se forman. Además, este nuevo método de creación de arrugas en superficie también permite la introducción de cargas sólidas en las mezclas iniciales fotosensibles (sílice, nanotubos de carbono, otras nanopartículas, etc.).

Por último, se han realizado ensayos con bacterias (*S. Aureus*) donde se confirma que la adhesión bacteriana está directamente asociada con la hidrofilicidad y la estructura de la superficie de contacto. En las muestras sintetizadas con copolímeros fluorados, no se observa adhesión bacteriana, mientras que las muestras en las que hay PAA, se observa la adhesión selectiva de las bacterias en la parte superior de las arrugas.